Post-Expedition Report for USGS T-3 Ice Island Heat Flow Measurements in the High Arctic Ocean, 1963-1973

Arthur H. Lachenbruch, B.Vaughn Marshall*, and Carolyn Ruppel

2019

USGS Field Activity: 1963-FA-001

Lachenbruch, A.H., Marshall, B.V., and Ruppel, C.D., 2019, Post-expedition report for USGS T-3 Ice Island heat flow measurements in the High Arctic Ocean, 1963-1973: U.S. Geological Survey data release, https://doi.org/10.5066/P91XQ3IS.

deceased

Notes from Carolyn Ruppel (USGS), February 2019

Suggested citation: *Lachenbruch, A.H., Marshall, B.V., and Ruppel, C.D., 2019, Post-expedition report for USGS T-3 Ice Island heat flow measurements in the High Arctic Ocean, 1963-1973: U.S. Geological Survey data release, https://doi.org/10.5066/P91XQ3IS.*

Refer to the metadata accompanying this release for more background on this report.

This report originated with USGS scientists Arthur Lachenbruch and B. Vaughn Marshall in the early 1970s. Handwritten notations and hand-drawn contours in the document are theirs. The exact date of this report is unknown. However, based on references that pre-date 1974 and the fact that the report includes the final data USGS T-3 heat flow data acquired in 1973, it is thought to have been produced in ~1974. In 2019, USGS scientist Carolyn Ruppel added typed references (including DOI, when available), typed figure captions and some corrections, references to the accompanying data release, and correct figure numbering. Explanations concerning figure number are given in the metadata file.

The photocopied version of this unpublished report was provided to the Coastal/Marine Hazards and Resources Program in 2015. Due to the historically important nature of this report, it is being preserved intact within the USGS Coastal & Marine Field Activity System. The USGS is not releasing this report through the modern USGS publications system because aspects of this document cannot be altered to comply with current USGS practices and guidelines without the loss of critical historic information.

Attached as an appendix is an interim report on T-3 heat flow data. This was formulated in 1971.

Tables 1 and 2 in this report have been released, along with other data related to the T-3 heat flow studies, through sciencebase.gov: *Ruppel, C.D., Hutchinson, D.H., Lachenbruch, A.H., and Hall, J.K., 2019, Thermal Data and Navigation for T-3 (Fletcher's) Ice Island Arctic Ocean Heat Flow Studies, 1963-1973: U.S. Geological Survey data release, https://doi.org/10.5066/P97EPU2F.*

Post-Expedition Report for USGS T-3 Ice Island Heat Flow Measurements in the High Arctic Ocean

Art H. Lachenbruch and B. V. Marshall

Background

In February 1963, the U.S. Geological Survey began a study of heat flow in the Arctic Ocean Basin. These operations were carried out from the scientific station on T-3 Ice Island (also known as Fletcher's Ice Island). At that time, the location of the floating island was approximately 82° 00' N, 157° 45' W. T-3 was apparently part of the continental ice sheet from Ellesmere Island that broke off as it protruded into the sea (Crary, 1960; Marshall, 1960; Stoiber and others, 1960). It obtained its name from the fact that it was first sighted as a radar target by the U.S. Air Force in 1950. At that time, it was about 6.4 x 18.0 km in size and approximately 58 metres thick. At various times from March 1952 to October 1961, it was used as a weather and scientific station. It was then abandoned after having gone aground five months earlier in 39 metres of water, approximately 142 km NW of Barrow, Alaska. Heavy winds apparently helped to refloat it in early 1962 when a portion broke off. Then, reduced to approximately 4.8 x 9.7 km in size, it was rediscovered by aircraft from the Naval Arctic Research Laboratory (NARL). In February 1962 the NARL re-established T-3 as a research station and kept it operating continuously until September 28, 1974, when all remaining personnel were evacuated, and the station was abandoned. The U.S. Geological Survey heat-flow studies were part of the scientific effort supported by the NARL.

Operations

The size and stability of T-3 Ice Island ~~make~~ made it ideal for the establishment of a permanent camp. It is not subject to the formation of pressure ridges and is much less likely to break up than is the pack ice. However, while the camp was situated on the island, much of the scientific work was done from several hydrohuts located on the pack ice, where the ice was much thinner and easier to work through. Generally, each continuing project had its own hydrohut, but these facilities were often shared with short-term projects. T-3 has a natural indentation or bay in its configuration, which is called Colby Bay. Although the camp was moved occasionally, it was always close to Colby Bay where the hydrohuts were. In the summer of 1962 portions of the ice in the bay broke up. Every summer after that, however, the bay ice remained connected to the island and the summer break-up of the pack ice occurred along the mouth of the bay.

From February 18 - April 7, 1963, the USGS hydrohut was built, a 1.2 x 1.2 x 3.7 metre hole cut through the ice, and the first two casts for heat flow made. Two men returned in June and stayed until September 16 to make 23 more casts. The results of these first 25 casts were published previously (Lachenbruch and Marshall, 1966). At first, the fieldwork called for 2 to 3 short trips to T-3 (2 to 3 weeks each) from October to May, and a full summer's work from June through September. This plan was followed through September 1965 when it was decided that

T-3 was moving rapidly enough to warrant a continuous field program. Except for an occasional month or two hiatus the fieldwork was continuous from March 1966 through September 1972. By this time, the island was moving much slower in a congested field of pack ice north of Ellesmere Island. The remaining two field trips were in April-May and October-November 1973.

A fire completely destroyed the hydrohut in April 1966. A new hut, winch, tripod, and necessary heat-flow equipment were quickly flown in while the planes could still land on the island. The new setup was better. Two hinged gratings were installed flush with the deck of the hut over the hydrohole. This was a good safety feature, and it also helped to make the handling of the Thermograd (heat-flow corer) in the hut a one-man operation. After a cast, for example, the Thermograd was raised high enough in the tower of the hydrohut for the tip of the core barrel to clear the deck. The tip of the core barrel was then lifted into a sling attached to a pulley on a line that extended to the opposite end of the hut. The grating doors were closed, covering the hydrohole, and the coring head was then lowered onto a two-wheeled "dolly" on the grating. The Thermograd could then be pushed away from the hydrohole to a convenient place to remove the core. This one-man system was used from the fall of 1966 on. Other improvements were a better level-wind system with fleet angle compensator for the winch, and a better line-weight tensiometer with a strip-chart recorder for continuous monitoring of line tension.

The frequency of making a cast for heat flow depended on the movement of the island and the changes in bottom topography. Except for times when there were equipment problems, the frequency varied from one a week to one per day. Usually 2 to 3 a week was average. The actual density of heat-flow values varied also because of the erratic drift of the island. In addition to heat-flow casts, temperature profiles of the ocean and more detailed temperatures of the bottom 100 metres of water were obtained, and a few attempts to get more detailed sediment temperature 1 metre to 4 metres in the sediments were made.

Methods and equipment

Gradient. The geothermal gradient was measured, and core obtained using a Ewing-type piston corer (Thermograd) similar to the one developed at Lamont-Doherty Geological Observatory (Gerard and others, 1962). It had four thermistors on outriggers mounted on the core barrel approximately 1 metre apart. A fifth thermistor was mounted on the top of the corer on the instrument case housing to obtain the bottom-water temperature. Temperature differences were measured within a few thousandths of a degree Centigrade. The Thermograd used for the earlier casts was a Model 322 from Alpine Geophysical Associates, which recorded data on 35 mm film. New Thermograds were designed by the U.S. Geological Survey in Menlo Park using a Moseley 680 strip-chart recorder with a 15 cm wide chart for data recording. The recorder allowed for quicker and easier evaluation of records. A later modification allowed for the separation of the instrument package and corer when triggering occurred at the ocean bottom. Thermistor circuits were connected to the instrument package by extendable telephone cables. The USGS thermograds also increased the core barrel length from 3.05 metres (10 feet) to 3.66 metres (12 feet). The ~~larger~~ LONGER length was the same as that of the plastic core liner obtained, and allowed for a slighly wider spacing of the thermistors. Initially, water pipe was used for the core barrels. It was not strong enough, however, and after obtaining a few bent barrels, heavier-walled 4130 steel tubing (I.D. = 3.96 cm, O.D. = 5.08 cm) was used.

Thermal conductivity. Thermal conductivity (k) of the sediments through the depth of gradient measurements is required to obtain heat flow. All values of k were determined using the needle-probe method. (Von Herzen and Maxwell, 1959) with probes which were designed and built in our Menlo Park Laboratory. The latest design is shown in Figure 2. Each thermal conductivity probe was calibrated regularly in a fused silica rod of the same diameter as the core (3.5 cm) using Ratcliffe's (1959) formula. The silica in turn was checked against quartz standards by steady-state methods to determine its quality in reference to Ratcliffe's silica. The agreement was within 1%.

Most of the conductivities for the first 28 casts were determined in the field using a strip-chart recorder to measure the amplified imbalance of a wheatstone bridge which tested the thermistor circuit of the k-probe. The chart spans were calibrated with a decade resistance box. A constant current was supplied to the heater circuit of the probe with Invar Model 479 power supply and was measured with a L&N potentiometer testing across a standard 1 ohm resistor. Sections of the core were enclosed in a form-fitting styrofoam box which accommodated five sections and their conductivity probes. The core was cut into 15-cm sections for ease of handling and shipping.

The above system was replaced with a laboratory unit yielding resistance and time data on punched cards which were processed by an IBM 360/65 computer to provide thermal conductivity values and plots

of temperature versus ℓn (time) for each test. A North Hills precision DC current source with 0.02% absolute accuracy and digital current readout of 1 μA resolution provided the power to the probe heater circuit. The probe thermistor circuit was connected to a digital voltmeter with ohm-DC converter and then through a buffer circuit to the printing summary punch. A metal cabinet with 20 styrofoam-insulated compartments was used to house the core sections. Each compartment was wired with a connector compatible with the probes and a compartment selector switch was mounted on the cabinet. The temperature of each sample was monitored until it stabilized, or a sufficiently small temperature drift was obtained. A typical computer plot and printout from a thermal conductivity test using this system is shown in Figures 3 & 4.
A printout of resistance, temperature, time, and the thermal conductivities from least-square solutions of different time intervals was also provided. More than 14,700 thermal conductivity values were obtained from Arctic core. Corrections for depth and temperature were applied according to Ratcliffe (1959).

Core. A total of 584 casts were made from T-3 to measure heat flow. Approximately 1.486 km of core was obtained from 546 of these. The remaining 38 casts included two that had rocks stuck in the coring tip, preventing any sediment recovery, three where the complete probe was lost, and two where the cores were lost. The longest core was 5.54 metres and the average length was 2.72 metres.

Immediately after recovery of a core, the excess plastic liner was cut off; the liner with the core was capped, taped, and cut into 15 cm lengths which also were capped and taped. For the first 382 casts, all the core sections were placed in an olive jar which was then sealed with a water-tight lid. The sections from the cores after F-382 were sealed with wax and wrapped in a plastic bag instead of being placed in the glass jar. Most of the core sections were weighed at T-3 and at Menlo Park to determine any weight loss. Four thousand sections from some of the casts from F-92 - F-382 which were weighed indicated that 87.1% had lost 0.5 gm (2-3% of sample weights) or less, and 69.7% lost 0.25 gm or less. The same analysis for 1,413 waxed samples gave values of 98.2% of 0.5 gm or less loss, and 95.9% with a loss of 0.25 gm or less. It was more difficult to weigh accurately at T-3 than at Menlo Park because of a less stable base for the Mettler balance, but most of the loss in weight was probably due to water loss in the sample.

Care was taken to prevent the core from freezing so that it would remain as natural as possible. They were shipped in insulated cases

and received special handling when loaded in the plane at T-3 and while at Barrow, Alaska. Occasionally one would be frozen, so a test was made with the core from a cast with unusable temperature data, F-439. It had 22 core sections. Conductivity was tested at three locations on each section before and after freezing. Each section was frozen from three to five days at approximately -30°C. The average absolute difference was only 2.3%. A few had higher conductivities after freezing, but most were slightly lower in value.

In order to make optimum use of the core, arrangements were made with Dr. David Clark at the University of Wisconsin, in 1968, to send the cores there when the USGS was through testing them. As of February 1975, 381 cores had been shipped to the university for further studies, i.e., paleomagnetism, moisture content, mechanical analysis, CO_3 content, microfossil investigations, sedimentation rates, clay mineralogy, and other studies. Thirty-nine cores were tested by Carl Bunker (USGS - Denver) for radioactive heat production (Table __), and one core each was given to Lamont-Doherty Geological Observatory, H. A. Wollenberg (Lawrence Radiation Laboratory) and to the Navy Oceanographic Office.

Results

Heat-flow data of the Arctic Ocean obtained from this study are presented in Table 2 along with the thermal gradients and harmonic thermal conductivities over the different depth intervals for each successful cast. The five thermistor positions were numbered consecutively beginning with the one closest to the tip of the core barrel. Position one penetrated deepest into the sediments ~~most deeply~~, and position five was mounted either on the coring head or instrument package, or on the core barrel when attempts for longer cores were made. Three-hundred fifty-six heat-flow values are listed; all except the first 19 are new. No values are listed where core was not obtained at the site or where the core was frozen, even though the later situation may have had a minor effect. Heat-flow calculations were made only for those gradient intervals where the recovered core extended over at least half of the interval.

THERMAL CONDUCTIVITIES

Thermal conductivity values, k, obtained in this study were highly variable. This was generally true when comparing mean values from different cores and also when observing conductivity values over a few centimeters in a single core. Most of the cores were collected in the Amerasia Basin of the Arctic Ocean where certain major features of the floor provide natural areas and boundaries for discussing the data. Figures 5 to 8 are histograms of the conductivity values for some of these. The number of data for each plot represents the number of core sections providing mean k-values. Each $\overline{k}$ is the mean conductivity of from one to five thermal conductivity tests. Mean thermal conductivity values per area range from 2.40 mcal/cm sec °C for the NW Canada Plain to 3.10 mcal/cm sec °C for the eastern Alpha Ridge. The division between the eastern and western Alpha Ridge is arbitrarily taken at the 90°W longitude except that F-537 and F-538 are included in west Alpha. According to Beal (1966) this would identify the eastern area as the junction of the Lomonosov Ridge and Ellesmere Island. The Mendeleyev Plain is the name suggested by Hall (1970) for that plain lying northwest of the Chuckchi Cap at a depth of about 3300 metres. The Mendeleyev Ridge includes the Arlis Plateau, Sargo Plateau and the T-3 Plateau (Hall, 1970).

Much of the sediment studied was either a grey or brown lutite, often showing mottling. X-ray diffraction analysis of the less than two

micron fraction from 25 cores indicated an average clay composition of 37% illite, 32% chlorite, 27% kaolinite and 3% montmorillonite (Darby, 1971). These cores were from the Canada Plain, Alpha Ridge (west), and Mendeleyev Ridge; and these percentages held regardless of sediment color.

The area of least variable conductivity was the NW Canada Plain (Area E, Figure 9). It lies between the Chuckchi Cap and the Alpha Ridge. A large portion of this plain is extremely flat. Twenty-nine cores (F-229 - F-266) were recovered over an area of approximately 1736 km^2 from an average depth of 3809 metres (line depth). The standard deviation of depth was 16 metres. The mean conductivity value for 688 core sections was 2.40 mcal/cm sec °C (Figure 8). Campbell (1973) correlated a fine grained, plane-laminated turbidite in the cores from this area. It overlaid a 1-10 mm thick brown foraminiferal lutite which averaged 6.34 cm below the sediment-water boundary. None of the k values are identified with this shallow turbidite. Only 2.5% of the cored sediment in this area was identified as turbidite. Figure 10 plots conductivity against depth and suggests that a larger number of the higher conductivities are concentrated close to the depths of about 1 metre and 3.4 metres. The same data was averaged over 30 cm depth increments. The standard deviation was then plotted as a horizontal line with midpoint at the mean conductivity value (Figure 11). The reason for the larger conductivities is not known, but possibly they are associated with a slightly different mineral assemblage and/or a different grain size distribution which is not associated with turbidity currents.

A typical plot of conductivity, moisture content and coarse fraction with depth for a single core in this area is shown in Figure 12.

Turbidites were found more frequently in cores from other portions of the Canada Plain where 27% of the cored sediment was turbidite (Campbell, 1973). Although some well-sorted fine-grained sands were found in these areas, most of the turbidity current deposits were classified as silts and sandy silts (Campbell, 1973). Campbell showed that the average mineral composition of the sand fraction of 19 turbidites from the Canada Plain was 54% quartz, 13% chert and 11.4% detrital calcite. Also the Canada Plain turbidites tested were composed of large weight percentages of silt-sized particles with large weight percentage variations of sand and small percentage variations of clay. The larger variation of conductivity in the northern and southern parts of the Canada Plain compared with the NW Canada Plain is seen from their histograms and depth distribution plots (Figures 13 & 14). Detailed data for thermal conductivity, moisture content, coarse fraction of grain size and turbidites were not always made on the same cores. Such data was available for core F-31 shown in Figure 15. The different properties were not measured at exactly the same depths which accounts for some offset at correlation depths. The two turbidites identified in F-31 are associated with increased k-values. The highest k-value is a reflection of the low moisture content just above the two-metre depth. It is interesting to note that conductivity values of 3.35 and 3.86 mcal/cm sec °C were found in the turbidite at about 1.2 meters even though the moisture content was more than 50%.

Cores F-196, 197, 207, 208 were from the Mendeleyev Plain. Figure 6 displays the histogram of conductivity values. The mean conductivity value is close to that for the north Canada Plain with a standard deviation of about 12%. Section averages of several physical properties for core F-207 on the Mendeleyev Plain are plotted in Figure 16. The bed of coarser sediments at about 1.4 meters registers increases of all plotted parameters. Here is another instance where a change in moisture content correlated positively with increases of conductivity and percent coarse grains. The coarse fraction included 20% detrital carbonates and 40% Foraminifera (Hoffman, 1972). This was one of the few cores tested that had such a high percent of Foraminifera.

Histograms of the thermal conductivity values for the different undersea ridges mentioned are presented in Figures 5 to 6. Figure 17 plots individual conductivity versus depth data for the Mendeleyev Ridge. Of the three ridges, the Mendeleyev Ridge had the least standard deviation from the mean k-value; about 8% compared to approximately 12% for the other two. It also had the lowest mean conductivity, 2.52 mcal/cm sec °C. This was almost identical to the value for the Canada Plain South, although the ridge had a standard deviation more than twice as large. The conductivity values for the Mendeleyev Ridge included data from stations F-110, 156, 165, 193, and 198 from which no heat-flow values were obtained.

The mean conductivity value increased from the 2.52 mcal/cm sec °C for over 1,000 section mean values for the Mendeleyev Ridge to 2.77 mcal/cm sec °C for over 3,900 section means from the west Alpha Ridge

to 3.10 mcal/cm sec °C for over 500 section mean values for the east Alpha Ridge. Darby (1971) identified 7 significant carbonate layers from cores peripheral to the Canada Plain. Nearly all carbonate peaks were related to an increase in coarse material. He found that Foraminifera (which constitute 99% of the carbonate secreting organisms in Arctic sediment) do not contribute significantly to the carbonate peaks and that in the detrital material dolomite was three to five times as abundant as calcite. Hoffman (1972) studied pink layers from 32 of the cores from the margins of the Canada Plain. With only two exceptions, these pink layers were associated with beds of coarse (greater than 62 microns) sediment; the average being sediment with 22% (by weight) coarse material. The coarse fractions averaged 27% quartz, 44.5% carbonate, 11.4% Foraminifera. He also found non-pink beds of similar grain size distributions whose coarse fractions averaged 49.5% quartz, 22.5% carbonate, and 12.6% Foraminifera. Data from core F-116 from the Mendeleyev Ridge (Figure 18) demonstrates the relationship of one pink layer with other physical properties. The data plotted are section mean values. A single k-test at the depth of the pink layer measured 4.3 mcal/cm sec °C.

Section mean values for thermal conductivity, percent water, coarse fraction, and percent carbonate are plotted with depth for F-221 in Figure 19. The remainder of such plots (Figure 20 to 32) present individual values with depth, for more detail. F-216, 221, and 223 were peripheral cores from the north Chuckchi Cap. F-557 and F-559 were taken from the east Alpha Ridge. The remainder of the plots of individual tests are from cores from the west Alpha Ridge. In general,

the percent moisture correlated negatively with conductivity, and the coarse percent and percent carbonate correlated positively with conductivity. These correlations offered no surprise, but some of the values did, i.e., at a depth of about 0.4 metres in core F-322 the thermal conductivity value was 5.31 mcal/cm sec °C even though the water content was almost 30%. The reason is probably the high carbonate content at this depth along with the moderate percent of coarse material. Another exceptional core was F-533. Even though a large amount of coarse material was present (apparently volcanic) the conductivities between 2-3 metres were controlled by the extremely high moisture content.

The two most unusual cores obtained were F-422 and F-437. The mean conductivity of F-422 from 0.08 metre depth to the bottom of the core was 1.57 mcal/cm sec °C. Core F-437, from 0.4 metres to the end of the core at 2.8 metres, had a mean conductivity value of 1.52 mcal/cm sec °C. Because of their uniqueness compared to our other Arctic cores, they were shipped immediately to University of Wisconsin. Their real value was reported by Ling and Clark (1973).

All available data were used to plot different combinations of thermal conductivity, moisture content and percent coarse. Figure 33 graphs thermal conductivity and percent water; 1,740 core section mean values are plotted. The resultant equation for conductivity is $K = (125 + 6.59\ w)^{-1}$. We do not use this to estimate conductivities of Arctic sediments from moisture content, but it is presented here as a comparison to Bullard and Day's (1961) equation of $K = (161 + 6.51\ w)^{-1}$

which is often used for estimates of k in other oceans. The Arctic values for water content greater than 65% came from cores F-422, 437, and 533. Data from these cores are treated separately in Figures 34 and 35. In the first of these, 1,825 core sections values show the relation of conductivity and percent coarse. The lower line represents data for k greater than 1.9 mcal/cm sec °C. The next graph (Figure 35) displays 1,810 section values relating water content to percent coarse. The upper line was determined from data where the percent water is greater than 65%.

HEAT FLOW

Values of heat flow for each successful station are listed in Table 2. Mean heat-flow values for different areas in the Amerasia Basin are shown in Table 3, and some are presented graphically in the histograms of Figures 36 to 39. None of the mean values could be considered high, in fact, those from the larger geographic divisions (upper table) range only from 1.19 HFU for the Mendeleyev Ridge to 1.70 HFU from the east Alpha Ridge. The highest individual value was 2.86 HFU measured at station F-389 on the west Alpha Ridge. Four nearby values varied from 1.20 - 1.26 HFU indicating that the high heat-flow value must reflect a minor local condition. On the southwest base of Crary Seamount, F-278 had a value of 2.00 HFU among three other values measuring from 1.25 - 1.28 HFU. This higher heat flow is probably also a local anomaly since the remaining five values are not rejected from normality by the Kolmogorov-Smirnov statistic (Lilliefors, 1967). Only four other individual values equaled or exceeded 2.00 HFU; these were all found on the east Alpha Ridge and ranged from 2.19 - 2.37 HFU. They were in the province of highest mean heat flow.

The 29 values listed from the northwest Canada Plain (area E) are from a very flat portion of that area and provide the most reliable mean value of any area, with a standard error of 0.4%. The cores obtained full penetration into the sediments at all these stations,

permitting a comparison of temperatures at specific depths over the area. The sub-bottom depths compared were: 0.0 cm, 66.0 cm, 167.6 cm, 268.0 cm and 368.3 cm. The largest standard deviation was 0.0085 °C at 66.0 cm. A regression line calculated from these points had a correlation coefficient of 0.89 and indicated the temperature gradient was 69.7 °C/km. It was from these cores that Campbell (1973) suggested an average sedimentation rate of 83 mm/1000 years, dependent on a correlation with cores described by Hunkins and Kutschale (1967).

The data from each physiographic province and each sub-area listed in table 3 were tested for normal distribution by means of the Kolmogorov-Smirnov statistic (K-S statistic). The Alpha Ridge and west Alpha Ridge data were rejected; however, when the high heat-flow value from F-389 was excluded, the west Alpha Ridge data was not rejected. Data from some of the other areas are plotted with their confidence level curves in Figures 43 to 57. The depth boundaries used for the Alpha Ridge and Mendeleyev Ridge were 3450 meters and 3100 meters respectively. These and other boundary restrictions excluded 25 heat-flow values from the analyses in the upper part of the table. Essentially, all those remaining were from areas close to the boundaries between abyssal plains and ridges or escarpments.

The data were further divided into populations suggested by their areal distribution. Detailed bathymetry maps from Hall (1970) are used in Figures 40 to 42 to view some of those heat-flow data more closely. Areas are identified by letter, heat-flow values by numbers in HFU, and the numbers in parenthesis are the number of values per area.

Twelve heat-flow values were obtained at the north Chukchi Rise - Canada Plain boundary. The 10 values from depths below 3450 m at area D had a mean of 1.39 HFU. Data from only three of the sub-areas, with four or more values, were rejected from being normal populations--areas M, C, and S. Areas C and M were not rejected when the highest value from each area was not used. The values in areas D, F, and G were all at depths below 3450 m. The mean heat-flow values for each of these three areas, area LR (depths 2280 - 3300 m), area N (2500 - 2700 m), and the single value for F-89 (3799 m) were very close to 1.41 HFU.

All heat-flow values from areas K, L, Q, R, S, and T were combined to produce a mean value of 1.15 HFU. When values from areas M and N were included, the mean was 1.19 HFU. In either case, a normal population was suggested by the K-S statistic and the mean heat-flow value was very close to that for the Mendeleyev Ridge. Area L was where Hall (1970) found hyperbolic echoes which he interpreted as buried linear sediment ridges.

Between 90° - 120° west longitude on the Alpha Ridge, areas P, V and W individually had mean heat-flow values from 1.30 - 1.32 HFU and collectively had a mean of 1.31 HFU with 0.04 standard error for the 28 values. Area Z includes stations F-537 and F-538 which were less than 7 km apart. The heat-flow values were 0.73 HFU and 0.82 HFU. They were considered reliable, but their significance is not known because of the sparse data. Excluding areas Z, C, and H, the mean heat-flow

values for groups of areas increased eastward: 1.19 HFU (areas K, L, M, N, Q, R, S, T), 1.31 HFU (area V, P, W), and 1.70 HFU (east Alpha).

Hall (1970) suggested a particular fracture pattern for parts of the Alpha and Mendeleyev Ridges and located what he thought to be the dislocated axes of an old spreading center. Using those suggested axes, 272 heat-flow values were plotted against distance from the spreading center (Figure 58). This was possible for data as far east as area V. The regression line indicates an increase of 0.0011 HFU/km with distance from the ridge crest, which is at least compatible with the idea that the Alpha Ridge is an extinct spreading center. A plot of heat flow versus water depth (Figure 59) shows essentially no correlation.

The USSR have obtained heat-flow data from the Arctic. Most of their stations were west of the 180° meridian, but one value of 1.80 HFU was reported at 86° 03' N latitude and 115° 20' W longitude. This is about 34 km NE of area S. While this single value is significantly higher than the mean value of 1.11 HFU for area S, it is consistent with the variability of individual values found on the Alpha Ridge.

Ocean temperatures

Five temperature profiles to the ocean bottom were obtained as part of some early heat-flow casts. In 1968, separate casts for ocean temperatures were added to the field program, and 75 more profiles were acquired. The temperature range was set at the surface and was not adjustable during the test, so only the gross temperature structure was visible. The first two of the separate profiles and the five early profiles were over the Canada Plain; the remainder were over the Alpha Ridge. Table 4 lists locations for the various water profiles, and the two detailed sediment temperature tests. The profiles were divided into groups suggested by the data and identified in Figure 60. Mean values at the measured depths were obtained for each group and plotted on the same figure. No distinctive relation is presented by the grouped data in the upper 400 metres. In this depth interval, group three has the coldest temperatures at every depth but one. Below 400 metres, this group has the coldest profile to its depth of 2000 m. Group three consists of six profiles SE of Hall Seamount at area "v," but nothing unique or specially unusual is known about the area. Profiles below 400 metres for the remaining three groups become progressively colder eastward. This means that the thickness of the Atlantic water layer decreases slightly eastward. For group one the Atlantic layer lies approximately between 300-940 metres, and for group four its limits are approximately 280-780 metres. These are consistent with the limits

of 200-900 metres reported by Coachman and Aagaard (1974). Some reduction in Atlantic water thickness from heat losses is expected, especially by the time this water has circulated as far as the area north of Ellesmere Island. (The residence time of the Atlantic water is approximately 10 years.) The temperature of group four at 500 metres is 0.328°C.

A few attempts were made to obtain more detailed temperature data from the bottom 100 metres of ocean water. The narrower temperature range used meant the recording instrument was off scale except for depths near the bottom. The procedure was to lower the pressurized recording system with one external thermistor to the ocean bottom, obtain a 5-10 minute reading and then, raising it, take similar readings one metre apart to ten metres and then at ten-metre intervals to 100 metres. Nine of the twelve attempts were usable, and plots for these are shown in Figures 61 to 69. No time series was attempted. Profiles three and four were taken approximately 19 km apart at comparable depths, and with a 13-day interval of time. Their bottom temperatures are essentially equal (-0.273 °C and -0.274°C), but number three has a greater temperature decrease one metre from the bottom. The least-square temperature gradient for profile three is 0.087 °C/km. The gradient for number four (10-70 metres) is 0.094 °C/km. At this depth the adiabatic gradient is approximately 0.084 °C/km. The suggestion from the profile of a small transient temperature change in the bottom water is supported by the temperature records of some nearby

heat-flow casts. FL 379, 380, 382, 383, and 384 each indicate a temperature reduction of from 0.010 to 0.015 °C of the water at the water-sediment boundary. The mean change was 0.011 °C. At these particular heat-flow stations a partial pull-out of the corer was attempted to obtain more sediment temperatures. Using a step change of temperature and assuming a 0.003 °C change of temperature to be significant and detectable, the 20-50 cm depths yielding these changes indicate they occurred roughly 10-60 days before the sediment measurements.

These bottom-temperature profiles clearly suggest superadiabatic temperature gradients near the bottom, probable small scale convection and micro "thermals" (Bodvarsson, 19__).

The results of the two successful detailed sediment temperature probes are plotted in Figure 70 and 71. They indicate near-surface steady-state conditions at the two localities. The small differences in temperature gradient probably reflect minor thermal conductivity changes.

Note added by C. Ruppel in February 2019: The figures that should be numbered 70 and 71 (originally referred to as 69 and 70) are missing from the version of the report that the USGS has. They are also missing from other known copies of the report.

REFERENCES

REFERENCES

References were typed, DOI added, and some corrections made by Carolyn Ruppel in 2019.

BEAL, M. A. et. al., The floor of the Arctic Ocean: Geographic Names, ARCTIC, 19 (3), 215-219, 1966.

Beal, M.A., Edvalson, F., Hunkins, K., Molloy, A, and N. Ostenso, The floor of the Arctic Ocean: Geographic Names, Arctic, 19(3), 215-219, 1966, https://doi.org/10.14430/arctic3430.

BODVARSSON, GUNNAR, Heat Transfer and Temperature Microstructure at the Ocean Floor, JÖKULL

Bodvarsson , G., Heat transfer and temperature microstructure at the ocean floor, Jokull, 16(3), 175-183, 1966.

BULLARD, E.C., and A. DAY, The flow of heat through the floor of the Atlantic Ocean, GEOPHYS. J., 4 (SPEC. SUPL.), 282-292, 1961

Bullard, E.C. and A. Day, The flow of heat through the floor of the Atlantic Ocean, Geophysical Journal Int., 4, Issue Supplement 1, 282–292, 1961, https://doi.org/10.1111/j.1365-246X.1961.tb06820.x

CAMPBELL, JOHN S., Pleistocene Turbidites of the Canada Abyssal Plain, Arctic Ocean, TECH. REPORT: CLARKE (13), MASTER'S THESIS, UNIVERSITY OF WISCONSIN, 1973

Campbell, J.S., Pleistocene turbidites of the Canada abyssal plain, Arctic Ocean, M.S. thesis, University of Wisconsin, 1973.

COACHMAN, L.K., and K. AAGAARD, Physical oceanography of Arctic and subarctic seas, in Marine geology and oceanography of the Arctic seas, edited by Yvonne Herman, pp 1-72, Springer-Verlag, New York, 1974

Coachman L.K. and K. Aagaard, Physical Oceanography of Arctic and Subarctic Seas. In: Herman Y. (eds) Marine Geology and Oceanography of the Arctic Seas, pp. 1-72, Springer-Verlag, New York, 1974, https://doi.org/10.1007/978-3-642-87411-6_1

CRARY, A. P., Arctic ice island and ice shelf studies, in Geophysical research papers, No. 63, pp 1-37, AFCRC-TR-57-232 (3), 1960.

Refer to:

Crary, A.P., Arctic Ice Island and Ice Shelf Studies: Part I. Arctic, 11(1), 2-42, 1958, https://doi.org/10.14430/arctic3731.

Crary, A.P., Arctic Ice Island and Ice Shelf Studies: Part II. Arctic, 13(1), 32-50, 1960, https://doi.org/10.14430/arctic3687.

Darby, Dennis A., Carbonate cycles and clay mineralogy of Arctic Ocean sediment cores, unpublished PhD thesis, University of Wisconsin, 1971.

Darby, D.A., Carbonate cycles and clay mineralogy of Arctic Ocean sediment cores, Ph.D. thesis, University of Wisconsin, 1971.

HALL, John K., Arctic Ocean geophysical studies: the Alpha cordillera and Mendeleyev Ridge, unpublished PhD thesis, Columbia University, 1970

Hall, J.K., Arctic Ocean geophysical studies: the Alpha Cordillera and Mendeleyev Ridge, Ph.D. thesis, Columbia University, 1970.

HOFFMAN, Thomas F., The origin and stratigraphic significance of pink layers in late Cenozoic sediments of the Arctic Ocean, Tech. Report: Clark (11), Master's thesis, University of Wisconsin, 1972

Hoffman, T.F., The origin an stratigraphic significance of pink layers in late Cenozoic sediments of the Arctic Ocean, M.S. thesis, University of Wisconsin, 1972.

Hunkins, Kenneth and Henry Kutschale, Quaternary sedimentation in the Arctic Ocean, in Sears, M., ed., Progress in Oceanogr., v. 4: Pergamon Press Ltd., London, p 89-94, 1967

See:
Hunkins, K. and H. Kutschale, Quaternary sedimentation in the Arctic Ocean, Progress in Oceanography, 4, 89-94, 1965, https://doi.org/10.1016/0079-6611(65)90042-X.

Lachenbruch, A. H. & B. V. Marshall, Heat flow through the Arctic Ocean floor: the Canada Basin - Alpha Rise boundary, J. Geophys. Res., 71(4), 1223-1248, 1966

Lachenbruch, A. H., and B. V. Marshall, Heat flow through the Arctic Ocean floor: The Canada Basin - Alpha Rise Boundary, J. Geophys. Res., 71(4), 1223–1248, 1966, doi:10.1029/JZ071i004p01223.

Lilliefors, Hubert W., On the Kolmogorov-Smirnov test for normality with mean variance unknown, J. Am. Stat. Assoc., v. 62, pp 399-402, 1967

Lilliefors, H.W., On theh Kolmogorov-Smirnov test for normality with mean variance unknown, J. Amer. Statistical Assoc., 62(318), 399-402, 1967, doi: 10.2307/2283970

Ling, H.Y., L.M. McPherson, and D.C. Clark, Late Cretaceous (Maestrichtian?) Silicoflagellates from the Alpha Cordillera of the Arctic Ocean, Science, vol 180, pp 1360-1361, 29 June, 1973.

Ling, H.Y., McPherson, L.M., and D.L. Clark, Late Cretaceous (Maestrichtian?) silicoflagellates from the Alpha Cordillera of the Arctic Ocean, Science, 180, 1360-1361, 1973, doi: 10.1126/science.180.4093.1360.

Marshall, W. E., Structure and stratigraphy of T-3 and the Ellesmere Ice Shelf, in Geophysical Research Papers, no. 63, pp 45-5 AFCRC-TR-59-232(3), 1960

Marshall, E.W., Structure and stratigraphy of T-3 and the Ellesmere ice shelf, in: Bushnell, V.C. (eds.), Scientific Studies at Fletcher's ice island T-3 (1952-1955), Geophys. Res. Paper 6, vol. 3, 45-57, Geophysics Research Directorate, Air Force Cambridge Research Laboratory, 1960.

RATCLIFFE, E. H., thermal conductivities of fused and crystalline quartz, Brit. J. Appl. Phys. 10, 22-25, 1959

Ratcliffe, E.H., Thermal conductivities of fused and crystalline quartz, Brit. J. Applied Phys., 10(1), 22-25, 1959.

Stoiber, R. E., et al, Petrographic evidence on the source area and age of T-3, in Geophysical Research Papers, no. 63, pp 58-72 AFCRC-TR-59-232(3), 1960

Stoiber, R.E., Lyons, J.B., Elbertz, W.T., and R.H. McCrehon, Petrographic evidence on the source area and age of T-3. In: Bushnell, V. (ed.), Scientific Studies of Fletcher's Ice Island, T-3 (1952-1955), vol. 3., Air Force Cambridge Research Center.

VON HERZEN, R. P., and A. E. MAXWELL, the measurement of thermal conductivity of deep-sea sediments by a needle-probe method, J. Geophys. Res., 64(10), 1557-1563, 1959

Von Herzen, R., and A. E. Maxwell, The measurement of thermal conductivity of deep - sea sediments by a needle - probe method, J. Geophys. Res., 64(10), 1557–1563, 1959, doi:10.1029/JZ064i010p01557.

TABLE 1. Radioactive heat generation for selected early T-3 cores. This table and associated metadata are available in digital form in: Ruppel, C.D., Hutchinson, D.H., Lachenbruch, A.H., and Hall, J.K., 2019, Thermal Data and Navigation for T-3 (Fletcher's) Ice Island Arctic Ocean Heat Flow Studies, 1963-1973: U.S. Geological Survey data release, https://doi.org/10.5066/P97EPU2F.

RADIO-ACTIVE HEAT GENERATION (H) OF SELECTED EARLY CORES
H (MASS UNITS = MICRO-CALORIES/GRAM YEAR

FL- 1	82-30N	156-26W	3747METERS	H(MASS UNITS)= 6.57	
FL- 2	82-12N	156-36W	3742METERS	H(MASS UNITS)= 6.60	
FL- 3	82-32N	156-54W	3741METERS	H(MASS UNITS)= 6.78	
FL- 6	82-43N	158-00W	3740METERS	H(MASS UNITS)= 6.73	
FL- 7	82-44N	158-14W	3742METERS	H(MASS UNITS)= 6.73	NO H.F.
FL- 8	82-40N	157-33W	3742METERS	H(MASS UNITS)= 6.70	
FL- 9	82-46N	157-05W	3743METERS	H(MASS UNITS)= 6.67	
FL- 10	82-57N	155-47W	3507METERS	H(MASS UNITS)= 4.49	
FL- 12	83-05N	155-51W	3473METERS	H(MASS UNITS)= 4.24	
FL- 13	83-08N	156-50W	3577METERS	H(MASS UNITS)= 4.58	
FL- 14	83-08N	157-11W	3216METERS	H(MASS UNITS)= 4.02	
FL- 15	83-00N	158-18W	3137METERS	H(MASS UNITS)= 4.18	
FL- 21	83-03N	163-31W	3494METERS	H(MASS UNITS)= 5.19	
FL- 22	82-54N	163-18W	3750METERS	H(MASS UNITS)= 6.45	
FL- 23	82-41N	163-18W	3748METERS	H(MASS UNITS)= 6.47	
FL- 24	82-23N	162-03W	3743METERS	H(MASS UNITS)= 6.54	
FL- 27	80-47N	140-25W	3706METERS	H(MASS UNITS)= 5.99	
FL- 30	80-30N	139-45W	3706METERS	H(MASS UNITS)= 5.76	
FL- 35	80-46N	136-49W	3680METERS	H(MASS UNITS)= 5.56	
FL- 38	80-36N	137-41W	3686METERS	H(MASS UNITS)= 5.85	
FL- 47	80-42N	135-09W	3645METERS	H(MASS UNITS)= 5.84	
FL- 53	80-32N	136-49W	3671METERS	H(MASS UNITS)= 5.93	
FL- 66	75-28N	141-14W	3700METERS	H(MASS UNITS)= 6.21	
FL- 74	75-50N	139-13W	3685METERS	H(MASS UNITS)= 5.98	
FL- 78	75-22N	140-10W	3678METERS	H(MASS UNITS)= 6.04	
FL- 84	75-23N	156-08W	2212METERS	H(MASS UNITS)= 8.46	NO H.F.
FL- 88	75-54N	152-23W	3782METERS	H(MASS UNITS)= 6.48	
FL- 93	77-48N	175-25W	1564METERS	H(MASS UNITS)= 4.52	
FL-101	77-40N	174-20W	2072METERS	H(MASS UNITS)= 5.63	NO H.F.
FL-112	77-57N	173-41W	1743METERS	H(MASS UNITS)= 5.61	NO H.F.
FL-126	78-22N	175-53W	1178METERS	H(MASS UNITS)= 4.48	
FL-183	79-18N	175-06W	2213METERS	H(MASS UNITS)= 4.80	NO H.F.
FL-194	80-11N	174-01W	2209METERS	H(MASS UNITS)= 4.63	
FL-217	80-36N	157-59W	3712METERS	H(MASS UNITS)= 4.23	
FL-222	80-29N	159-13W	3630METERS	H(MASS UNITS)= 3.89	
FL-228	80-49N	158-49W	3632METERS	H(MASS UNITS)= 3.91	NO H.F.
FL-271	83-11N	153-54W	3523METERS	H(MASS UNITS)= 4.18	
FL-274	83-14N	153-04W	2745METERS	H(MASS UNITS)= 4.47	
FL-280	83-52N	148-23W	2639METERS	H(MASS UNITS)= 4.42	NO H.F.

TABLE 1

TABLE 2. Heat flow data. This table and associated metadata are available in digital form in: Ruppel, C.D., Hutchinson, D.H., Lachenbruch, A.H., and Hall, J.K., 2019, Thermal Data and Navigation for T-3 (Fletcher's) Ice Island Arctic Ocean Heat Flow Studies, 1963-1973: U.S. Geological Survey data release, https://doi.org/10.5066/P97EPU2F.

STA	LAT	LONG	(M) DEPTH	GRADIENT 1-2	2-3	3-4	4-5	<K> 1-2	2-3	3-4	4-5	Q(HEAT FLOW) 1-2	2-3	3-4	4-5	Q	AVE % DEV	MAX DEV
F 2	82 11.81	156 55.50	3742	69.0	66.2			2.06	2.17			1.42	1.44			1.43	.69	.02
F 3	82 31.81	156 54.04	3741	68.0	67.9	66.5		2.28	2.20	2.23		1.55	1.49	1.49		1.51	1.76	.05
F 6	82 42.66	157 59.77	3740	62.6	62.7			2.17	2.14			1.36	1.34			1.35	.74	.02
F 8	82 39.50	157 33.24	3742	66.5	67.3	65.1		2.24	2.26	2.20		1.49	1.52	1.44		1.48	1.94	.07
F 9	82 45.45	157 04.58	3743	64.3	63.2	62.6		2.16	2.27	2.17		1.39	1.43	1.36		1.39	1.75	.07
F 10	82 56.73	155 46.83	3507	47.1	49.5	51.6		2.78	2.92	2.67		1.31	1.45	1.38		1.38	3.38	.14
F 11	82 59.78	155 56.92	3520	52.5	55.5			2.74	2.61			1.40	1.45			1.42	1.75	.05
F 12	83 04.80	155 51.22	3473	53.9	56.7			2.85	2.68			1.54	1.52			1.53	.65	.02
F 13	83 07.87	156 50.04	3577	56.5	52.7			2.67	2.55			1.51	1.35			1.43	5.59	.15
F 14	83 07.72	157 11.04	3216	38.5	39.9			2.44	2.95			.94	1.18			1.06	11.32	.23
F 15	82 59.51	158 17.57	3137	30.0	29.7	30.1		2.77	2.62	2.69		.83	.78	.81		.80	2.20	.04
F 16	83 01.09	158 54.48	2247	37.7	30.0			2.77	2.80			1.04	.84			.94	10.63	.19
F 17	82 58.69	159 06.88	2215	32.5	26.8				2.65				.71			.71		
F 19	83 03.43	162 49.13	3417	37.6	45.2	49.4		2.42	2.53	2.42		.91	1.15	1.20		1.08	10.83	.28
F 21	83 02.70	163 30.76	3494	47.3	46.0	50.2		2.63	2.68	2.68		1.25	1.23	1.34		1.27	3.49	.10
F 22	82 53.81	163 18.16	3750	69.7	63.7	66.5		2.31	2.17	2.20		1.61	1.38	1.46		1.48	5.69	.22
F 23	82 40.69	163 18.09	3748	72.2	62.1	68.7		2.21	2.12	2.19		1.59	1.32	1.50		1.47	6.80	.27
F 24	82 22.47	162 03.31	3743	53.2	57.6	60.7		2.97	2.32	2.40		1.58	1.34	1.45		1.45	5.64	.23
F 25	82 26.94	160 36.77	3750	66.1	61.3	62.1		1.94	2.24	2.13		1.28	1.37	1.33		1.32	2.34	.09
F 26	80 48.26	140 29.77	3707	56.6	48.8	55.0		2.42	2.67	2.53		1.37	1.30	1.39	5.99	1.35	2.62	.09
F 27	80 47.04	140 24.81	3706	59.9	50.9	55.1		2.31	2.81	2.50		1.38	1.43	1.38	5.99	1.39	1.59	.05
F 28	80 47.75	140 22.41	3705	54.3	47.6	55.1		2.39	2.46	2.51		1.30	1.17	1.39	5.99	1.28	6.04	.21
F 29	80 29.50	139 50.66	3706	56.6	52.0	57.4		2.38	2.64	2.23		1.35	1.37	1.28	5.76	1.33	2.66	.09
F 30	80 29.87	139 45.39	3706	59.9	53.1			2.38	2.60			1.43	1.38		5.76	1.40	1.77	.05
F 31	80 32.43	139 55.64	3709	55.5	52.0			2.43	2.60			1.35	1.35		5.76	1.35		
F 35	80 46.05	136 48.95	3680	51.0	42.9			2.43	2.82			1.24	1.21		5.56	1.22	1.22	.03
F 38	80 35.85	137 40.62	3686		48.7	55.5			2.68	2.41			1.30	1.34	5.85	1.32	1.51	.04
F 43	80 32.42	134 24.22	3629		47.0	46.0			2.66	2.88			1.25	1.33	5.84	1.29	3.10	.07
F 46	80 33.17	134 20.91	3620		46.9	52.0				2.63				1.37	5.84	1.37		
F 47	80 41.45	135 09.12	3645	46.3	49.3			2.79	2.86			1.29	1.41		5.84	1.35	4.44	.12
F 48	80 37.30	135 59.10	3660	39.1	47.1				2.67				1.26		5.84	1.26		
F 49	80 35.05	136 08.38	3658	50.1	46.5	53.3		2.62	2.93	2.96		1.31	1.36	1.55	5.84	1.40	6.79	.23
F 50	80 31.95	135 42.35	3655	36.5	46.7	52.5			2.93	2.71			1.37	1.42	5.84	1.39	1.79	.05
F 51	80 32.93	135 36.99	3658	54.8	44.4	50.2		2.87	2.90	2.80		1.57	1.29	1.41	5.93	1.42	6.86	.28
F 52	80 40.61	136 18.24	3667	47.4	50.5			2.49	2.79			1.18	1.41		5.93	1.29	8.88	.22
F 53	80 32.30	136 48.62	3671		42.9	49.7			2.68	2.35			1.15	1.17	5.93	1.16	.86	.02
F 55	76 35.20	138 01.87	3602	37.0	52.2				2.36				1.23		6.21	1.23		
F 56	76 35.70	138 06.34	3609	61.4	57.5			2.55	2.39			1.57	1.37		6.21	1.47	6.80	.19
F 57	76 38.46	138 18.74	3613	54.7	64.7			2.56	2.14			1.40	1.38		6.21	1.39	.71	.02
F 63	76 12.85	142 02.92	3698	40.5				3.40				1.38			6.21	1.38		
F 65	75 33.09	141 44.20	3706		63.8	61.1			2.28	2.27			1.45	1.39	6.21	1.42	2.11	.06
F 66	75 28.24	141 14.10	3700	74.5	65.3	57.5		2.02	2.22	2.42		1.50	1.45	1.39	6.21	1.44	2.61	.11

1.32 ± 0.07

1.32 ± 0.12

TABLE (2) SUMMARY OF DATA FOR SUCCESSFUL HEAT FLOW STATIONS (SEPT '75)

STA	LAT	LONG	(M) DEPTH	GRADIENT 1-2	2-3	3-4	4-5	<K> 1-2	2-3	3-4	4-5	Q(HEAT FLOW) 1-2	2-3	3-4	4-5	$\bar{Q}$	AVE % DEV	MAX DEV
F 71	75 43.48	140 37.00	3706	31.2				2.94				.91			5.96	.91		
F 74	75 49.57	139 12.98	3685		34.7	41.8			2.34	2.46			.81	1.03	5.98	.92	11.95	.21
F 75	75 52.59	139 03.24	3675	41.9				3.21				1.35			5.98	1.35		
F 76	75 32.74	139 22.82	3665	46.2	43.4			2.50	2.58			1.15	1.12		6.02	1.13	1.32	.03
F 78	75 22.26	140 10.31	3678	57.1	44.9			2.43	2.51			1.39	1.12		6.04	1.25	10.75	.27
F 79	75 23.20	140 15.30	3678	47.3	54.5			2.34	2.31			1.10	1.26		6.04	1.18	6.77	.15
F 89	75 38.45	151 08.53	3799		63.8	67.9			2.23	2.18			1.42	1.48	6.48	1.45	2.06	.06
F 92	77 37.76	174 43.90	2075			52.0				2.32				1.21		1.21		
F 93	77 48.00	175 25.41	1564		48.1	43.9			2.46	2.57			1.18	1.13		1.15	2.16	.05
F 94	77 53.03	175 51.67	1608	45.9	45.4	40.6		2.42	2.38	2.30		1.11	1.08	.93		1.04	7.05	.17
F 95	78 02.21	176 17.79	1348		50.9	48.3			2.69	2.58			1.37	1.25		1.31	4.58	.11
F103	77 37.59	173 47.26	1874		36.7	38.7			2.31	2.35			.85	.91		.88	3.40	.05
F104	77 36.52	173 46.10	1845		37.6	37.6			2.53	2.47			.95	.93		.94	1.06	.02
F106	77 38.04	173 43.74	1853	47.5	45.3	49.2		2.45	2.48	2.34		1.17	1.12	1.15		1.14	1.55	.05
F107	77 37.68	173 42.56	1870	46.8	44.0	46.2		2.51	2.48	2.33		1.17	1.09	1.08		1.11	3.39	.09
F108	77 42.25	173 20.80	2094	53.9	42.3	63.2		2.68	2.58	2.38		1.44	1.09	1.51		1.34	12.70	.41
F111	77 52.64	173 10.97	2023	56.2	44.7	50.6		2.39	2.41	2.39		1.34	1.08	1.21		1.21	7.16	.26
F113	78 00.06	174 06.70	1677	48.9	65.8	54.1		2.41	2.43	2.45		1.18	1.60	1.32		1.36	11.38	.41
F115	78 04.14	174 49.64	1500		51.4	50.6			2.83	2.43			1.45	1.23		1.34	8.20	.21
F116	78 05.38	174 48.53	1567			65.5				2.45				1.60		1.60		
F117	78 07.09	174 53.94	1331	40.8	48.9	38.0		2.50	2.56	2.57		1.02	1.25	.98		1.08	10.25	.27
F118	78 07.58	174 57.84	1345		53.3	43.6			2.56	2.34			1.37	1.02		1.19	14.64	.35
F119	78 06.67	174 49.80	1359	42.0	41.4			2.78	2.44			1.15	1.01			1.08	6.48	.14
F120	78 05.27	174 27.29	1845	50.1	53.5			2.52	2.41	2.41		1.26	1.29			1.27	1.17	.03
F122	78 08.03	174 22.87	1834		45.2	45.0			2.37	2.42			1.07	1.09		1.08	.92	.02
F123	78 10.21	174 30.23	1760		52.2	55.1			2.42	2.41			1.26	1.33		1.29	2.70	.07
F124	78 13.50	174 42.17	1513		47.4	40.0				2.36				.94		.94		
F125	78 15.22	175 23.44	1285		52.0	38.5			2.75	2.73			1.43	1.05		1.24	15.32	.38
F126	78 21.75	175 52.65	1178		48.7	46.0			2.72	2.45			1.32	1.13		1.22	7.75	.18
F128	78 33.07	175 54.76	1576	47.5	43.8	37.9		2.50	2.49	2.47		1.19	1.09	.94		1.07	8.28	.24
F129	78 33.69	175 55.80	1450		44.9	46.2			2.53	2.39			1.14	1.11		1.12	1.33	.03
F130	78 33.00	176 04.54	1291		39.9	45.5			2.88	2.63			1.15	1.20		1.17	2.12	.05
F131	78 32.24	176 14.36	1197		41.8	54.7			2.53	2.52			1.06	1.38		1.22	13.11	.32
F132	78 30.04	176 16.98	1196		41.8	68.3			2.65	2.51			1.11	1.71		1.41	21.27	.60
F134	78 30.28	176 07.37	1213		44.0	61.1			2.43	2.34			1.07	1.43		1.25	14.40	.36
F135	78 32.28	176 17.96	1378		47.8				2.46				1.17			1.17		
F136	78 33.27	176 26.01	1378		46.9	44.9			2.50	2.40			1.17	1.08		1.12	4.00	.09
F137	78 36.51	176 31.54	1362		40.3	57.2			2.38	2.39			.96	1.37		1.16	17.59	.40
F138	78 36.53	176 24.03	1357		44.8	46.9			2.53	2.46			1.13	1.15		1.14	.87	.02
F140	78 39.92	176 30.72	1562		46.9	46.2			2.47	2.37			1.16	1.10		1.13	2.65	.06
F145	78 31.52	175 49.69	1429		43.7				2.59				1.13			1.13		
F146	78 29.46	175 59.15	1233		47.6	49.9			2.46	2.38			1.17	1.19		1.18	.84	.02

STA	LAT	LONG	(M) DEPTH	GRADIENT 1-2	2-3	3-4	4-5	<K> 1-2	2-3	3-4	4-5	Q(HEAT FLOW) 1-2	2-3	3-4	4-5	$\bar{Q}$	AVE % DEV	MAX DEV
F147	78 30.14	176 08.07	1186		46.2	37.4			2.47	2.56			1.14	.96		1.05	8.57	.17
F148	78 31.63	176 12.75	1159	52.6	37.9	41.8		2.52	2.53	2.61		1.33	.96	1.09		1.12	12.03	.36
F149	78 34.15	176 08.18	1419	53.4	40.5	39.7				2.37				.94		.94		
F151	78 37.28	175 22.68	1742	48.0	46.5	49.2		2.52	2.44	2.61		1.21	1.13	1.28		1.20	4.23	.14
F152	78 39.49	175 17.93	1791	____	46.9	____		____	2.38	____		____	1.11	____		1.11		
F154	78 43.09	175 21.32	1817		45.6	51.3			2.59	2.31			1.18	1.19		1.18	.42	.01
F155	78 45.73	175 29.69	1741		48.1	49.1				2.56				1.26		1.26		
F160	78 46.05	176 02.17	1557		42.9	52.4			2.57	2.53			1.10	1.33		1.21	9.46	.22
F163	78 50.10	176 24.79	1580		56.2	55.3				2.45				1.36		1.36		
F168	78 39.98	175 57.24	1662	50.2				2.65				1.33				1.33		
F169	78 39.23	175 50.43	1640		45.0	52.6			2.60	2.48			1.17	1.31		1.24	5.64	.13
F170	78 39.71	175 55.72	1652		44.4	57.8			2.61	2.60			1.16	1.50		1.33	12.78	.34
F171	78 40.92	175 54.49	1675		47.6	49.8			2.56	2.46			1.22	1.23		1.22	.40	.01
F178	78 53.96	176 30.45	1589	43.1	34.6	60.3		2.63	2.57	2.44		1.14	.89	1.47		1.16	17.33	.57
F179	78 52.47	176 40.59	1642		46.0	48.8			2.61	2.33			1.20	1.13		1.16	3.00	.07
F180	78 49.74	176 42.15	1626	48.4	47.5	46.9		2.70	2.65	2.36		1.30	1.26	1.11		1.22	6.17	.18
F181	78 48.66	175 30.71	1494		56.1	72.6				2.54				1.82		1.82		
F182	78 56.88	175 21.03	1066			48.1				2.85				1.37		1.37		
F185	79 36.31	173 04.65	2680		31.5				2.79				.88			.88		
F188	79 38.23	172 03.56	2267		43.1	36.8			2.68	2.56			1.15	.94		1.04	10.04	.20
F192	79 59.22	174 26.12	1958	59.9	55.6				2.72				1.51			1.51		
F196	80 33.83	171 34.85	3324	52.9	51.5			2.70	2.63			1.43	1.35			1.39	2.87	.08
F197	80 37.13	171 58.71	3322	51.0	42.6			2.41	2.64			1.23	1.12			1.17	4.68	.11
F199	80 12.15	172 47.69	2987	39.6	47.6			2.43	2.41			.96	1.15			1.05	9.00	.18
F200	80 10.55	172 19.63	3045	41.2	49.1			2.44	2.35			1.01	1.15			1.08	6.48	.14
F204	79 44.12	170 57.33	3154	46.8	49.1			2.80	2.75			1.31	1.35			1.33	1.50	.04
F207	79 41.84	170 09.99	3259	42.5	46.7	50.7		2.87	2.64	2.42		1.22	1.23	1.23		1.22	.36	.01
F208	79 45.30	170 14.94	3259	43.3	47.8	52.4		2.98	2.62	2.72		1.29	1.25	1.42		1.32	5.05	.16
F213	80 24.51	159 27.47	3346		45.9	43.7			2.79	3.18			1.28	1.39		1.33	4.11	.11
F215	80 17.25	159 25.23	3042	44.9	41.5	44.5		2.82	3.14	3.08		1.26	1.30	1.37		1.31	3.05	.11
F216	80 23.69	157 41.59	3575		42.2	45.5			2.83	2.[illegible]			1.19	1.33		1.26	5.55	.13
F217	80 36.31	157 58.61	3712	45.0		50.5				2.80				1.42		1.42		
F218	80 41.03	158 21.83	3653			50.5				2.77				1.40		1.40		
F219	80 38.56	159 18.65	3700		50.1	55.5			2.78	2.69			1.40	1.49		1.44	3.11	.09
F221	80 32.98	159 38.89	3635	54.1	50.5	50.4	52.8	2.46	2.76	2.93	3.04	1.33	1.39	1.48	1.61	1.45	6.36	.28
F222	80 29.05	159 12.69	3630		54.6	56.3				2.81				1.58		1.58		
F223	80 28.35	159 06.16	3616	56.9	49.6	52.7		2.62	2.81	2.79		1.49	1.39	1.47		1.45	2.75	.10
F224	80 27.74	158 48.81	3468	49.5	44.6	44.2		2.54	2.66	2.88		1.26	1.19	1.27		1.24	2.68	.07
F225	80 29.63	158 42.84	3607		50.1	52.7	48.8		2.74	2.85	2.78		1.37	1.50	1.36	1.41	4.25	.14
F227	80 50.09	158 25.18	3640	47.5	48.0	46.5		2.69	2.71	2.62		1.28	1.30	1.22		1.26	2.45	.07
F229	81 40.66	157 29.47	3817	66.1	71.6	68.6		2.44	2.31	2.45		1.61	1.65	1.68		1.64	1.48	.07
F231	81 50.90	157 32.68	3812		71.9	65.0			2.32	2.44			1.67	1.59		1.63	2.45	.08

STA	LAT	LONG	(M) DEPTH	GRADIENT 1-2	2-3	3-4	4-5	<K> 1-2	2-3	3-4	4-5	Q(HEAT FLOW) 1-2	2-3	3-4	4-5	$\bar{Q}$	AVE % DEV	MAX DEV
F233	81 55.35	158 05.40	3815		71.3	65.8			2.31	2.47			1.65	1.62		1.63	.91	.03
F238	82 05.64	157 18.02	3807	71.9		68.8		2.42		2.47		1.74		1.70		1.72	1.16	.04
F239	82 08.88	157 22.11	3798	68.2	12.8	65.5		2.49	2.35	2.50		1.70	1.71	1.64		1.68	1.71	.07
F240	82 10.04	157 11.63	3798	67.4	70.0	66.6		2.45	2.37	2.43		1.65	1.66	1.62		1.64	.94	.04
F241	82 11.14	156 56.56	3812	68.5	72.7	64.0		2.55	2.33	2.36		1.74	1.70	1.51		1.65	5.65	.23
F243	82 15.21	156 18.58	3798	66.0	70.9	67.0		2.50	2.26	2.52		1.65	1.60	1.69		1.64	1.88	.09
F244	82 18.63	156 24.81	3810	65.7	72.8	65.8		2.56	2.34	2.44		1.68	1.71	1.61		1.66	2.26	.10
F245	82 16.98	156 28.09	3808	62.8	71.2	65.3		2.43	2.80	2.45		1.53	1.63	1.60		1.58	2.38	.10
F246	82 15.95	156 45.62	3806	61.6	68.5	63.2		2.36	2.38	2.45		1.45	1.63	1.55		1.54	4.03	.17
F247	82 13.44	157 00.72	3803	65.8	70.2	65.3		2.48	2.35	2.43		1.63	1.65	1.58		1.62	1.64	.07
F249	82 14.32	156 55.90	3806	64.8	72.5	65.0		2.47	2.28	2.41		1.60	1.65	1.56		1.60	1.94	.09
F250	82 15.08	156 37.47	3813	66.3	69.4	66.8		2.54	2.27	2.47		1.69	1.57	1.65		1.63	2.71	.12
F252	82 17.23	157 03.24	3809	64.5	69.3	66.9		2.56	2.32	2.36		1.65	1.61	1.58		1.61	1.51	.07
F253	82 21.41	157 07.60	3802	68.3	73.1	68.5		2.54	2.40	2.33		1.74	1.77	1.60		1.70	4.04	.16
F254	82 26.03	157 22.85	3803	64.4	70.8	65.2		2.34	2.37	2.35		1.51	1.68	1.53		1.57	4.51	.17
F255	82 25.21	157 22.37	3791	66.5	72.4	62.1		2.53	2.33	2.37		1.68	1.68	1.47		1.61	5.79	.20
F256	82 17.03	157 28.08	3802	66.4	72.0	65.4		2.46	2.36	2.4[illegible]		1.63	1.70	1.60		1.64	2.29	.10
F257	82 15.40	157 39.39	3816	67.5	71.7	64.8		2.47	2.39	2.37		1.67	1.72	1.54		1.64	4.19	.18
F258	82 09.30	158 03.51	3812	68.6	75.5	65.8		2.51	2.32	2.40		1.72	1.75	1.58		1.68	4.09	.17
F259	82 15.16	158 39.70	3817	66.4	70.0	64.8		2.38	2.37	2.42		1.58	1.66	1.57		1.60	2.35	.09
F260	82 24.28	158 30.75	3816	67.4	69.8			2.41	2.28	2.43		1.62	1.60			1.61	.62	.02
F261	82 24.51	158 18.08	3818	68.9	72.7	65.7		2.50	2.34	2.43		1.72	1.70	1.59		1.67	3.19	.13
F262	82 38.86	158 35.68	3811	68.5	67.5	61.8		2.46	2.44	2.31		1.69	1.65	1.43		1.59	6.70	.26
F263	82 37.12	158 32.30	3815	69.9	71.9	65.3		2.45	2.32	2.37		1.71	1.69	1.55		1.65	4.04	.16
F264	82 34.07	158 00.53	3817	68.7	69.9	65.0		2.46	2.27	2.43		1.69	1.59	1.58		1.62	2.88	.11
F265	82 31.48	157 42.49	3814	70.4	72.9	64.8		2.37	2.33	2.44		1.67	1.70	1.58		1.65	2.82	.12
F266	82 33.85	157 42.50	3816	67.7	71.3	65.3		2.34	2.39	2.42		1.58	1.70	1.58		1.62	3.29	.12
F268	83 16.32	152 58.48	3053	63.8	66.0	59.7			2.69	2.75			1.77	1.62		1.69	4.42	.14
F269	83 14.31	153 13.96	3096		51.7				2.77				1.44			1.44		
F270	83 11.18	154 00.77	3277	48.3	44.6			2.66	2.78			1.29	1.24			1.26	1.97	.04
F271	83 10.67	153 53.54	3253	46.9	42.5	43.7		2.76	2.82	2.75		1.29	1.20	1.20		1.23	3.25	.08
F272	83 11.82	152 56.24	2283			44.0	48.3		2.75	3.00	2.78			1.32	1.34	1.33	.75	.02
F273	83 12.30	152 56.42	2322		48.3	44.2			2.96	2.99			1.43	1.32		1.37	4.00	.11
F274	83 13.49	153 04.31	2745	65.8	59.6	58.6			2.66	2.92			1.58	1.71		1.64	3.95	.13
F275	83 30.23	149 58.64	2883	45.1	49.0	42.4		2.70	2.68	2.88		1.22	1.31	1.22		1.25	3.20	.08
F277	83 34.55	149 26.45	2870	47.0	48.7	47.0			2.59	2.88			1.26	1.35		1.30	3.44	.09
F278	83 36.40	149 08.10	2722	75.5		71.6		2.68		2.77		2.02		1.98		2.00	.99	.03
F279	83 38.17	149 01.71	2730		45.5	45.3				2.83				1.28		1.28		
F284	83 47.34	145 50.92	2681		38.1	43.0			2.71	2.79			1.03	1.20		1.11	7.62	.17
F285	83 48.51	145 27.90	2652		50.9	46.7			2.65	2.91			1.35	1.36		1.35	.36	.01
F286	84 00.84	144 02.17	2315	51.0		39.5		2.62		2.80		1.34		1.10		1.22	9.83	.23
F287	84 05.19	144 01.15	2429	37.6		29.2		2.56		2.91		.96		.85		.90	6.07	.11

STA	LAT	LONG	(M) DEPTH	GRADIENT 1-2	2-3	3-4	4-5	<K> 1-2	2-3	3-4	4-5	Q(HEAT FLOW) 1-2	2-3	3-4	4-5	$\bar{Q}$	AVE % DEV	MAX DEV
F288	84 11.23	144 28.42	2413		70.0	63.6			2.67	2.73			1.87	1.73		1.80	3.88	.13
F289	84 14.69	144 16.97	2356		40.2	28.8				2.77				.80		.80		
F290	84 23.40	143 51.19	2261		39.1	32.9			2.67	2.73			1.04	.90		.97	7.21	.13
F291	84 26.67	144 08.60	2246		35.2	34.5				2.55				.88		.88		
F292	84 18.28	143 41.02	2329		57.8	59.1			2.68	2.77			1.55	1.64		1.59	2.82	.09
F293	84 25.00	143 04.57	2057		53.7	46.8				2.78				1.30		1.30		
F294	84 56.62	145 34.04	2233		46.6				2.71				1.27			1.27		
F295	84 57.40	145 30.63	2213	41.7	43.5				2.73				1.19			1.19		
F298	85 07.83	142 51.23	1971			58.4				2.73				1.59		1.59		
F300	85 18.53	144 02.85	2082		41.1	46.0			2.82	2.74			1.16	1.26		1.21	4.13	.09
F301	85 18.95	143 36.00	2100	----	39.0	----		----	2.69	----		----	1.05	----		1.05		
F302	85 19.28	142 36.62	2169	33.4	31.6			2.64	2.72	2.72		.88	.86			.87	1.14	.02
F303	85 26.39	142 28.07	2208		27.6	31.6			2.70	2.68			.74	.85		.79	6.91	.11
F304	85 28.28	143 08.52	2277		41.3	48.4			2.65	2.65			1.09	1.28		1.18	8.01	.18
F305	85 25.22	144 33.92	2257	35.8	33.8	43.3		2.97	2.70	2.70		1.06	.91	1.17		1.04	8.70	.25
F306	85 24.93	145 12.85	2263		41.6	42.4			2.77	2.67			1.15	1.13		1.14	.87	.02
F307	85 25.35	145 38.04	2278		38.4	45.6			2.75	2.73			1.06	1.24		1.15	7.82	.18
F308	85 30.27	143 08.18	2252	35.3	37.2			2.86	2.69			1.01	1.00			1.00	.49	
F309	85 34.92	142 31.03	2262	47.2	50.8	50.6	47.4	2.74	2.74	2.66	2.82	1.29	1.39	1.35	1.34	1.34	2.04	.10
F310	85 43.80	142 39.16	2424	34.1	36.8	40.7		2.72	2.76	2.65		.93	1.01	1.08		1.00	5.07	.14
F311	85 41.93	142 21.15	2332	44.0	48.9	42.1		2.76	2.82	2.73		1.22	1.38	1.15		1.25	6.93	.22
F312	85 41.02	142 11.99	2282		52.3	44.5			2.86	2.72			1.50	1.21		1.35	10.70	.29
F313	85 38.69	141 47.15	2243		48.2	45.4			2.81	2.82			1.35	1.28		1.31	2.66	.07
F314	85 27.00	139 23.54	1927		46.4	44.8			2.77	2.68			1.28	1.20		1.24	3.22	.07
F316	85 08.72	138 13.91	1785	38.3	35.9			2.65	2.80			1.01	1.00			1.00	.49	
F319	84 52.64	136 02.41	2016	34.5	35.5	32.1		2.71	2.69	2.82		.93	.96	.91		.93	1.90	.05
F320	84 45.72	136 23.71	2055		41.9	45.1			2.63	2.59			1.10	1.17		1.13	3.08	.07
F322	84 17.80	135 06.17	2674		51.0	47.1			3.10	3.36			1.58	1.58		1.58		
F324	84 12.73	135 29.76	2654	44.8	45.2	42.6		2.45	2.43	2.59		1.10	1.10	1.10		1.10		
F326	84 12.89	135 41.40	2653	45.7	46.5	43.2		3.13	3.23	3.25		1.43	1.50	1.40		1.44	2.61	.10
F327	84 13.49	135 35.08	2644	47.8	48.1	47.2		2.58	2.67	2.66		1.23	1.28	1.26		1.25	1.41	.04
F328	84 13.66	135 24.38	2644	45.6	45.0	41.2		2.61	2.75	2.70		1.19	1.24	1.11		1.18	3.95	.13
F329	84 14.13	135 06.30	2545	64.3	65.7	60.5		2.63	2.76	2.85		1.69	1.81	1.72		1.74	2.68	.11
F330	84 15.46	134 41.78	2563			65.8				2.74				1.80		1.80		
F331	84 16.02	134 37.65	2659	43.9	45.2	39.1		2.61	2.70	2.92		1.15	1.22	1.14		1.17	2.84	.08
F332	84 21.98	133 15.96	2733	50.5	50.2	48.7		2.52	2.62	2.7[illegible]		1.27	1.31	1.36		1.31	2.36	.09
F333	84 27.43	132 41.98	2694	46.9	48.6	41.0		2.56	2.69	2.[illegible]		1.20	1.31	1.12		1.21	5.50	.18
F334	84 36.92	132 26.68	2594		56.0	50.8			2.62	2.72			1.47	1.38		1.42	[illegible].15	.09
F335	84 53.30	132 29.56	1822		54.0	49.0			2.70	2.98			1.46	1.46		1.46		
F337	84 47.77	131 33.61	2286	48.2	54.4	40.8		2.53	2.71	2.67		1.22	1.47	1.09		1.26	11.11	.38
F338	84 46.84	132 03.29	2266	36.7	42.8	37.6		2.56	2.69	2.85		.94	1.15	1.07		1.05	7.17	.20
F340	84 48.60	131 17.96	2290	32.8	28.5	27.1		2.52	2.63	2.74		.83	.75	.74		.77	4.88	.08

STA	LAT	LONG	(M) DEPTH	GRADIENT 1-2	2-3	3-4	4-5	<K> 1-2	2-3	3-4	4-5	Q(HEAT FLOW) 1-2	2-3	3-4	4-5	$\bar{Q}$	AVE % DEV	MAX DEV
F341	84 51.74	130 58.43	2343	44.2	42.7	40.9		2.59	2.64	2.83		1.14	1.13	1.16		1.14	.97	.03
F342	84 59.74	130 20.91	1966		33.6	32.4			2.56	2.67			.86	.86		.86		
F343	85 04.50	130 38.04	1753	33.6	37.8	32.4		2.60	2.69	2.67		.87	1.02	.87		.92	7.24	.14
F344	85 01.28	130 57.73	1769	41.3	40.1	40.2		2.53	2.65	2.84		1.04	1.06	1.14		1.08	3.70	.10
F345	84 55.19	130 45.69	2292	45.1	40.0	44.2		2.58	2.68	2.75		1.16	1.07	1.22		1.15	4.63	.15
F346	84 51.22	130 42.69	2372	46.0	36.9	44.1		2.52	2.66	2.68		1.16	.98	1.18		1.10	7.63	.19
F347	84 46.46	130 32.98	2448	42.8	42.9	42.6		2.66	2.63	2.67		1.14	1.13	1.14		1.13	.39	.01
F348	84 47.29	130 33.08	2457		46.0	44.9			2.62	2.77			1.21	1.24		1.22	1.22	.03
F349	84 47.92	131 03.69	2371	41.8	40.2	43.0		2.51	2.65	2.74		1.05	1.06	1.18		1.09	5.06	.13
F350	84 44.70	130 39.89	2490	31.9		30.4		2.61		2.71		.83		.82		.82	.60	
F351	84 44.13	130 42.75	2478	37.5		38.3		2.44		2.55		.91		.98		.94	3.70	.07
F352	84 48.71	130 55.69	2368		46.7	41.7			2.67	2.70			1.25	1.13		1.19	5.04	.12
F353	84 51.55	131 10.02	2313		51.0	43.2			2.59	2.73			1.32	1.18		1.25	5.59	.13
F354	84 53.42	130 59.81	1917	37.3	49.2	42.3		2.55	2.64	2.57		.95	1.30	1.09		1.11	11.17	.34
F355	84 56.22	131 18.77	1920	44.0	40.5	44.3		2.62	2.80	2.84		1.15	1.13	1.26		1.18	4.51	.12
F356	84 55.87	130 50.82	2287		51.5	44.9			2.65	2.63			1.36	1.18		1.27	7.08	.17
F357	84 57.78	130 20.00	2213	47.9	51.1	49.6		2.60	2.72	2.83		1.25	1.39	1.40		1.34	4.78	.14
F358	84 54.73	129 45.29	2377	56.5	62.7	54.2		2.50	2.66	2.77		1.41	1.67	1.50		1.52	6.25	.26
F359	84 52.93	129 43.84	2400	26.7	35.2	34.6		2.56	2.56	2.50		.68	.90	.87		.81	11.15	.22
F360	84 52.50	129 55.37	2365	46.2	49.4	46.3		2.59	2.51	2.64		1.20	1.24	1.22		1.22	1.09	.04
F361	84 56.78	130 02.51	2365		35.9	35.4			2.69	2.89			.97	1.02		.99	2.51	.04
F362	84 54.57	130 10.15	2385			43.6				2.73				1.19		1.19		
F363	84 47.90	129 57.58	2460		47.4	43.9			2.63	2.62			1.25	1.15		1.20	4.16	.10
F364	84 32.14	131 01.37	2639			40.5				2.63				1.07		1.07		
F365	84 28.48	131 22.31	2732	33.6		31.9		2.53		2.68		.85		.86		.85	.58	
F366	84 26.74	131 20.78	2778	47.0		44.4		2.57		2.73		1.21		1.21		1.21		
F367	84 25.83	131 06.28	2762	33.6		33.5		2.58		2.67		.87		.89		.88	1.13	.02
F369	84 35.84	129 20.23	2539	42.6	50.2	44.4		2.54	2.72	2.62		1.08	1.36	1.17		1.20	8.67	.28
F370	84 34.91	129 01.19	2542	42.2		43.2		2.66		2.76		1.12		1.19		1.15	3.03	.07
F372	84 35.58	128 45.33	2580	____	51.3	____		____	2.64	____		____	1.35	____		1.35		
F374	84 43.03	129 46.48	2458	46.0		47.0		2.57		2.72		1.18		1.27		1.22	3.67	.08
F375	84 37.25	128 50.07	2349	____	42.2	____		____	2.69	____		____	1.14	____		1.14		
F376	84 35.50	128 42.99	2605	____	60.3	____		____	2.67	____		____	1.61	____		1.61		
F377	84 34.31	128 15.95	2648	44.1				2.58				1.14				1.14		
F378	84 39.05	128 57.49	2299	43.4				2.54				1.10				1.10		
F379	84 38.19	128 44.84	2268	52.0	52.7	49.0		2.51	2.67	2.80		1.30	1.41	1.37		1.36	2.94	.11
F380	84 37.54	128 27.89	2401	49.1	41.7	41.4		2.58	2.61	2.85		1.26	1.09	1.18		1.17	4.91	.16
F382	84 37.01	127 25.28	2542	34.1	38.2	32.8		2.58	2.60	2.71		.88	.99	.89		.92	5.07	.11
F383	84 37.32	127 17.20	2543	38.3		35.9		2.66		2.66		1.02		.95		.98	3.55	.06
F384	84 38.21	127 12.89	2581	48.3	48.3	45.2		2.50	2.68	2.66		1.21	1.30	1.20		1.23	3.41	.09
F385	84 48.33	126 57.19	2225			44.6				2.74				1.22		1.22		
F386	84 48.03	126 58.17	2266	49.4	45.0	45.4		2.50	2.70	2.94		1.24	1.21	1.33		1.26	3.70	.11

STA	LAT	LONG	(M) DEPTH	GRADIENT 1-2	2-3	3-4	4-5	<K> 1-2	2-3	3-4	4-5	Q(HEAT FLOW) 1-2	2-3	3-4	4-5	$\bar{Q}$	AVE % DEV	MAX DEV
F387	84 46.86	127 13.88	2321	43.0	47.8	44.2		2.57	2.65	2.77		1.11	1.27	1.23		1.20	5.17	.15
F388	84 46.06	127 23.28	2343	47.5	45.8			2.51	2.77			1.19	1.27			1.23	3.25	.07
F389	84 46.63	127 35.74	2271		109.0	104.0			2.57	2.80			2.80	2.92		2.86	2.09	.12
F390	84 51.41	125 46.54	1976		55.0	38.1			2.59	2.55			1.43	.97		1.20	19.16	.45
F395	84 41.51	125 53.40	2502		48.3	40.3			2.89	3.35			1.39	1.35		1.37	1.45	.04
F396	84 38.53	126 04.65	2589	51.4	59.5	37.7		2.72	2.90	3.20		1.40	1.72	1.21		1.44	12.77	.51
F397	84 36.77	125 50.35	2597	44.9	44.9	44.8		2.58	2.74	2.93		1.16	1.23	1.31		1.23	4.14	.14
F398	84 36.42	125 48.14	2596	49.0	45.9	37.3		2.69	2.66	3.11		1.32	1.22	1.16		1.23	4.68	.15
F399	84 36.81	125 48.08	2594	49.1	47.7	44.5		2.68	2.74	2.97		1.31	1.31	1.32		1.31	.33	.01
F400	84 30.81	126 21.43	2690	46.9	51.0	49.5		2.66	2.80	2.73		1.25	1.43	1.35		1.34	4.63	.17
F401	84 23.30	126 54.61	2733	46.1	42.4	41.3		2.75	2.85	3.09		1.27	1.21	1.28		1.25	2.30	.06
F402	84 22.83	126 20.54	2698		48.0				2.61				1.25			1.25		
F404	84 28.99	127 11.14	2231		54.1				2.71				1.47			1.47		
F405	84 31.36	128 12.92	2753		53.1	53.3			2.66	2.72			1.41	1.45		1.43	1.39	.04
F406	84 32.46	128 38.10	2711		46.2	41.6			2.62	2.72			1.21	1.13		1.17	3.41	.08
F407	84 23.21	129 03.37	2813	55.5	50.3			2.70	2.92			1.50	1.47			1.49	1.01	.03
F408	84 23.51	127 52.45	2758	51.2	51.1	52.8		2.74	2.71	3.[illegible]		1.40	1.38	1.67		1.48	8.38	.29
F409	84 27.51	127 00.21	2742	49.4	49.9	48.5		2.74	2.72	3.25		1.36	1.36	1.58		1.43	6.82	.21
F410	84 28.13	126 52.41	2737	49.2	41.3	46.1		2.70	2.94	3.24		1.33	1.21	1.49		1.34	7.27	.28
F411	84 29.67	126 39.96	2693	48.1	44.4	43.2		2.62	2.73	2.85		1.26	1.21	1.23		1.23	1.44	.04
F412	84 27.79	125 01.34	2521	39.5	43.1			2.68	2.87			1.06	1.24			1.15	7.82	.18
F413	84 25.56	125 15.22	2390	40.1		39.2		3.07		3.01		1.23		1.18		1.20	2.07	.05
F414	84 21.36	124 39.69	2082			37.4				2.95				1.10		1.10		
F417	84 29.88	124 06.28	2381	51.7	47.2	41.4		2.84	2.74	3.14		1.47	1.29	1.30		1.35	5.74	.18
F418	84 30.27	124 30.10	2356	49.1	36.3			2.52	2.68			1.24	.98			1.11	11.71	.25
F419	84 32.43	124 38.88	2432	47.7	43.7			2.49	2.68			1.19	1.17			1.18	.84	.02
F420	84 46.59	122 55.14	2248	43.4	31.5			2.58	2.73			1.12	.86			.99	13.13	.25
F421	84 48.11	123 43.15	2238	52.3	46.9			2.51	2.67			1.31	1.25			1.28	2.34	.05
F422	84 53.48	124 32.87	2049		88.4				1.58				1.39			1.39		
F423	84 55.72	126 43.37	1532		30.0				2.90					.87		.87		
F425	85 02.61	127 54.11	2282	48.4	41.4	48.7		2.58	2.69	2.66		1.25	1.11	1.29		1.21	5.84	.17
F427	86 01.82	134 44.84	2216	45.8	48.6			2.68	2.78			1.23	1.35			1.29	4.65	.11
F429	86 03.08	133 55.29	2215	42.4	54.4	42.8		2.70	2.68	2.77		1.14	1.46	1.18		1.26	10.58	.32
F430	85 59.45	133 20.49	1860	38.6	44.4	32.7		2.71	2.75	2.86		1.04	1.22	.93		1.06	9.82	.28
F431	85 55.63	132 14.44	1505		50.9	49.7			2.79	2.80			1.42	1.39		1.40	1.06	.03
F432	85 58.04	130 51.91	1674		27.2	26.5			2.66	2.76			.73	.73		.73		
F433	85 58.95	129 51.75	1624	51.5	70.7			2.75	2.70			1.42	1.91			1.66	14.71	.48
F434	86 01.05	129 26.45	2058	37.6	31.2	55.5		2.63	2.80	2.76		.99	.87	1.53		1.13	23.59	.65
F435	86 03.41	129 32.49	2272		55.4	54.0			2.82	2.82			1.56	1.52		1.54	1.29	.04
F436	85 59.78	130 13.13	1780		34.0	47.9			2.72	2.84			.93	1.36		1.14	18.77	.42
F438	86 01.27	128 42.44	2149	44.4	38.6	40.7		2.59	2.76	2.69		1.15	1.07	1.09		1.10	2.81	.08
F441	85 56.70	121 14.46	2431	45.2	35.8	42.1		2.70	2.66	2.67		1.22	.95	1.13		1.10	9.09	.26

STA	LAT	LONG	(M) DEPTH	GRADIENT 1-2	2-3	3-4	4-5	<K> 1-2	2-3	3-4	4-5	Q(HEAT FLOW) 1-2	2-3	3-4	4-5	$\bar{Q}$	AVE % DEV	MAX DEV
F442	86 02.49	121 12.58	2431		49.4	51.0			2.68	2.72			1.32	1.39		1.35	2.58	.07
F443	85 57.96	121 07.71	2436		39.3	35.9			2.69	2.71			1.06	.97		1.01	4.43	.08
F444	85 45.89	119 57.68	2126	36.4	36.9	35.3		2.67	2.76	2.83		.97	1.02	1.00		.99	1.78	.04
F446	85 55.68	117 29.12	2342	43.7	38.7	35.0		2.66	2.79	3.02		1.16	1.08	1.06		1.10	3.63	.10
F461	85 33.45	120 17.26	1221	38.0				2.91				1.11				1.11		
F462	85 33.67	120 07.15	1209	39.3				2.83				1.11				1.11		
F465	85 34.94	114 59.36	1356		51.9	41.6			3.14	3.14			1.63	1.31		1.47	10.88	.32
F468	85 22.92	113 18.37	1239			39.7				3.32				1.32		1.32		
F474	85 20.88	110 00.23	1647		35.6	32.1			3.01	3.26			1.07	1.05		1.06	.94	.02
F475	85 18.48	110 07.86	1805		44.1					3.30				1.45		1.45		
F476	85 15.87	110 00.54	1910		50.3	40.0			3.06	3.21			1.54	1.28		1.41	9.21	.26
F479	85 26.09	110 11.43	1198		39.4				3.13				1.23			1.23		
F483	84 28.06	112 56.20	1381			39.2				3.32				1.30		1.30		
F486	84 20.40	113 30.78	1749	39.1				2.74				1.07				1.07		
F487	84 20.91	112 39.49	1714		40.3				2.79				1.12			1.12		
F488	84 14.34	114 04.90	2129		43.9	46.3			2.95	2.90			1.29	1.34		1.31	1.90	.05
F489	84 11.90	114 51.52	2275	43.0	48.6	50.2		2.82	2.78	2.87		1.21	1.35	1.44		1.33	6.16	.22
F493	84 17.01	112 34.63	1801		64.6				2.88				1.86			1.86		
F495	84 16.94	112 33.73	1808	36.1				2.79	3.06			1.01				1.01		
F501	84 18.82	112 17.74	1750		47.6	61.8			3.04	2.71			1.44	1.67		1.55	7.39	.22
F502	84 16.00	112 38.50	1780	40.5		45.7		3.05		2.96		1.24		1.36		1.30	4.61	.11
F503	84 16.89	112 22.72	1776	42.1	47.2	50.2			3.13	2.83			1.47	1.42		1.44	1.73	.05
F505	84 16.53	112 24.67	1753		42.6	45.6			3.14	3.03			1.34	1.38		1.36	1.47	.04
F506	84 06.62	112 43.87	1871		31.3	43.8			2.81	2.95			.88	1.29		1.08	18.89	.40
F508	84 07.50	112 13.00	1866		46.9					2.94				1.38		1.38		
F509	84 11.80	111 29.60	1787		43.7					3.07				1.34		1.34		
F511	84 03.30	112 41.60	1960			44.5				2.73				1.22		1.22		
F513	84 04.80	112 28.40	1917			39.4				3.20				1.26		1.26		
F514	84 14.00	110 57.90	1733	45.7		34.8		2.75		3.11		1.26		1.08		1.17	7.69	.17
F528	84 45.00	100 33.70	1943		62.4	65.3			2.98	3.03			1.86	1.98		1.92	3.12	.12
F529	84 48.60	99 28.40	1889	48.0	45.5			2.55	2.67	3.13		1.22	1.21			1.21	.41	.01
F530	84 49.70	99 30.60	1985	41.4		41.1		2.59		2.82		1.07		1.16		1.11	4.03	.09
F532	85 03.30	98 23.00	2116	49.4	49.9			2.97	2.82			1.47	1.41			1.44	2.08	.06
F533	85 05.90	98 17.80	1855				34.9				3.22				1.12	1.12		
F537	85 24.20	88 46.60	2025	26.4		26.9			2.66	2.86		.70		.77		.73	4.[illegible]6	.06
F538	85 24.20	88 47.30	2029	24.1	38.6	26.4		2.74	2.77	2.75		.66	1.07	.73		.[illegible]2	20.32	.40
F545	84 54.90	83 22.80	2126		56.0	60.1			2.91	2.8[illegible]			1.63	1.70		1.66	2.10	.07
F548	84 37.10	83 38.20	2019	56.9	57.9	60.0		3.60	3.40	3.01		2.05	1.97	1.81		1.94	4 57	.23
F549	84 37.30	82 26.70	1708		56.6	55.1			3.05	3.12			1.73	1.72		1.72	.28	.01
F550	84 36.90	82 16.90	1708	54.6	54.0	51.5		3.43	3.43	3.37		1.87	1.85	1.73		1.81	3.18	.13
F551	84 36.80	82 20.70	1706	50.3	57.4	54.1		3.34	3.11	3.19		1.68	1.79	1.73		1.73	2.17	.10
F552	84 17.70	85 58.20	1829			52.2				3.23				1.69		1.69		

STA	LAT	LONG	(M) DEPTH	GRADIENT 1-2	2-3	3-4	4-5	<K> 1-2	2-3	3-4	4-5	Q(HEAT FLOW) 1-2	2-3	3-4	4-5	$\bar{Q}$	AVE % DEV	MAX DEV
F556	84 20.90	85 24.50	1822	58.2	22.4	54.5		3.01	3.05	2.74		1.75	.68	1.49		1.30	31.97	1.06
F557	84 20.80	85 15.20	1820		6.9	65.9	74.6			3.41	2.94			2.25	2.20	2.22	1.12	.05
F559	84 23.60	84 34.60	1791		27.0	54.8	82.9		3.06	2.76	3.19		.83	1.51	2.64	1.66	39.35	1.80
F560	84 23.50	84 28.10	1790		27.7	64.6	64.5		3.13	2.91	3.31		.87	1.87	2.13	1.62	30.93	1.25
F561	84 22.30	84 34.70	1790	56.6	17.4	55.1	62.9	2.58	2.93	2.99	3.56	1.46	.51	1.65	2.24	1.46	32.76	1.72
F562	84 11.70	86 34.30	1835		18.0	54.2	66.5		3.21	2.98	3.08		.58	1.61	2.05	1.41	39.30	1.46
F563	84 11.90	87 20.30	1896		28.5	37.0			3.29	2.99			.94	1.11		1.02	8.29	.16
F565	84 07.00	87 51.80	1658		25.9	44.9			3.27	3.30				1.48		1.48		
F566	84 07.00	86 32.50	1675		44.3				3.33				1.48			1.48		
F567	84 08.50	86 33.30	1817			69.7				3.15				2.20		2.20		
F569	84 12.90	83 02.80	1735		52.3	55.9	58.2		3.00	2.85	2.76		1.57	1.59	1.61	1.59	.83	.04
F571	84 06.00	84 28.00	1697		78.4	79.1			3.04	2.99			2.38	2.37		2.37	.21	.01
F573	83 58.50	84 48.00	1694		49.2	62.9			3.21	2.79			1.58	1.75		1.66	5.10	.17
F576	83 46.40	88 59.30	1570		47.5				3.49				1.66			1.66		
F578	83 41.10	85 28.80	1608		60.2	53.8	48.7		3.10	3.08	2.98		1.87	1.66	1.45	1.66	8.43	.41
F579	83 41.00	85 27.80	1610		49.4	52.1			3.07	3.05			1.52	1.59		1.55	2.25	.07
F580	83 41.10	85 27.50	1610		46.8	47.3			3.05	2.94			1.42	1.39		1.40	1.06	.03
F582	83 49.00	78 45.00	1247			73.8				2.97				2.19		2.19		
F583	83 50.60	78 53.00	1295		60.1		60.0		2.99		3.17		1.80		1.90	1.85	2.70	.10
F584	83 50.30	78 52.00	1297		58.2	57.1			3.03	3.07			1.76	1.75		1.75	.28	

Table 3. Kolmogorov-Smirnov tests on heat flow data by regions. The letters in the middle and bottom parts of the table refer to areas in Figure 9.

TABLE 3

KOLMAGOROV – SMIRNOV TESTS

AREA	— DESCRIPTION	NUM	$\bar{Q}$	σ	DMAX	(COL.	ROW)	SIGNIF. LEVEL
ALPHA	< 3500 m – F12, 21, 389	~~207~~	~~1.28~~	~~0.01~~	– REJECTED –			
W. ALPHA	W. of 90°; + F537, 538; – F12, 21, 389	181	1.22	0.23	0.072	5	20	0.01
E. ALPHA	LONG ≤ 90° – F537, 538	26	1.70	0.30	0.159	4	19	0.05
MEND. R.	< 3200 m	59	1.19	0.16				
MEND. P.	> 3200 m	4	1.28	0.10	0.228	1	1	0.20
C. PLAIN S.		13	1.27	0.19	0.149	1	10	0.20
C. PLAIN N.		17	1.33	0.07	0.095	1	14	0.20
C. PLAIN NP		30	1.30	0.14	0.135	2	19	0.15
NW C. PLAIN		29	1.63	0.04	0.110	1	19	0.20
C	CRAY, SBAINSCHT – F278 (2.00)	5	1.26	0.09	0.154	1	2	0.20
D	incl. F224 > 3500 m	10	1.39	0.11	0.191	1	7	0.20
F	F21 – F25 > 3450 m, incl. F21	5	1.40	0.10	0.197	1	2	0.20
G	F3 – F13 > 3450 m incl. F12	8	1.44	0.07	0.164	1	5	0.20
DFG		23	1.41	0.09	0.111	1	18	0.20
H	F14 – F19	5	0.92	0.16	0.168	1	2	0.20
LR		7	1.42					
K	ALL IN AREA	8	1.14	0.38	0.302	5	5	0.01
L	332 – 374 + 425 NEXT TO M	37	1.14	0.185	0.083	1	20	0.20
M	– F389	42	1.24	0.16	0.103	1	20	0.20
LM		79	1.19	0.18	0.081	1	20	0.20
N		8	1.41	0.27	0.218	1	5	0.20
V Ø		17	1.30	0.20	0.169	2	14	0.15
P		6	1.32	0.16	0.175	1	3	0.20
Q		18	1.17	0.19	0.108	1	15	0.20
R	F427 – F438	10	1.23	0.26	0.135	1	7	0.20
~~S~~	/ / / /	~~7~~	~~1.14~~	~~0.12~~	– REJECTED –			
W	F528 – F533	5	1.31	0.40	0.199	1	2	0.20
VØPW		28	1.31	0.23	0.130	1	19	0.20
KLTQRS		83	1.15	0.21	0.065	1	20	0.20
KLTQRSNM		133	1.19	0.21	0.082	5	20	0.01
KLTQRSM		125	1.18	0.20	0.066	1	20	0.20

Table 4. Water column temperature profiles collected from T-3.

USGS TEMPERATURE PROFILES IN THE ARCTIC OCEAN
DATA OBTAINED FROM T-3 ICE ISLAND

TABLE (4

DATE DY	MO	YEAR	TIME GMT	POSITION LATITUDE	LONGITUDE	STATION NUMBER	DEPTH
EARLY TEMPERATURE PROFILES MADE WITH HEAT FLOW CASTS (SUCCESSFUL)							
03	09	1963	0122	82 22.47	-162 03.31	FL-024	3743
10	05	1964	0347	80 29.50	-139 50.66	FL-029	3709
12	07	1964	0027	80 35.85	-137 40.62	FL-038	3689
04	08	1964	0110	80 32.42	-134 24.22	FL-043	3632
25	08	1964	0049	80 37.30	-135 59.10	FL-048	3663
SEPERATE PROFILE CASTS (SUCCESSFUL)							
6	5	1968	157	82 19.82	-158 50.30	TP- 1	3824
19	5	1968	2326	82 33.72	-157 59.21	TP- 2	3820
14	7	1968	155	83 36.94	-149 7.57	TP- 4	2671
26	8	1968	44	84 19.30	-143 55.30	TP- 5	2354
19	11	1968	2150	84 58.19	-136 16.82	TP- 6	1900
13	12	1968	421	84 24.29	-133 39.00	TP- 7	2641
18	12	1968	830	84 44.37	-132 22.05	TP- 8	2388
26	12	1968	1344	84 44.41	-131 48.39	TP- 9	2293
7	1	1969	1031	84 59.44	-130 47.02	TP-10	1870
15	1	1969	759	84 47.84	-130 51.11	TP-11	2381
23	1	1969	1105	84 52.83	-131 13.24	TP-12	2299
3	2	1969	1722	84 55.23	-129 40.75	TP-13	2378
13	2	1969	1226	84 45.35	-130 15.44	TP-14	2566
21	2	1969	1229	84 24.94	-130 56.65	TP-15	2778
28	2	1969	2109	84 35.61	-128 45.25	TP-16	2574
18	3	1969	850	84 34.40	-128 20.51	TP-17	2638
23	3	1969	1109	84 37.38	-128 23.31	TP-18	2617
31	3	1969	1217	84 40.10	-127 9.03	TP-19	2561
14	4	1969	030	84 48.10	-127 3.35	TP-20	2282
28	5	1969	2255	84 27.79	-126 39.50	TP-21	2704
9	6	1969	804	84 22.09	-128 29.89	TP-23	2816
26	6	1969	726	84 22.43	-124 50.22	TP-24	1958
7	7	1969	1517	84 30.04	-123 49.49	TP-25	2420
15	7	1969	707	84 33.22	-124 16.29	TP-26	2409
22	8	1969	2010	86 3.03	-133 45.46	TP-27	2207
1	9	1969	404	86 2.47	-130 11.18	TP-28	1988
25	9	1969	059	85 44.58	-119 21.02	TP-29	2031
8	12	1969	0525	85 29.67	-113 26.59	TP-30	1365
21	12	1969	0140	85 21.23	-110 4.00	TP-31	1619
9	2	1970	0440	84 27.29	-112 47.18	TP-32	1444
8	6	1970	0204	84 13.1	-112 37.1	TP-35	1936
17	6	1970	0220	84 05.4	-112 27.6	TP-36	1901
23	6	1970	0322	84 06.7	-111 50.0	TP-37	1871
25	6	1970	0225	84 10.8	-111 08.4	TP-38	1818
3	7	1970	1415	84 24.8	-107 11.7	TP-39	1307
4	7	1970	2256	84 25.1	-107 11.0	TP-40	1298
15	7	1970	1500	84 48.2	-106 14.2	TP-41	1404
18	7	1970	0106	84 44.1	-106 27.4	TP-42	1442
29	7	1970	0210	84 35.6	-106 22.6	TP-44	1358
31	7	1970	2259	84 39.4	-105 51.1	TP-45	1490

2	8	1970	0157	84	38.6	-105	57.9	TP-46	1499
3	8	1970	2226	84	35.5	-106	22.0	TP-47	1327
8	8	1970	0103	84	29.4	-106	55.3	TP-48	1302
11	8	1970	2210	84	27.3	-106	51.0	TP-49	1282
15	8	1970	2224	84	20.3	-107	47.6	TP-50	1537
21	8	1970	0945	84	12.0	-107	04.2	TP-52	1740
24	8	1970	2257	84	20.7	-106	01.6	TP-53	1492
26	8	1970	1659	84	21.4	-104	50.4	TP-54	1400
28	8	1970	0342	84	23.4	-104	32.4	TP-55	1419
11	9	1970	0824	84	51.1	-099	23.4	TP-56	2009
13	9	1970	0358	84	49.4	-099	18.2	TP-57	1991
15	9	1970	0306	84	50.6	-099	17.5	TP-58	1978
17	9	1970	0324	84	51.1	-099	25.3	TP-59	1988
23	9	1970	0126	84	49.5	-099	01.5	TP-60	1739
9	11	1970	2148	85	05.9	-099	11.3	TP-62	2107
16	3	1971	0218	85	28.7	-089	17.8	TP-63	1939
15	07	1971	2222	84	37.3	-088	01.2	TP-64	1933
12	08	1971	0504	84	43.4	-087	19.9	TP-65	2023
17	11	1971	1238	84	35.3	-084	55.2	TP-66	1671
03	12	1971	0758	84	36.8	-082	20.3	TP-67	1702
06	04	1972	0752	84	22.50	-084	43.40	TP-69	1792
14	06	1972	0807	84	11.10	-086	30.60	TP-70	1864
27	06	1972	748	84	6.20	-087	40.50	TP-71	1615
10	07	1972	0502	84	08.00	-086	33.00	TP-72	1708
15	07	1972	1113	84	06.80	-086	47.40	TP-73	1756
04	08	1972	0716	84	09.40	-083	52.20	TP-74	1775
07	08	1972	0745	84	10.50	-083	50.30	TP-75	1658
22	08	1972	0656	84	07.90	-084	21.00	TP-76	1478
20	09	1972	0646	83	45.80	-088	53.30	TP-77	1475
21	09	1972	0255	83	45.50	-088	48.40	TP-78	1472
23	09	1972	0709	83	44.9	-088	36.4	TP-79	1458
01	05	1973	0807	83	42.1	-085	24.5	TP-80	1629
04	05	1973	0031	83	41.3	-085	30.3	TP-81	1609
12	05	1973	0224	83	41.1	-085	26.5	TP-82	1600
03	11	1973	0621	(83	49.5	-081	24.0)	TP-83	1321

DETAILED BOTTOM TEMPERATURE PROFILES (SUCCESSFUL)

~~14~~	~~1~~	~~1969~~	~~744~~	~~84~~	~~47.59~~	~~-130~~	~~35.76~~	~~DBP- 1~~	~~2436~~
18	3	1969	1519	84	34.81	-128	25.85	DBP- 3	2588
31	3	1969	1811	84	40.04	-127	9.38	DBP- 4	2567
14	2	1970	0020	84	27.1	-112	36.5	DBP- 5	1447
14	8	1970	0027	84	27.7	-106	58.9	DBP- 7	1278
10	9	1970	2346	84	49.1	-099	26.3	DBP- 8	1965
19	9	1970	0704	84	49.3	-099	32.8	DBP- 9	1996
23	9	1970	0941	84	49.5	-098	44.3	DBP-10	1727
08	12	1971	0520	84	36.7	-082	23.2	DBP-11	1701
05	05	1973	0459	83	41.1	-085	28.9	DBP-12	1608

DETAILED SEDIMENT TEMPERATURES (SUCCESSFUL)

05	09	1973	0405	83	41.1	-085	26.3	DST-02	1608
11	11	1973	0008	(83	51.3	-078	50.0)	DST-05	1304

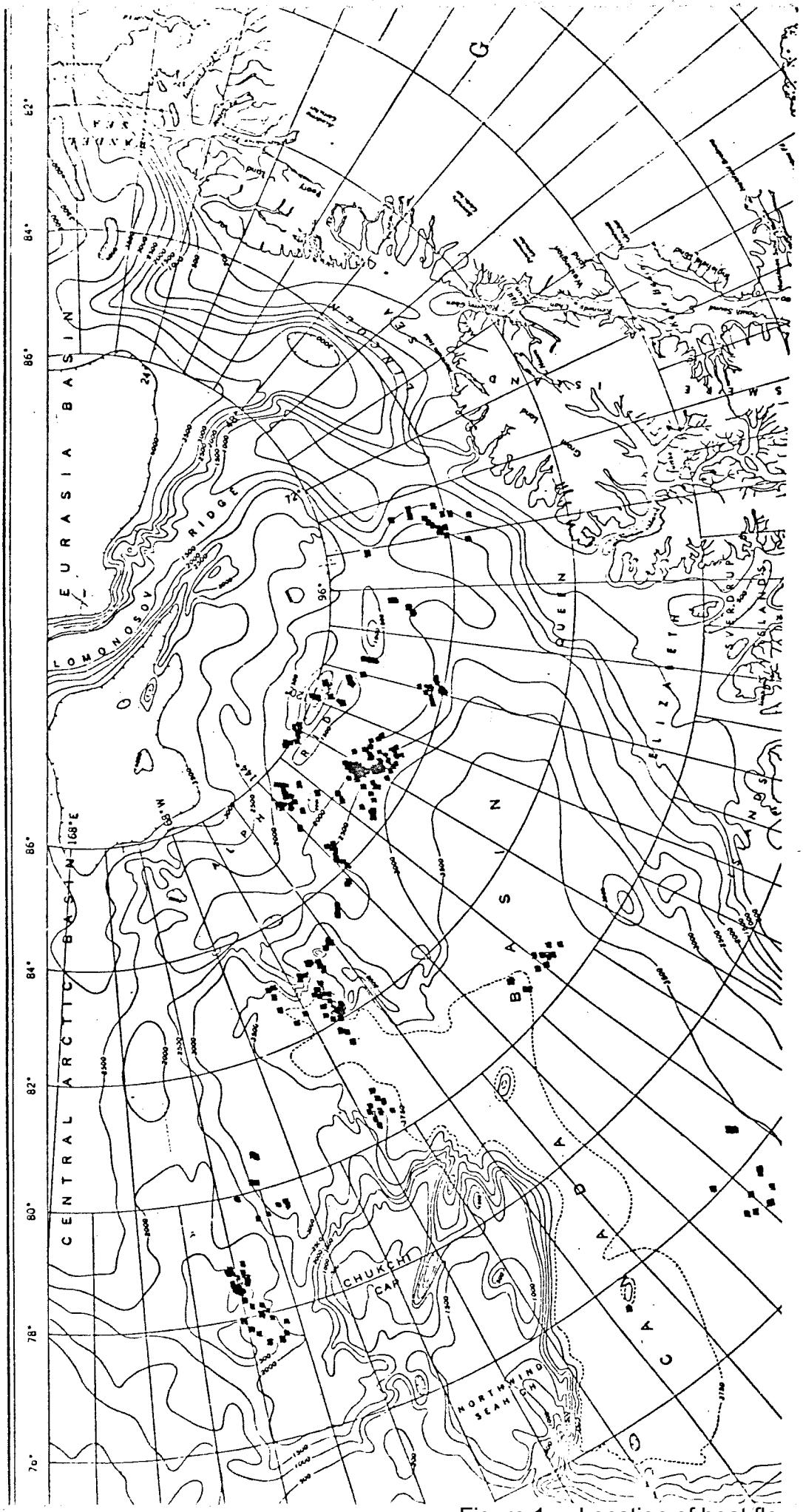

Figure 1. Location of heat flow stations.

FIG 1 LOCATION OF HEAT FLOW STATIONS

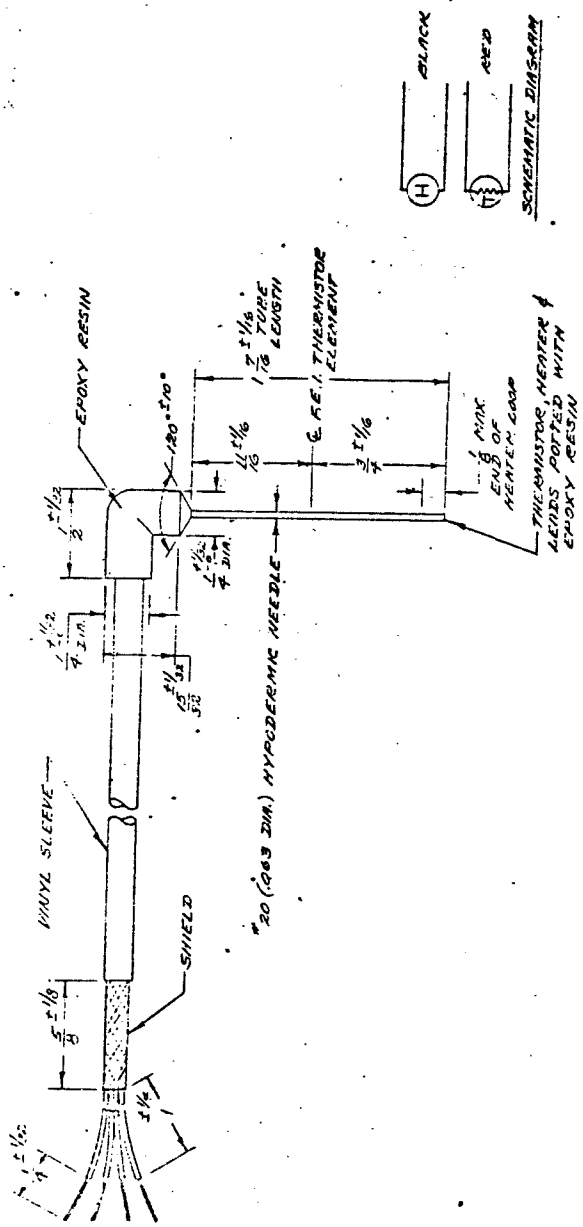

FIG 2 THERMAL CONDUCTIVITY PROBE

Figure 2. Schematic of thermal conductivity probe.

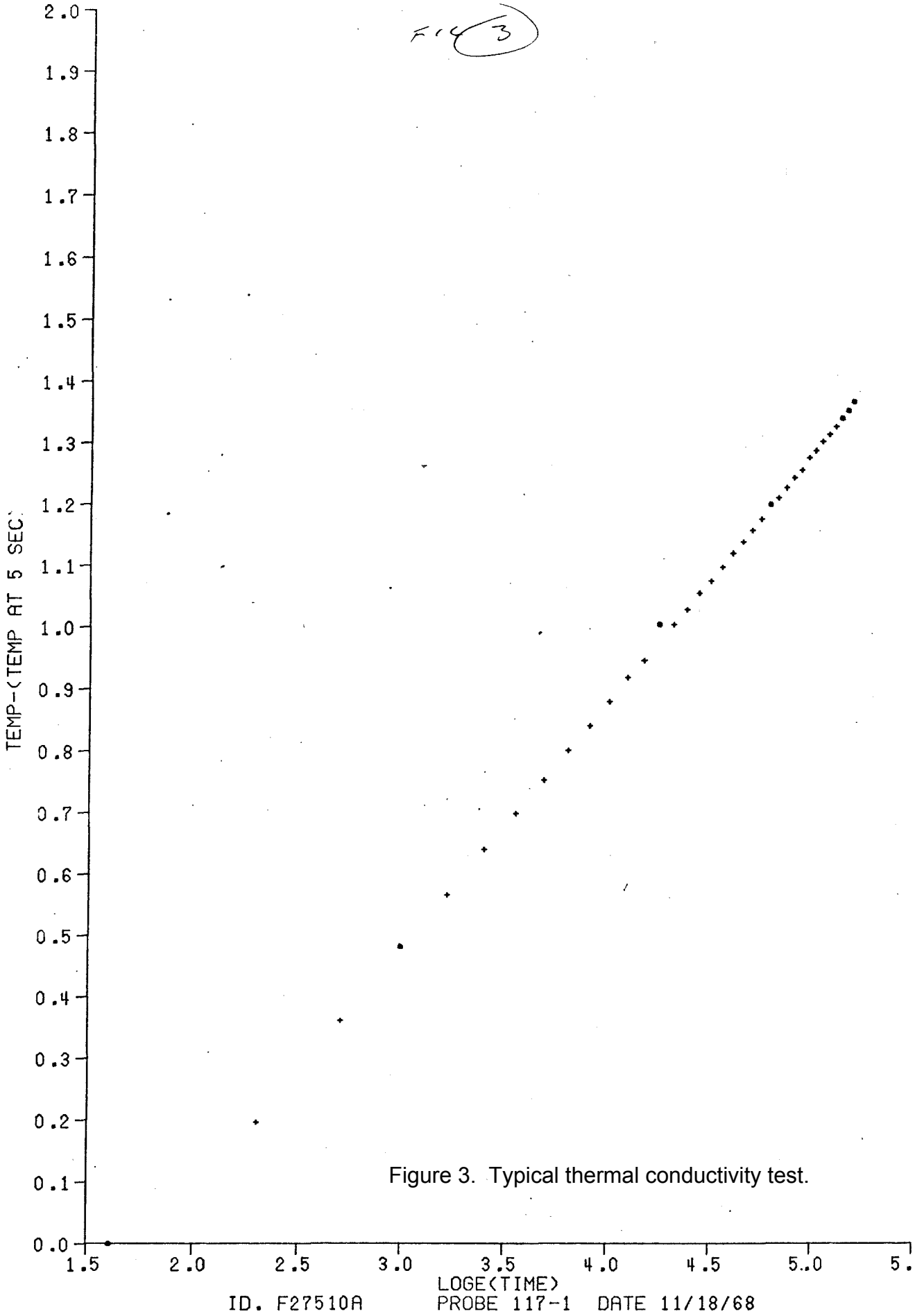

Figure 3. Typical thermal conductivity test.

IDENTIFICATION: F27510A HOLE DEPTH: PROBE: 117 TRIAL: 1 DATE: 11/18/68
CURRENT: 92.000 PROBE CONST: 0.14590
DEL TIME: DRIFT=60, RUN= 5 DEPTH= 2881.00 TEMP= 0.0 COR= -0.03880 EPS= 0.005

DRIFT...RESISTANCE	DEL RES.	TEMPERATURE	TIME	DRIFT SLOPE
4542.5		21.7383	0	
4542.5	0.0	21.7383	60	
4542.1	0.4	21.7406	120	
4541.9	0.2	21.7418	180	
4541.4	0.5	21.7446	240	0.000027

RUN.....RESISTANCE	TEMPERATURE	TIME	CONDUCTIVITY	DEL THETA	LEAST SQUARE SOLUTIONS INIT.PT.	SLOPE	CONDUCTIVITY	POINTS
4541.4	21.745	0 8PTS	3.2525 MC/CSC	0.16057	22.845	0.4017	2.9552	1-15
4233.9	23.574	5- 40	3.3221	-0.081863 *	22.848	0.4011	2.9594	4-20
4202.2	23.771	10- 45	2.9626	-0.000534	-101.090	11.6330	0.1020	4-36
4176.0	23.935	15- 50	2.9722	-0.001846				
4156.9	24.055	20- 55	3.0351	-0.006744 *				
4143.6	24.139	25- 60	2.9782	-0.001358				
4131.9	24.214	30- 65	2.9615	-0.002380				
4122.8	24.272	35- 70	2.9701	0.001617				
4114.3	24.326	40- 75	2.6680	0.001007				
4106.7	24.375	45- 80	2.9768	-0.000290				
4100.5	24.414	50- 85	2.8493	0.002335				
4094.4	24.453	55- 90	2.9301	0.001511				
4088.2	24.493	60- 95	3.2388	-0.003357				
4084.0	24.520	65-100	2.9596	0.001801				
4074.9	24.579	70-105	3.5981	-0.027161 *				
4074.9	24.579	75-110	3.0142	0.000687				
4071.2	24.603	80-115	2.9325	0.002762				
4067.0	24.630	85-120	3.0237	0.0				
4064.0	24.649	90-125	2.7745	0.003601				
4060.5	24.672	95-130	2.9039	0.002747				
4057.0	24.694	100-135	2.8281	0.000687				
4054.1	24.713	105-140	2.8677	0.001572				
4051.2	24.732	110-145	3.0044	0.001480				
4048.4	24.750	115-150	2.7829	0.001205				
4044.8	24.773	120-155	3.0275	-0.005127 *				
4043.1	24.784	125-160	2.7587	0.000336				
4040.5	24.801	130-165	2.7908	-0.000778				
4038.1	24.817	135-170	2.9041	-0.001175				
4036.1	24.830	140-175	2.7484	0.000473				
4033.1	24.849	145		-0.004929				
4031.2	24.861	150		-0.003647				
4029.0	24.876	155		-0.004807				
4027.1	24.888	160		-0.004333				
4025.2	24.900	165		-0.004318				
4023.2	24.913	170		-0.005386 *				
4021.2	24.926	175		-0.006729 *				
4019.1	24.940	180		-0.009094 *				

Figure 4. Digital data from typical thermal conductivity test.

FIG (4)

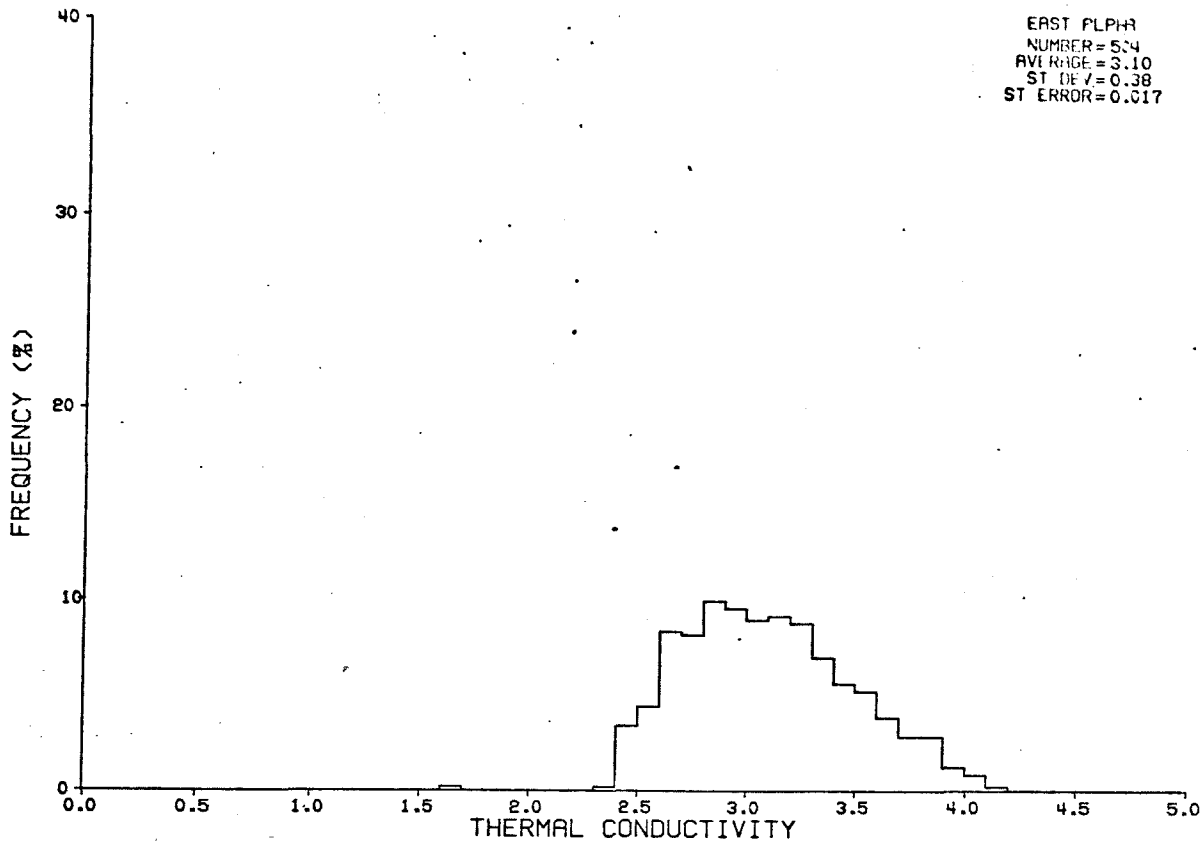

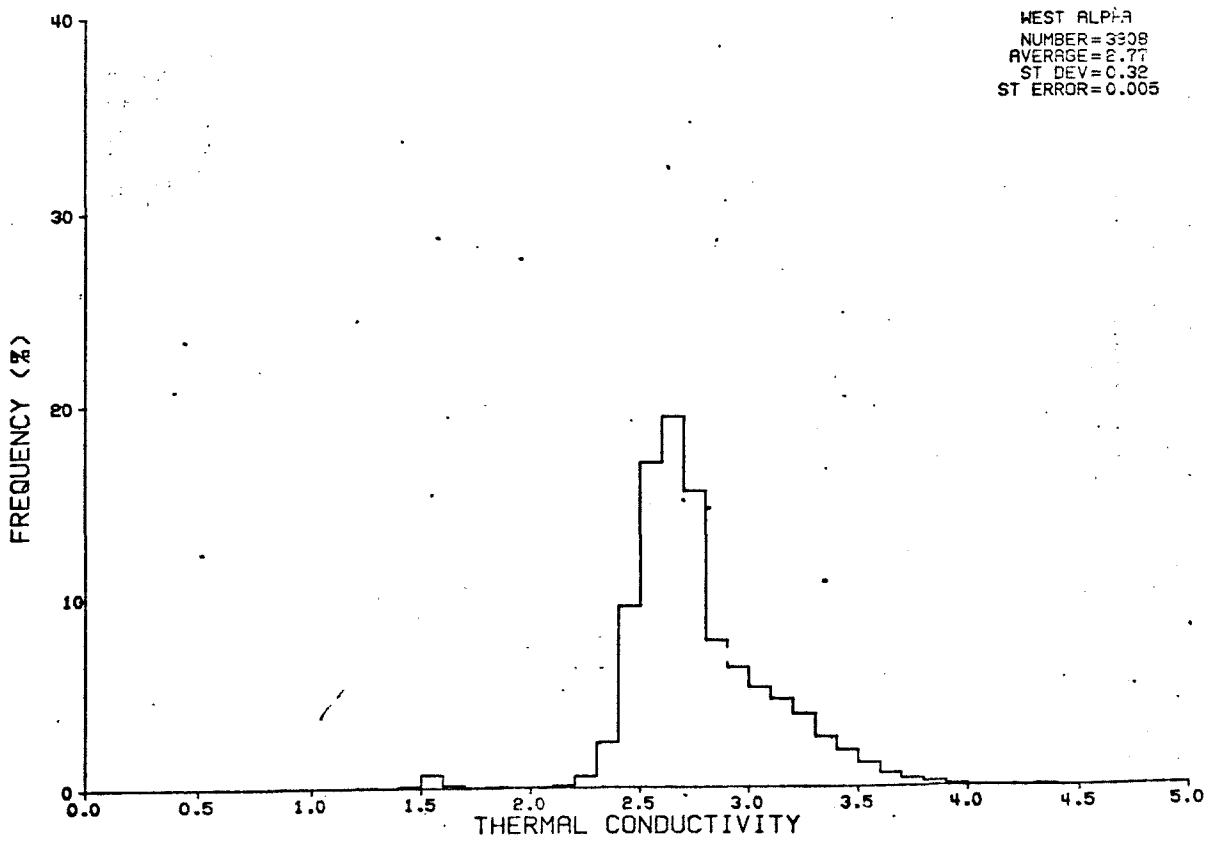

Figure 5. Histograms of thermal conductivity values from East Alpha (top) and West Alpha (bottom) ridges.

FIG 5

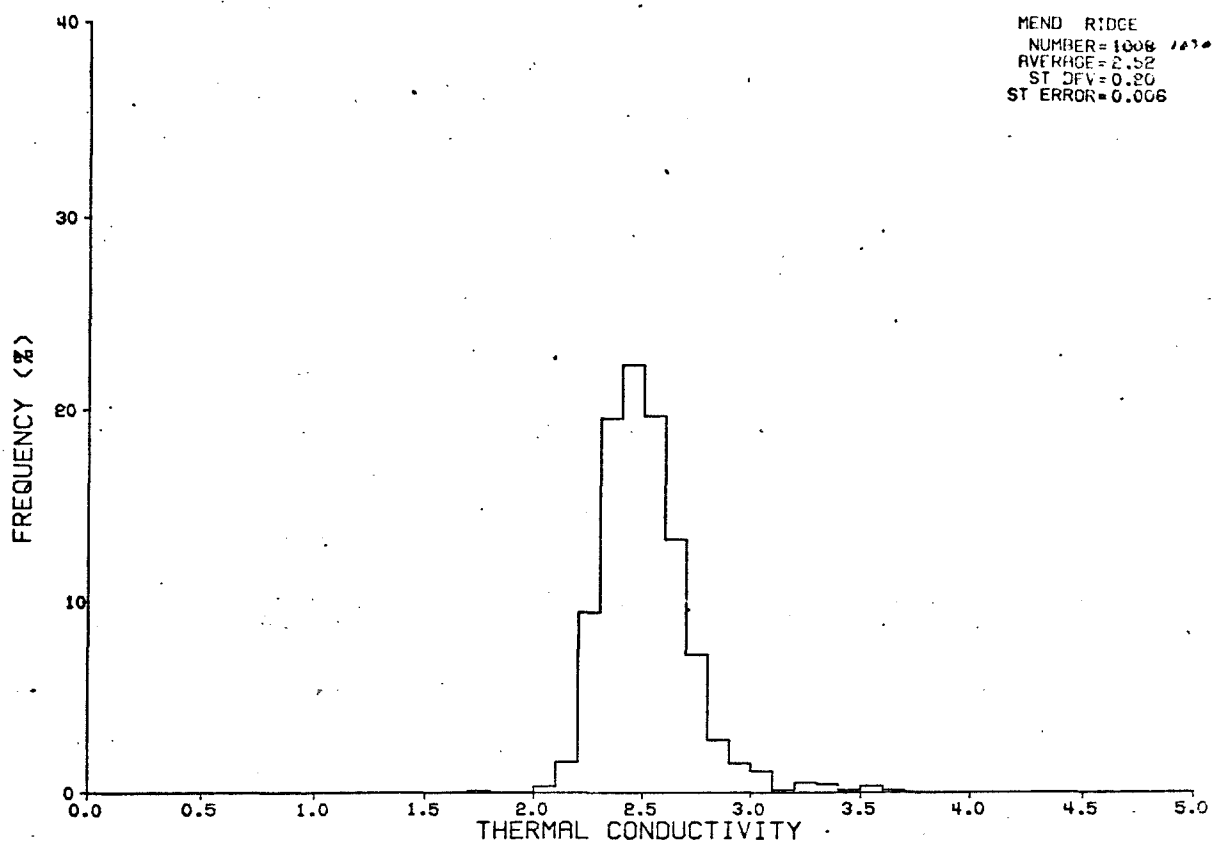

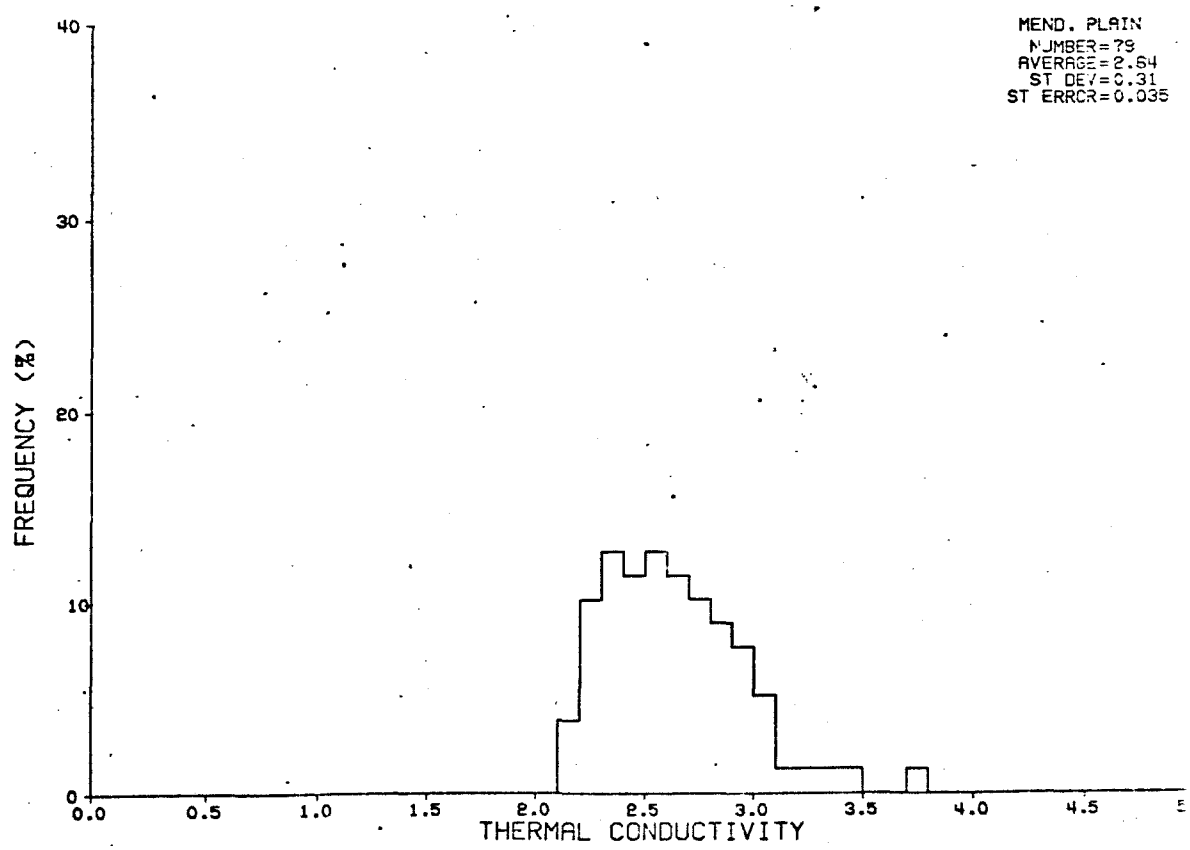

Figure 6. Histogram of thermal conductivity values from Mendeleev Ridge (top) and Mendeleev Plain (bottom).

FIG. 6

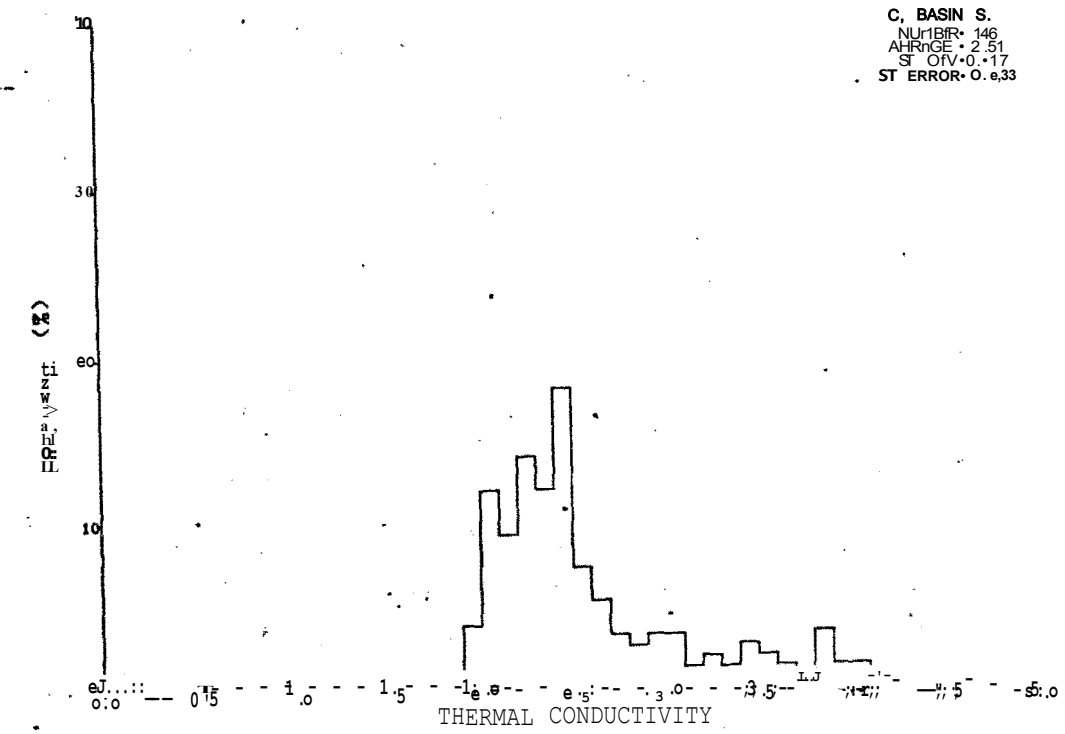

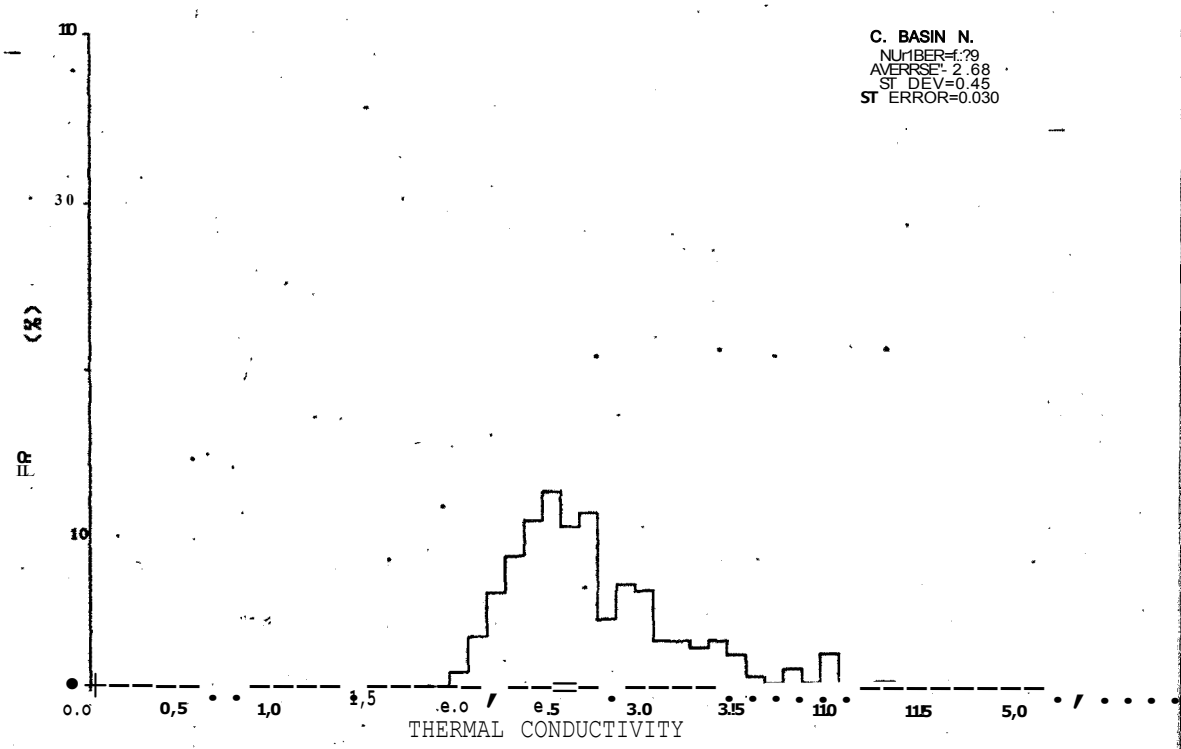

Figure 7. Histograms of thermal conductivity values from Canada Basin south (top) and Canada Basin north (bottom).

FIG 7

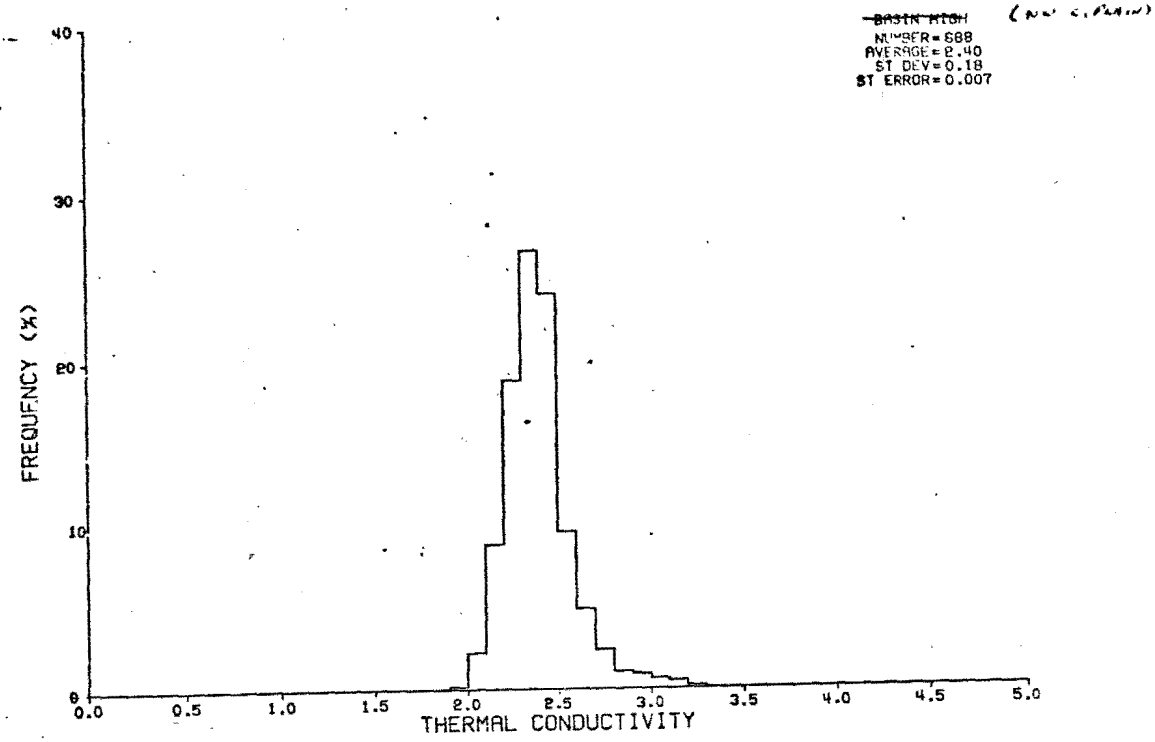

Figure 8. Histogram of thermal conductivities from NW Canada Basin, now known as the Nautilus Basin.

FIG 8

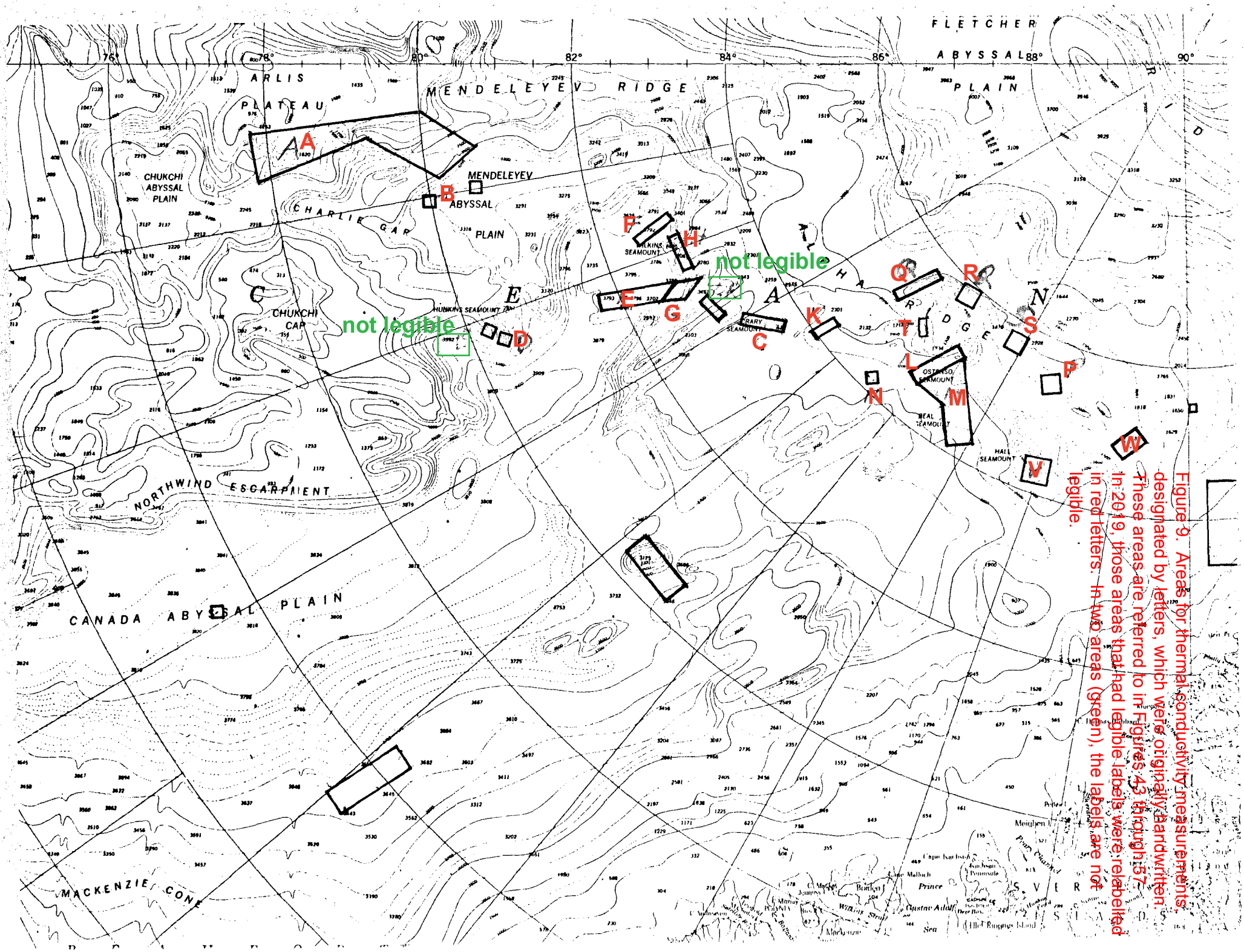

Figure 9. Areas for thermal conductivity measurements, designated by letters, which were originally handwritten. These areas are referred to in Figures 43 through 57. In 2019, those areas that had legible labels were relabelled in red letters. In two areas (green), the labels are not legible.

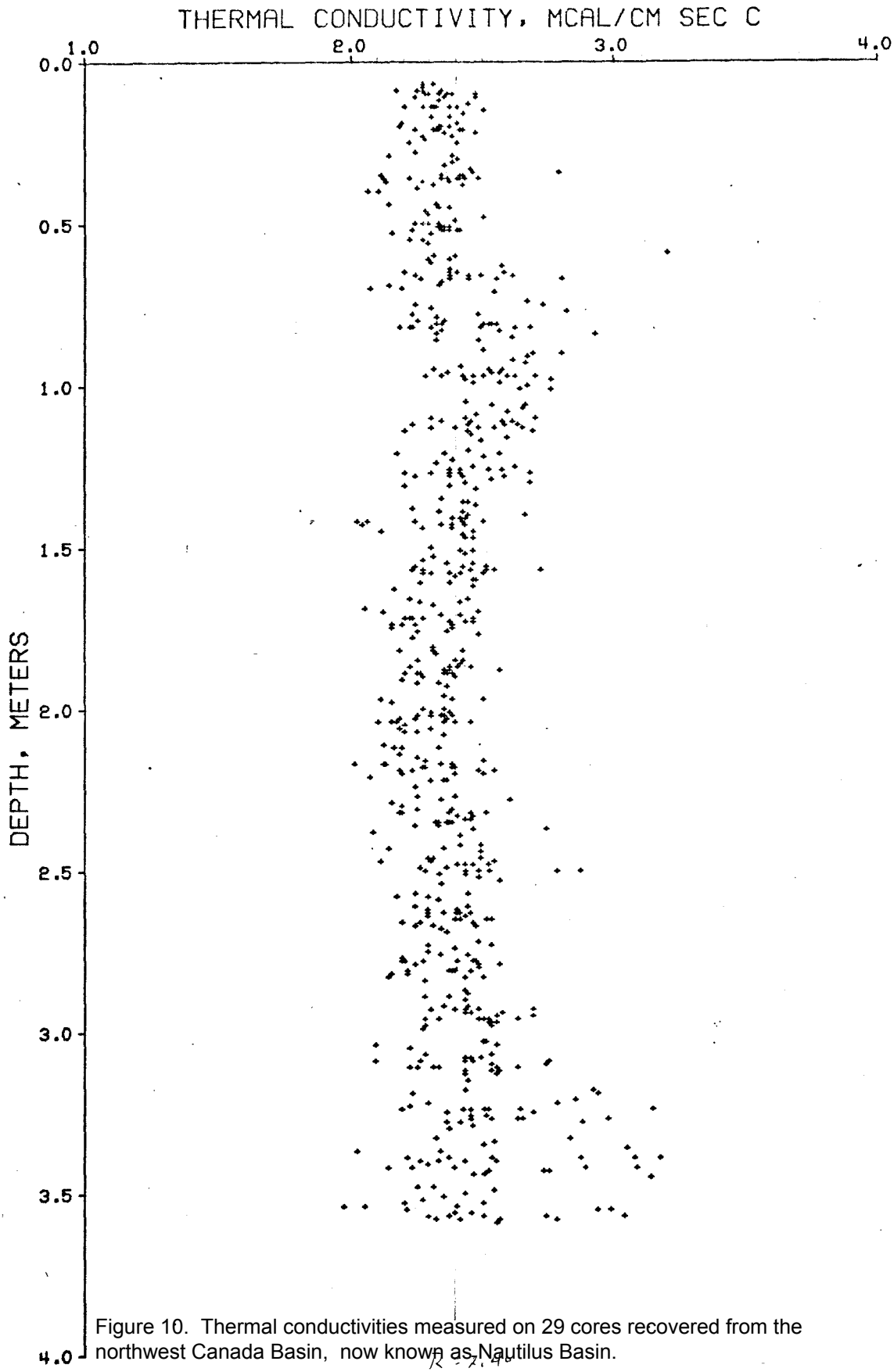

Figure 10. Thermal conductivities measured on 29 cores recovered from the northwest Canada Basin, now known as Nautilus Basin.

FIG. 10 THERMAL CONDUCTIVITIES ~~FROM~~ OF 29 CORES FROM THE NW CANADA BASIN

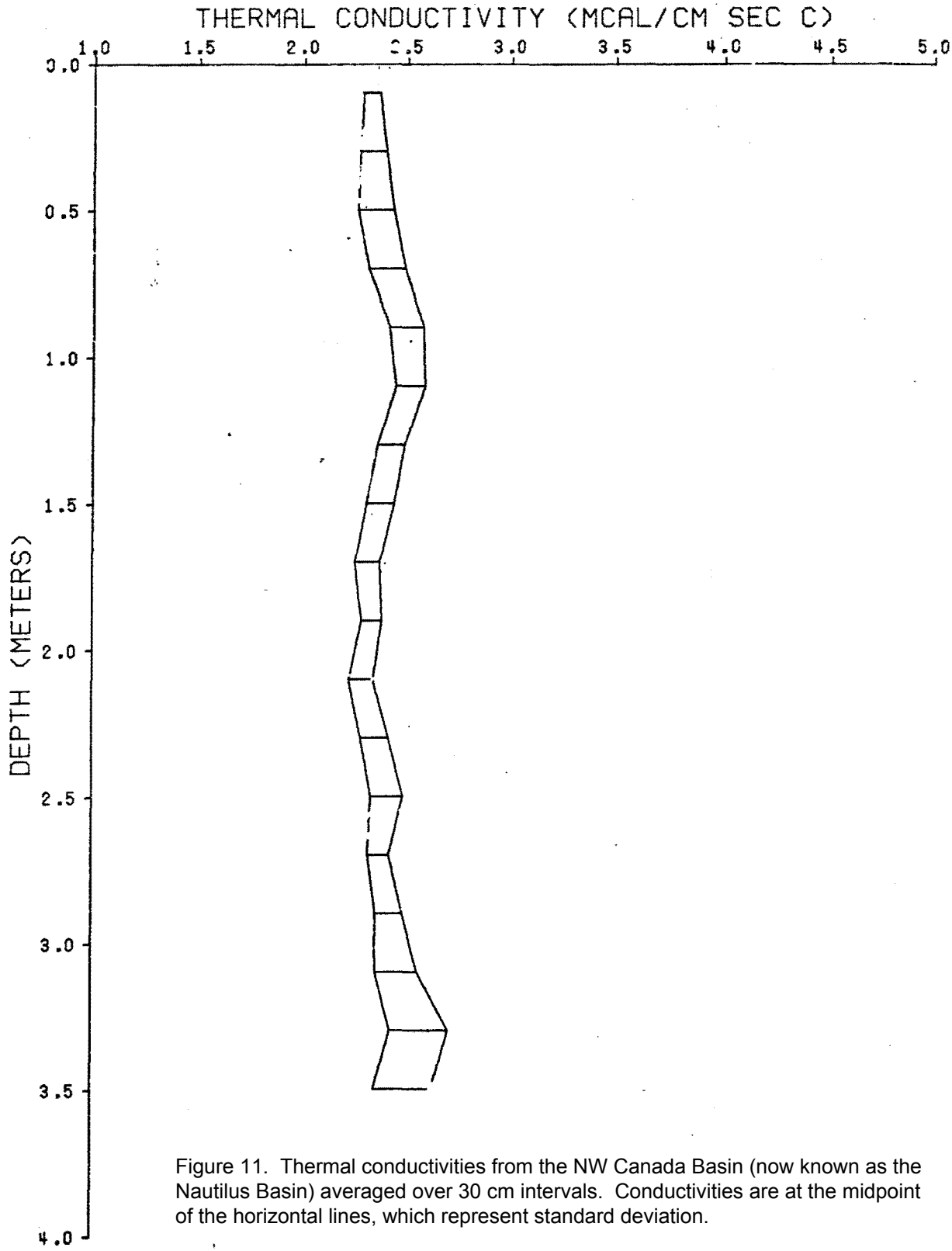

Figure 11. Thermal conductivities from the NW Canada Basin (now known as the Nautilus Basin) averaged over 30 cm intervals. Conductivities are at the midpoint of the horizontal lines, which represent standard deviation.

FIG. (11) Thermal conductivities from NW Canada Basin averaged over 30 cm depth intervals. Conductivities are at midpoint of each horizontal line, which represents standard deviation

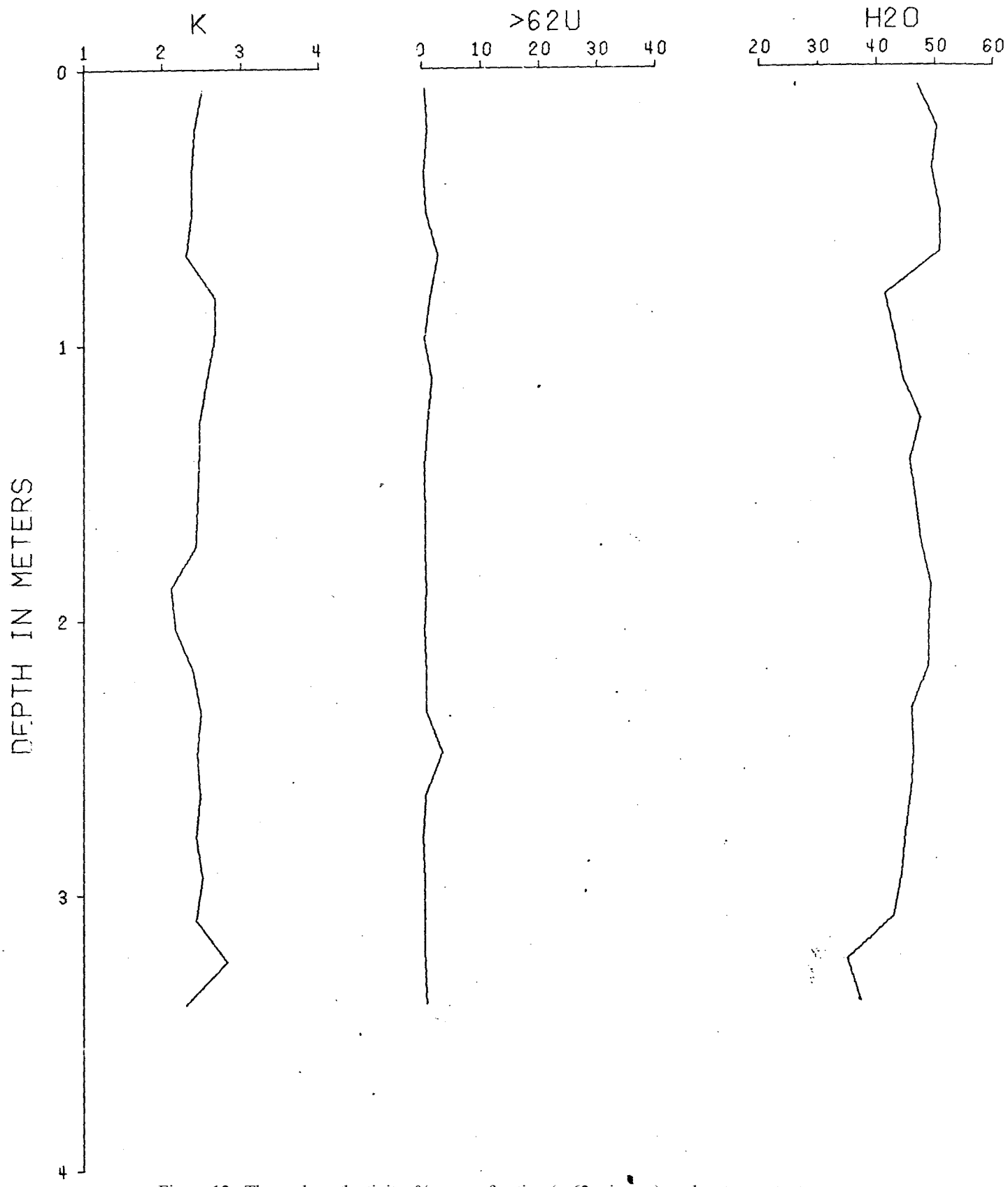

Figure 12. Thermal conductivity, % coarse fraction (> 62 microns), and water content measured on a sediment core recovered at FL-239.

FL239

Fig 13

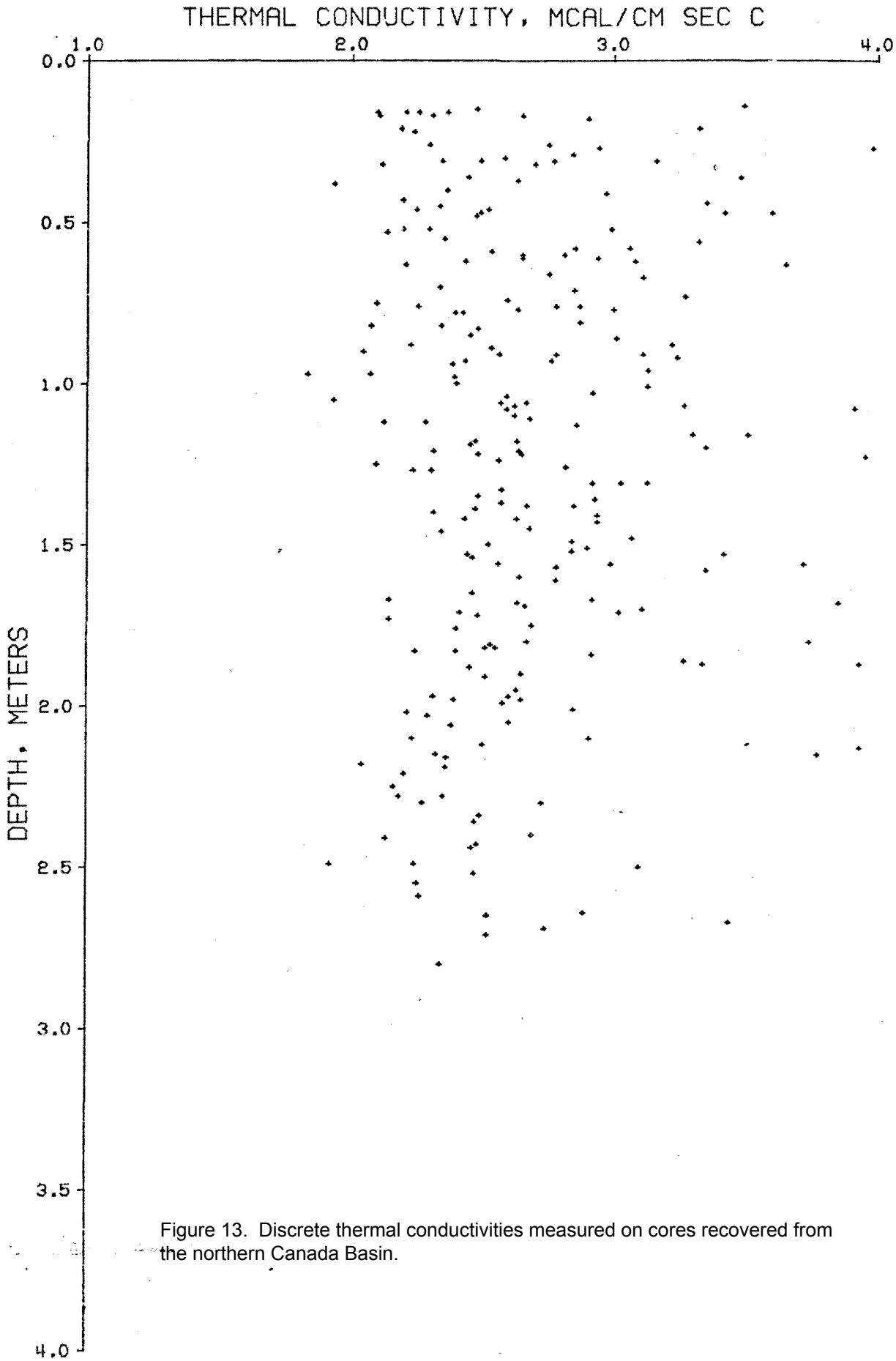

Figure 13. Discrete thermal conductivities measured on cores recovered from the northern Canada Basin.

FIG. (13) DATA FROM N. CANADA PLAIN

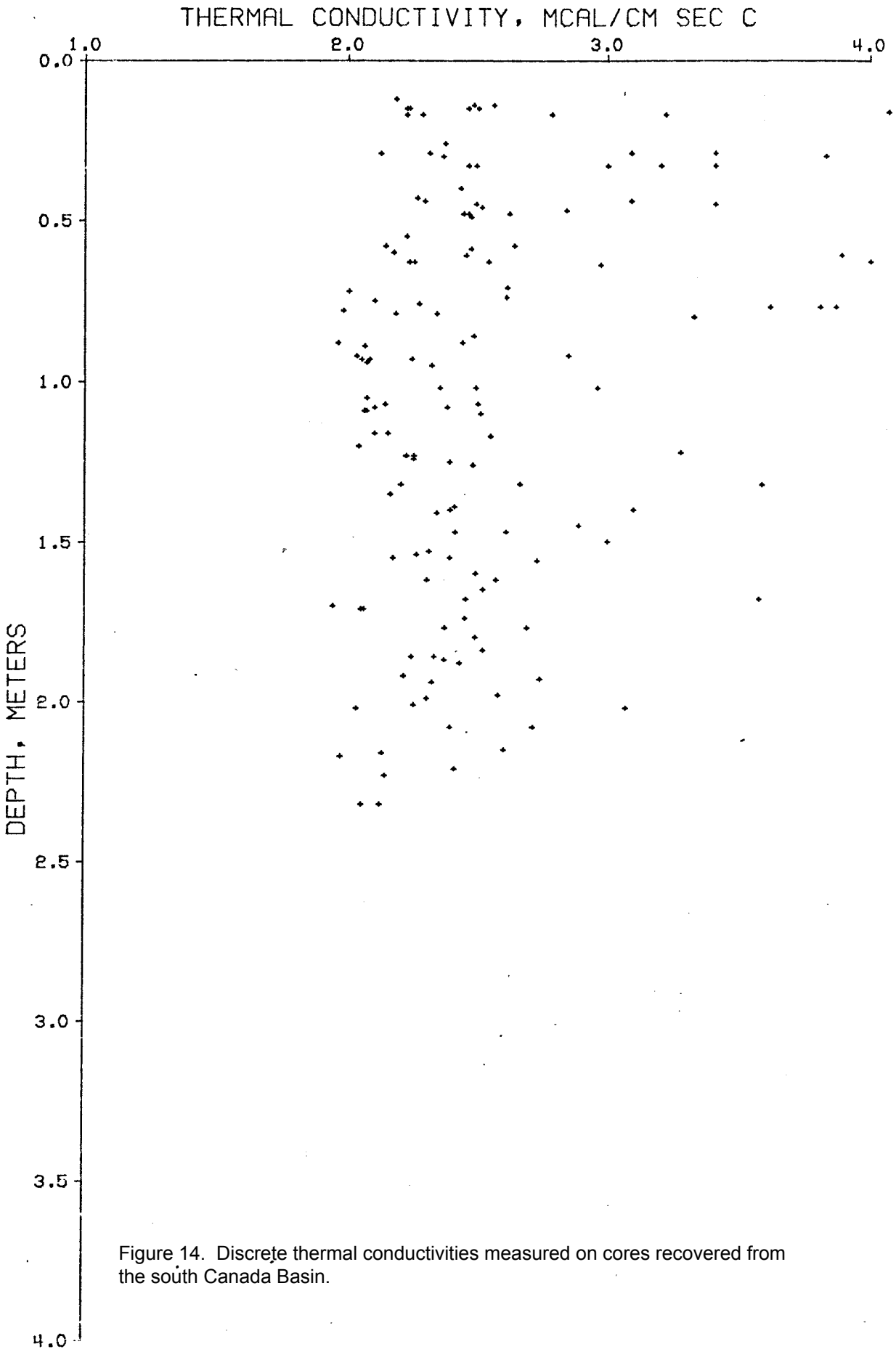

Figure 14. Discrete thermal conductivities measured on cores recovered from the south Canada Basin.

FIG. (14) DATA FROM S. CANADA BASIN

Figure 15. Thermal conductivity, % coarse fraction (> 62 microns), and water content measured on a sediment core recovered at FL-31 in the northern Canada Plain. Values are discrete measurements.

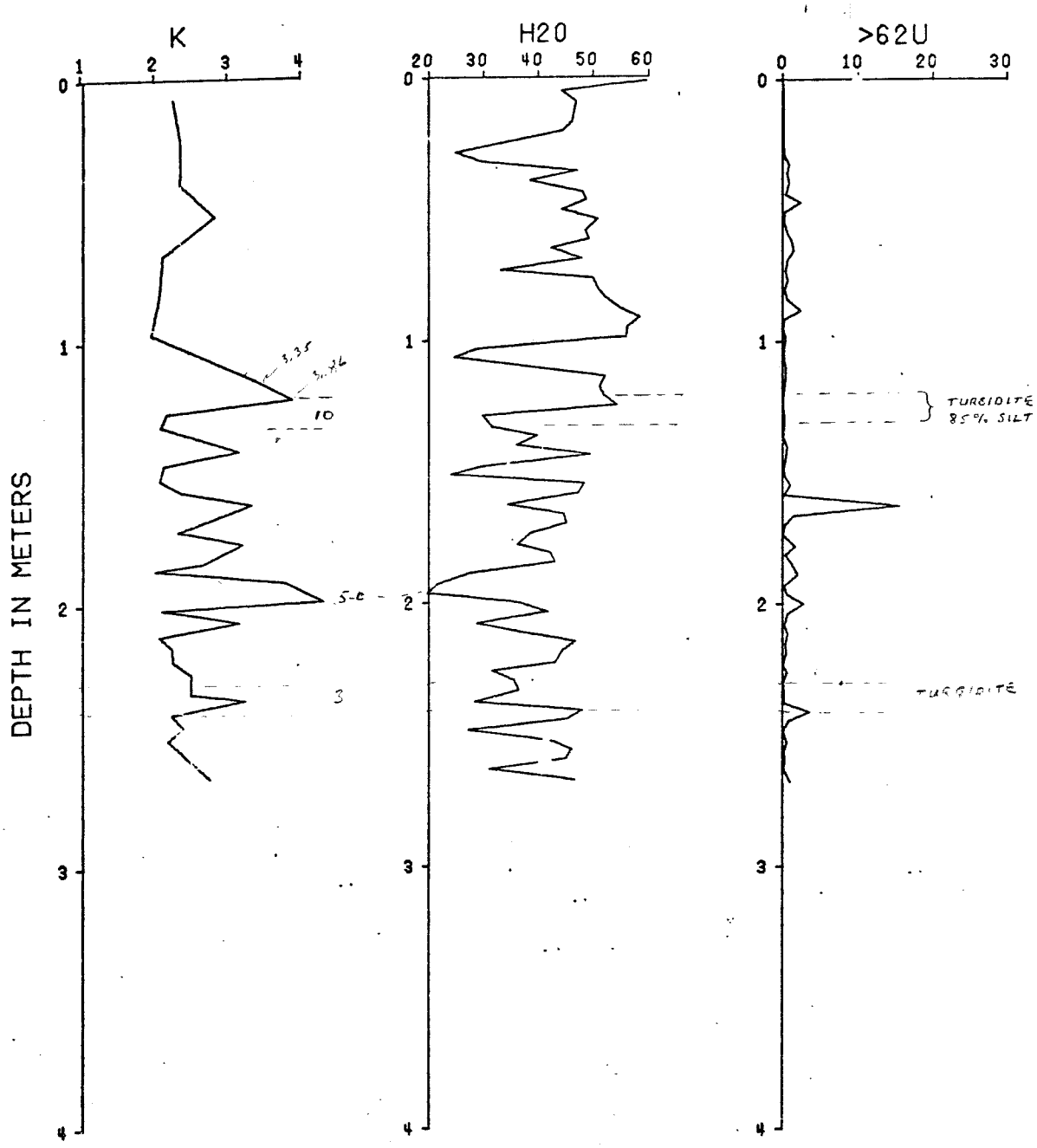

FL 31

FIG. 15 STATION FC31 was in N. CANADA PLAIN
DATA ARE SINGLE VALUES.

Figure 16. Thermal conductivity, % coarse fraction (> 62 microns), water content, and % carbonate measured in a sediment core recovered at FL-207. Values are section averages.

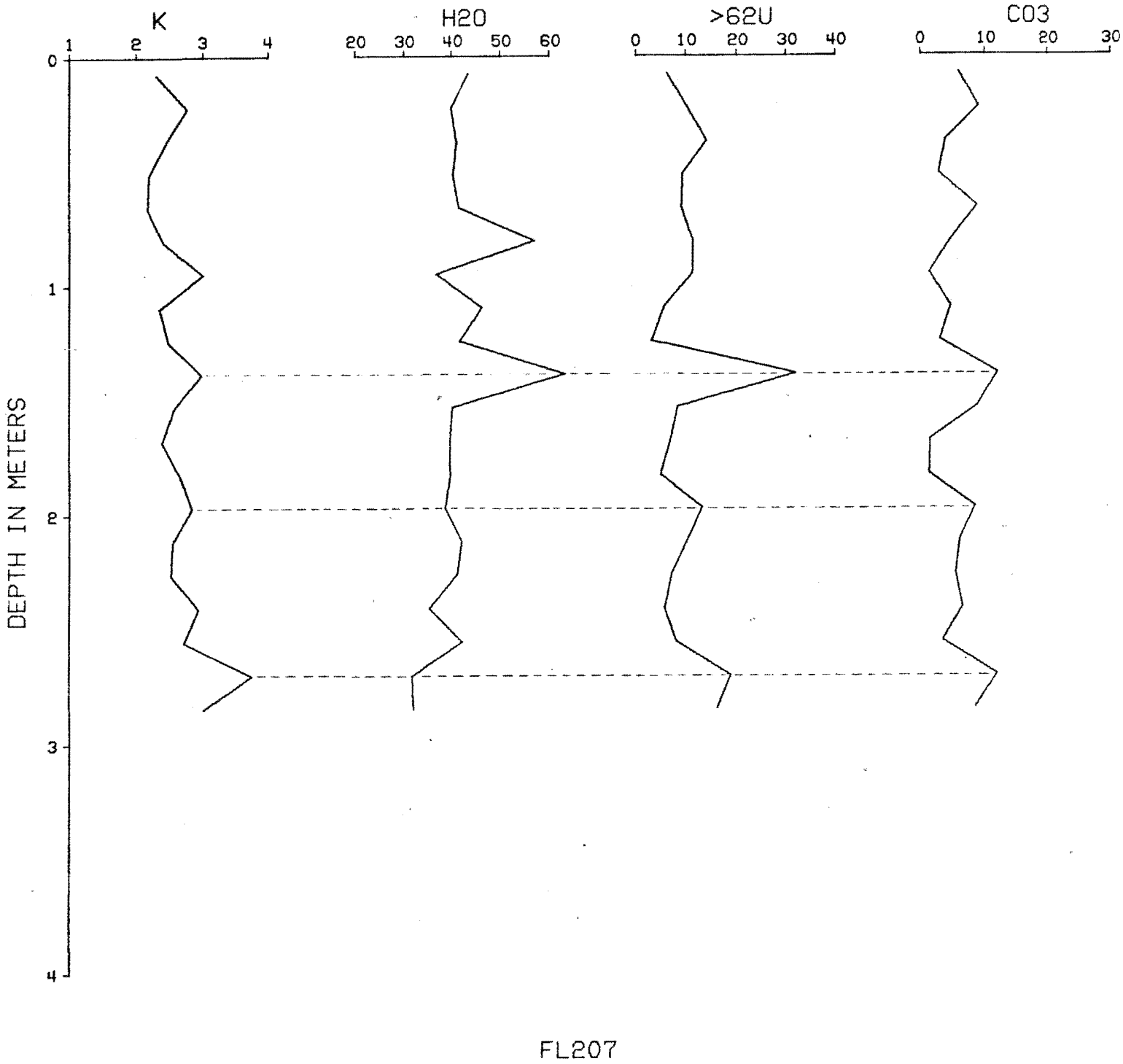

FIG. 16 HEAT FLOW STATION FL207. VALUES ARE SECTION AVERAGES.

Figure 17. 953 discrete thermal conductivities measured on sediments recovered from the Mendeleev Ridge, plotted as a function of depth beneath the seafloor.

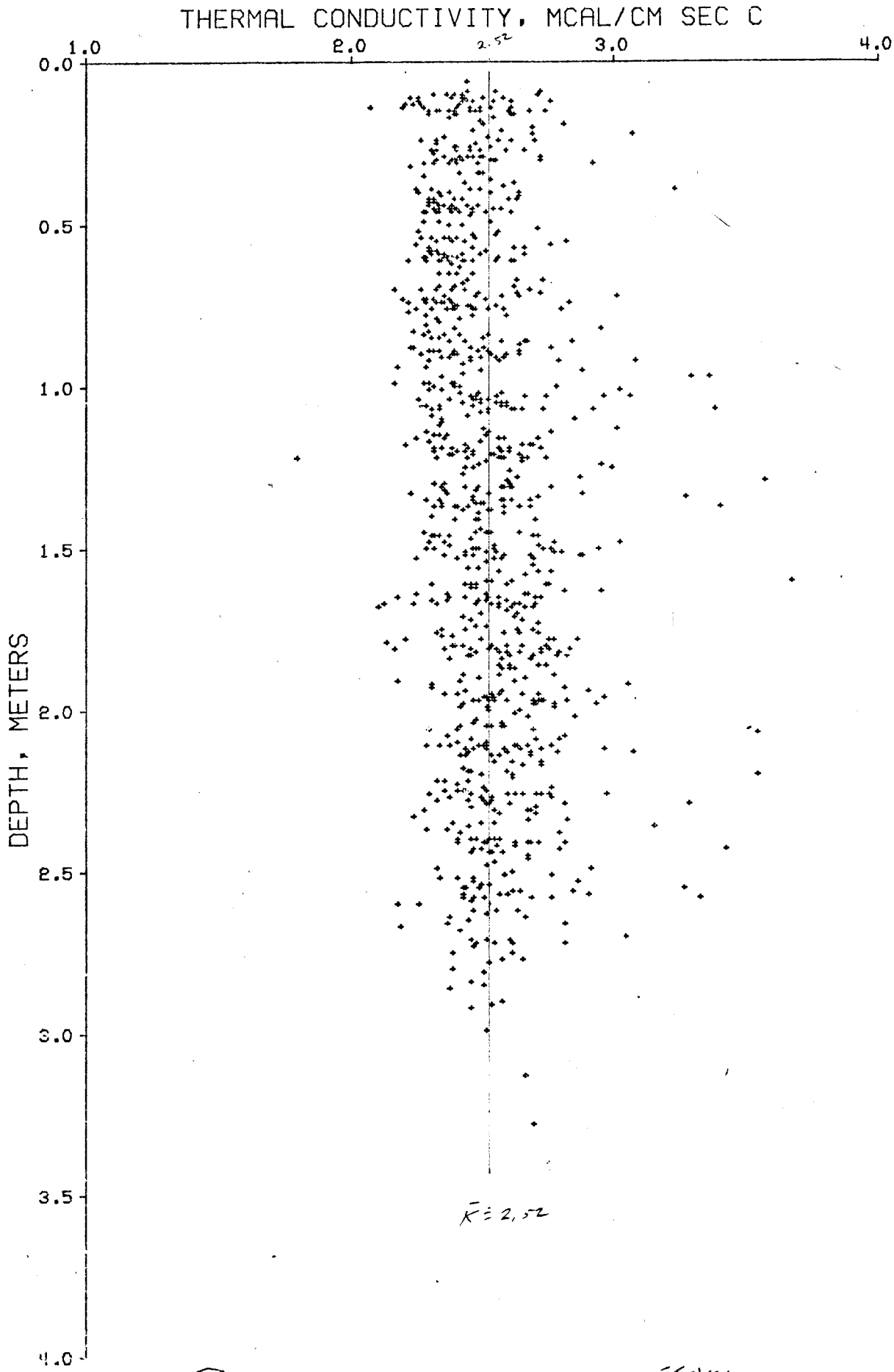

FIG. 17 THERMAL CONDUCTIVITY VALUES FROM MENDELEYEV RIDGE, 953 values.

REV. R. 9/57

Figure 18. Thermal conductivity, % coarse fraction (> 62 microns), water content, and % carbonate measured in a sediment core recovered at FL-116, Mendeleev Ridge. Values are section averages.

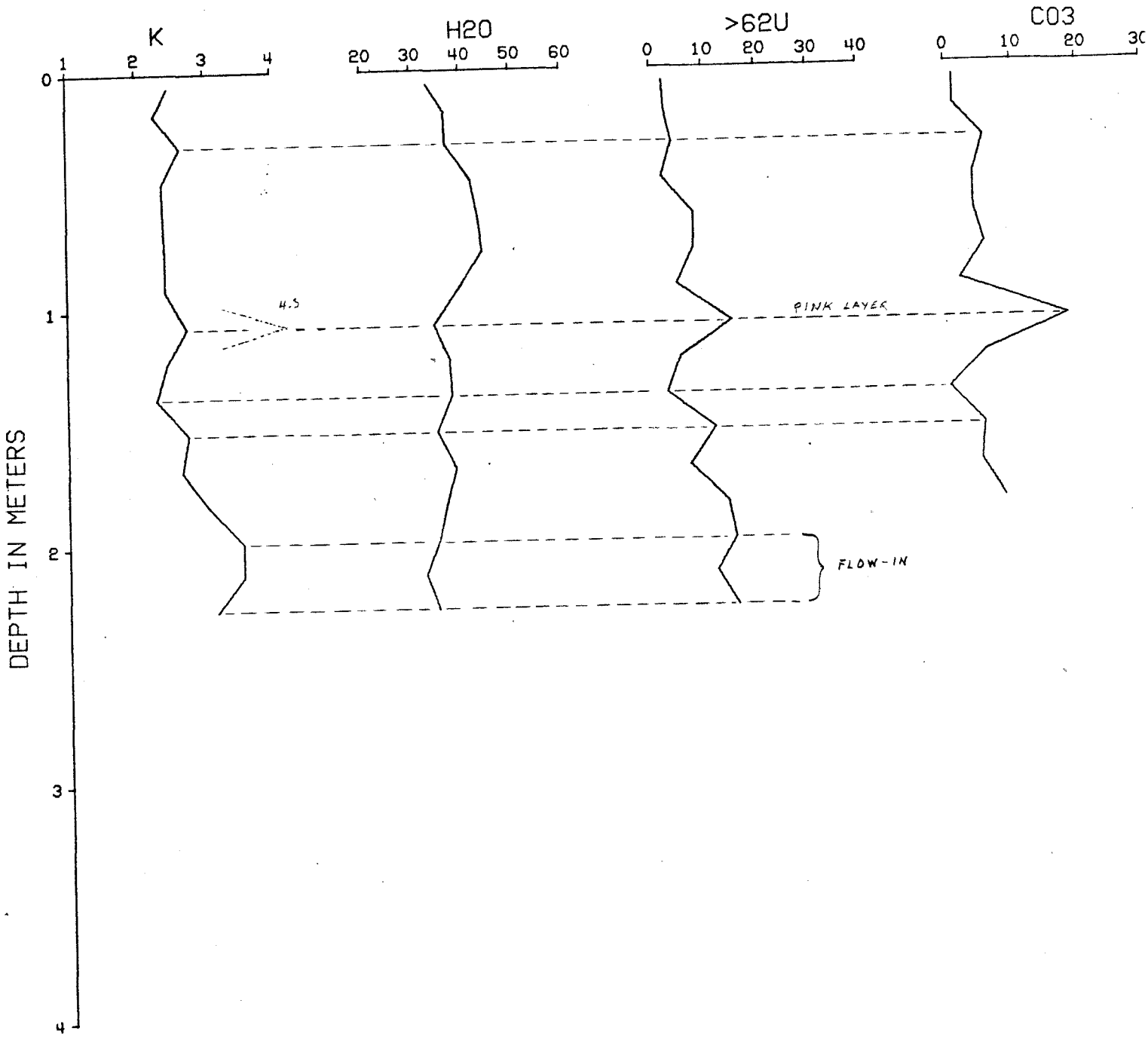

FL116

FIG (18) DATA FROM CORE FL 116. Values are core section means.

Figure 19. Thermal conductivity, % coarse fraction (> 62 microns), water content, and % carbonate measured in a sediment core recovered at FL-221, Mendeleev Plain. Values are section averages.

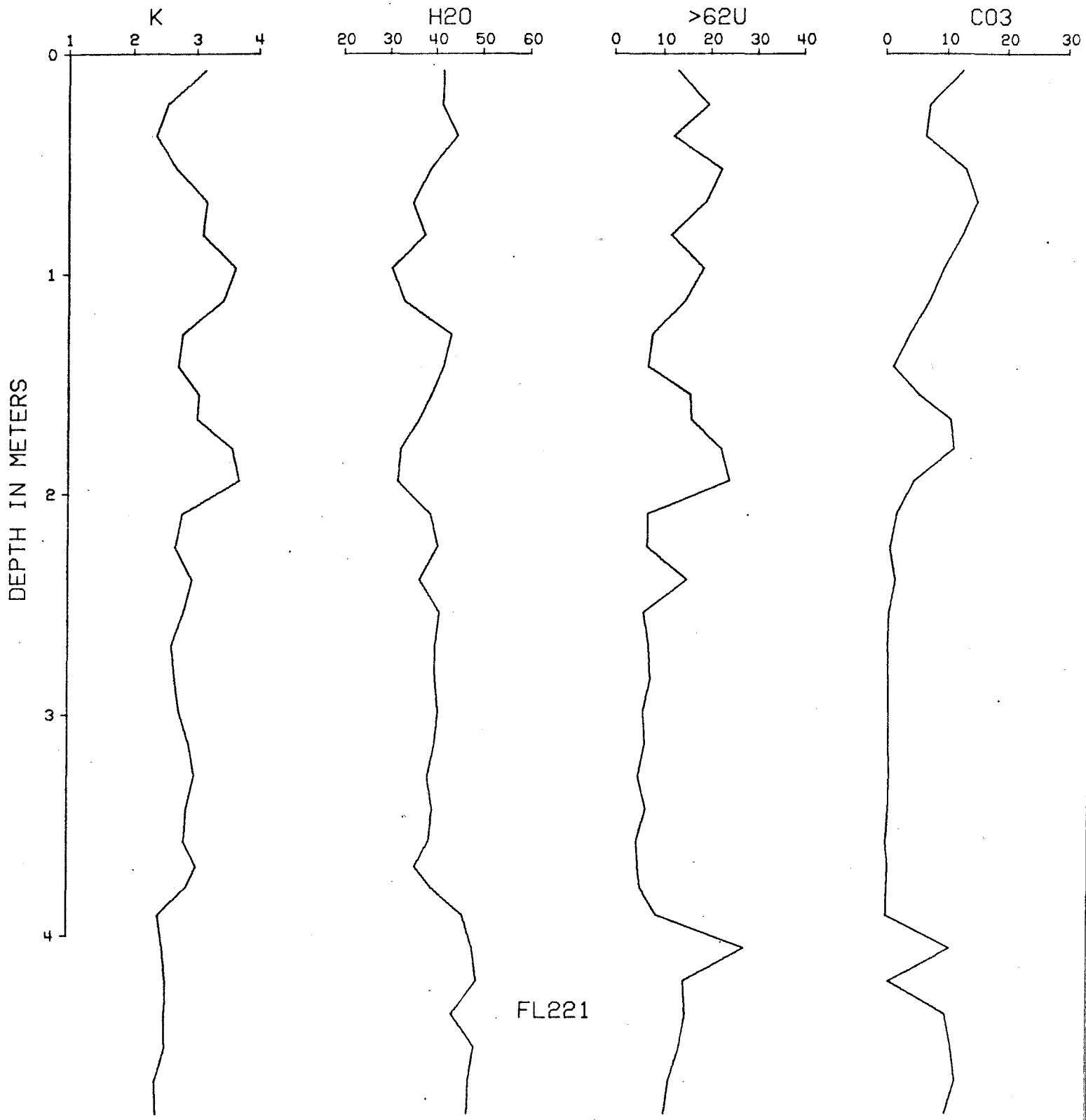

FIG. 19 SECTION MEAN VALUES

Figure 20. Thermal conductivity, % coarse fraction (> 62 microns), water content, and % carbonate measured in a sediment core recovered at FL-216, Mendeleev Plain. Values are discrete measurements.

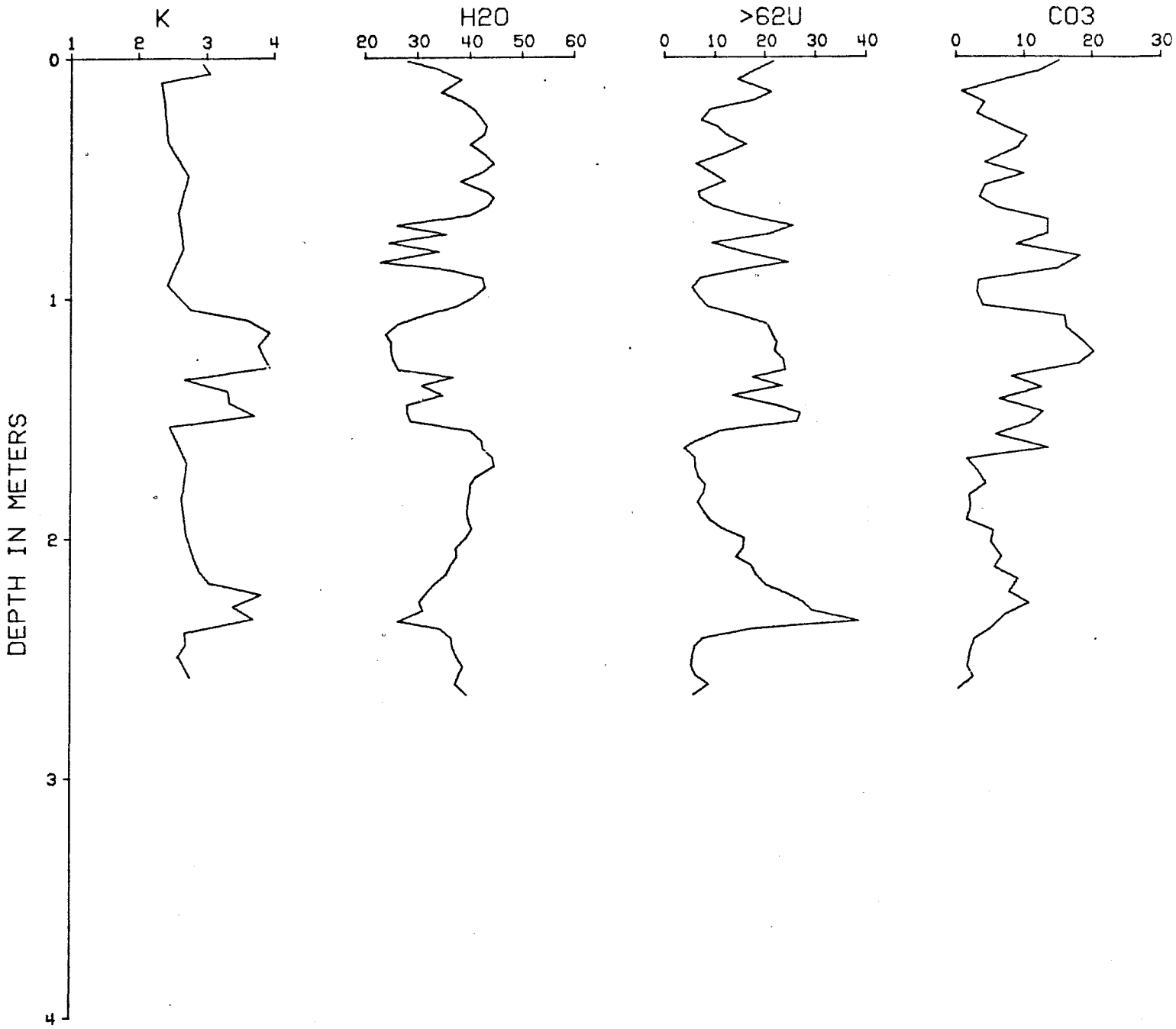

FL216

FIG. (20) INDIVIDUAL VALUES

Figure 21. Thermal conductivity, % coarse fraction (> 62 microns), water content, and % carbonate measured in a sediment core recovered at FL-223, Mendeleev Plain. Values are discrete measurements.

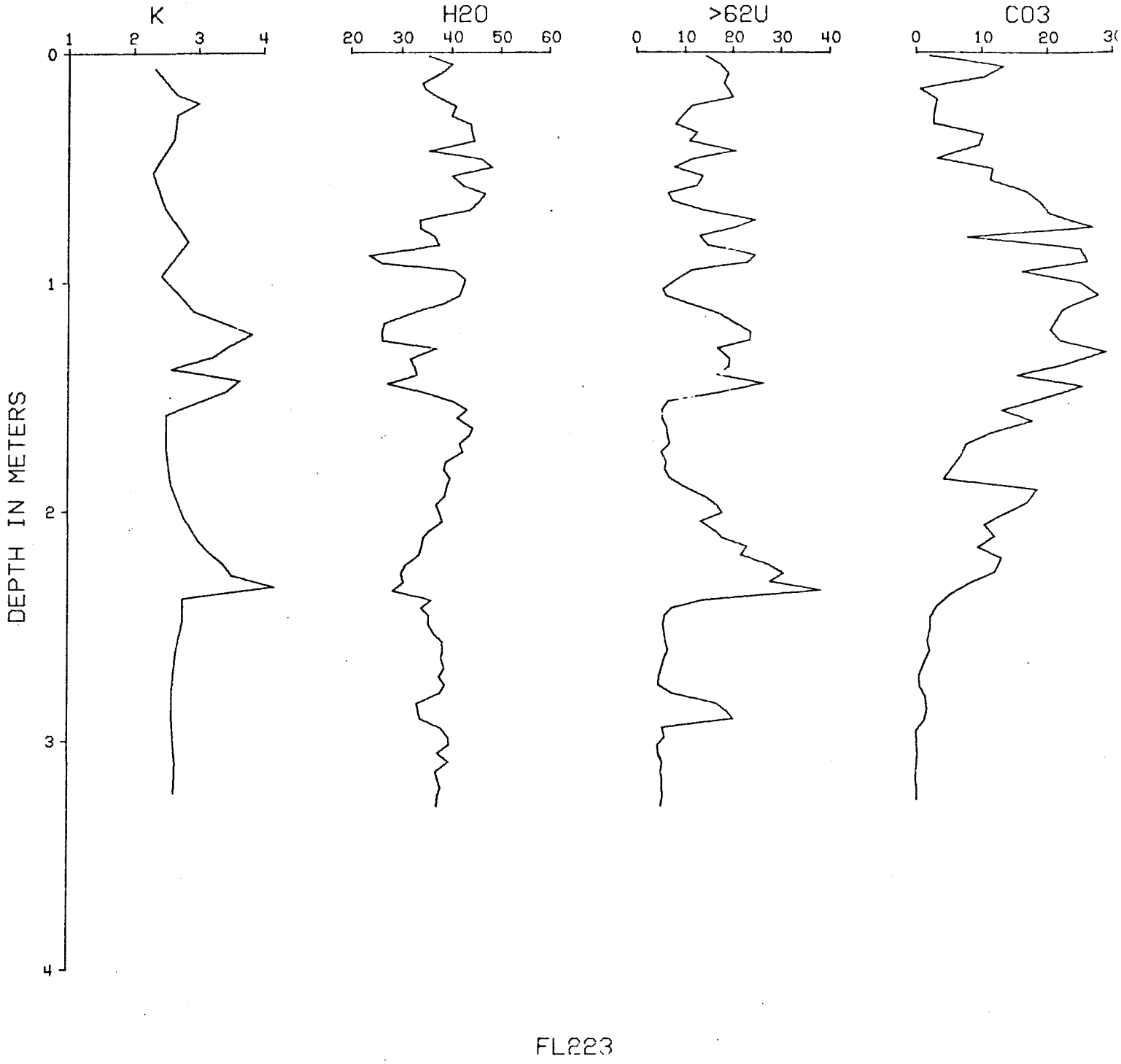

FIG (21) INDIVIDUAL VALUES

Figure 22. Thermal conductivity, % coarse fraction (> 62 microns), water content, and % carbonate measured in a sediment core recovered at FL-322, Alpha Ridge. Values are discrete measurements.

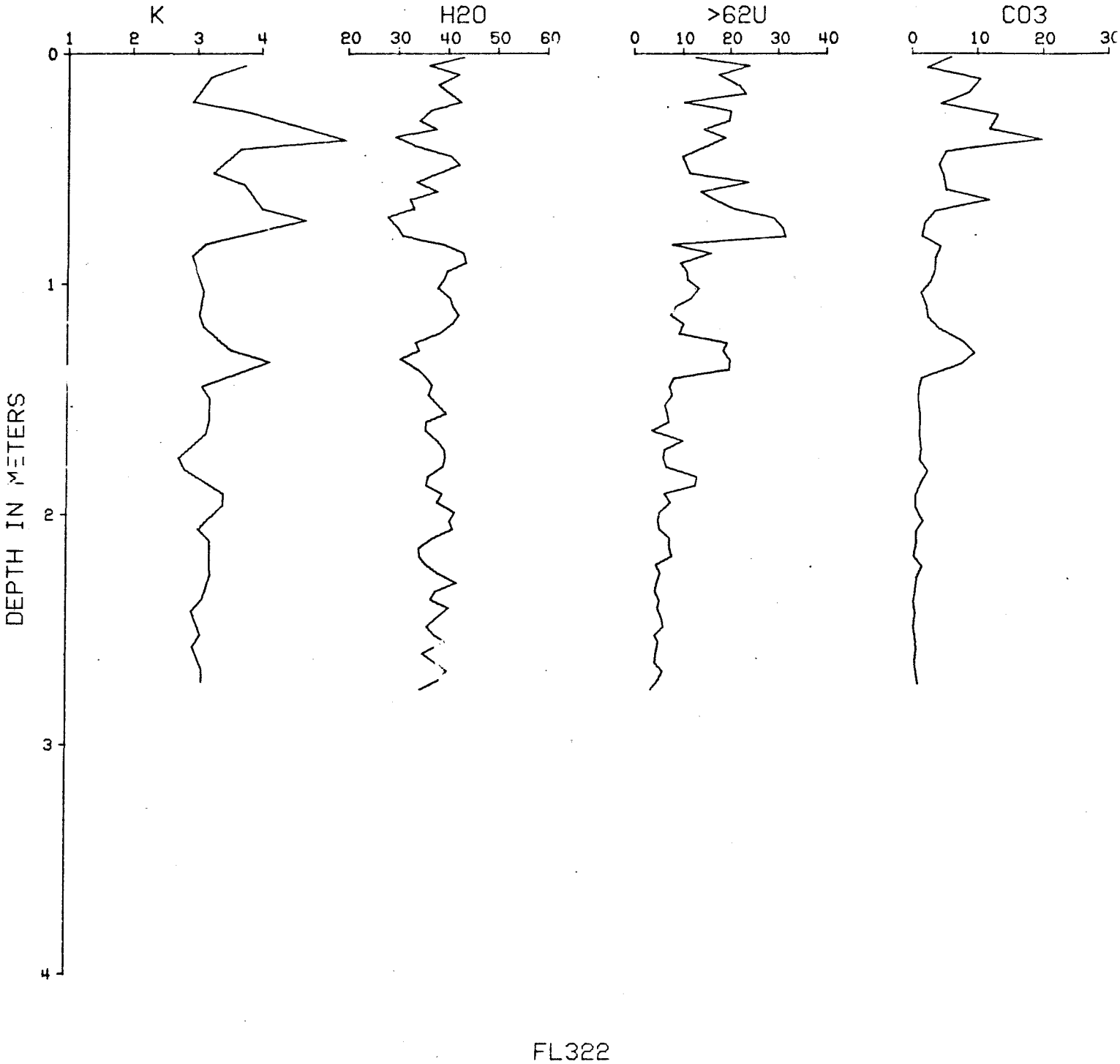

FIG. (22) INDIVIDUAL VALUES

Figure 23. Thermal conductivity, % coarse fraction (> 62 microns), water content, and % carbonate measured in a sediment core recovered at FL-326, Alpha Ridge. Values are discrete measurements.

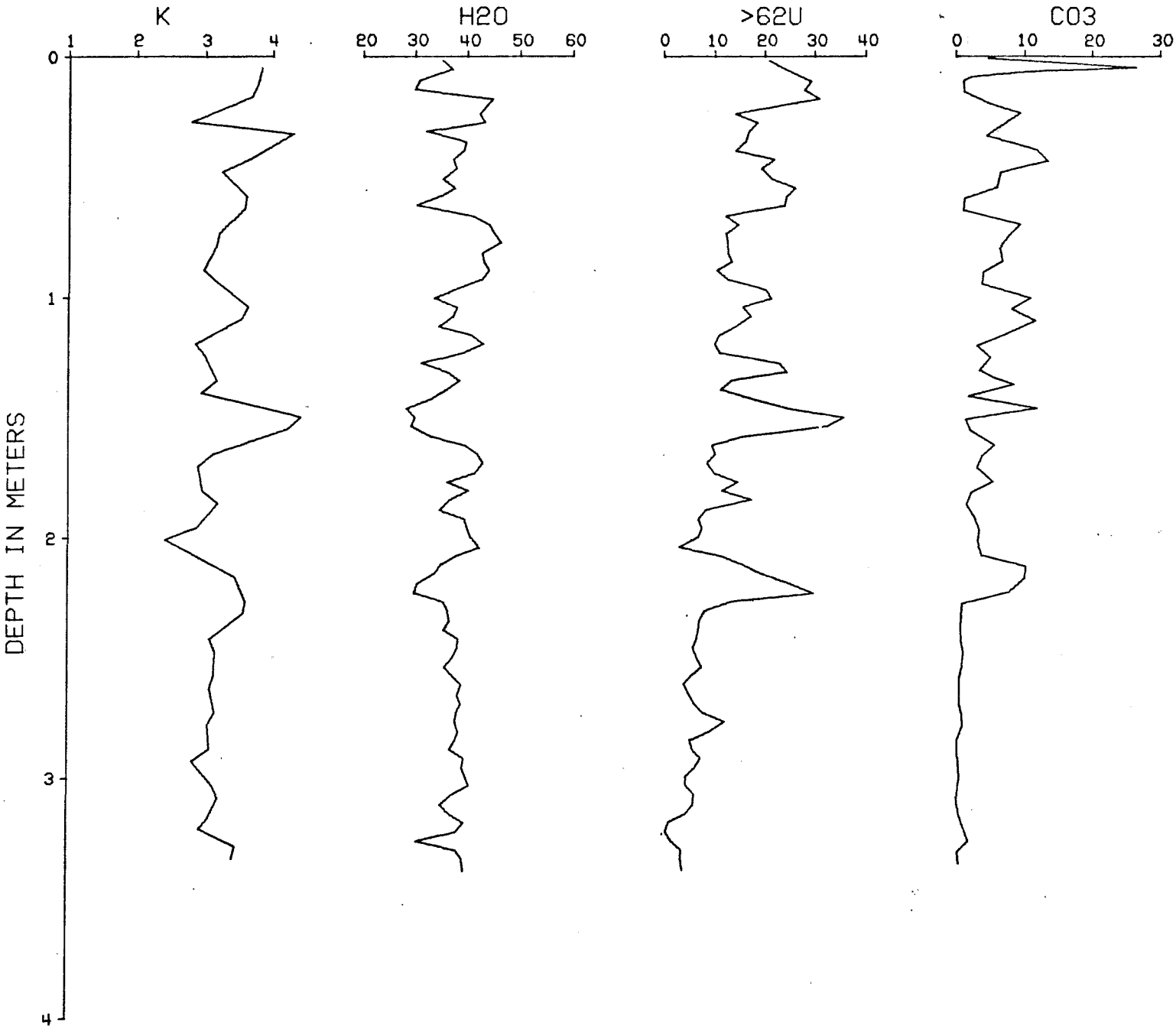

FL326

FIG (23) INDIVIDUAL VALUES

Figure 24. Thermal conductivity, % coarse fraction (> 62 microns), water content, and % carbonate measured in a sediment core recovered at FL-395, Alpha Ridge. Values are discrete measurements.

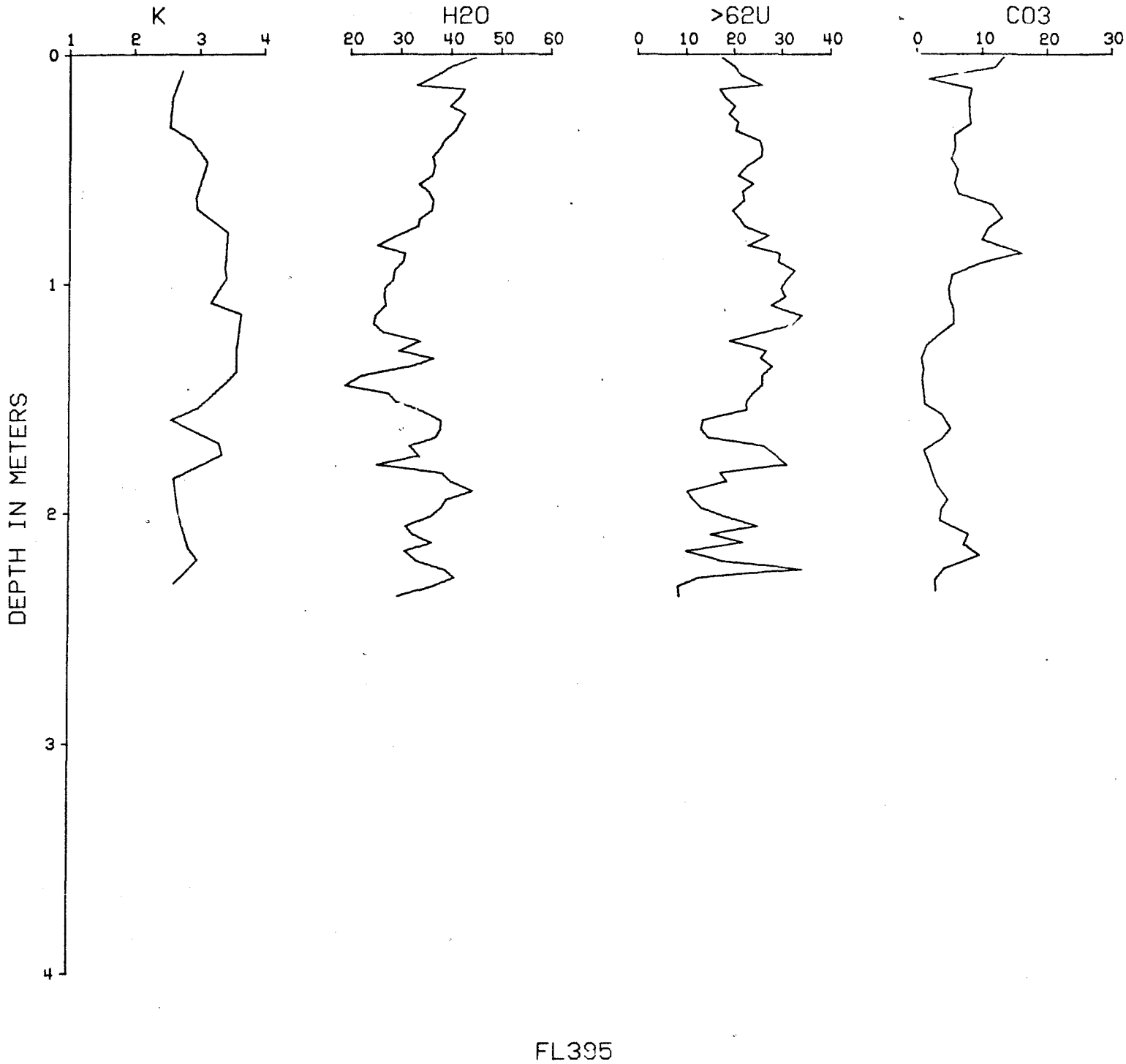

FIG (24) INDIVIDUAL VALUES

Figure 25. Thermal conductivity, % coarse fraction (> 62 microns), water content, and % carbonate measured in a sediment core recovered at FL-413, Alpha Ridge. Values are discrete measurements.

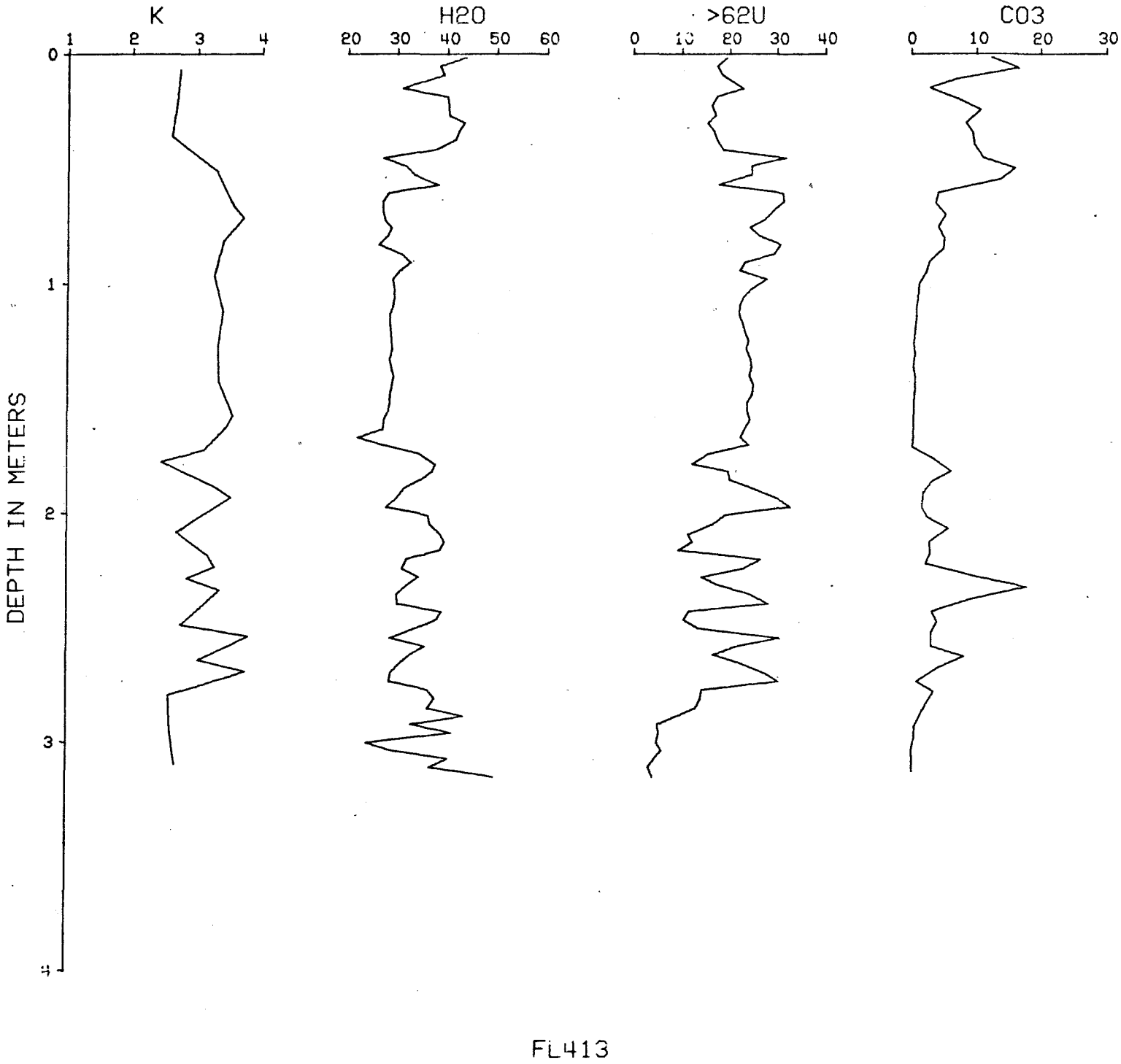

FIG. 25 INDIVIDUAL VALUES

Figure 26. Thermal conductivity, % coarse fraction (> 62 microns), water content, and % carbonate measured in a sediment core recovered at FL-433, Alpha Ridge. Values are discrete measurements.

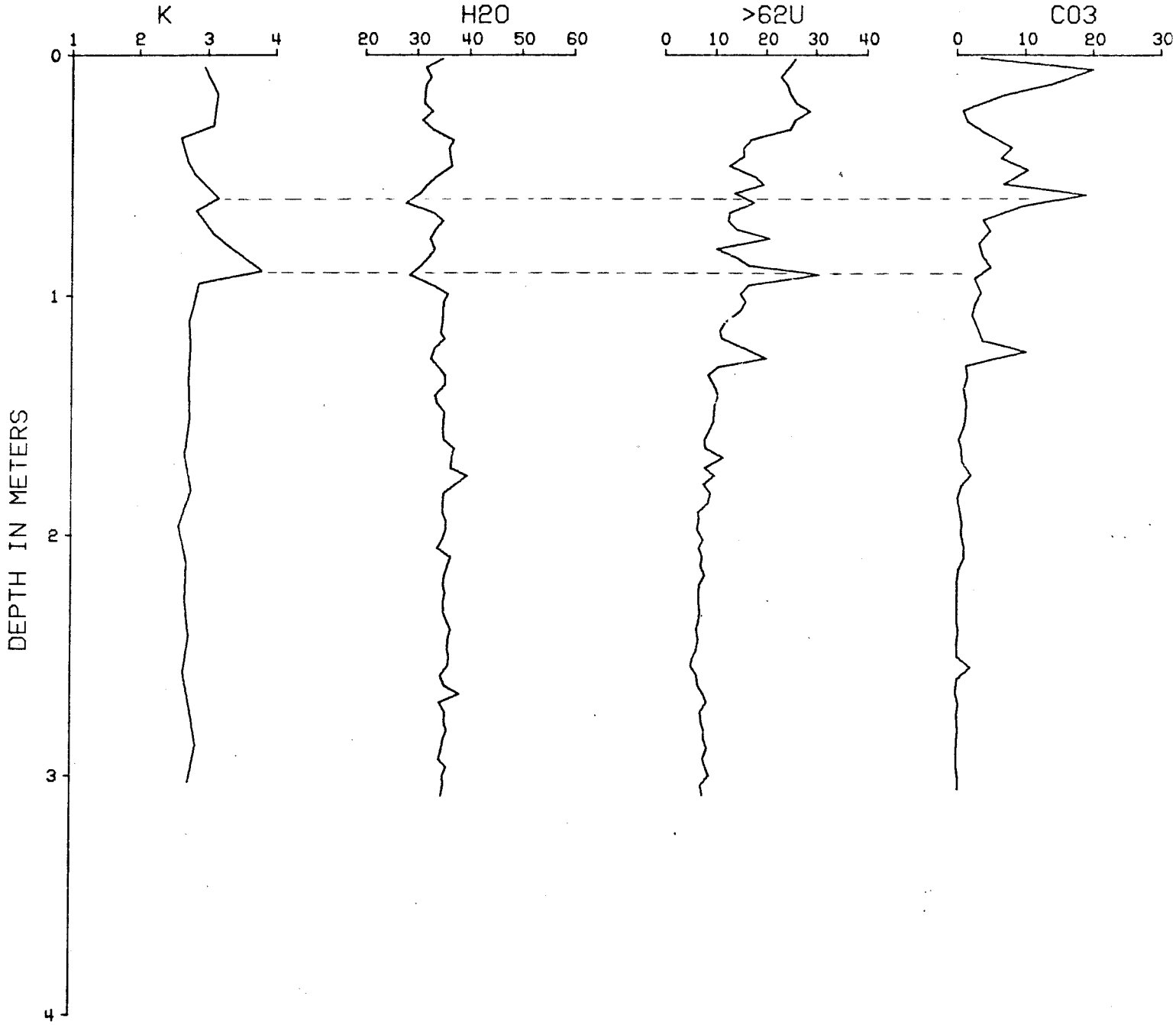

FL433

FIG. 26 INDIVIDUAL VACUÉS

Figure 27. Thermal conductivity, % coarse fraction (> 62 microns), water content, and % carbonate measured in a sediment core recovered at FL-434, Alpha Ridge. Values are discrete measurements.

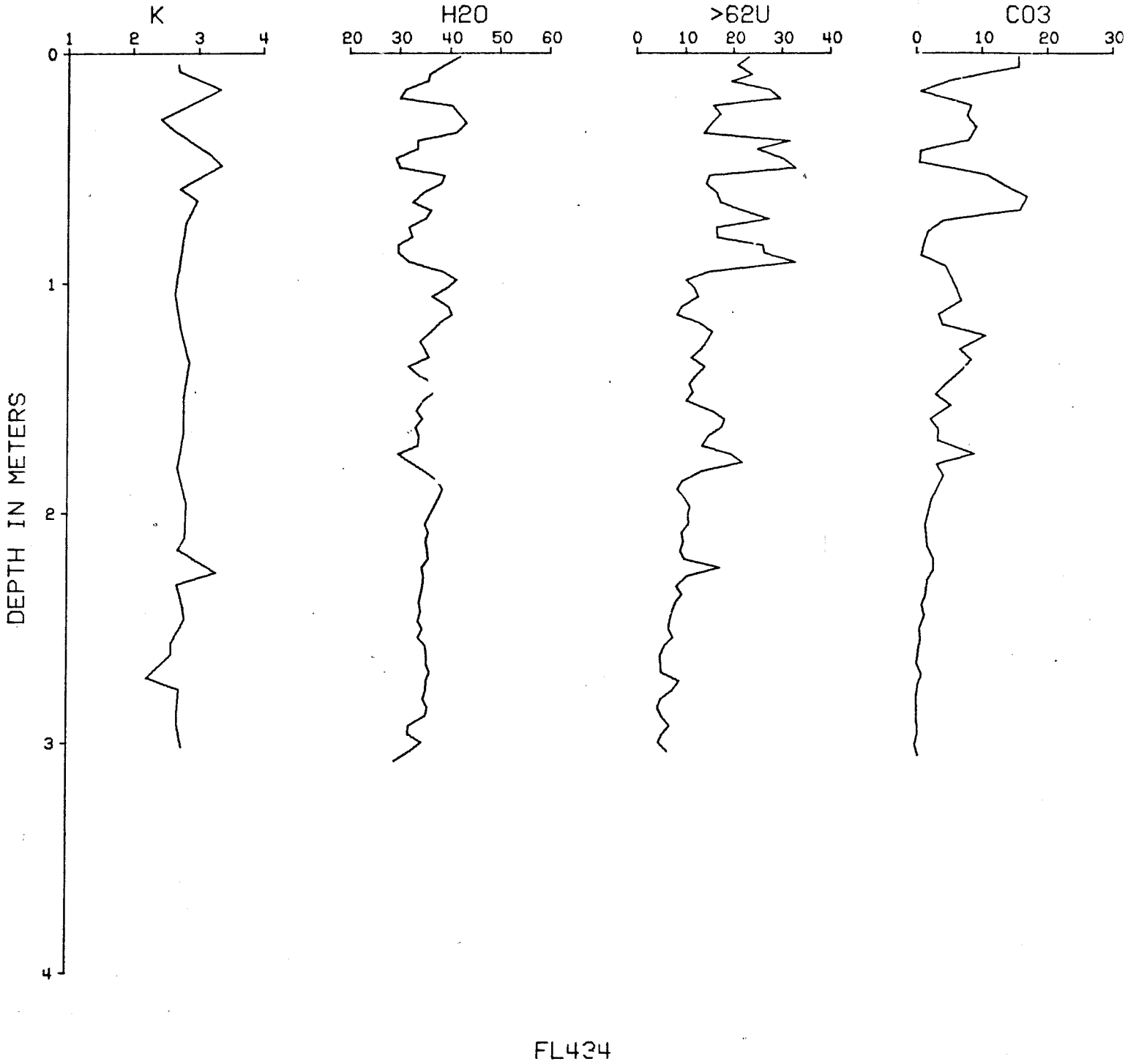

FIG. (27) INDIVIDUAL VALUES

Figure 28. Thermal conductivity, % coarse fraction (> 62 microns), water content, and % carbonate measured in a sediment core recovered at FL-474, Alpha Ridge. Values are discrete measurements.

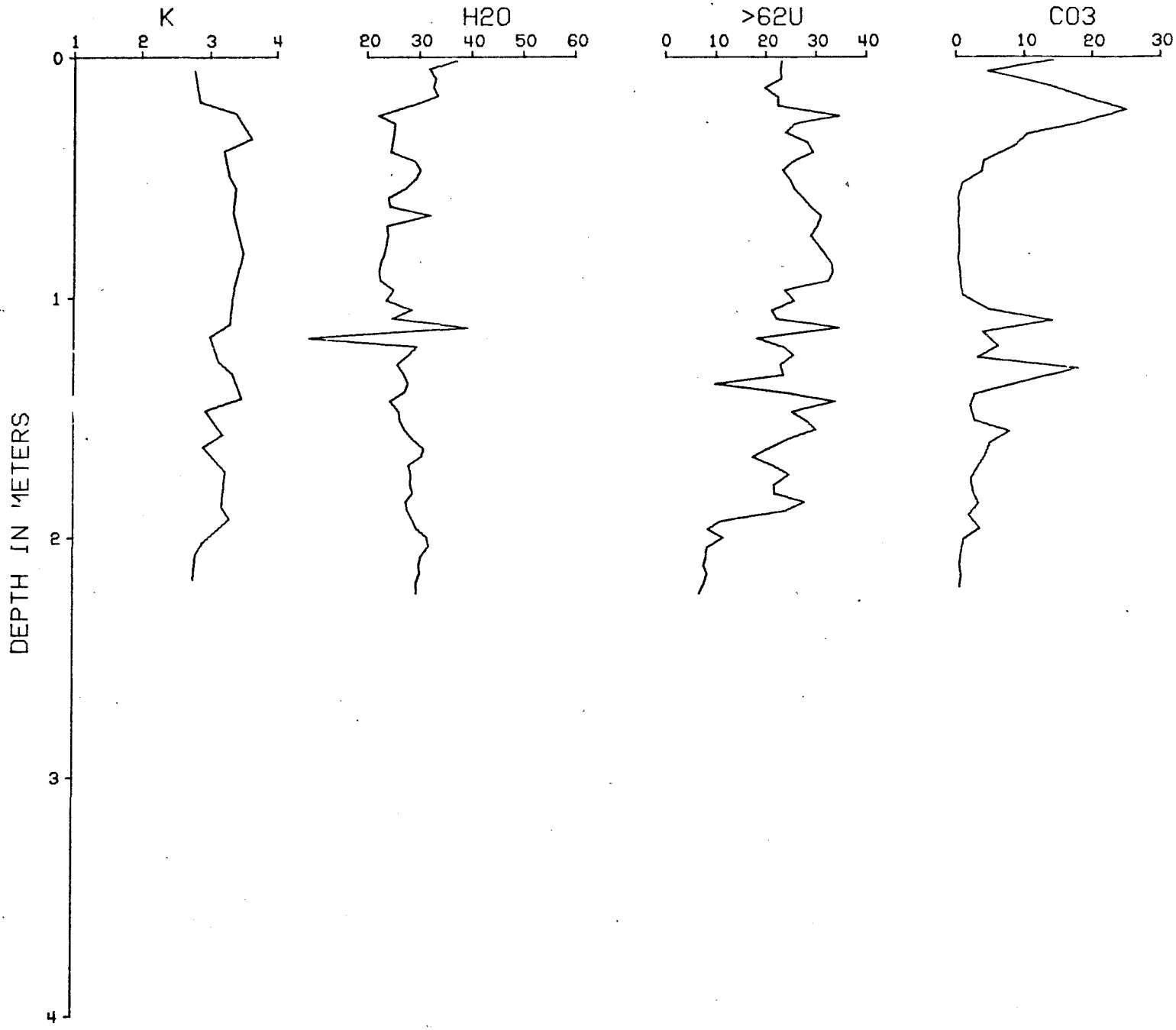

FL474

FIG. 28 INDIVIDUAL VALUES

Figure 29. Thermal conductivity, % coarse fraction (> 62 microns), water content, and % carbonate measured in a sediment core recovered at FL-503, Alpha Ridge. Values are discrete measurements.

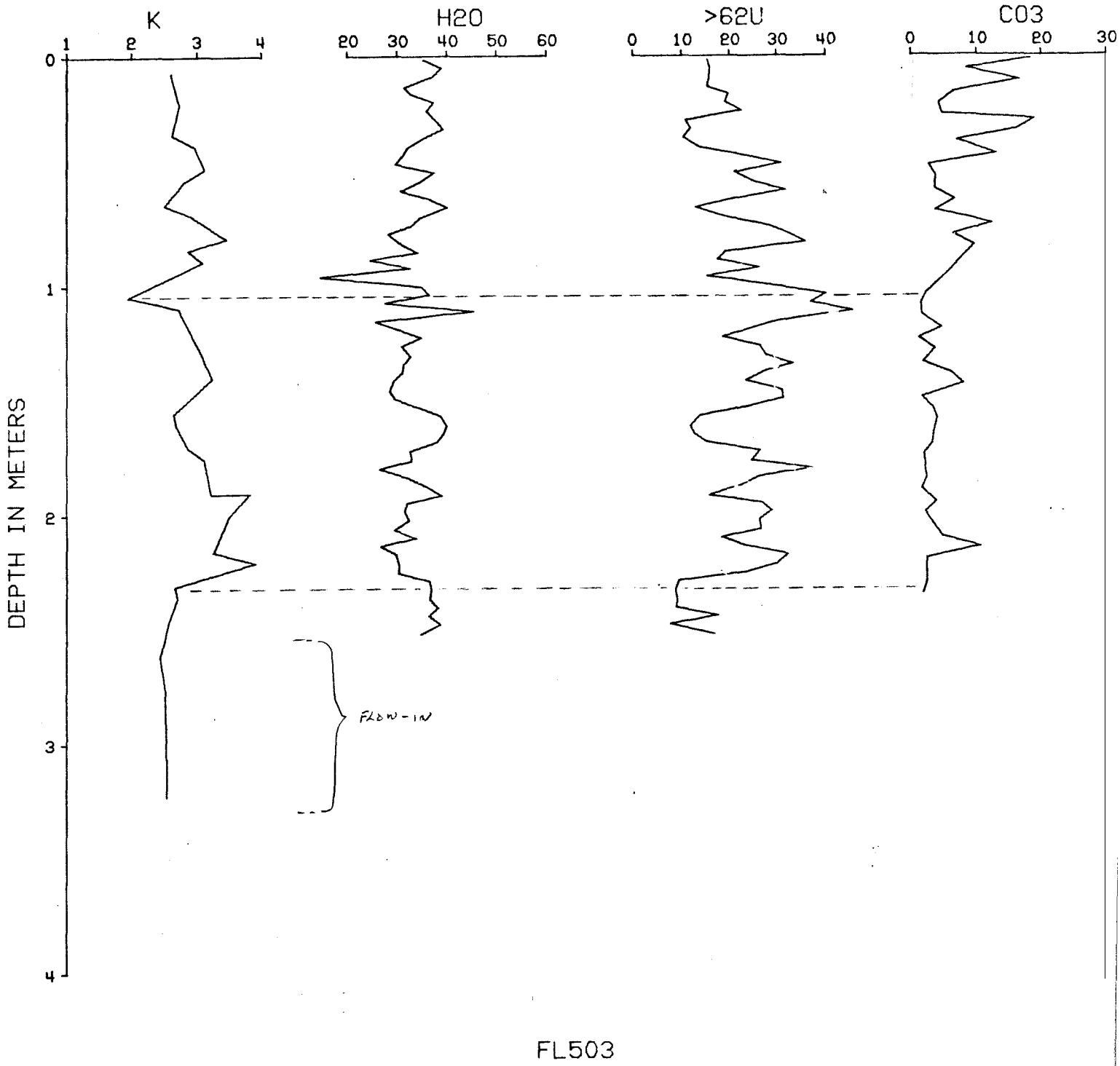

FIG. (29) INDIVIDUAL VALUES

Figure 30. Thermal conductivity, % coarse fraction (> 62 microns), water content, and % carbonate measured in a sediment core recovered at FL-533, Alpha Ridge. Values are discrete measurements.

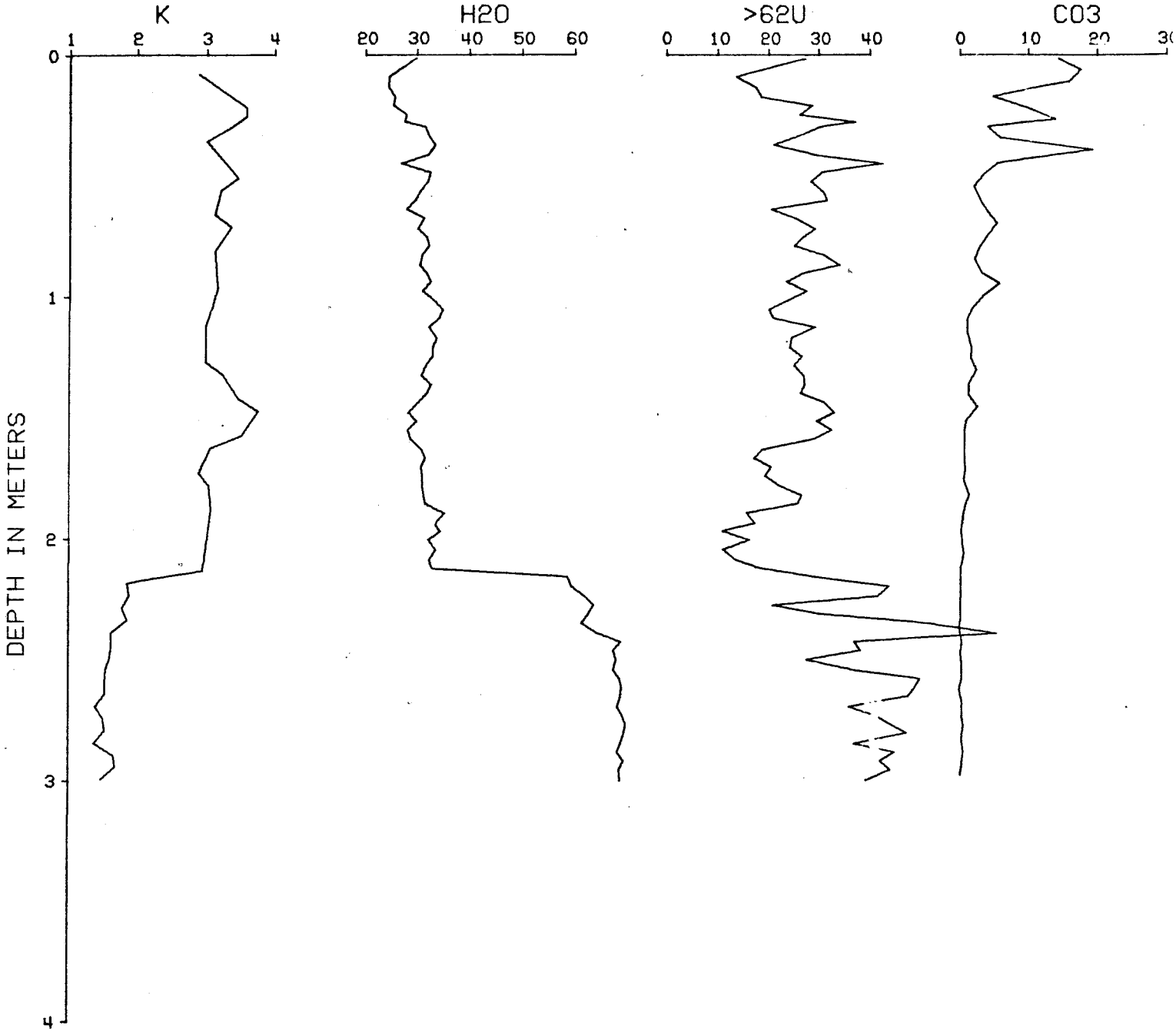

FL533

FIG. (3a) INTRINSIC VACCET

NO F

Figure 31. Thermal conductivity, % coarse fraction (> 62 microns), water content, and % carbonate measured in a sediment core recovered at FL-557, Alpha Ridge/Greenland Margin transition. Values are discrete measurements.

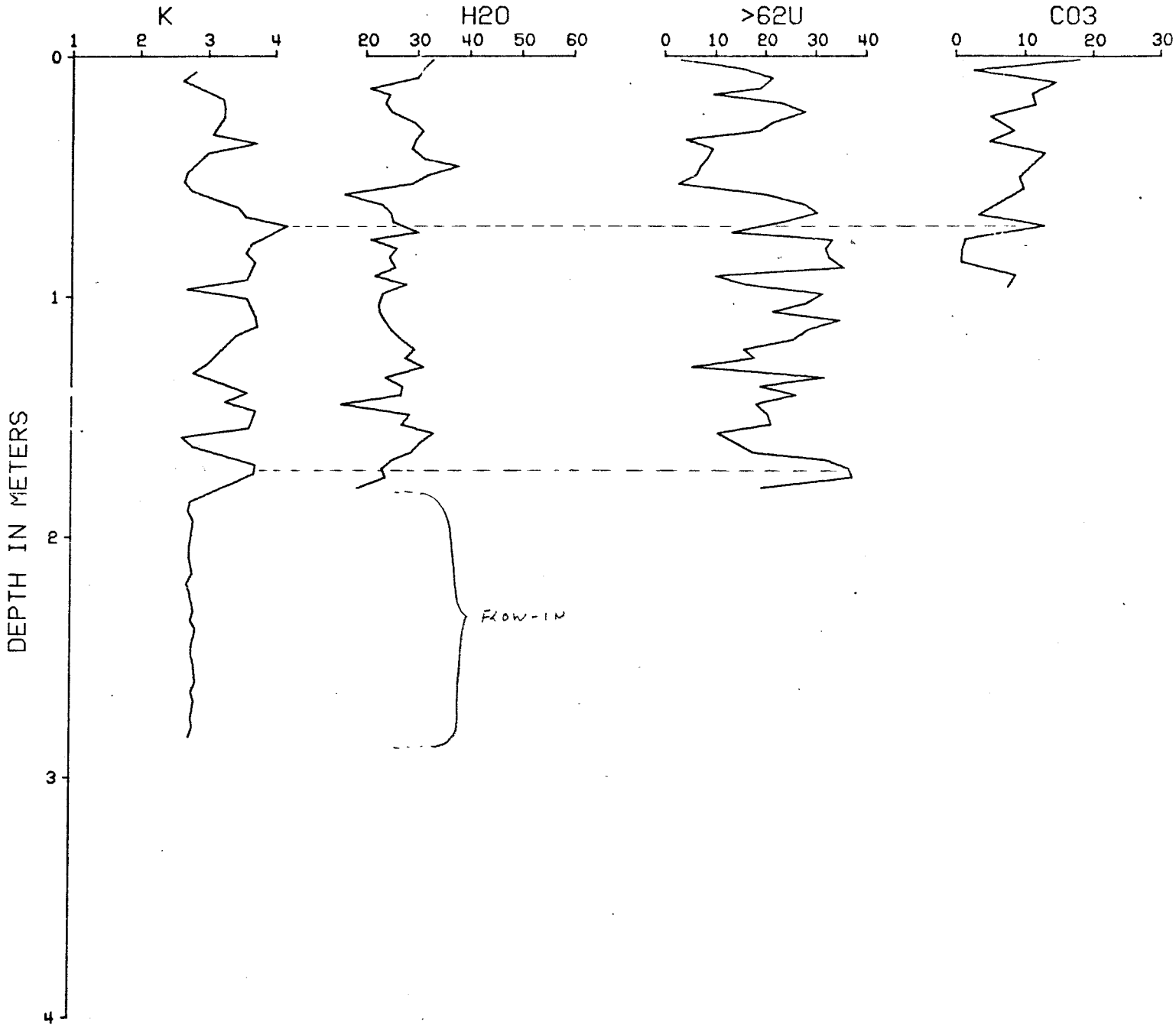

FL557

FIG. 31 INDIVIDUAL VALUES

Figure 32. Thermal conductivity, % coarse fraction (> 62 microns), water content, and % carbonate measured in a sediment core recovered at FL-559, Alpha Ridge/Greenland margin transition. Values are discrete measurements.

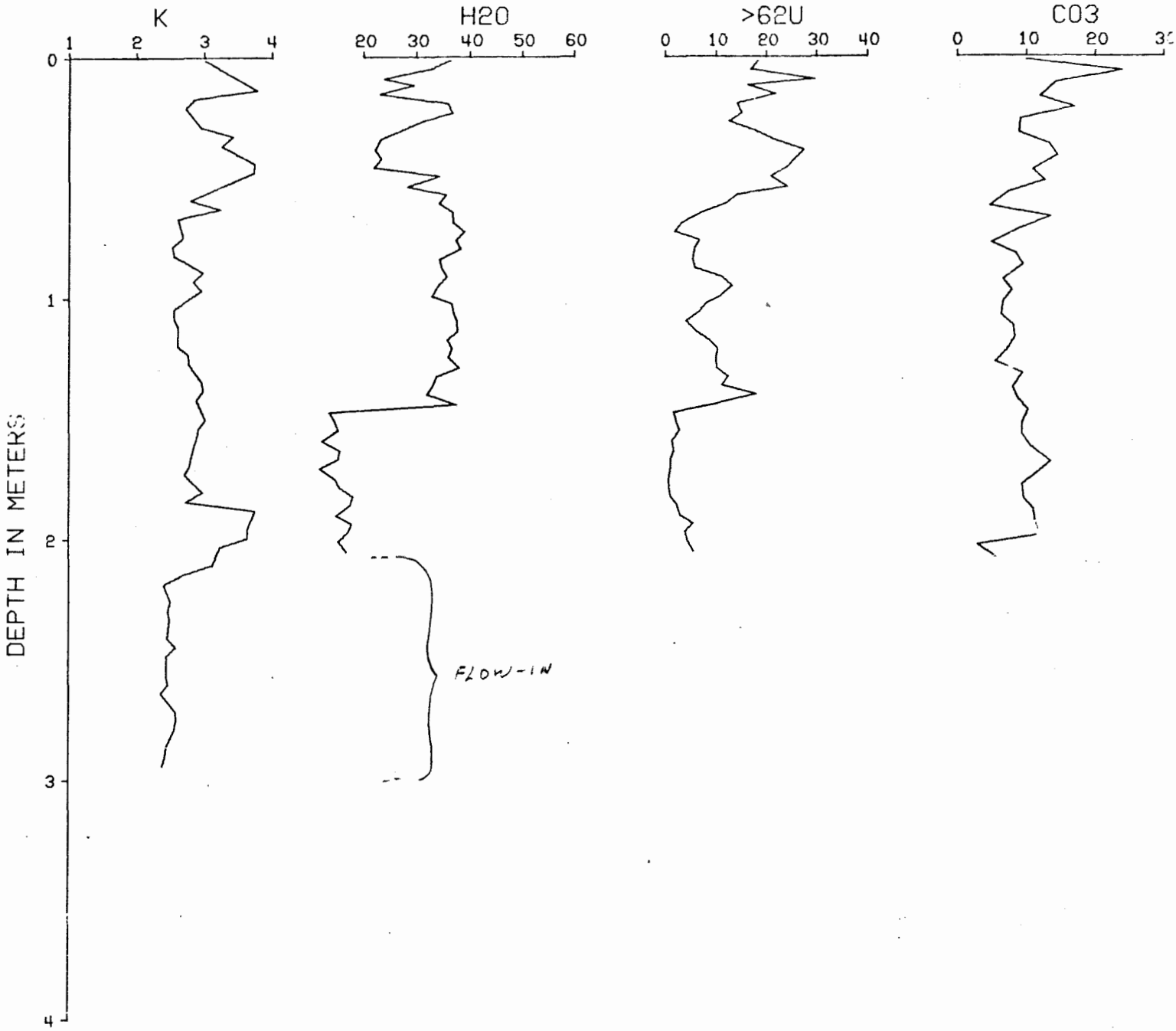

FL559

FIG. 32 INDIVIDUAL VALUES

Figure 33. Mean thermal conductivities measured in 1740 core sections and corresponding water content.

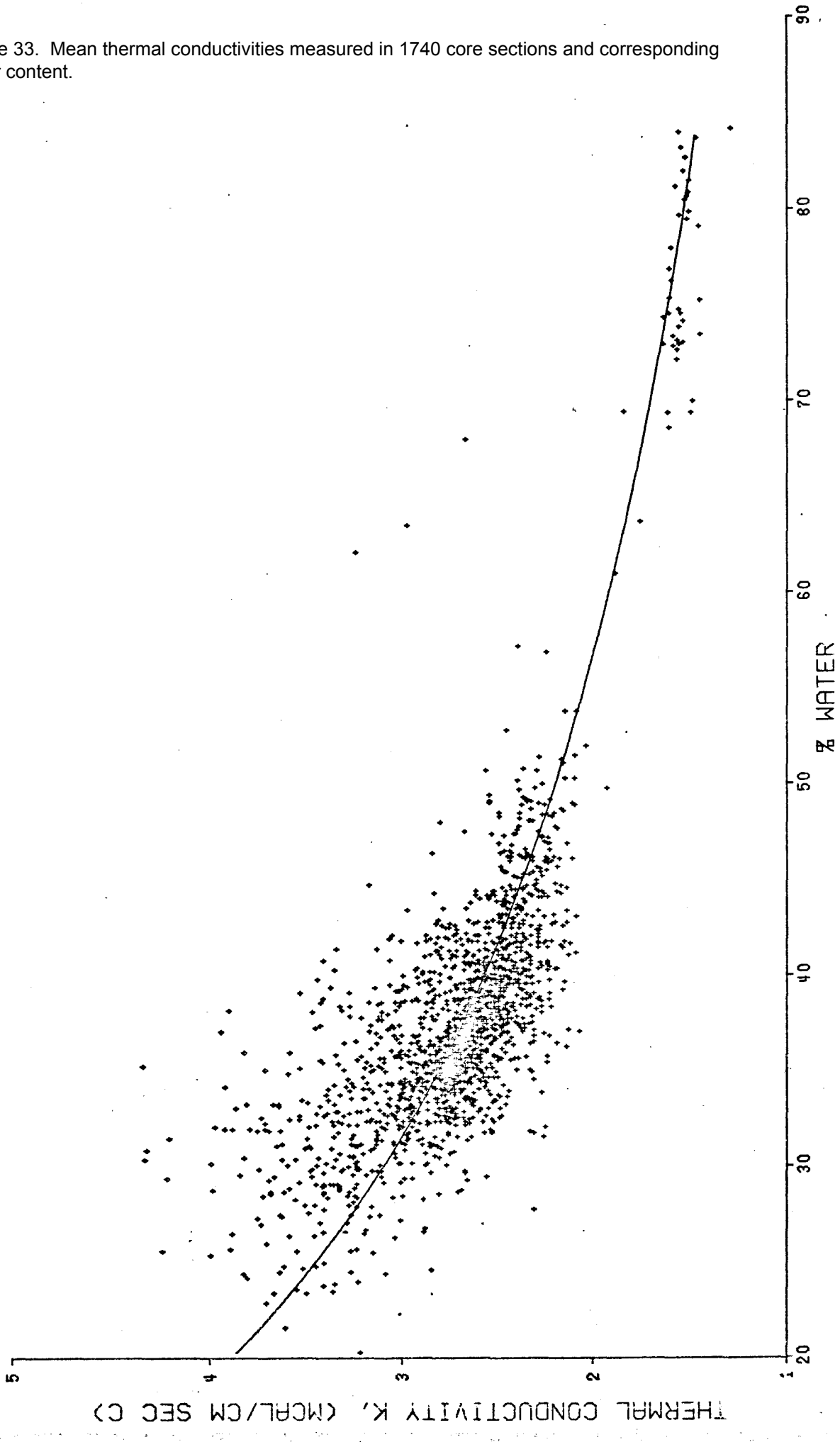

FIG. 33 MEAN VALUES FROM 1,740 CORE SECTIONS

Figure 34. Mean thermal conductivity and mean percentage of grains coarser than 62 microns, as measured in 1825 core sections. The lower line corresponds to values of K greater than 1.9 mcal/cm-sec-C.

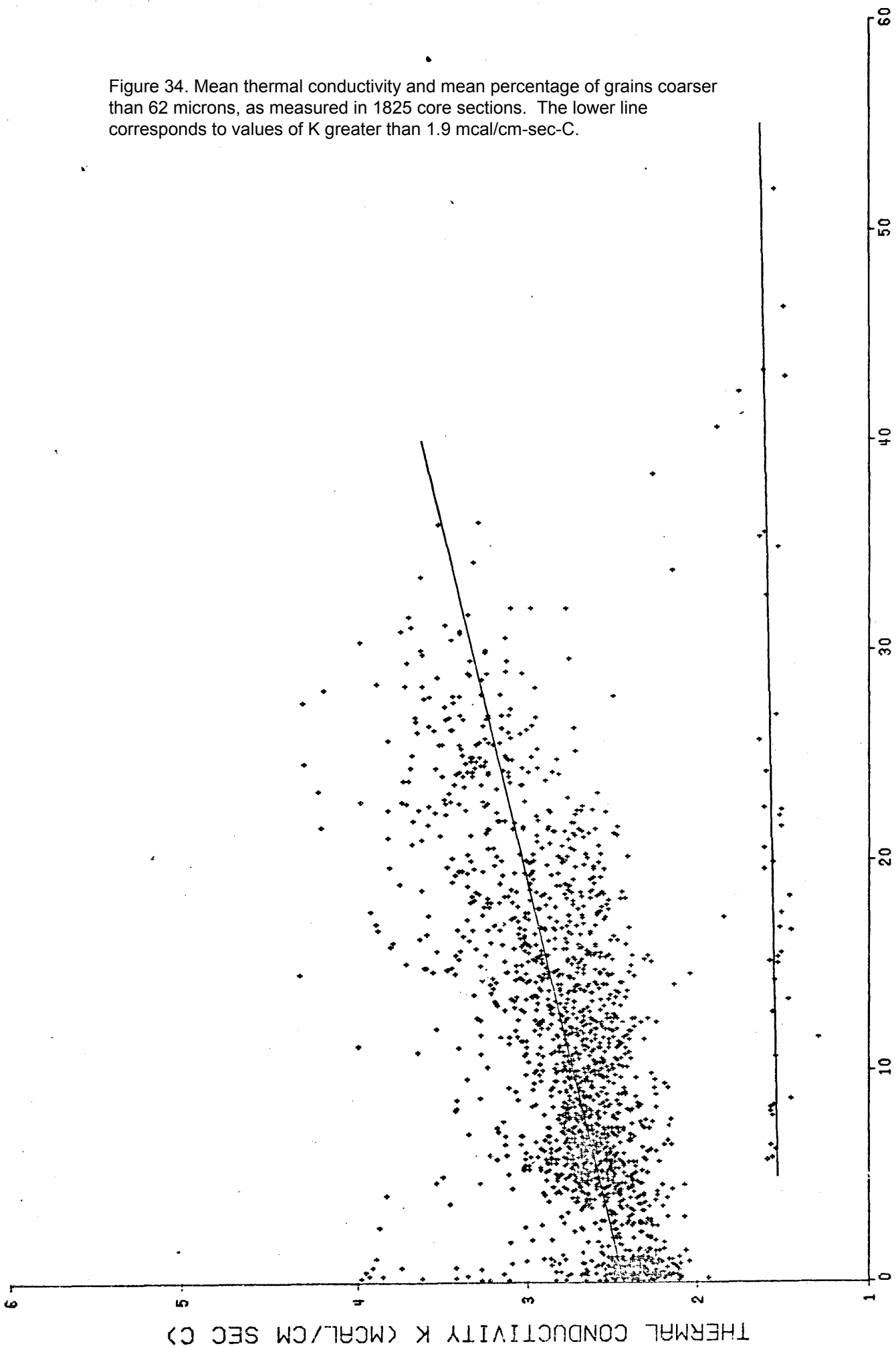

Figure 35. Mean water content and mean percentage of grains coarser than 62 microns, as measured in 1810 core sections. The upper line corresponds to water content greater than 65%.

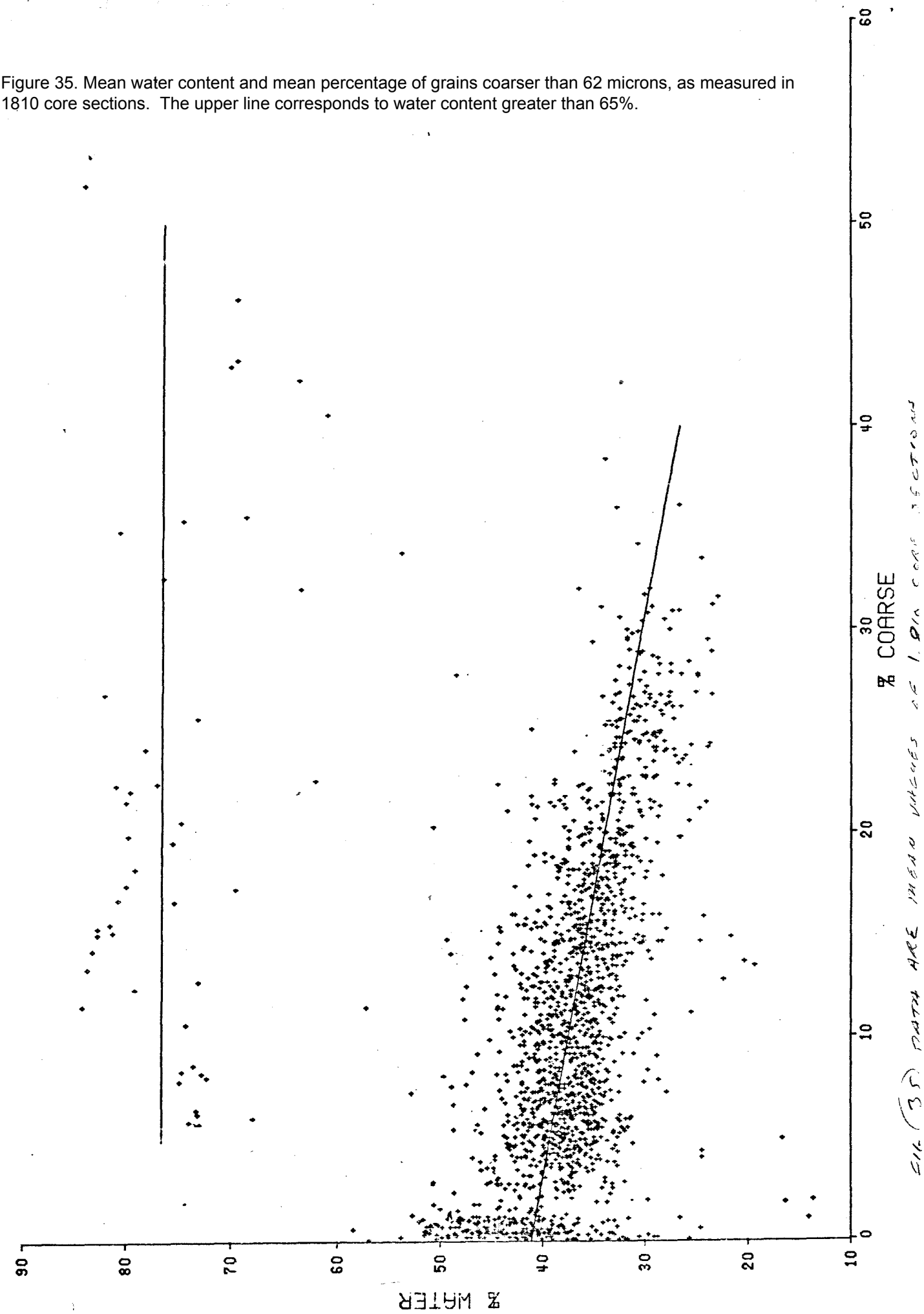

FIG (35) DATA ARE MEAN VALUES OF 1.0 IN CORE SECTIONS

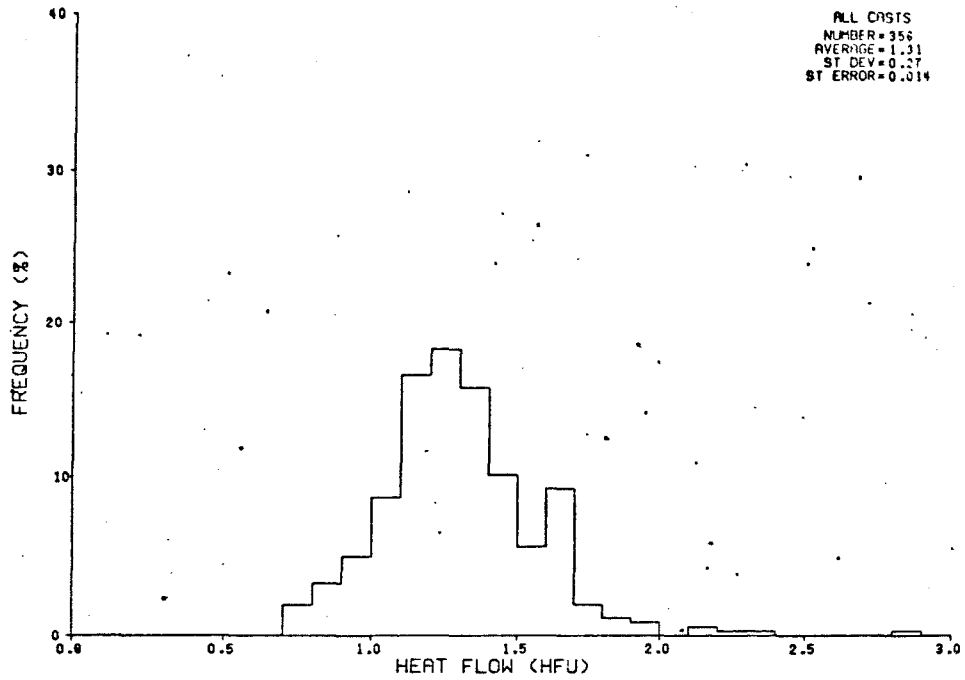

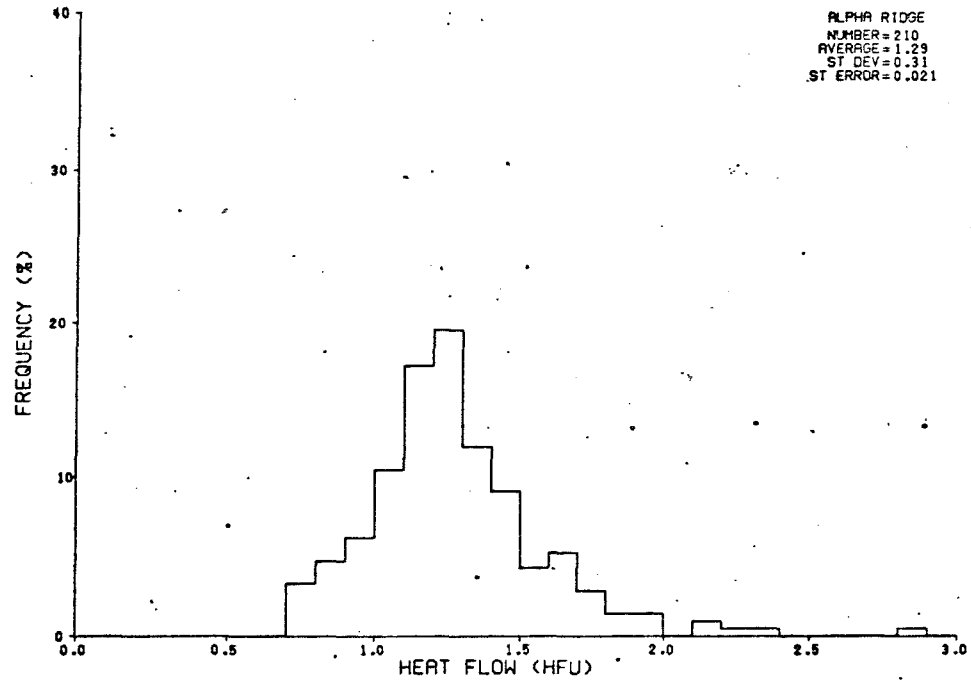

Figure 36. Histograms of measured heat flow for the entire dataset (top) and Alpha Ridge (bottom).

FIG. 36

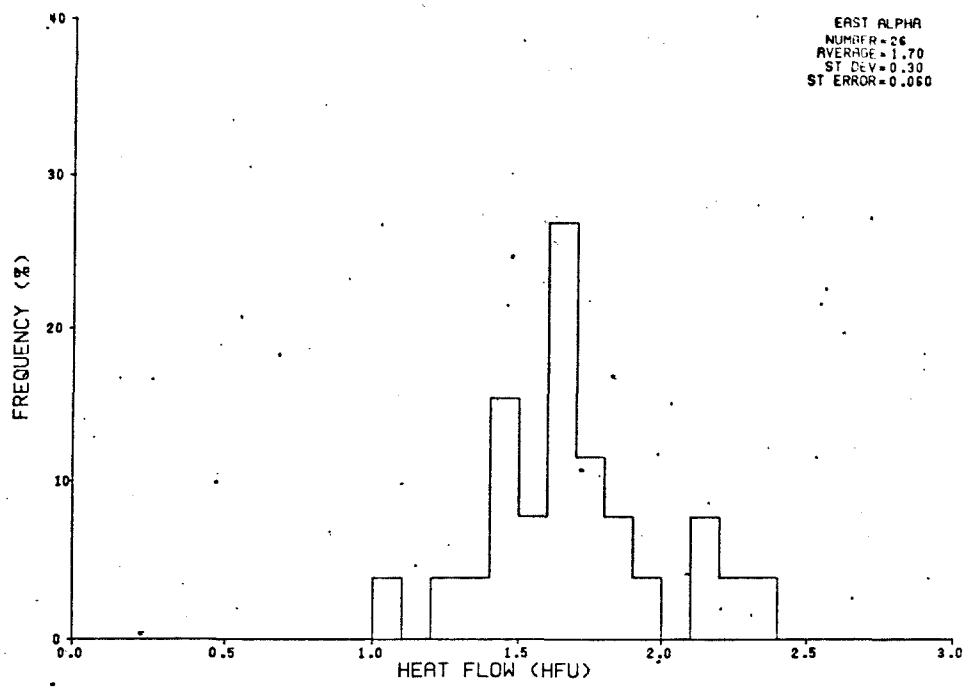

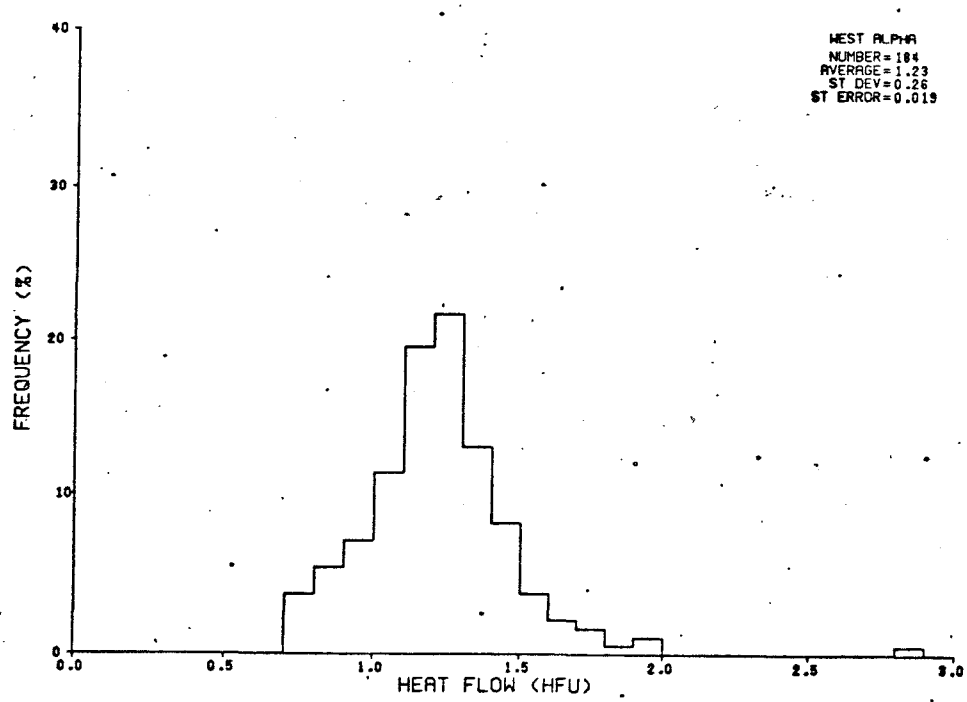

Figure 37. Histograms of measured heat flow for east Alpha Ridge (top) and west Alpha Ridge (bottom).

FIG. 37

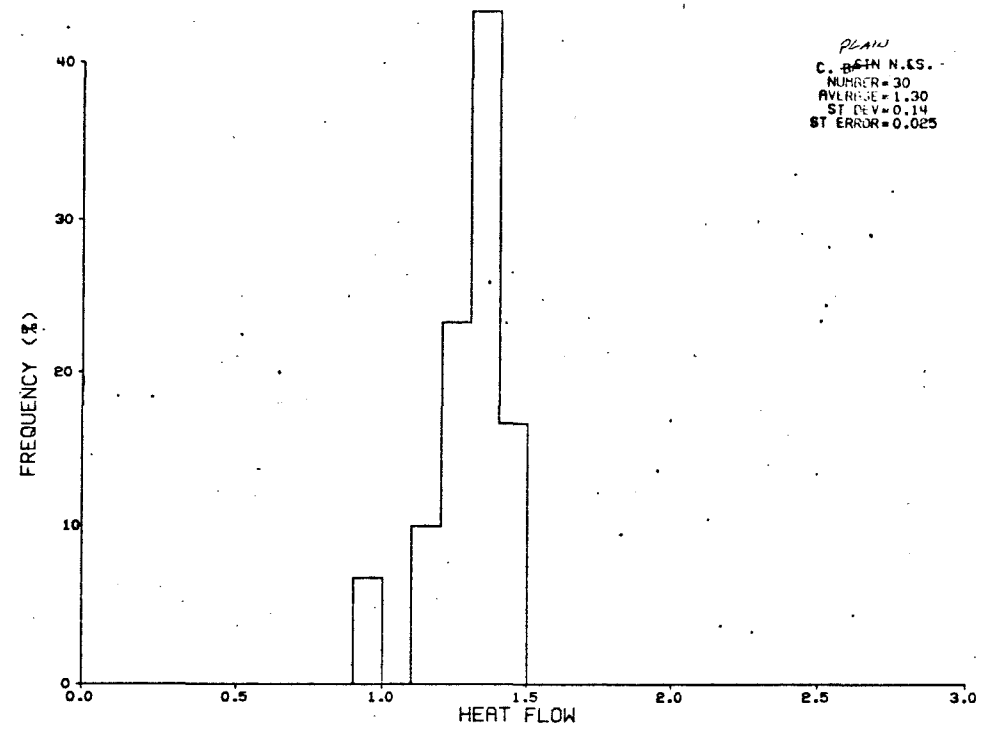

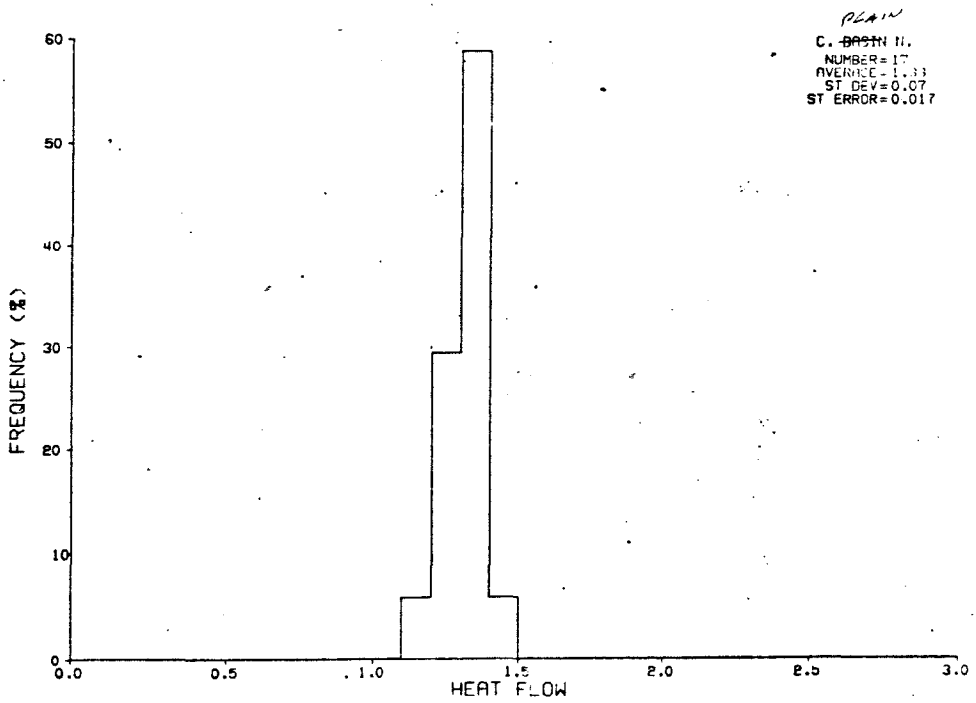

Figure 38. Histograms of measured heat flow for the all Canada Plain data (top) and for the subset of data from northern Canada Plain (bottom). Canada Plain referred to the deep, flat portion of Canada Basin east of Northwind Ridge. Refer to Figure 9.

FIG. 38

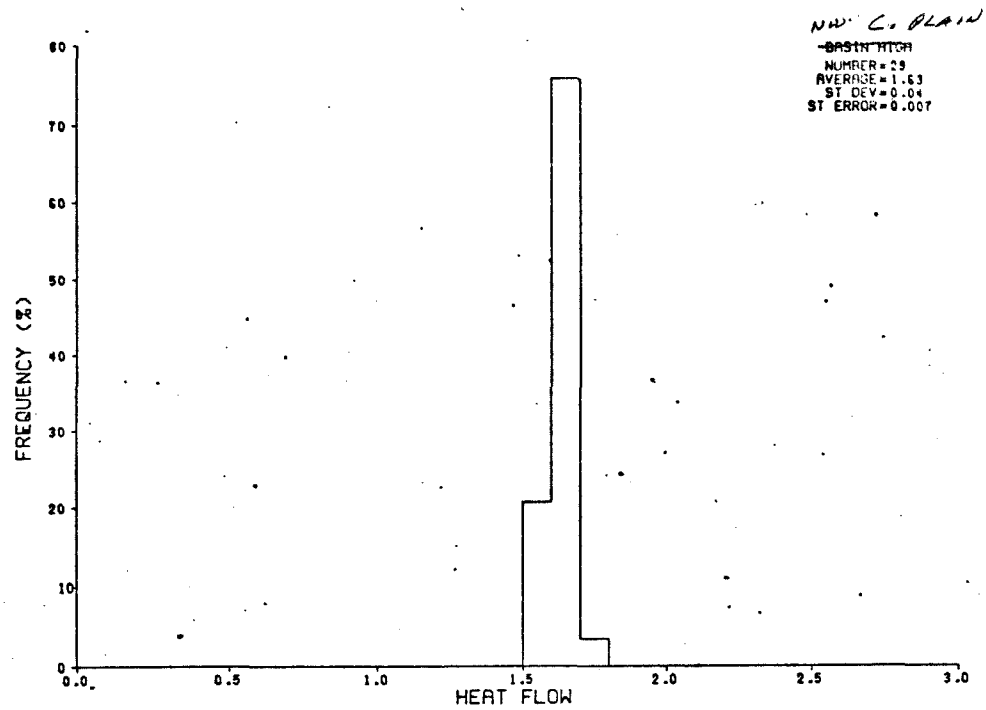

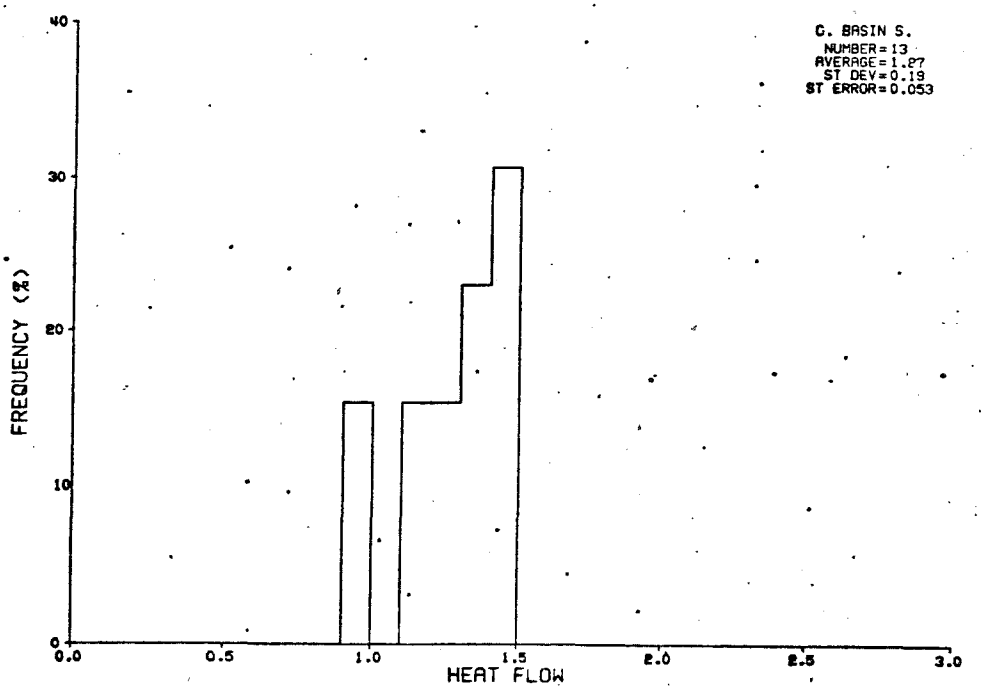

Figure 39. Histograms of measured heat flow for the NW Canada Basin (top), now known as Nautilus Basin, and for the southern Canada Basin (bottom).

FIG (39)

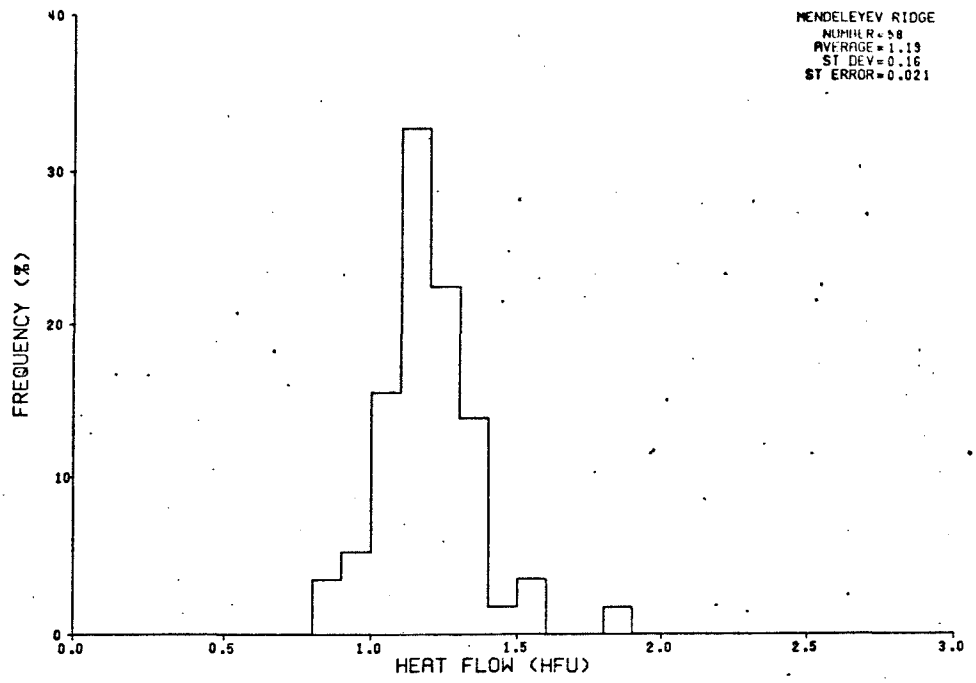

Figure 39 (continued). Histogram of measured heat flow for the Mendeleev Ridge.

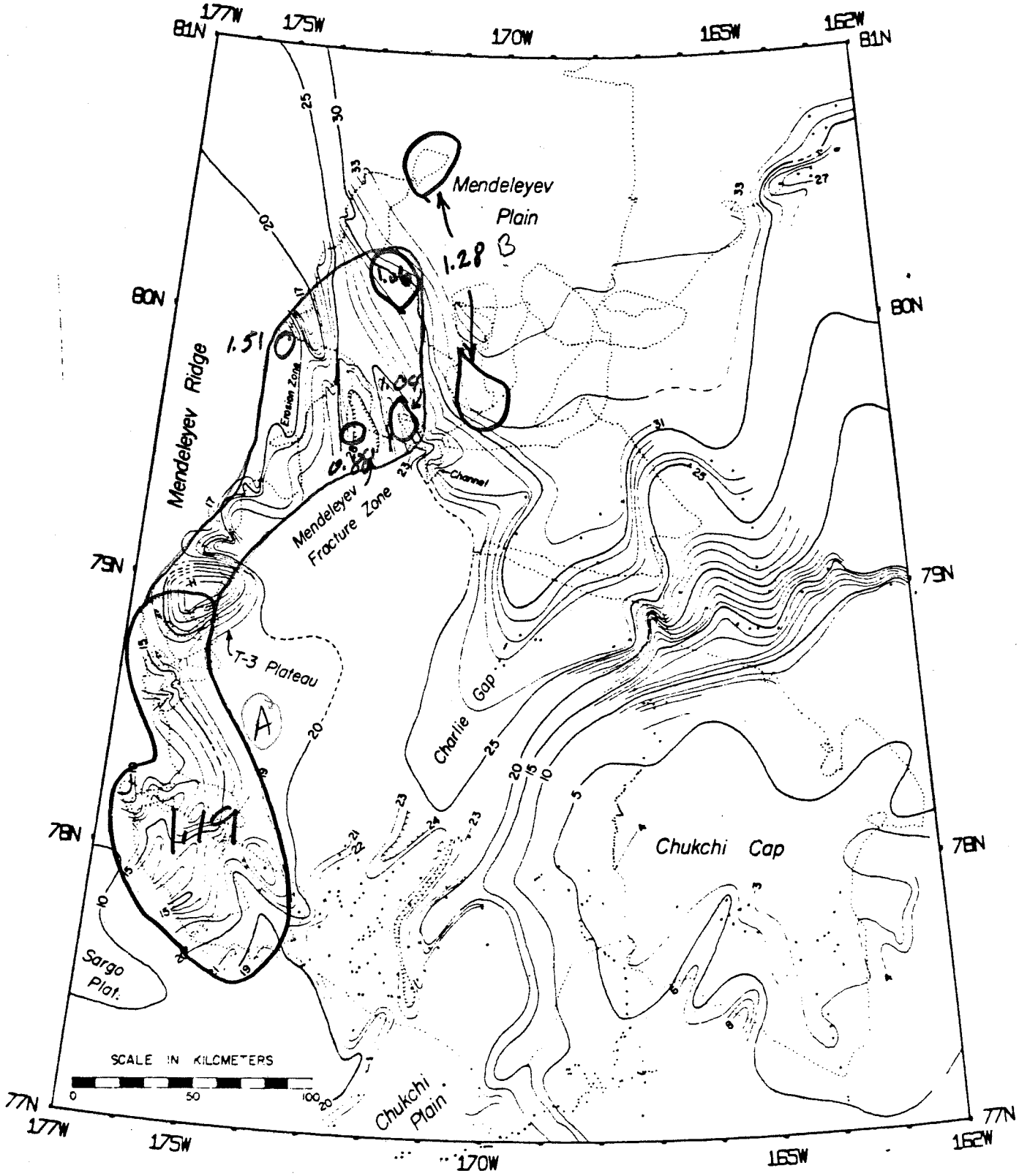

2089

AREA I BATHYMETRY

Figure ~~9~~ 40

Figure 40. Hand-contoured heat flow values superposed on bathymetry reported in meters divided by 100. Letter labels refer to Figure 9.

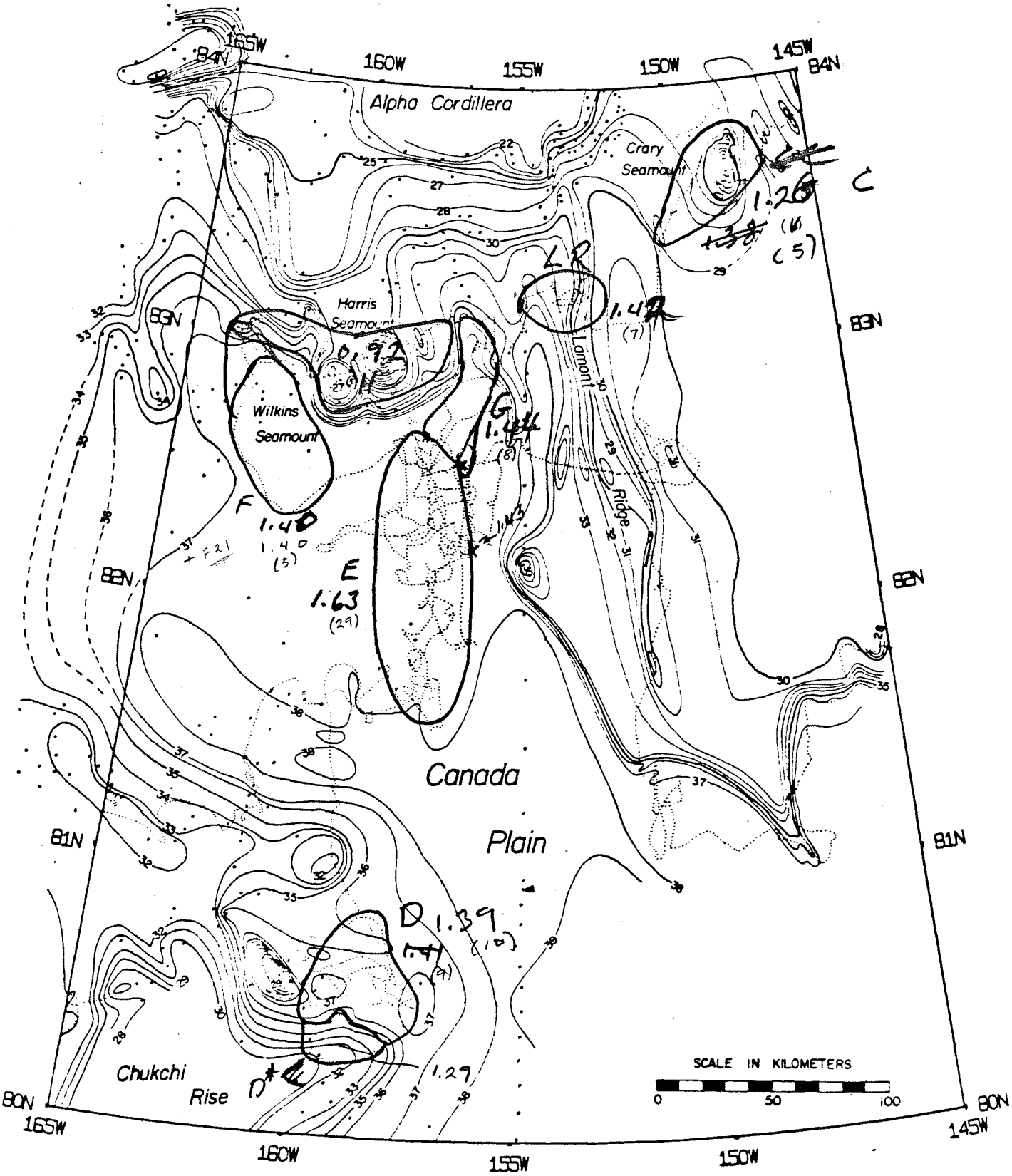

~~AREA II BATHYMETRY~~

~~Figure 10~~ (41)

Figure 41. Hand-contoured heat flow values superposed on bathymetry reported in meters divided by 100. Letter labels refer to Figure 9. Note in 2019: Some of the place names shown here are no longer used and may be morphologically incorrect (e.g., Mendeleev fracture zone).

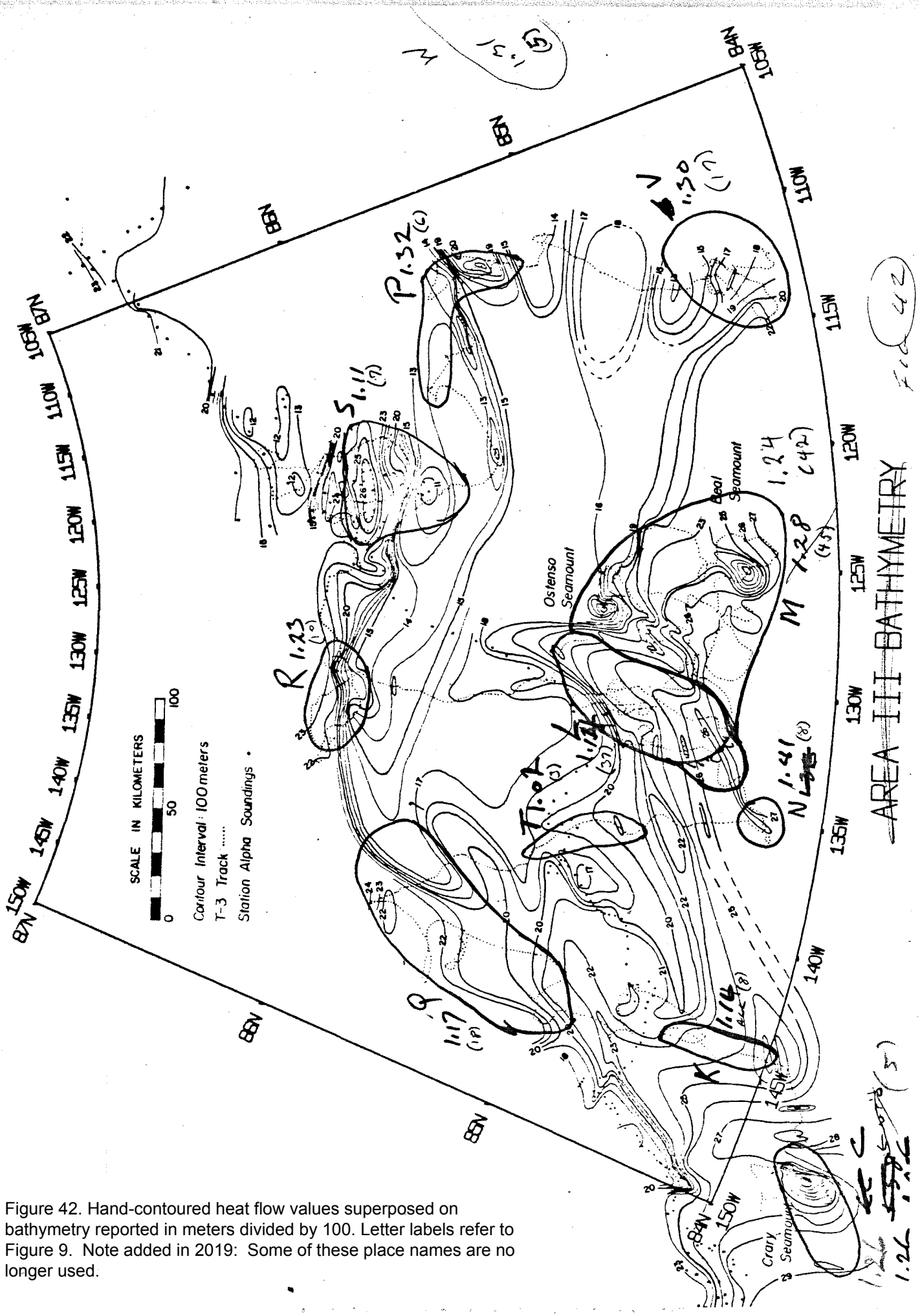

Figure 42. Hand-contoured heat flow values superposed on bathymetry reported in meters divided by 100. Letter labels refer to Figure 9. Note added in 2019: Some of these place names are no longer used.

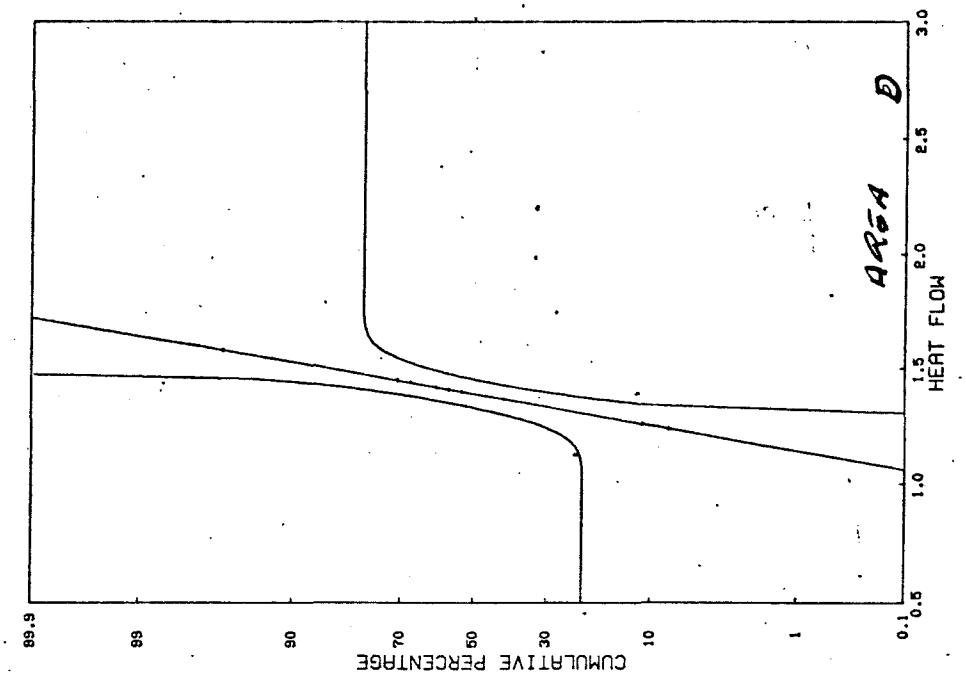

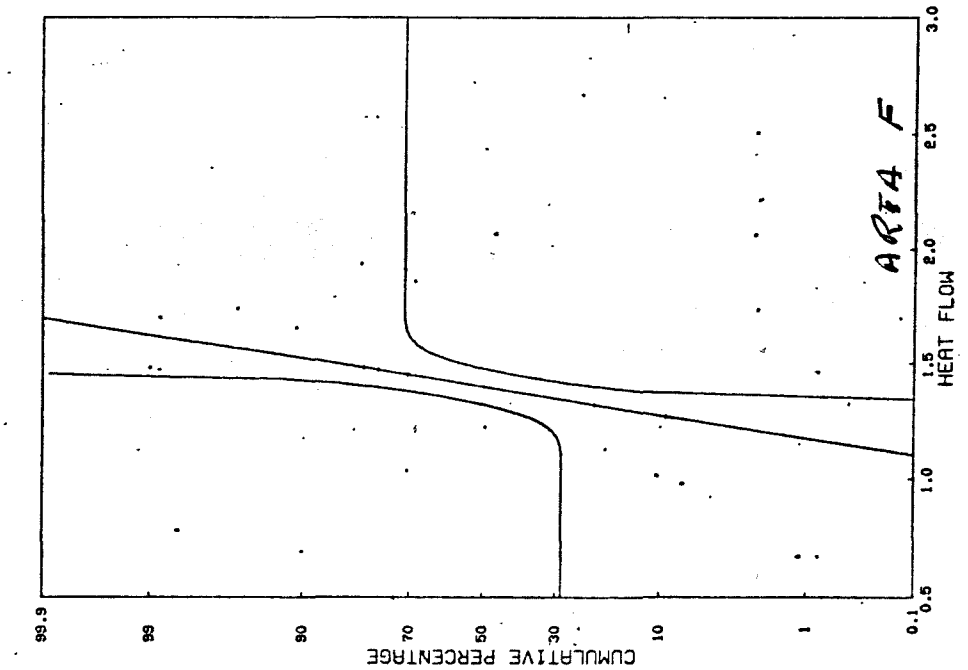

FIG 43

Figure 43. Heat flow data with confidence limits for Area F and Area D in Figure 9.

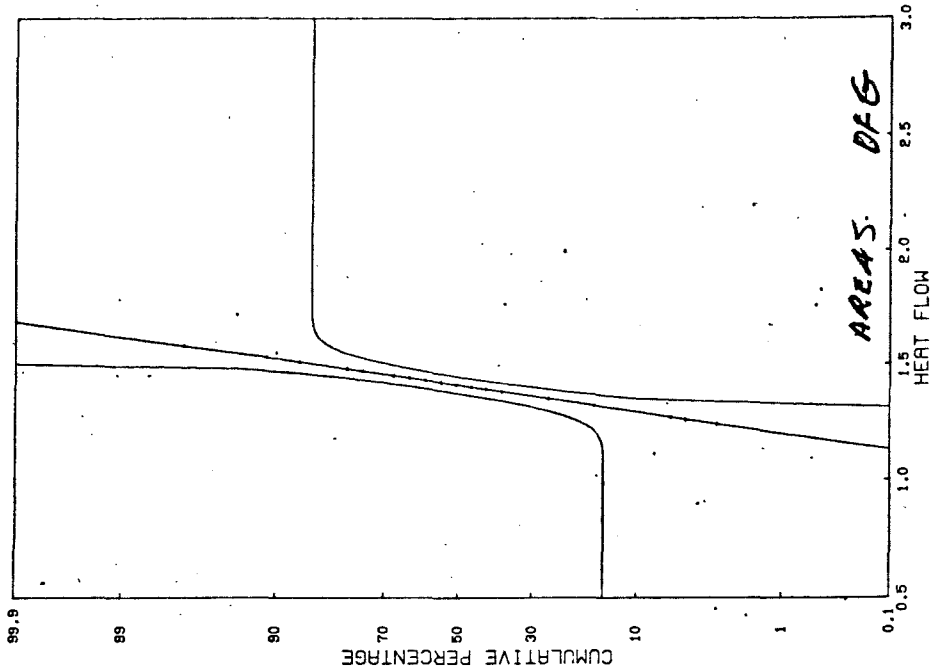

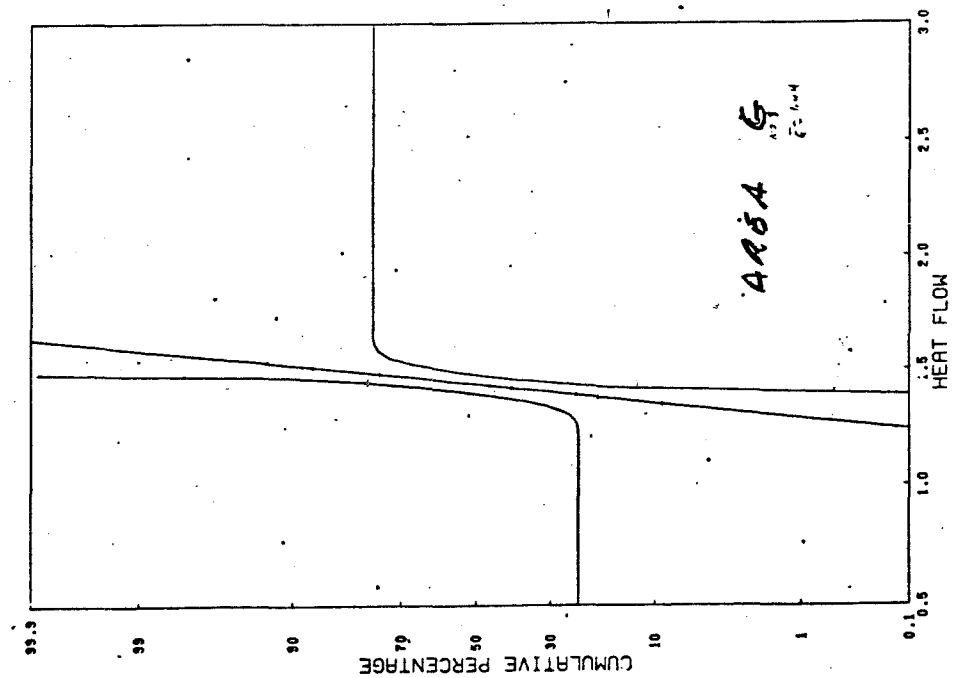

FIG C4

Figure 44. Heat flow data with confidence limits for Area G and Area D+G(??) in Figure 9.

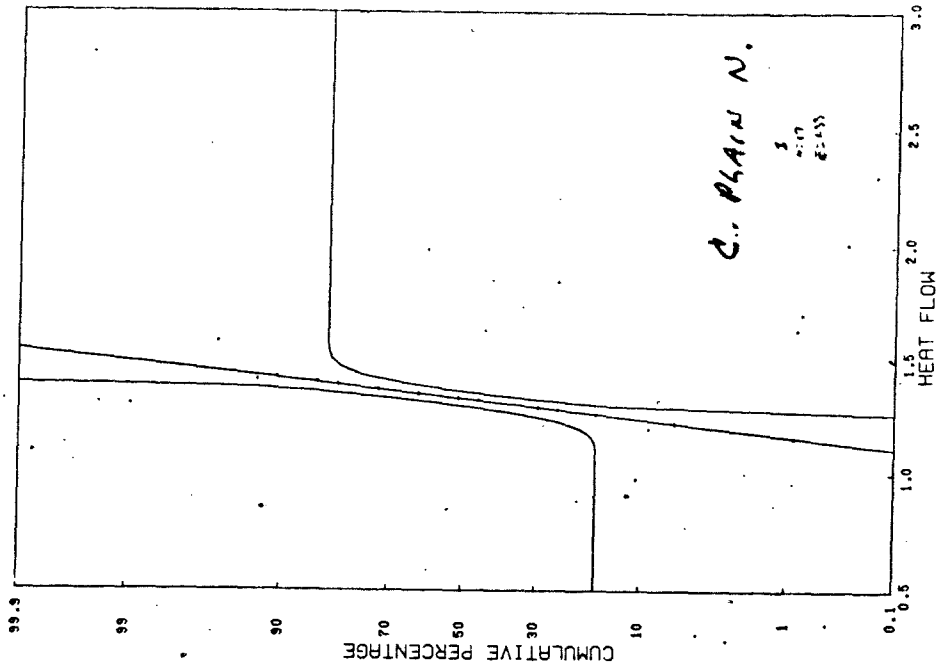

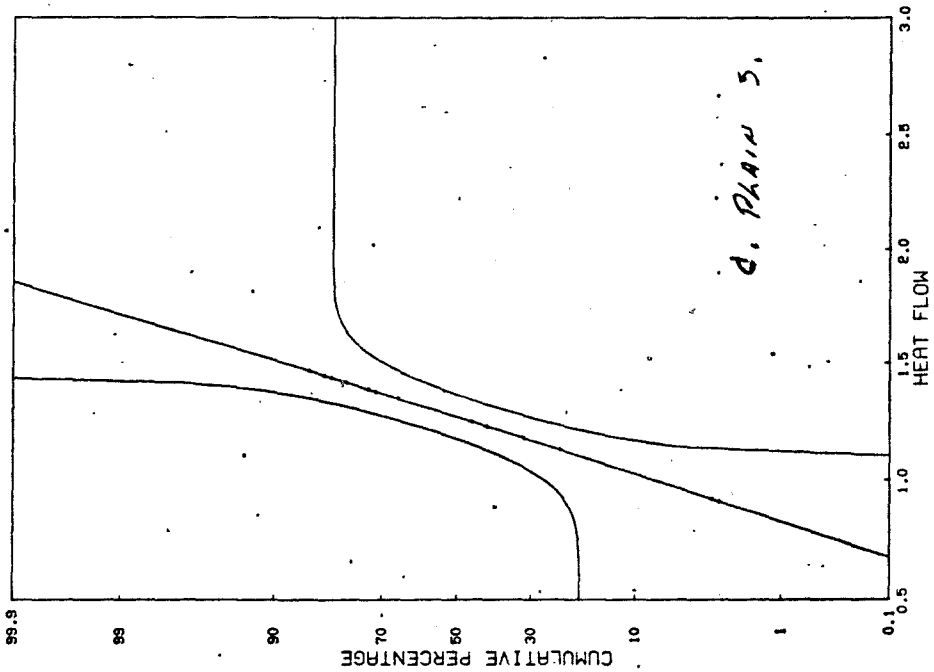

Figure 45. Heat flow data with confidence limits for south and north Canada Plain.

FIG (45)

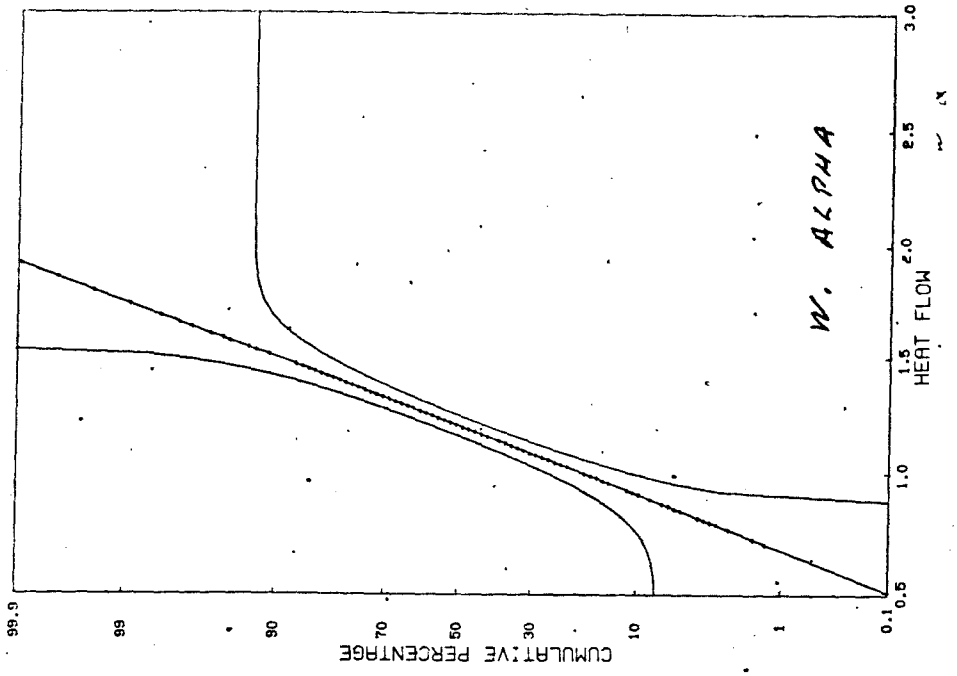

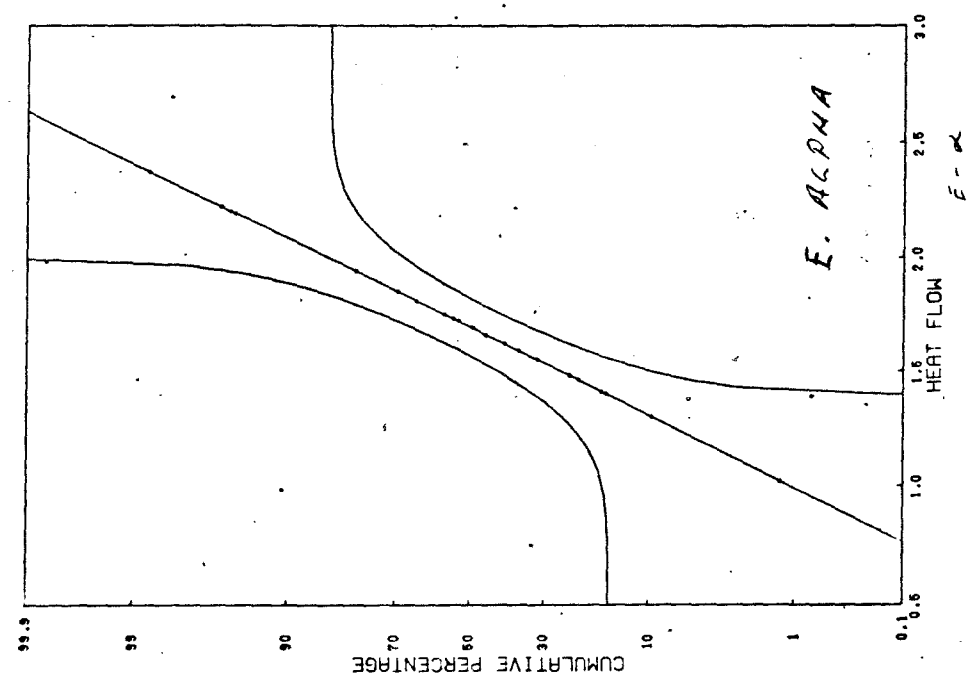

Figure 46. Heat flow data with confidence limits for east and west Alpha Ridge.

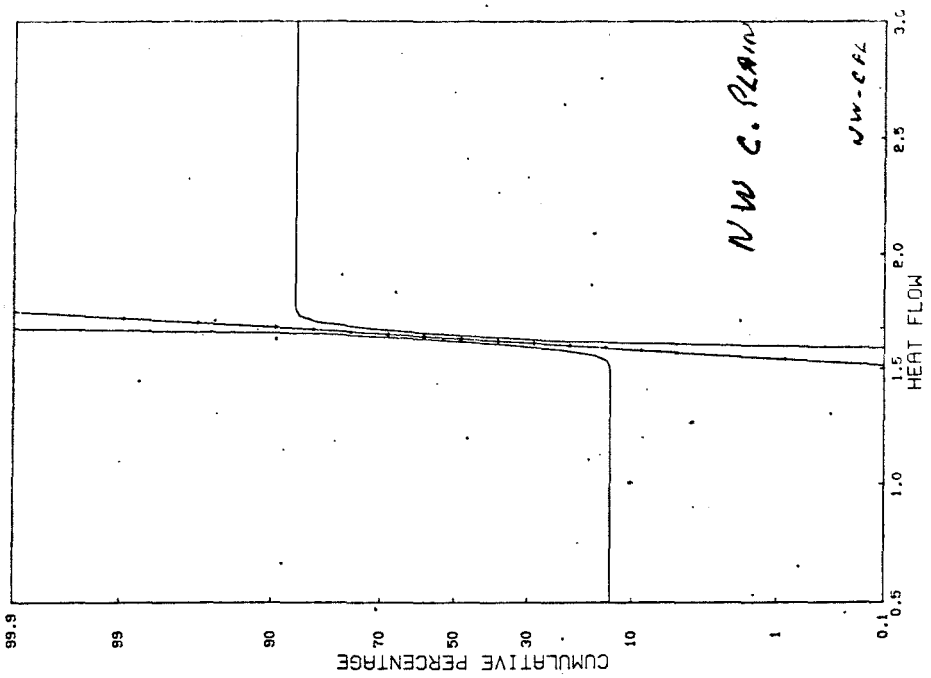

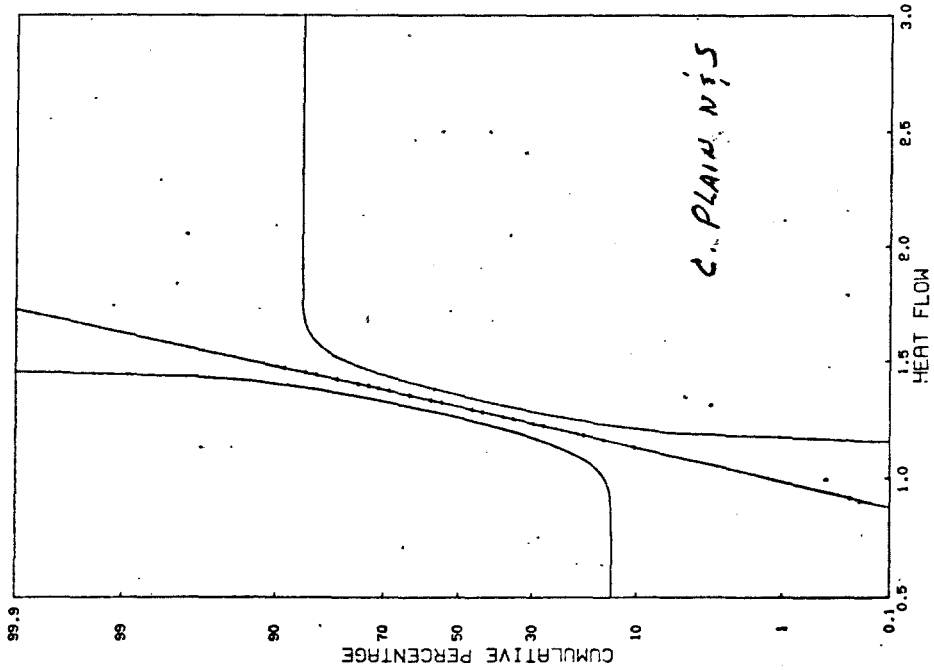

FIG 47

Figure 47. Heat flow data with confidence limits for Canada Plain and NW Canada Basin, now known as Nautilus Basin.

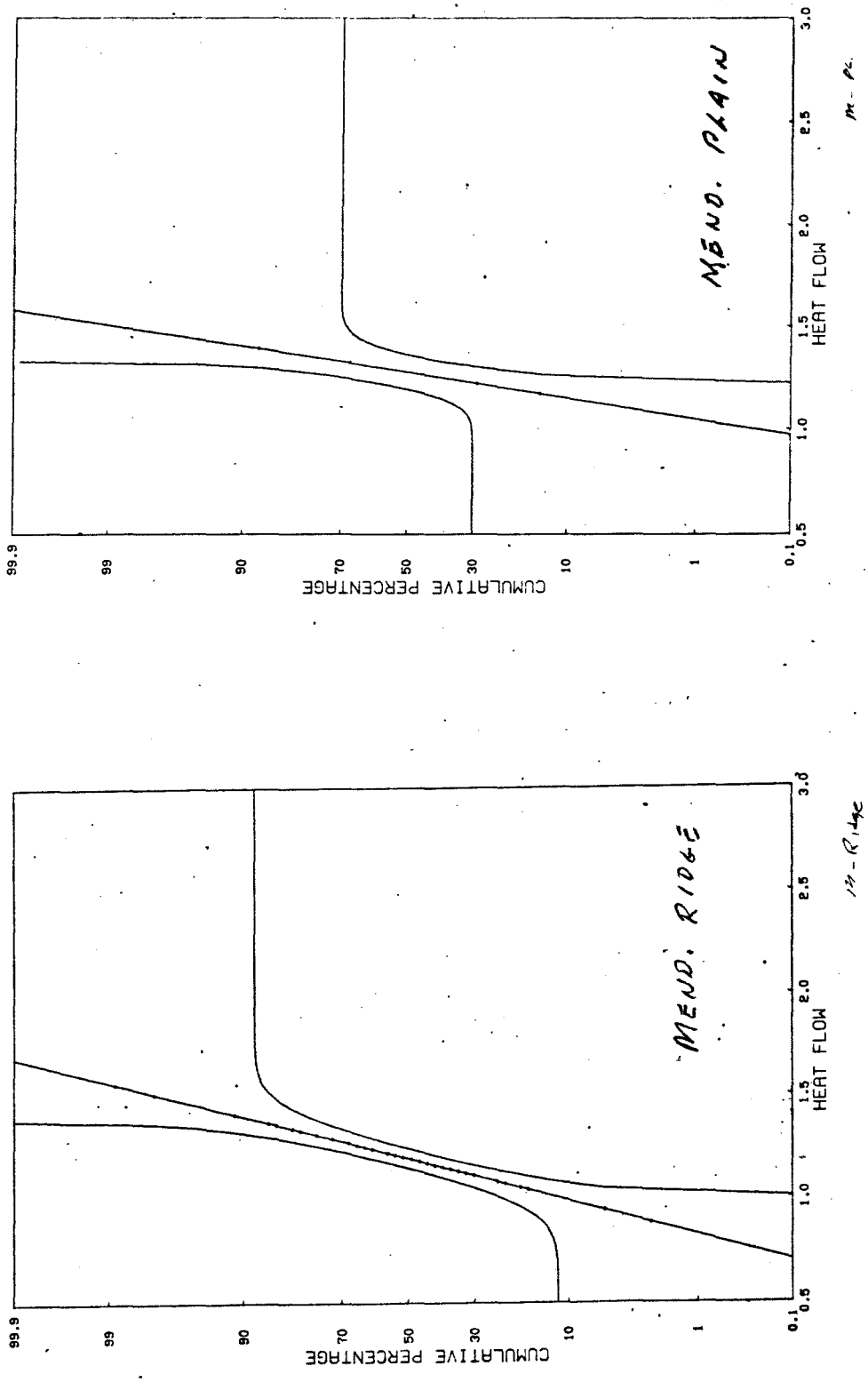

Figure 48. Heat flow data with confidence limits for Mendeleev Ridge and Mendeleev Plain.

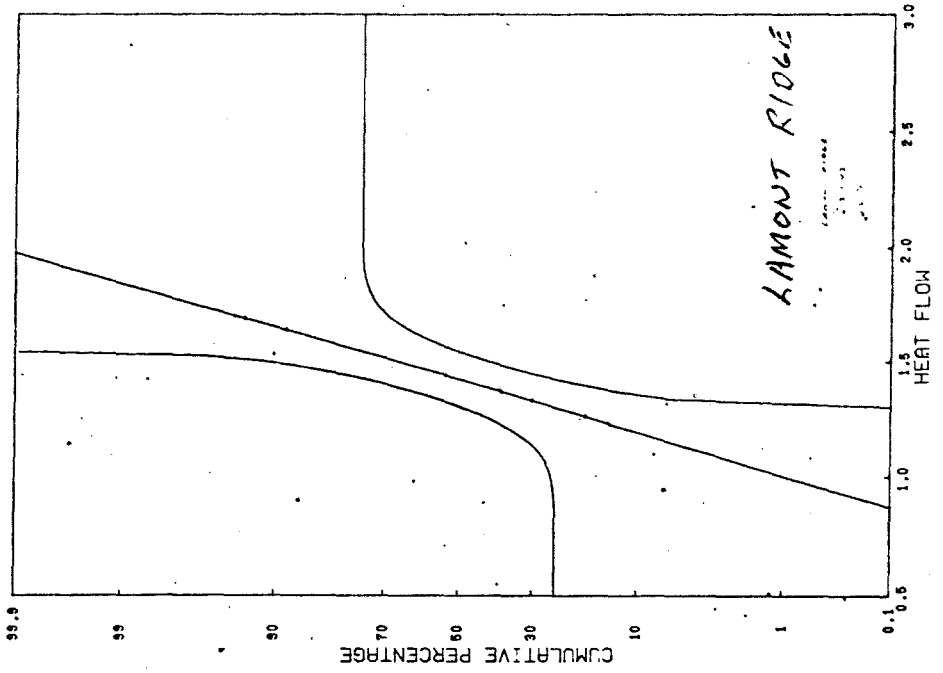

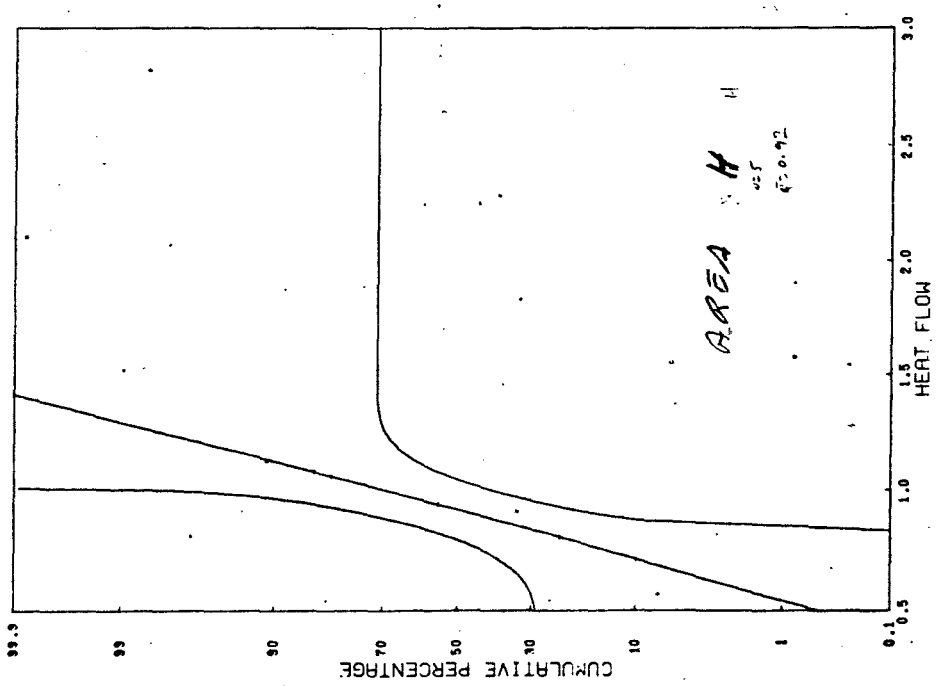

FIG. 49

Figure 49. Heat flow data with confidence limits for Area H from Figure 9 and Lamont Ridge, whose position is shown in Figure 41. Note added in 2019 by C. Ruppel: Lamont Ridge is east of the feature turned "NW Canada Basin" (now Nautilus Basin) in this report and forms part of what is now known as the Nautilus Spur.

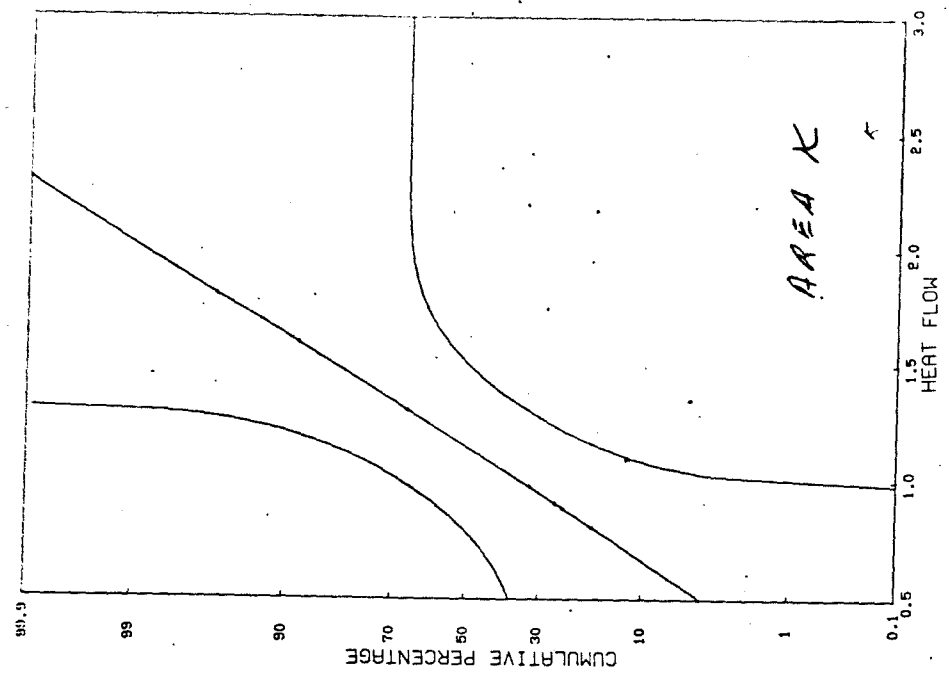

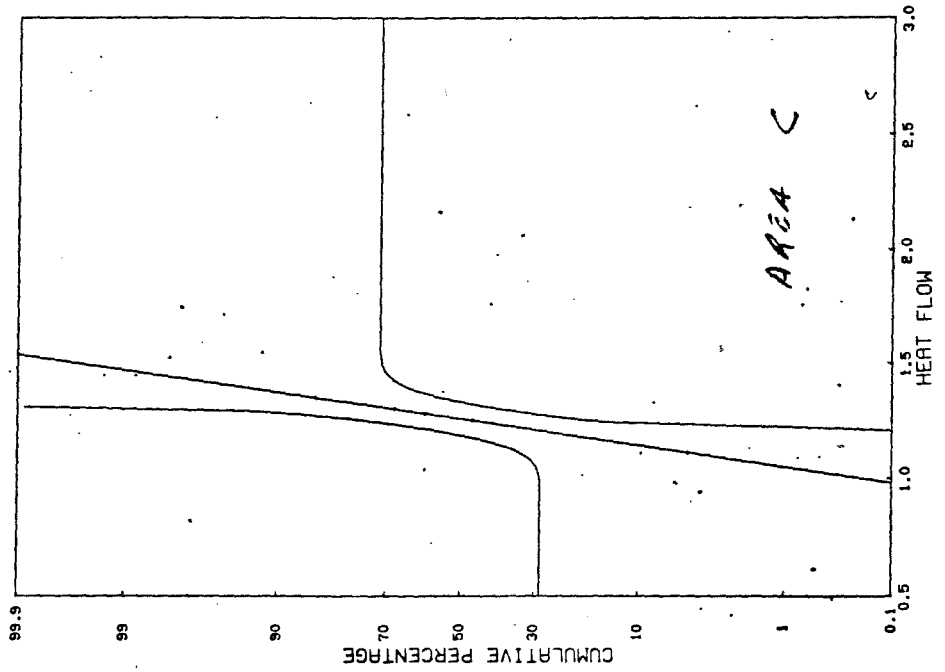

Figure 50. Heat flow data with confidence limits for Area C and Area K in Figure 9.

FIG (50)

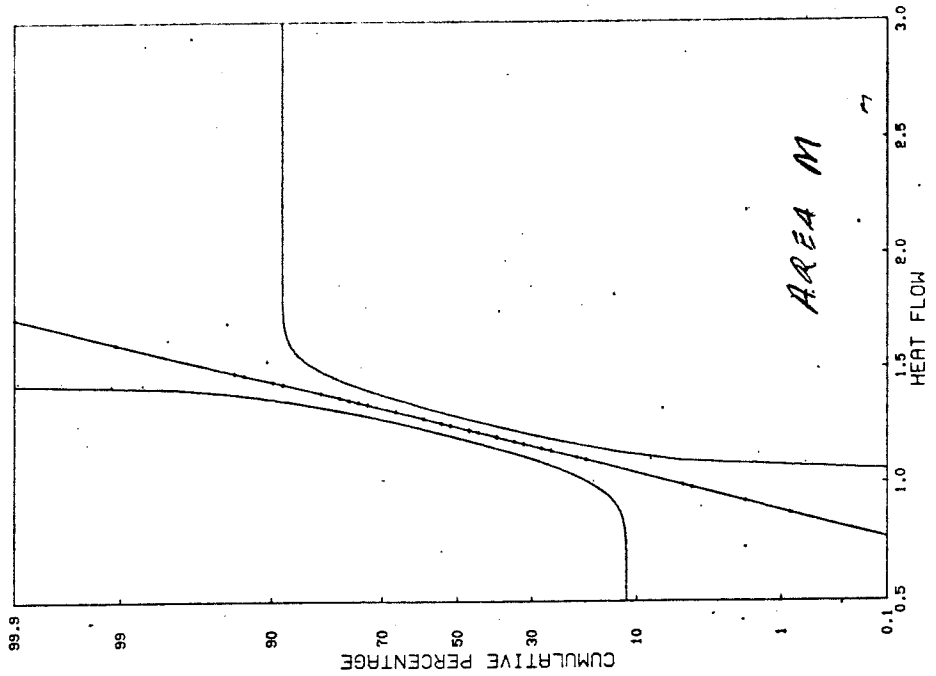

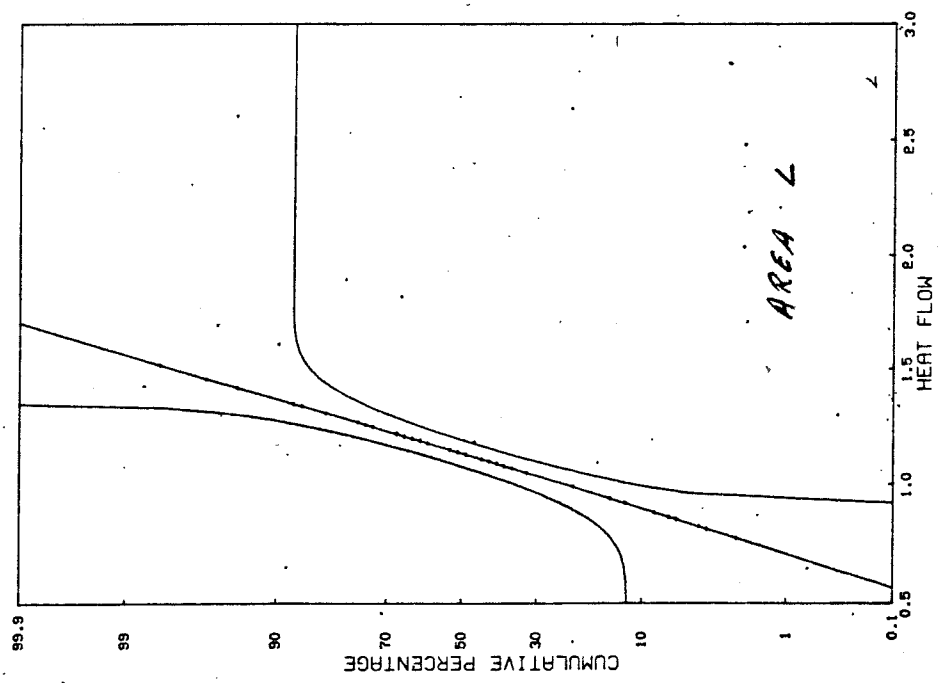

Figure 51. Heat flow data with confidence limits for Area L and Area M in Figure 9.

FIG (51)

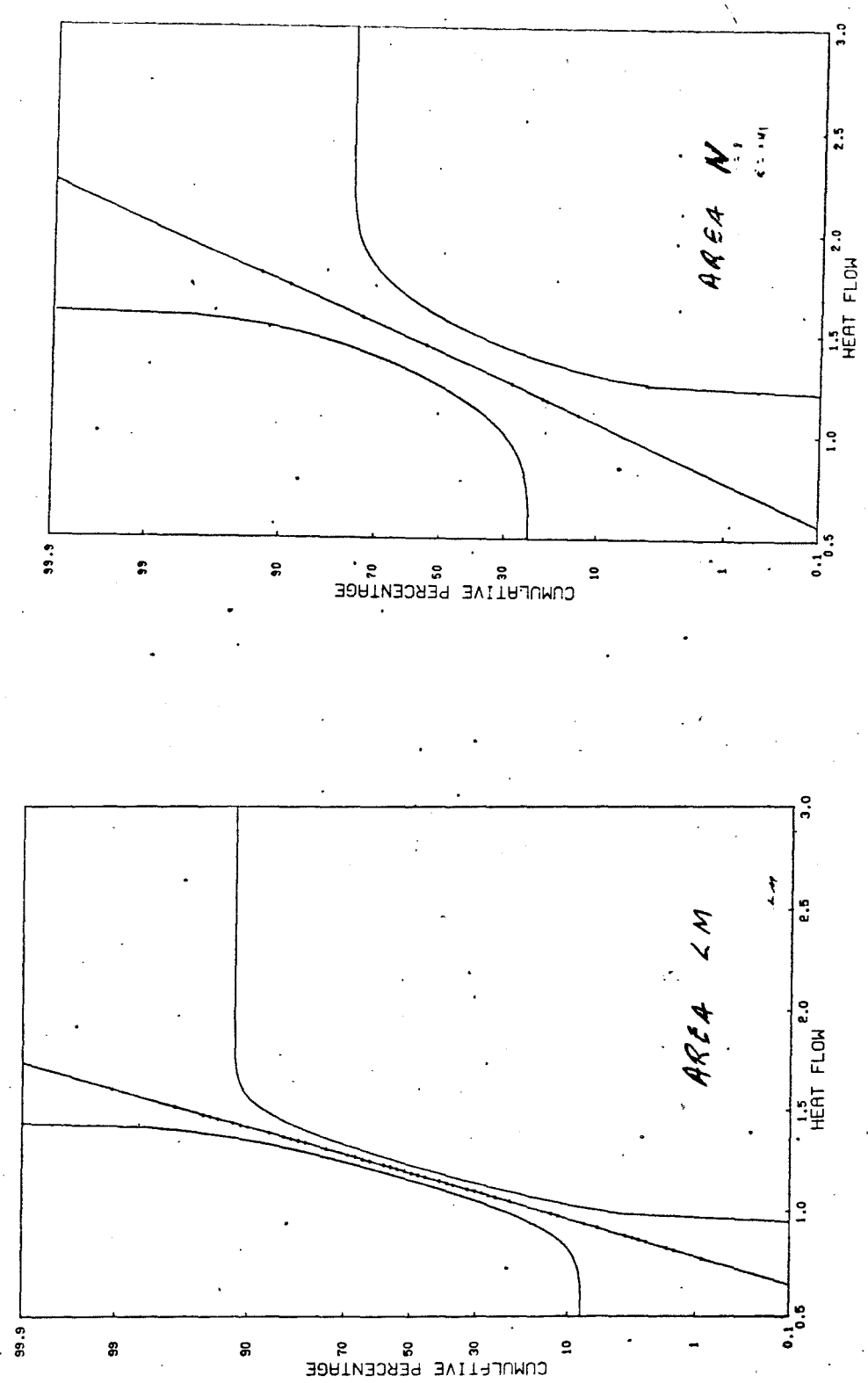

Figure 52. Heat flow data with confidence limits for Area L+M and Area N in Figure 9.

FIG. 52

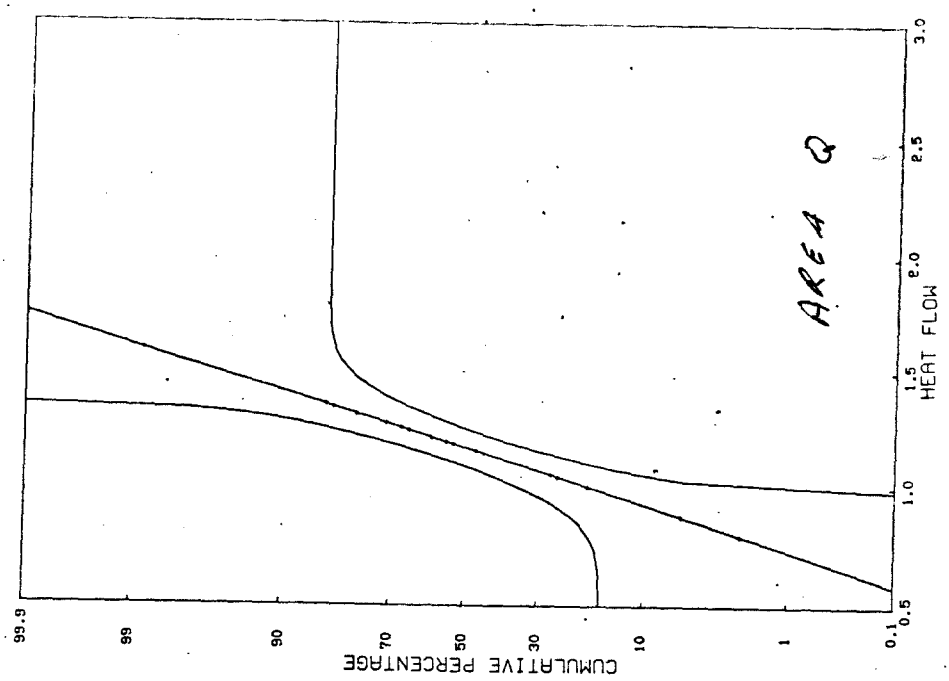

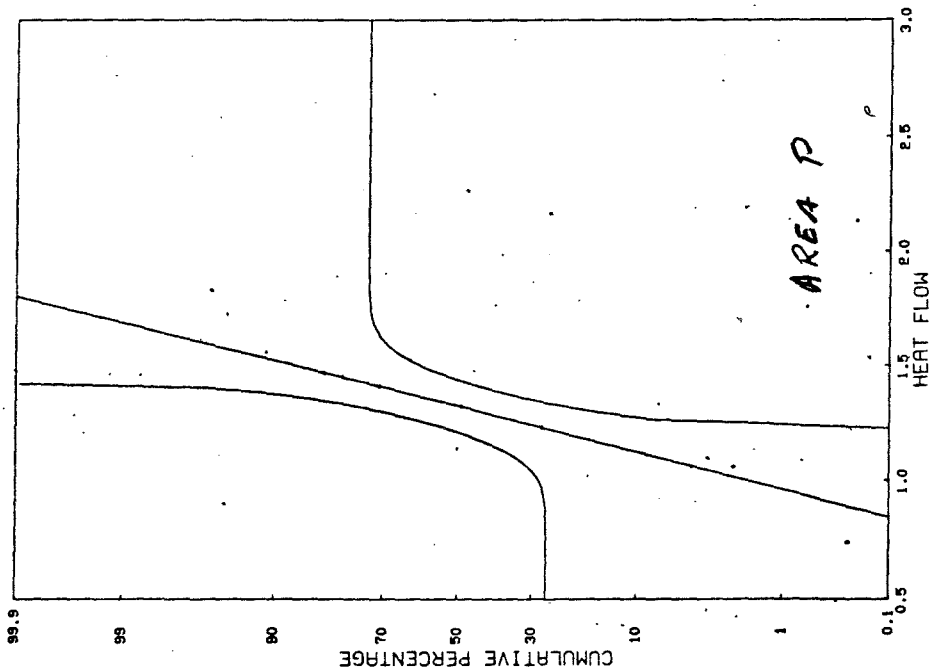

Figure 53. Heat flow data with confidence limits for Area P and Area Q in Figure 9.

F-6 (53)

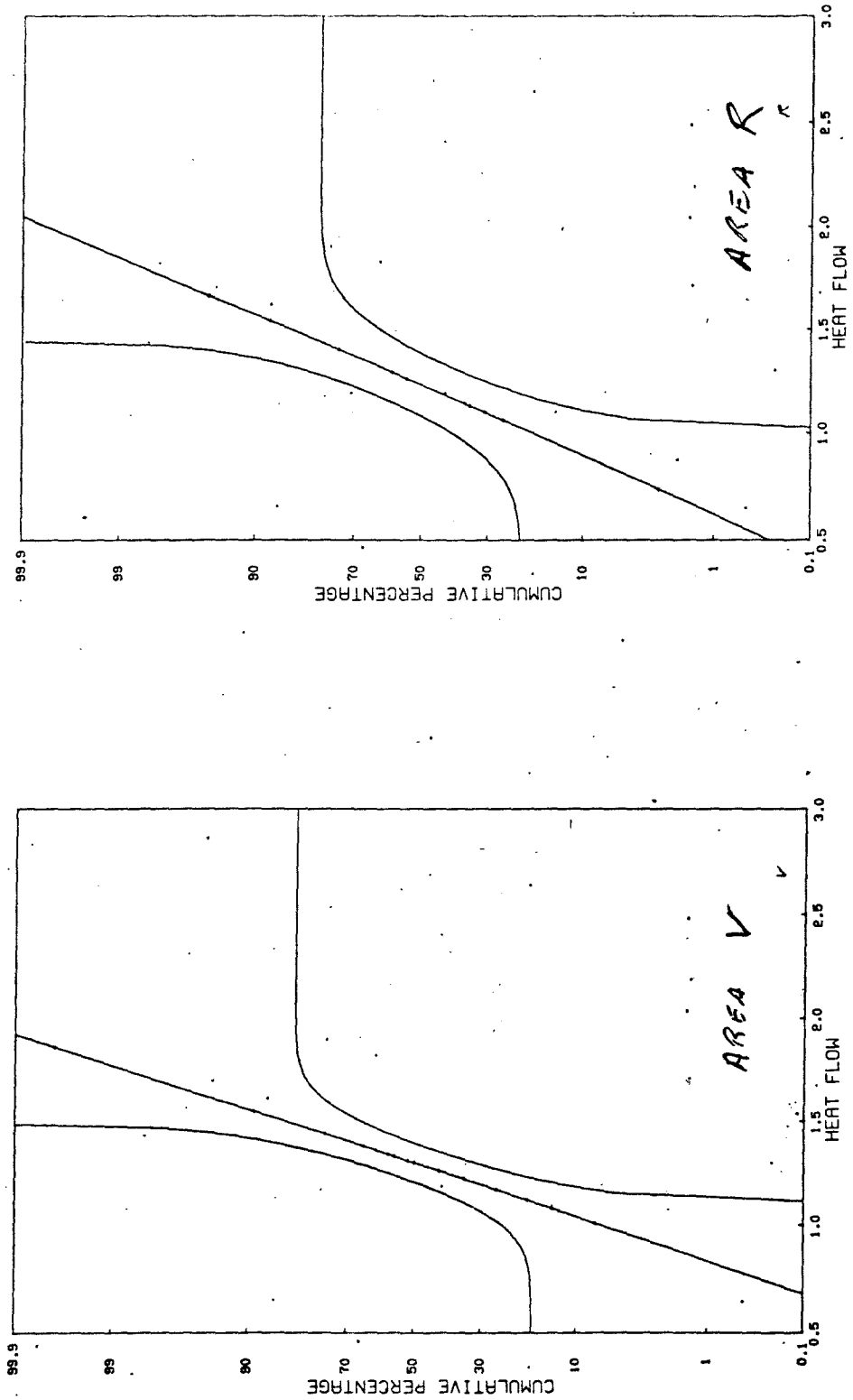

Figure 54. Heat flow data with confidence limits for Area V and Area R in Figure 9.

FIG. 54

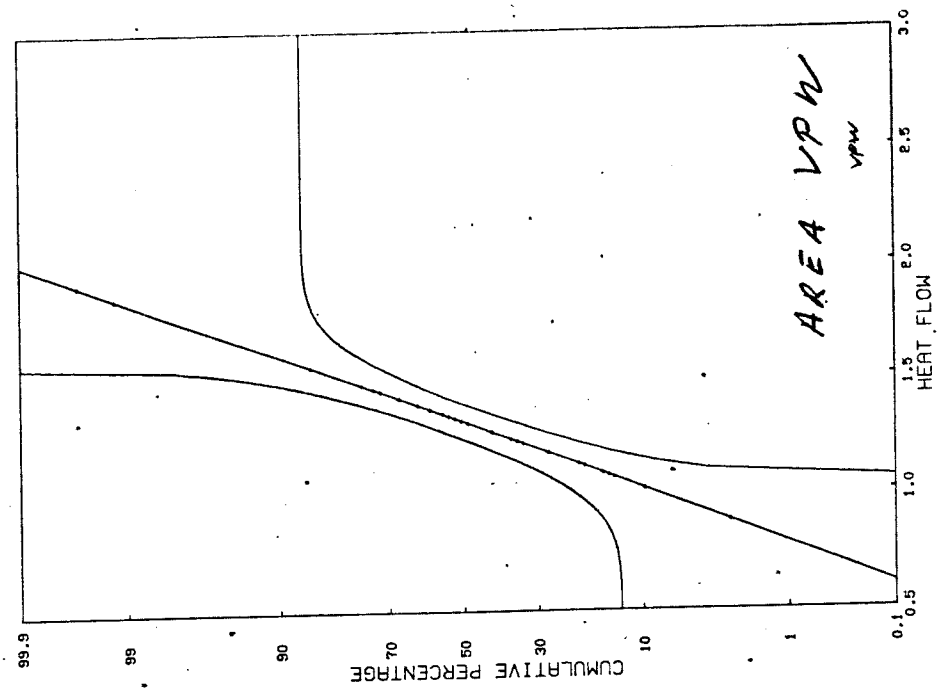

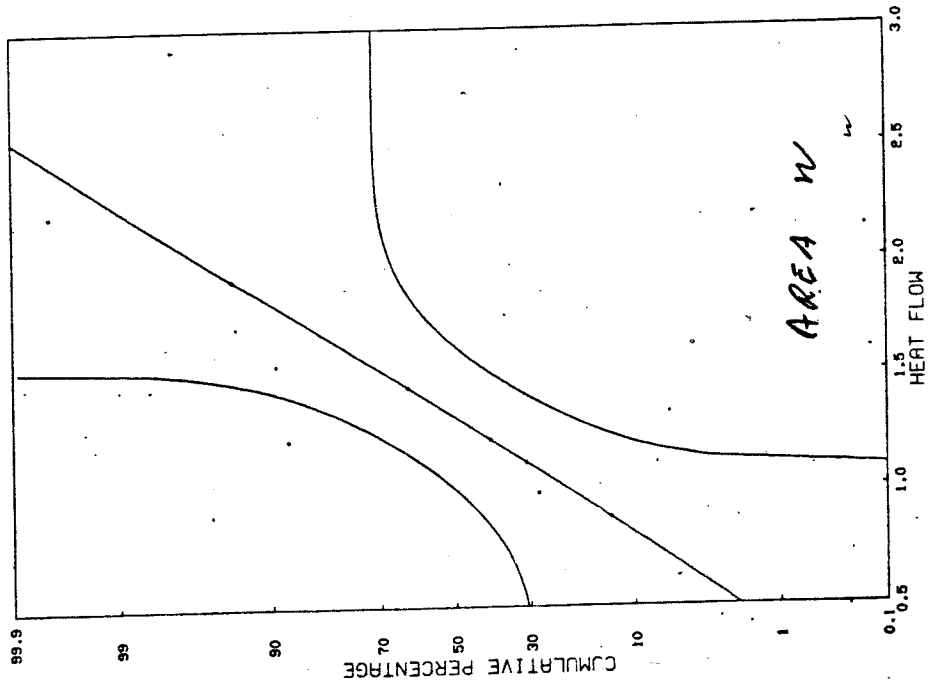

Figure 55. Heat flow data with confidence limits for Area W and Area VPW in Figure 9.

FIG (55)

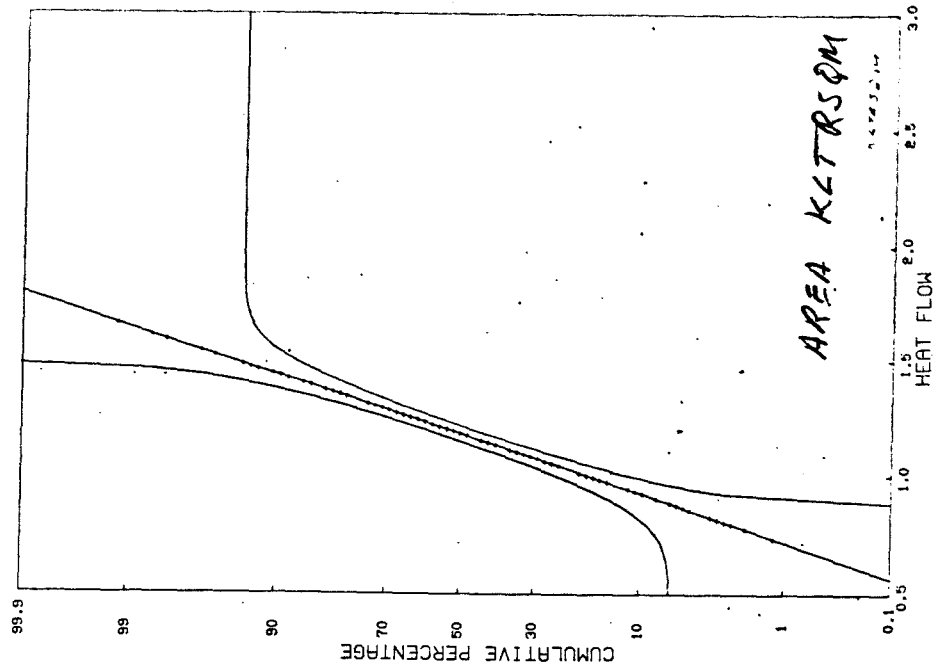

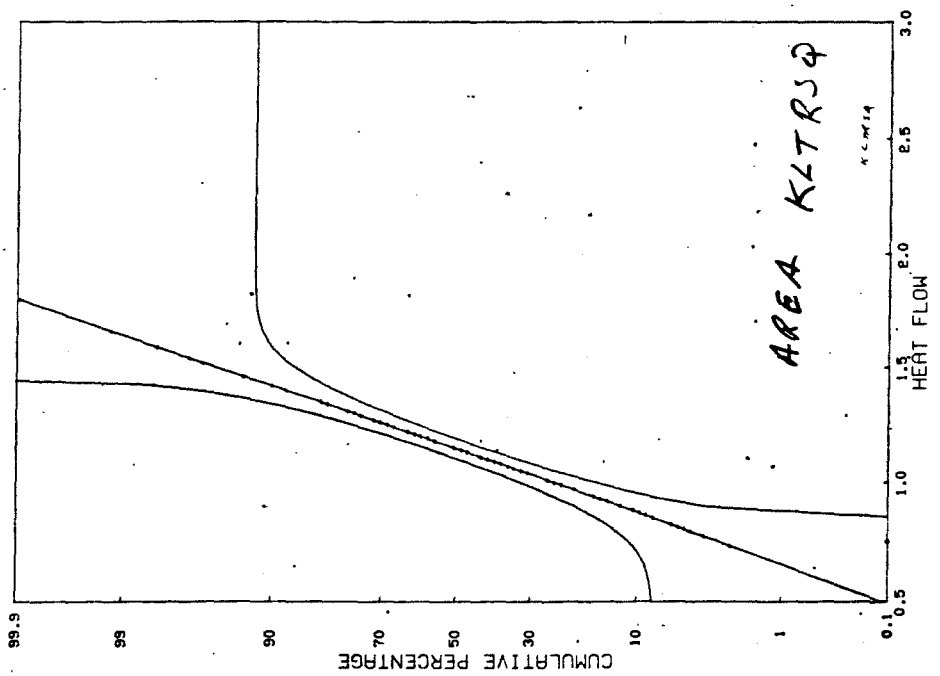

Figure 56. Heat flow data with confidence limits for Area KLTRSQ and KLTRSQM in Figure 9.

FIG 56

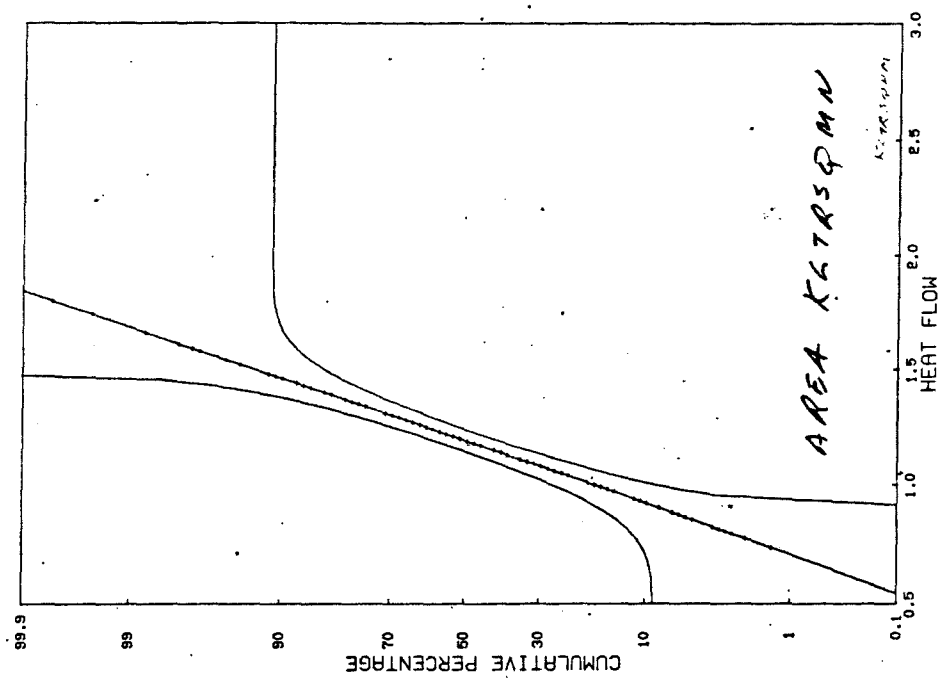

Figure 57. Heat flow data with confidence limits for Area KLTRSQMN in Figure 9.

FIG. 57

Figure 58. Heat flow data plotted with distance from the Alpha and Mendeleev Ridge crests as a test for a pattern associated with heat flow changes away from a spreading ridge. Note added by C. Ruppel, January 2019: In the decades following this report, it was shown that the AMR is not associated with seafloor spreading.

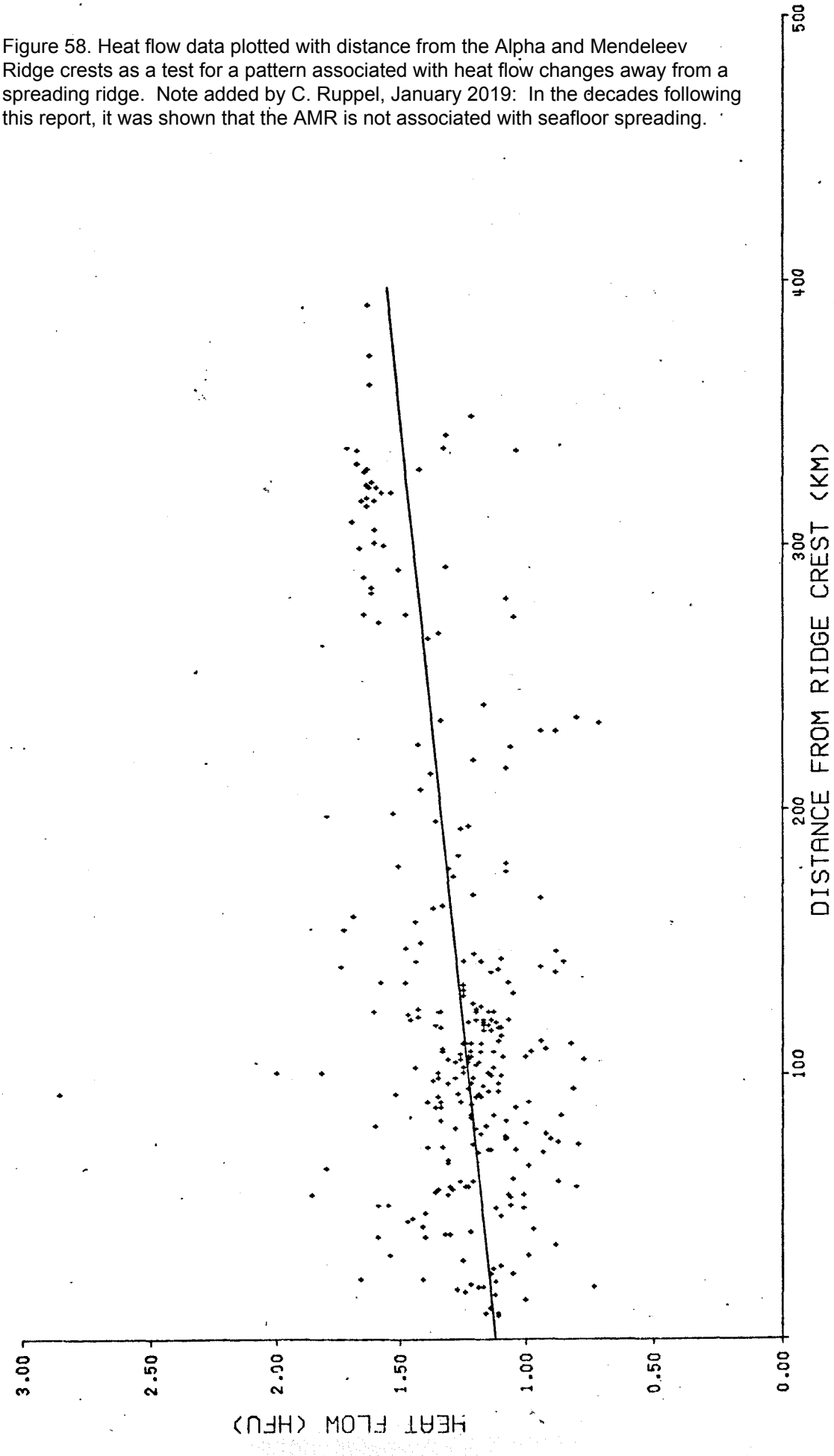

FIG 58

Figure 59. Heat flow data plotted with bathymetry for the Alpha Ridge data.

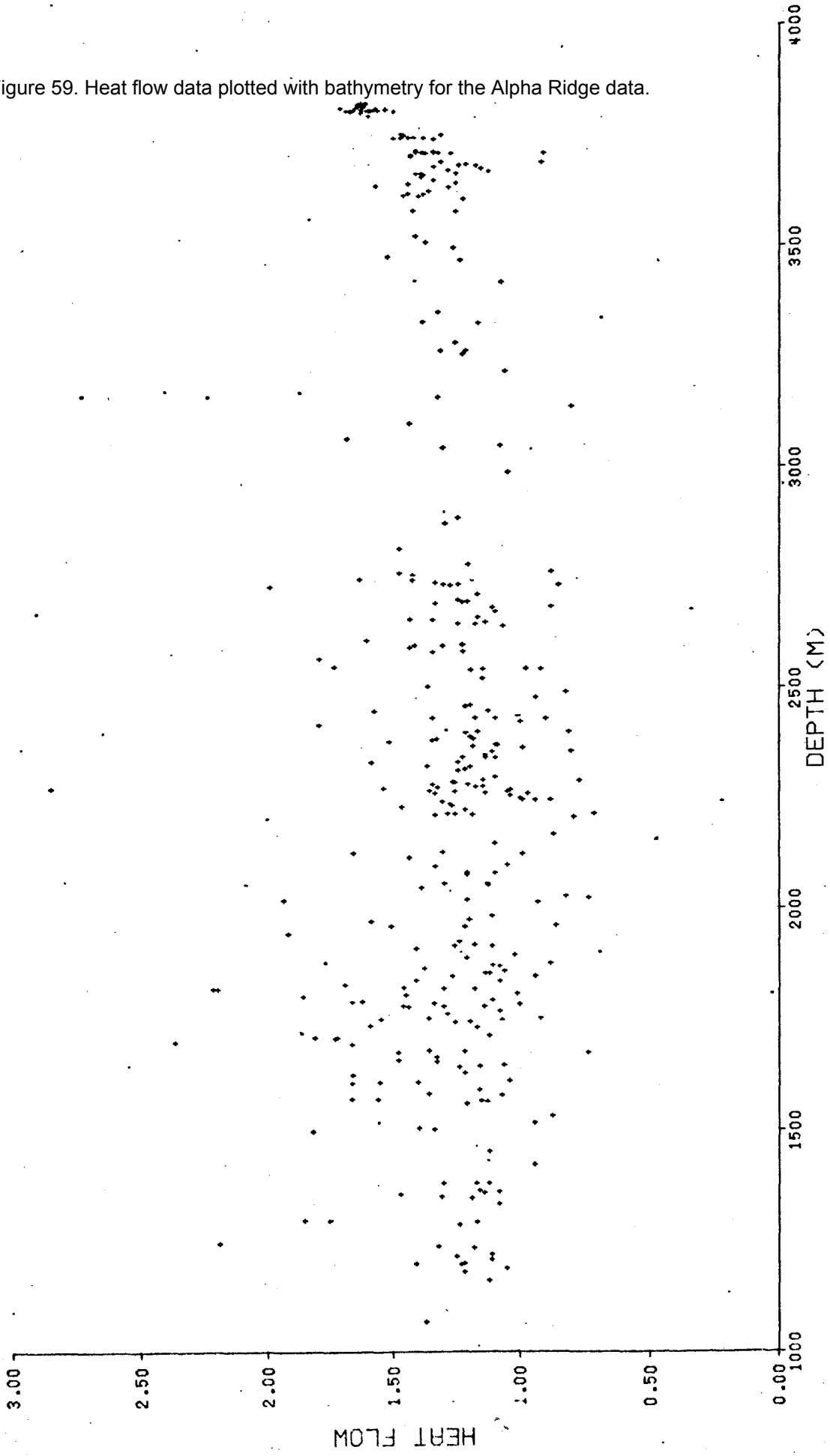

FIG 59

Figure 60. Water column temperatures measured during dedicated casts. Data in Table 4. Crosses for data from earlier than TP28 and for measurements made during heat flow casts. Squares for TP32 and 41-60. Circles correspond to TP 35-40, and triangles denote TP63-83.

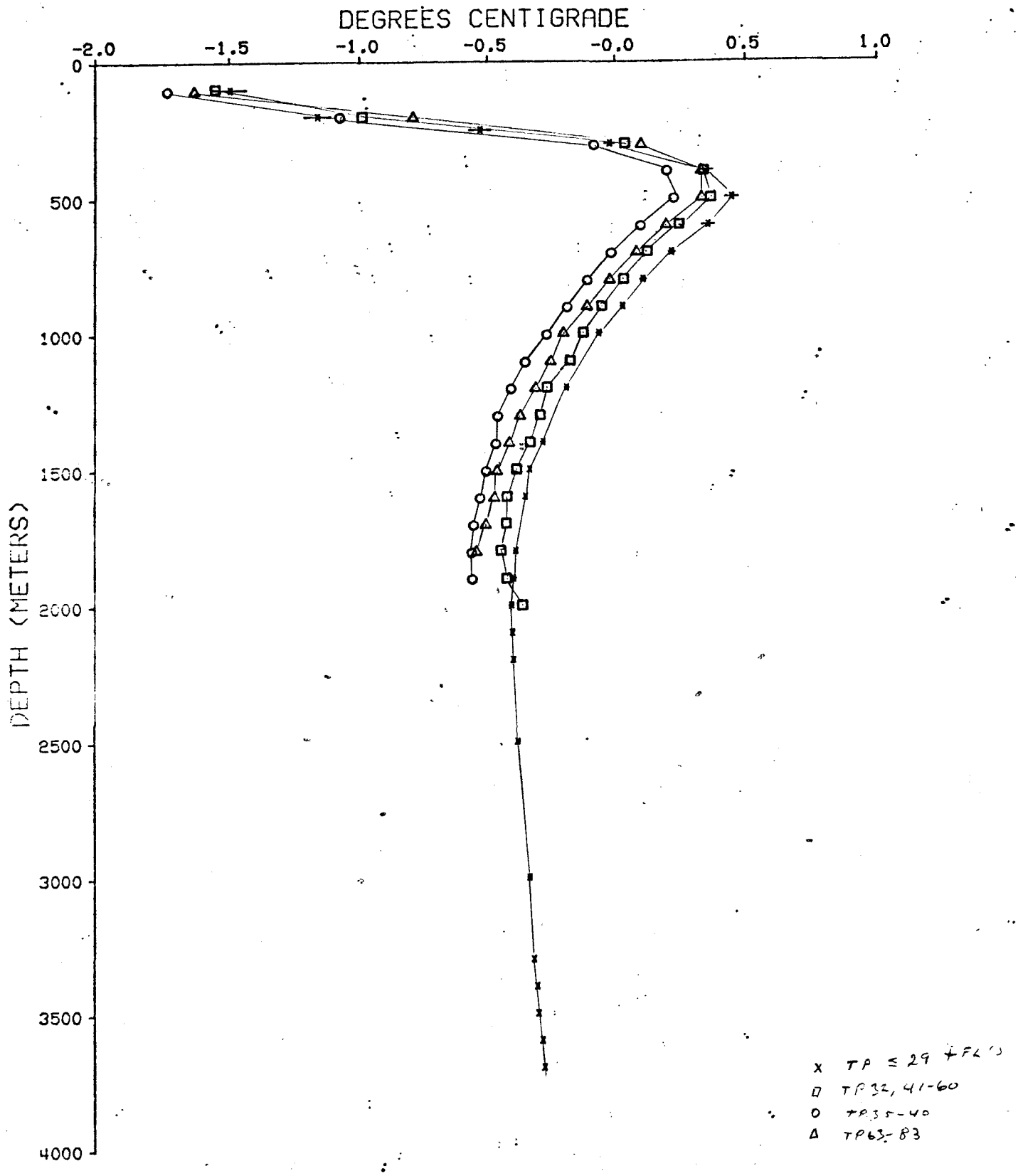

FIG. 59

Figure number incorrect in original. Should be Figure 60.

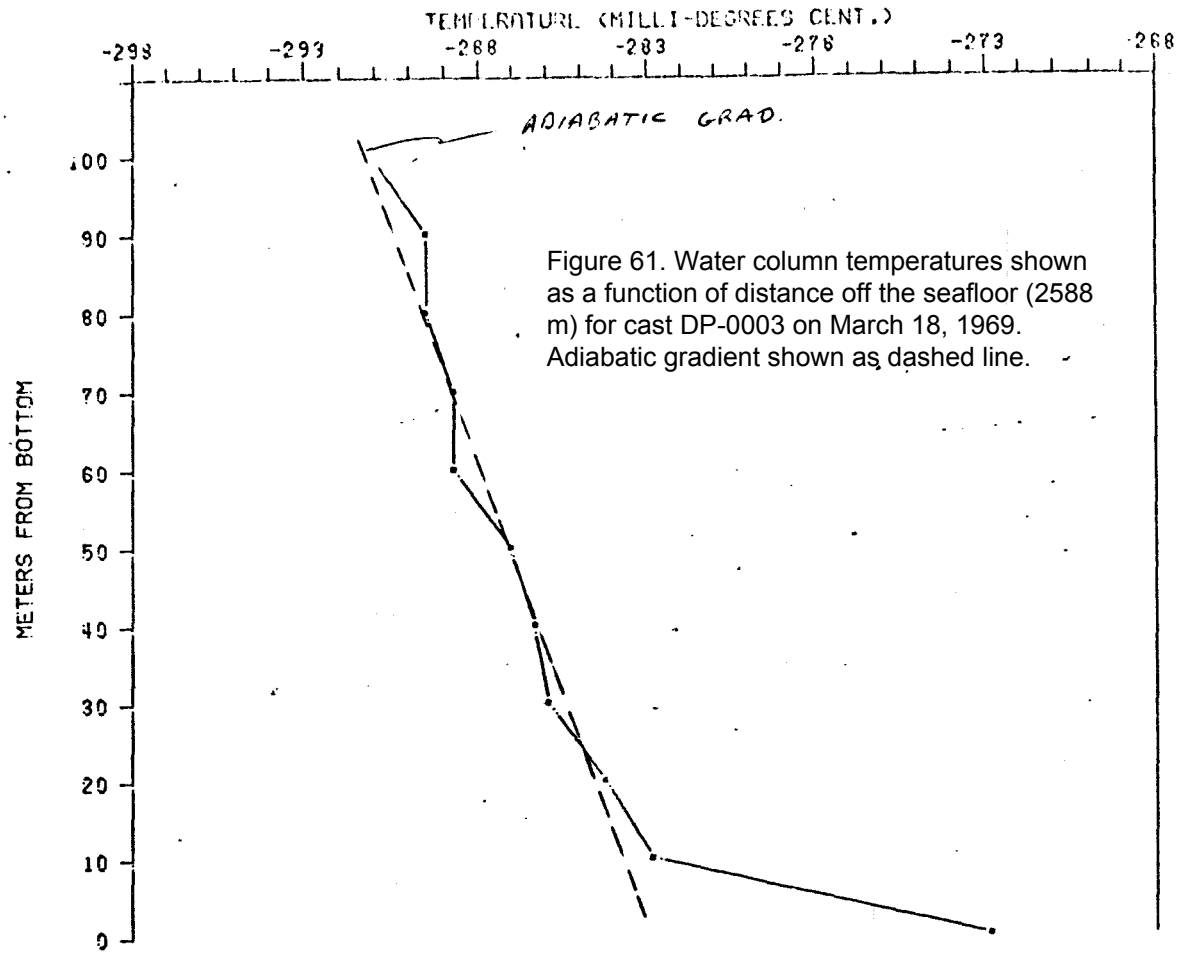

Figure 61. Water column temperatures shown as a function of distance off the seafloor (2588 m) for cast DP-0003 on March 18, 1969. Adiabatic gradient shown as dashed line.

Figure number incorrect in original. Should be Figure 61.

CAST NUMBER DP-0003 DATE 03-18-69

2546.0 M

FIG 60

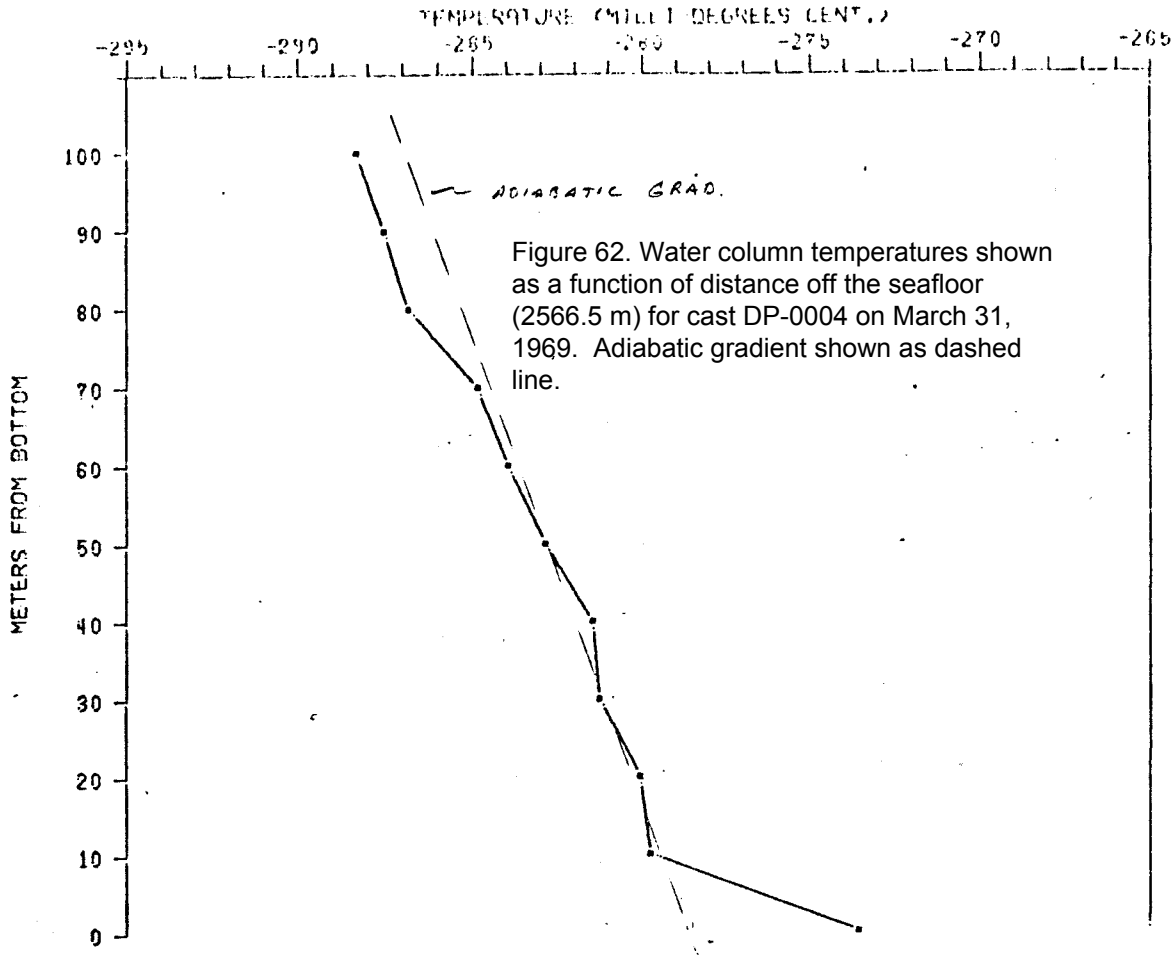

Figure 62. Water column temperatures shown as a function of distance off the seafloor (2566.5 m) for cast DP-0004 on March 31, 1969. Adiabatic gradient shown as dashed line.

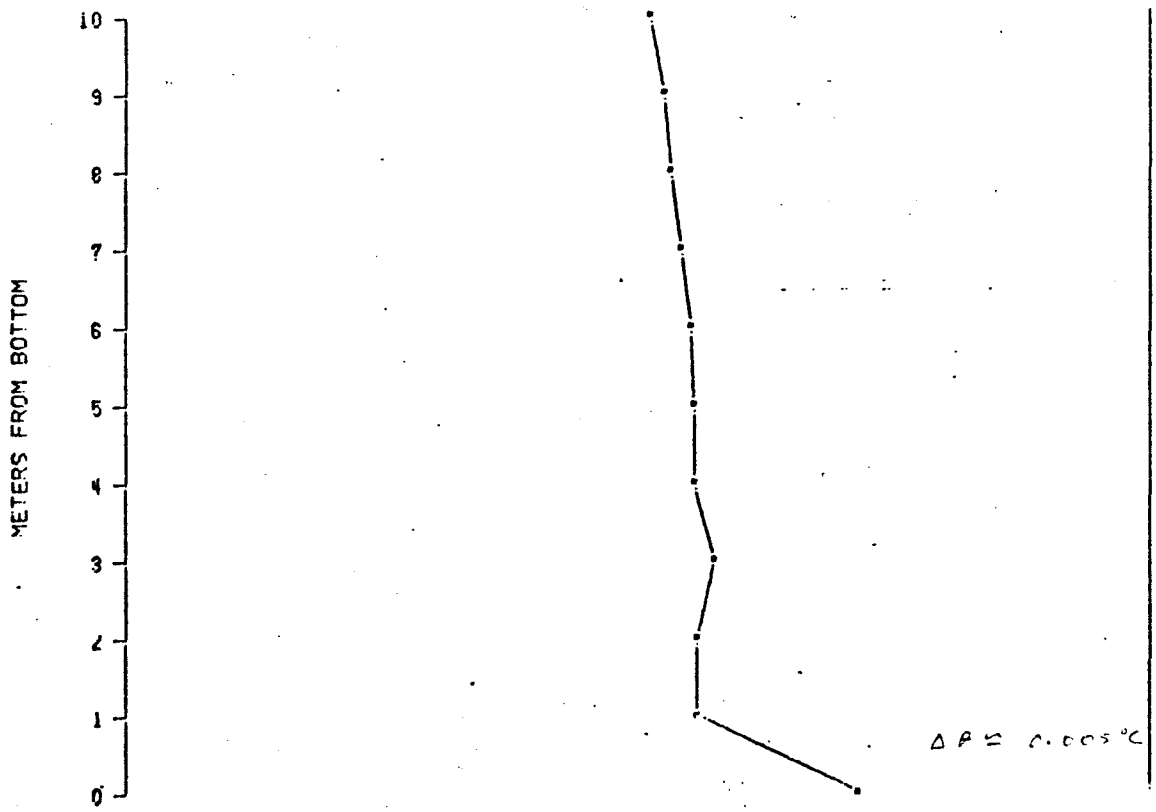

CAST NUMBER DP-0004 DATE 03-31-69

2566.5m

Figure number incorrect in original. Should be Figure 62.

FIG 61

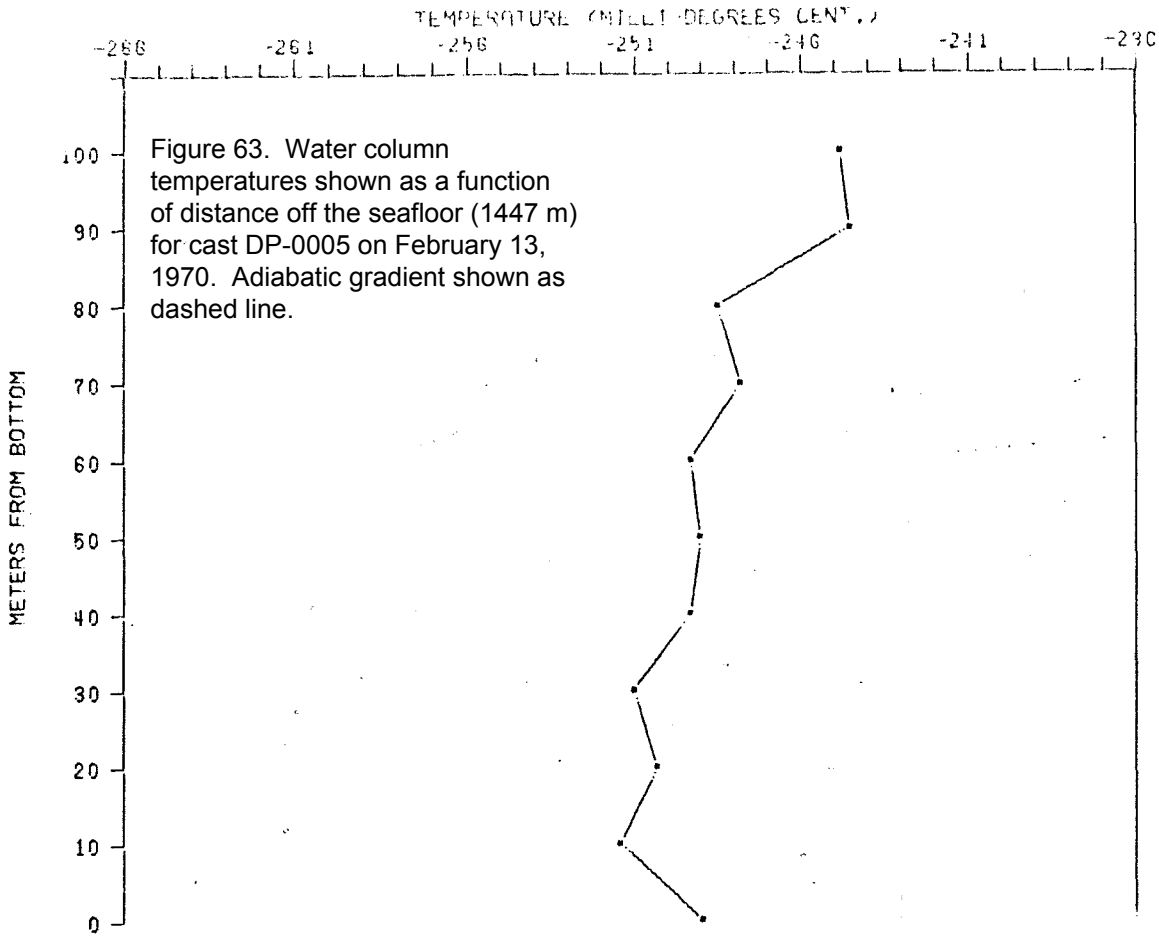

Figure 63. Water column temperatures shown as a function of distance off the seafloor (1447 m) for cast DP-0005 on February 13, 1970. Adiabatic gradient shown as dashed line.

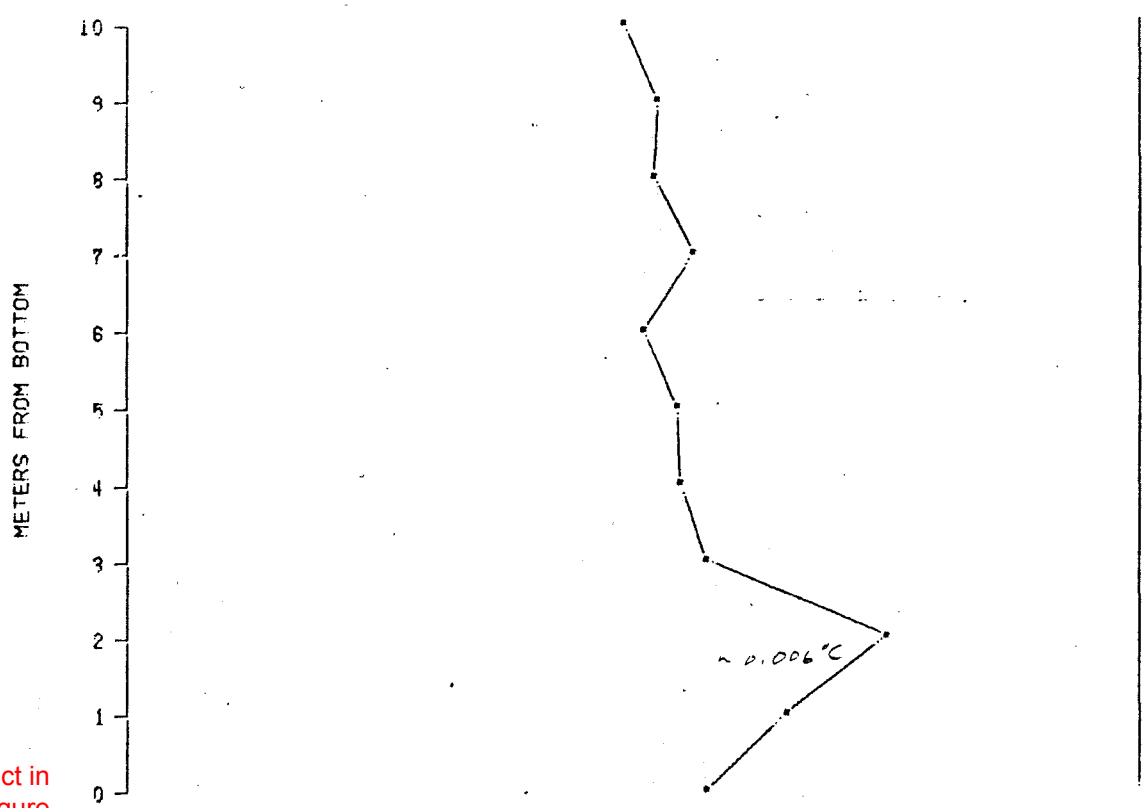

CAST NUMBER DP-0005 DATE 02-13-70

1447.0 m

Figure number incorrect in original. Should be Figure 63.

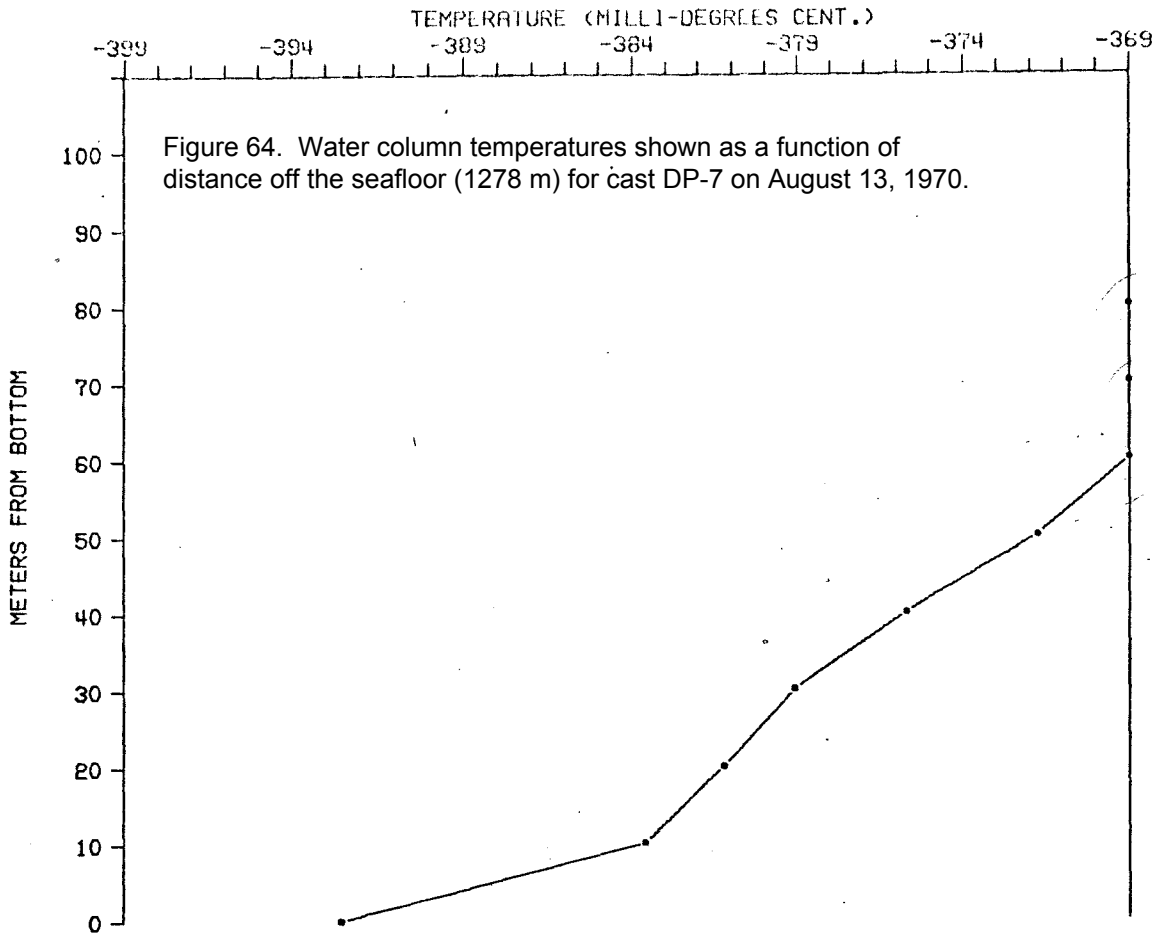

Figure 64. Water column temperatures shown as a function of distance off the seafloor (1278 m) for cast DP-7 on August 13, 1970.

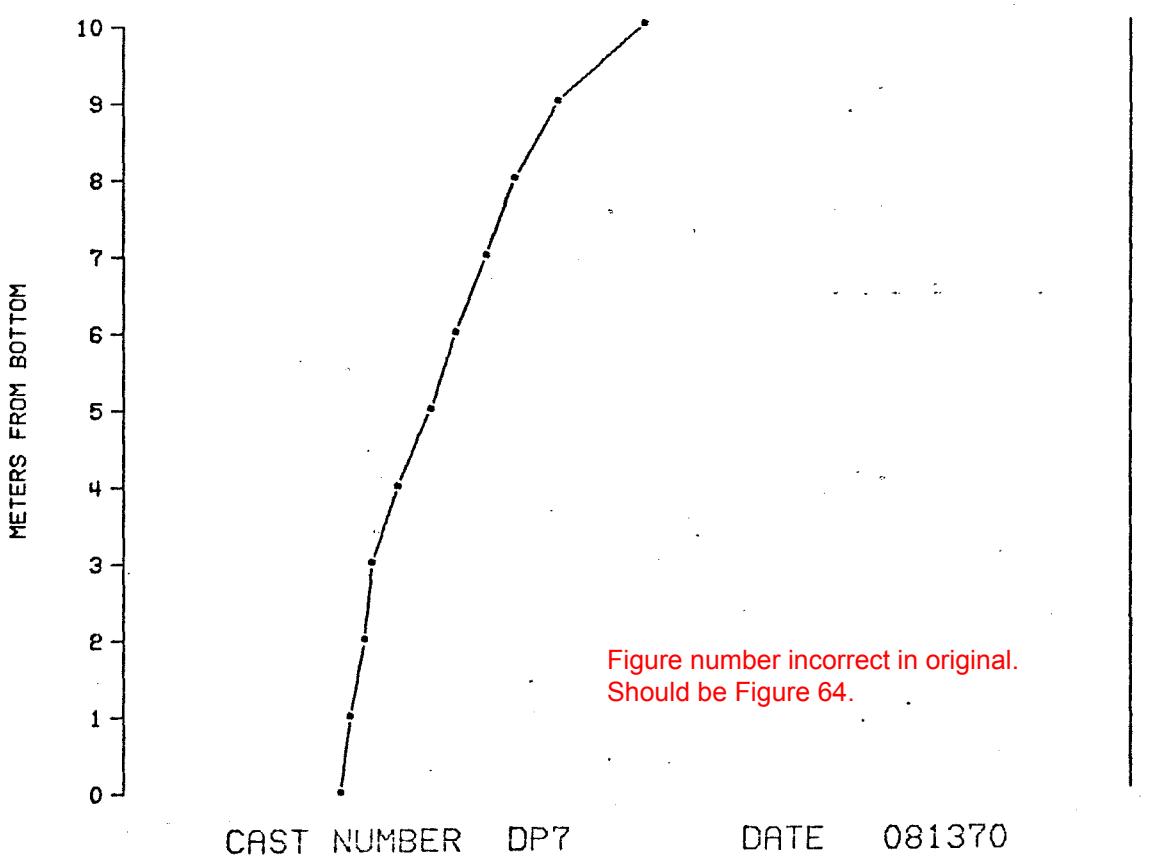

Figure number incorrect in original.
Should be Figure 64.

FIG (63)

1278 m

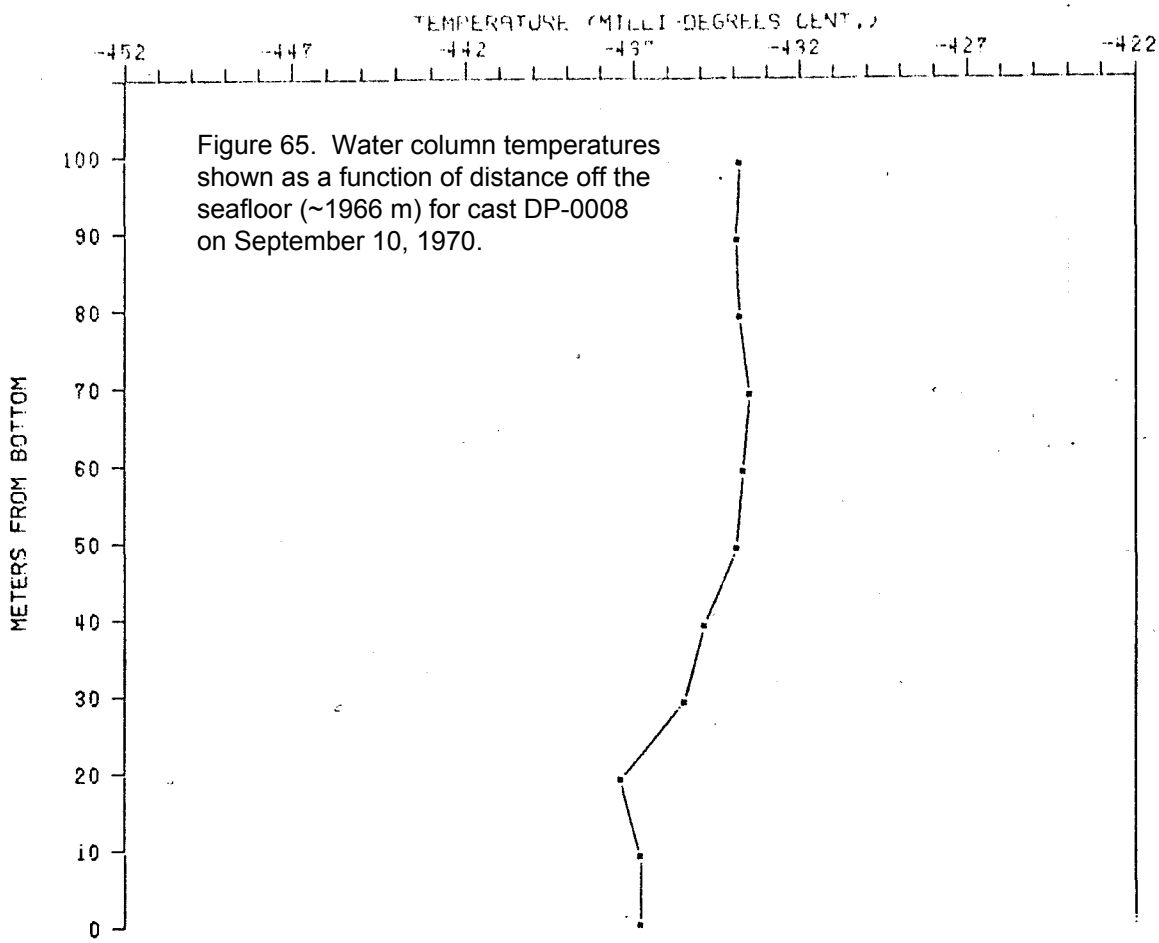

Figure 65. Water column temperatures shown as a function of distance off the seafloor (~1966 m) for cast DP-0008 on September 10, 1970.

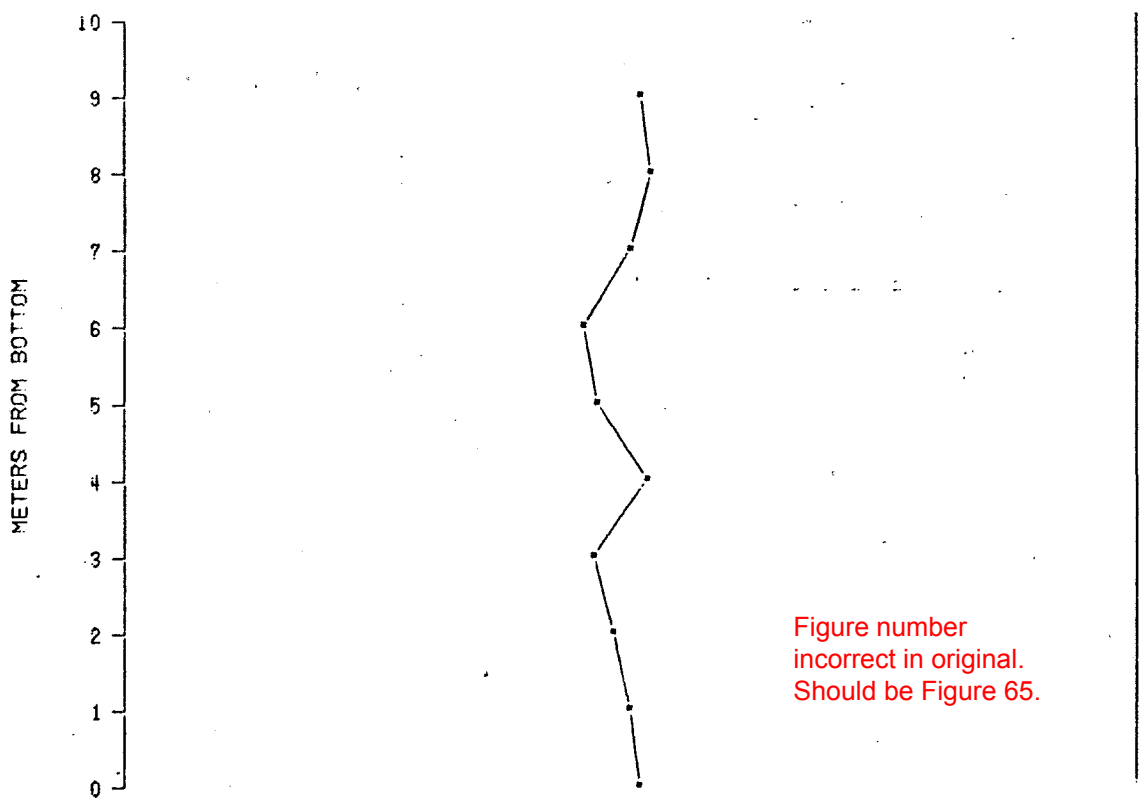

Figure number incorrect in original. Should be Figure 65.

CAST NUMBER DP-0008 DATE 09-10-70

1965.7

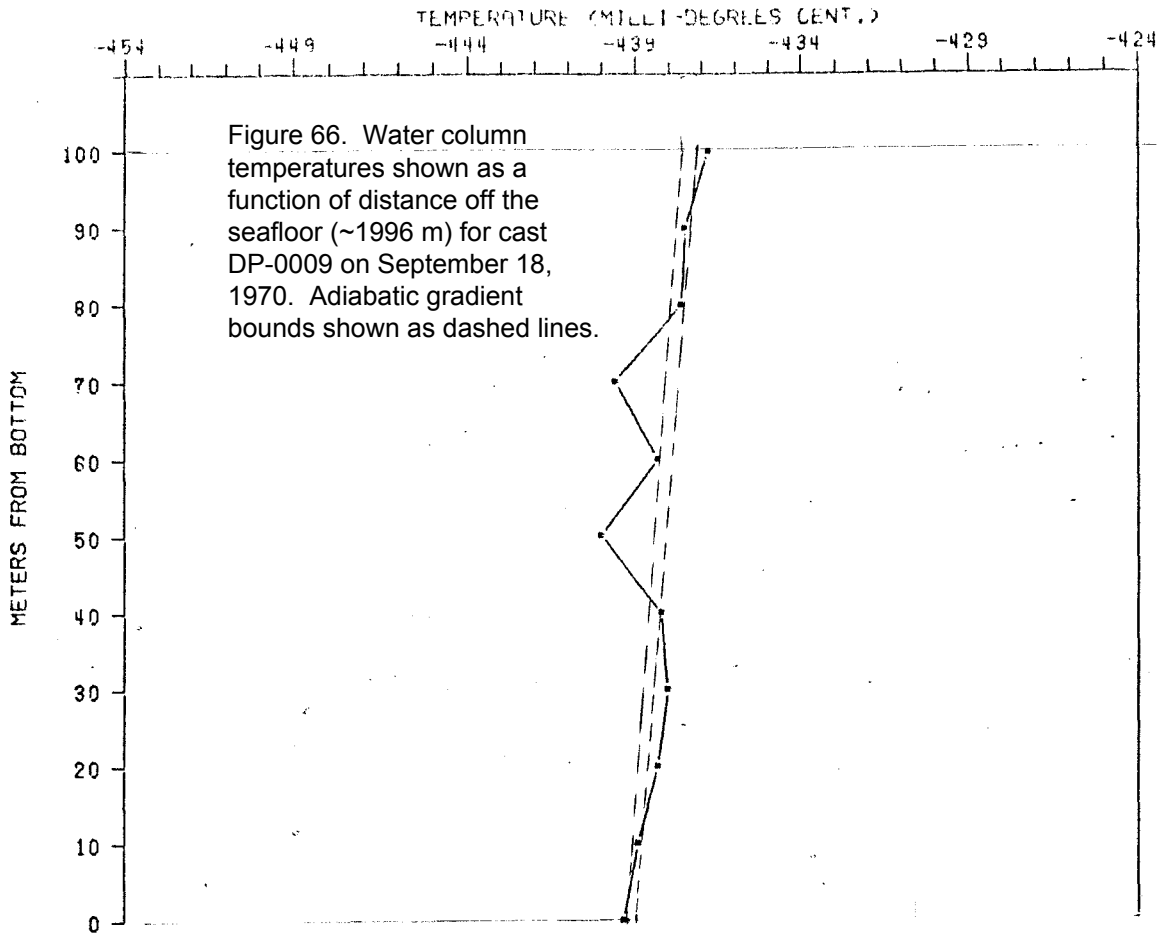

Figure 66. Water column temperatures shown as a function of distance off the seafloor (~1996 m) for cast DP-0009 on September 18, 1970. Adiabatic gradient bounds shown as dashed lines.

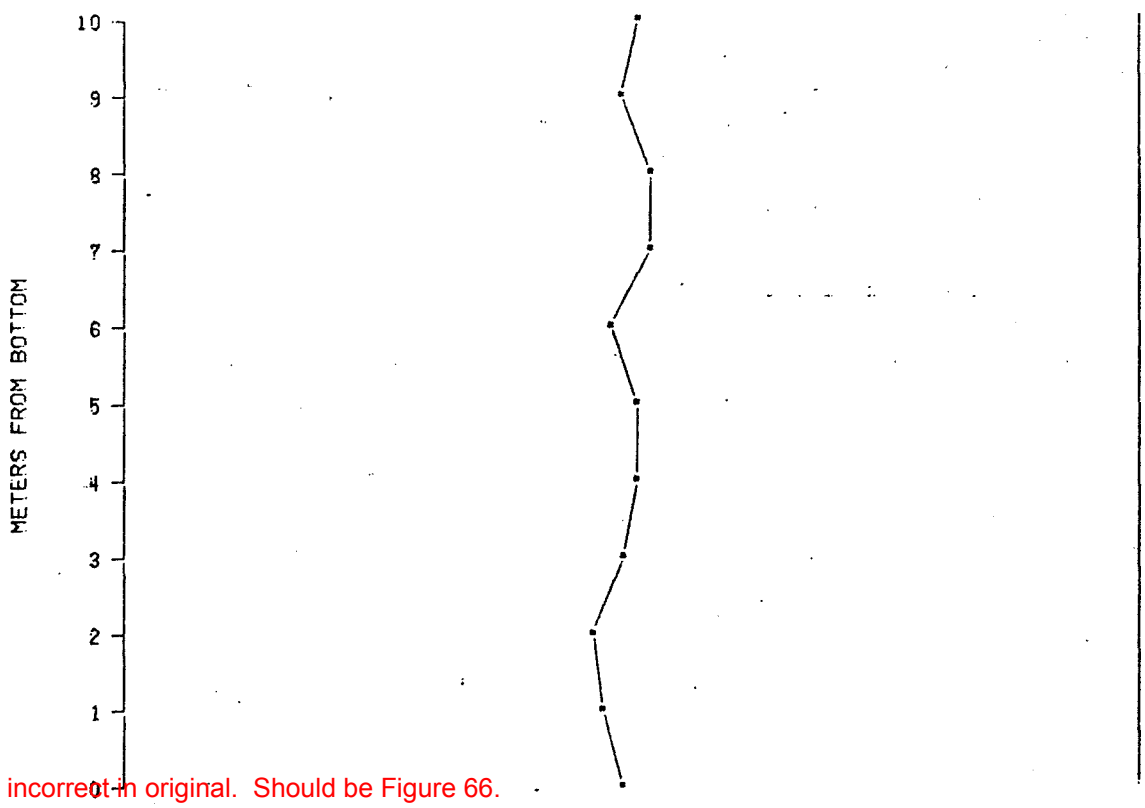

Figure number incorrect in original. Should be Figure 66.

CAST NUMBER DP-0009 DATE 09-18-70

1995.8m

FIG (65)

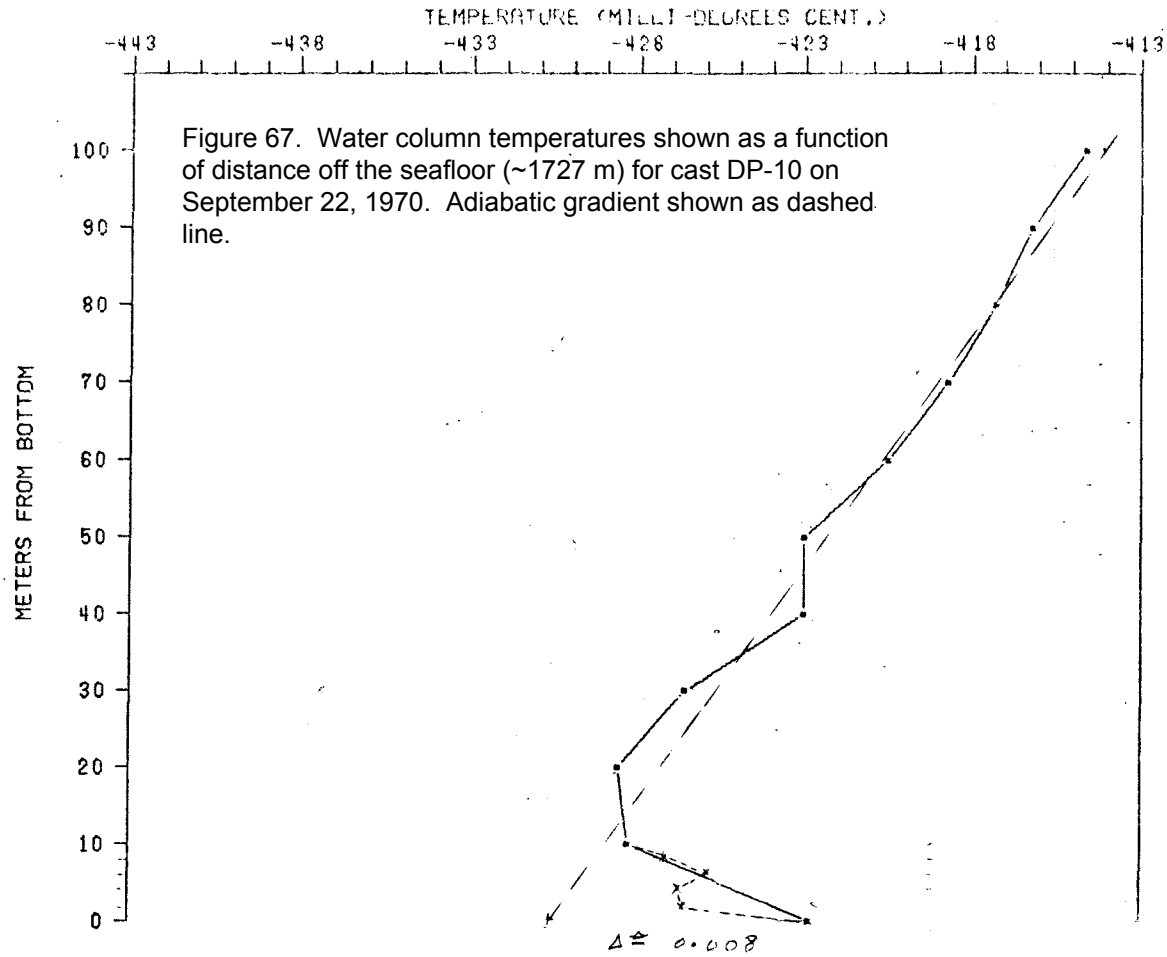

Figure 67. Water column temperatures shown as a function of distance off the seafloor (~1727 m) for cast DP-10 on September 22, 1970. Adiabatic gradient shown as dashed line.

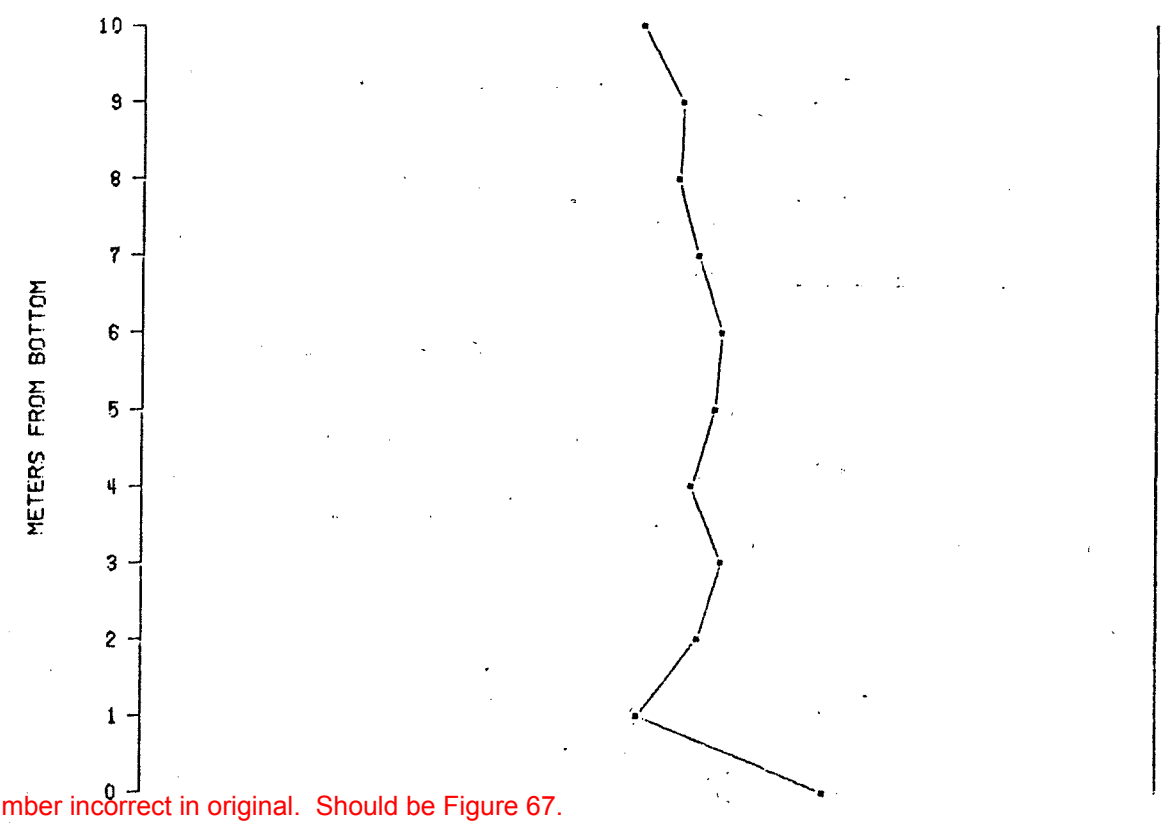

Figure number incorrect in original. Should be Figure 67.

CAST NUMBER DP-0010 DATE 09-22-70

1727.4

FIG. (66)

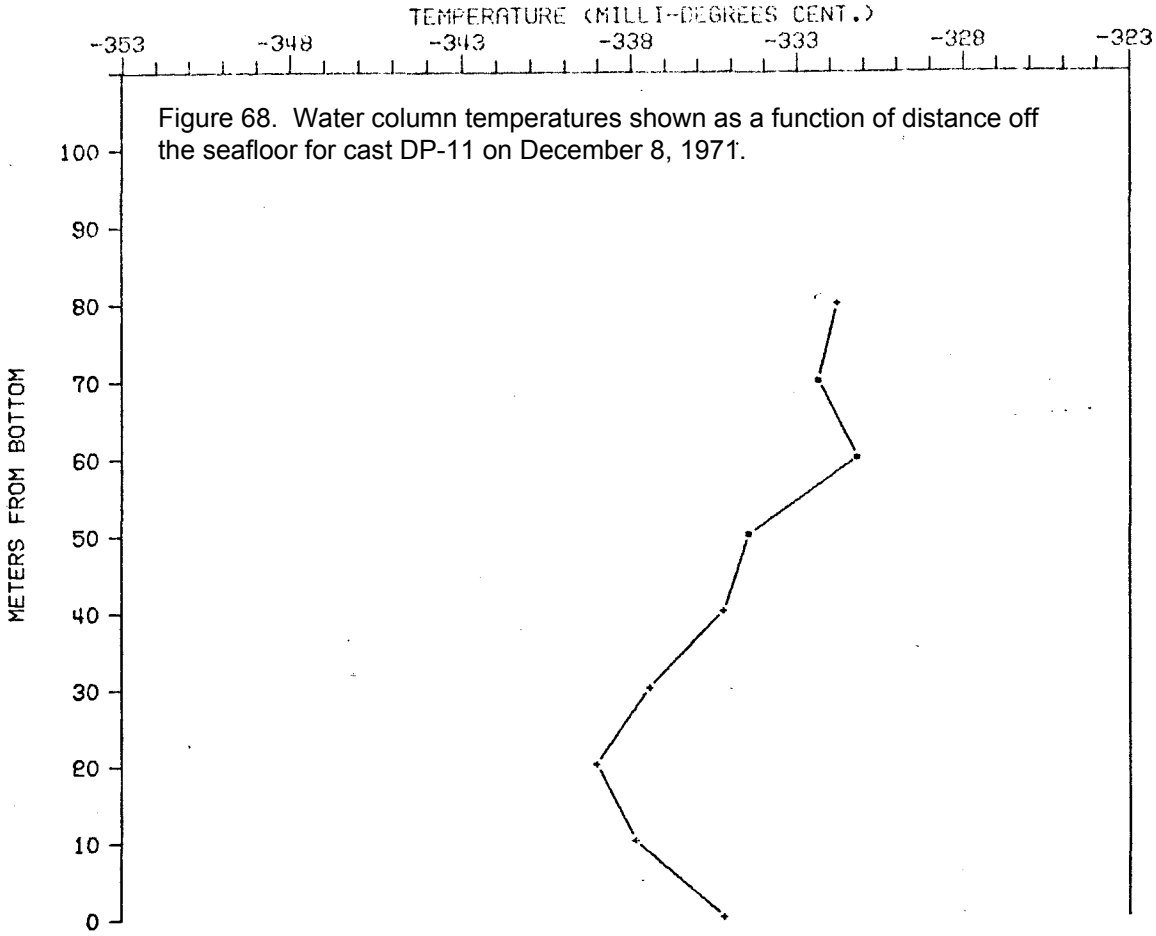

Figure 68. Water column temperatures shown as a function of distance off the seafloor for cast DP-11 on December 8, 1971.

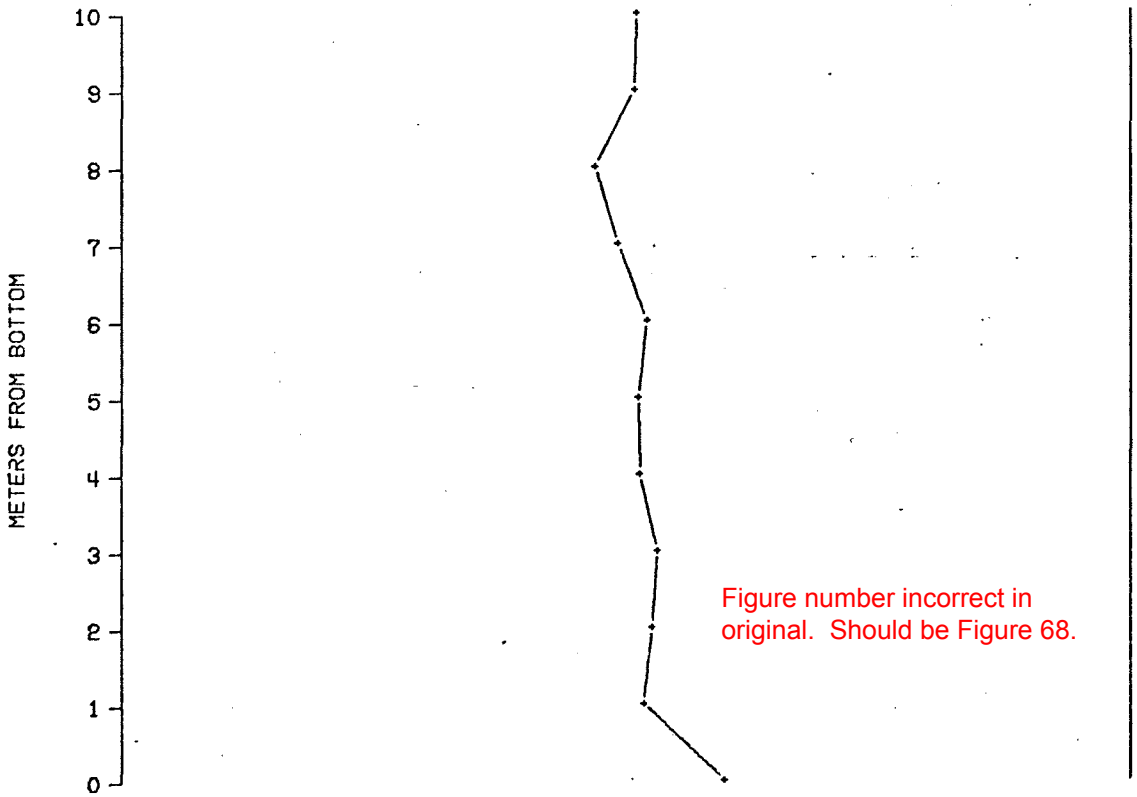

Figure number incorrect in original. Should be Figure 68.

CAST NUMBER DP11 DATE 120871

FIG. (67)

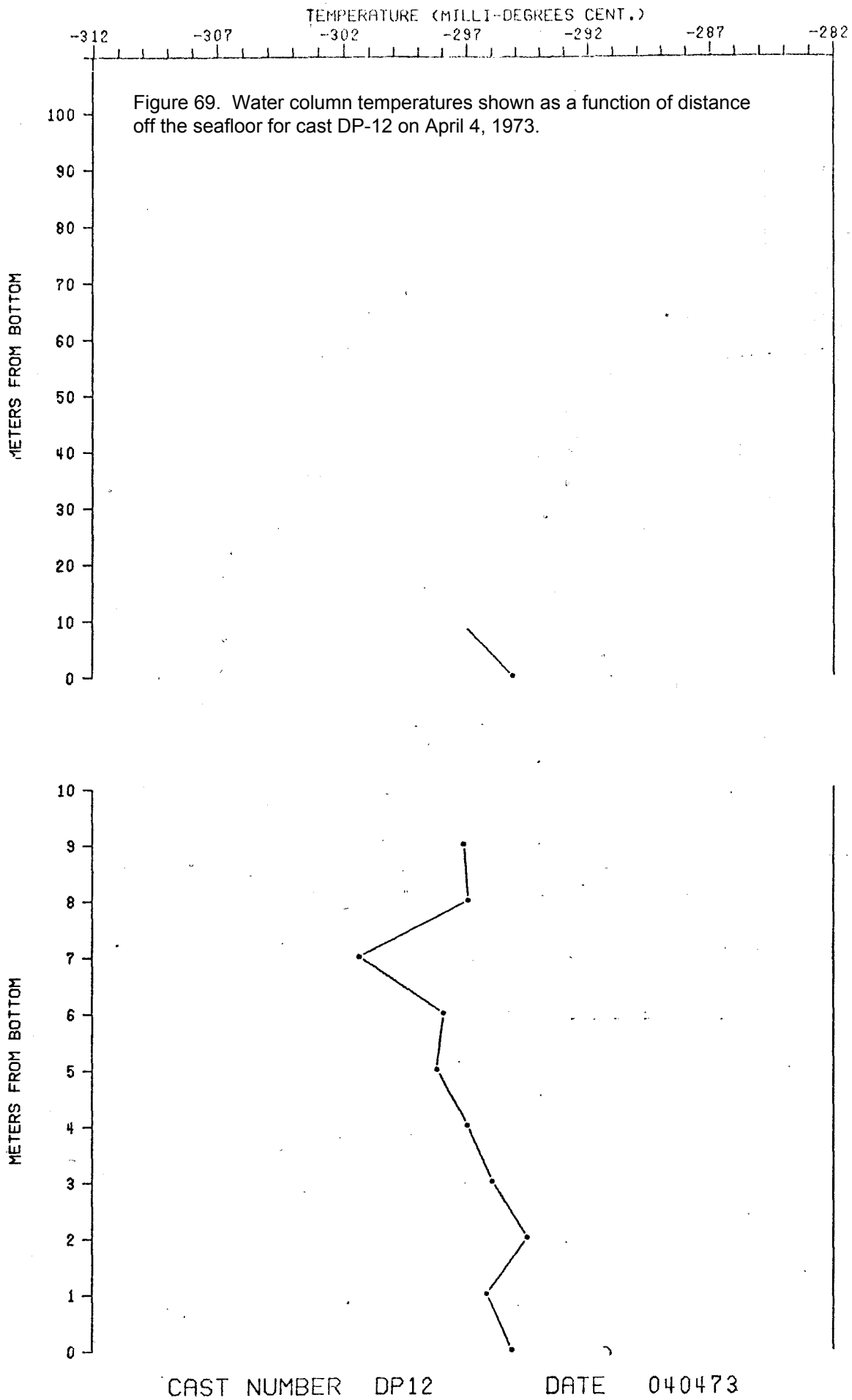

Figure 69. Water column temperatures shown as a function of distance off the seafloor for cast DP-12 on April 4, 1973.

Figure number incorrect in original. Should be Figure 69.

FIG. (68)

APPENDIX

The following interim report on T-3 heat flow was written by Art Lachenbruch and B. Vaughn Marshall in 1971, prior to completion of the T-3 heat flow dataset. The photocopy shown here was provided to C. Ruppel by Barbara Lachenbruch, daughter of Art Lachenbruch and professor emeritus at Oregon State University, in 2018.

GEOTHERMAL STUDIES OF THE ARCTIC OCEAN

INTERIM REPORT, MARCH 1971

by

Arthur H. Lachenbruch and B. Vaughn Marshall

Introduction

The purpose of this report is to outline the present status of the geothermal study of the Arctic Ocean, summarize some of the results to date, and indicate the future direction of the work.

The immediate objective of this program is to measure the distribution of heat flux from the solid earth beneath the Arctic Ocean basin, and insofar as possible to identify the factors controlling its magnitude and its variation. The broader objective is to understand these factors in relation to the world oceans.

The Arctic Ocean provides a unique opportunity for such studies for two reasons: 1) It is of manageable size, smaller by an order of magnitude than the major oceans of the world, and still containing a great variety of sharply delineated features including typical oceanic abyssal planes, a seismically active oceanic rift system, two aseismic ridges of different types and an assortment of continental slopes and shelves, and 2) much of it is accessible from stations on drifting ice for thermal measurements with a greater precision and observation density than is feasible from a vessel on the open sea. For these reasons it is believed that studies in the Arctic will lead to fundamental general information about the world oceans not readily obtainable elsewhere.

Several secondary scientific and technologic objectives are served in the process of determining the distribution of heat flow. These include precision measurements of the water temperature profile and of the thermal microstructure at the sea floor. These data bear on problems of gross circulation of Arctic water masses and of bottom currents and energy exchange at the lower boundary of the ocean. They may ultimately be important to an understanding of Arctic sedimentation and the distribution of pollutants, particularly radioactive wastes disposed in the sea. The bottom sediments are systematically cored, and detailed thermal conductivity testing is carried out in the laboratory. After the completion of these nondestructive tests, the cores are sent to the University of Wisconsin where they form the input for a comprehensive ONR-supported study of the sedimentology and magnetic and faunal stratigraphy under the direction of Professor David Clark. The material

collected by the project represents the most comprehensive suite of cores obtained by American workers from the Arctic basin, about 1500 meters of core from about 500 localities throughout an area of about 10^6 km^2 (most of the North American quadrant of the Arctic Ocean). Because of the slow sedimentation in the Arctic, typical 3-meter cores provide a sedimentary record over the past 2 million years and yield information that might contribute to our understanding of the history of ice cover on the ocean and its present delicate balance. The information obtained on physical properties of bottom sediments could be useful in assessing schemes involving technological utilization of the sea floor.

Additionally, the analysis of seismic sources in northern Siberia, whether from nuclear detonations or earthquakes, will depend to some extent on an understanding of thermal conditions in the earth's mantle beneath the Arctic Ocean basin.

Present status of the observations and data reduction

The interpretation of heat-flow observations involves an analysis of many types of data--water temperatures, sediment gradients and thermal properties, heat-production measurements, navigation and bathymetry, and results of related geophysical and oceanographic studies. In general, it is less efficient to attempt to keep current on data reduction in all these areas than to plan toward bringing them together after the ice has traversed a geographic region that forms an efficient interpretive unit. In the interim the effort is best devoted toward optimizing the quality and quantity of data being obtained. With the return of T-3 to the eastern Alpha Cordillera in the spring of 1970, an interesting geographic unit was circumscribed. During the last calendar year all of the project data to May 1970 was brought up to date on reduction, assembled on IBM cards and submitted to preliminary analysis and evaluation. This included more than 10,000 sediment conductivity values, several thousand water and sediment temperature measurements, and comparable numbers of navigational and bathymetric data. They have resulted in 318 reliable earth heat-flow determinations non-uniformly distributed over a 10^6 km^2 region including the Canada Basin and Alpha-Mendeleyev Cordillera. Preliminary inspection suggests that they contain important new information on the nature of extinct ocean rifts, the thermal state of the crust and upper mantle in the Arctic basin, the unique thermal properties of Arctic Ocean sediments, and on the thermal regime and possibly circulation patterns of Arctic waters, particularly near the sea floor. Results of earlier studies on this project, including those in the Denmark Strait have been discussed in the published literature, but systematic inspection of this large new block of data is only now getting under way. However, a few preliminary comments on the data can be made at this time.

Thermal conductivity. The heat flow through the sea floor is obtained by multiplying the thermal gradient by the thermal conductivity of the sediment in which the gradient was measured. Thus no matter how accurate the gradient measurement, the heat flow can be no more accurate than the conductivity value used. Several studies have indicated a functional relationship between moisture content and ocean sediment conductivity. As moisture content is easy to measure, it has been common practice in many oceanic heat-flow studies to measure only the water content and determine conductivity from an empirical curve, the most common being that of Bullard and Day (1961) (see dashed line, Figure 1). Preliminary project data (circles and crosses, Figure 1) from a small part of the Arctic basin ($\sim 10^2$ km in diameter) indicated that the Bullard-Day curves gave values that were systematically too low and that the water content was a poor indicator of conductivity in any case. Subsequent project measurements throughout a region, now 1000 km in diameter, confirm this. The small pluses in Figure 1 represent about 1000 of the additional conductivity

measurements. The solid line in Figure 1 is a least-square fit to the original Arctic data (Lachenbruch and Marshall, 1966). It is clear that even this relation can cause heat-flow errors of several tens of percent. Such errors would defeat the unique advantages afforded by an ice island to investigate the fine structure of the heat-flow field with closely spaced precision gradient measurements. For this reason extensive conductivity testing has been carried out with an automated digital system for several years. Heat flows are determined only when gradient and conductivity have been measured in the same material. The success of this approach is indicated by the good agreement between heat flows determined at different levels in the same core.

It was suggested (Lachenbruch and Marshall, 1966) that the anomalously high conductivities of Arctic sediments resulted from a large component ice-rafted material that must be highly dolomitic or silicic. This has now been confirmed by extensive analyses by Clark (oral communication), and it is likely that the conductivity data will be useful in stratigraphic studies. One group of cores, flagged by remarkably low conductivities (approximately the same as pure water), were subsequently found by Dr. Clark's laboratory to be a unique deposit of volcanic ash. A uniquely high thermal gradient in this material compensated for the low conductivity to yield a normal heat flow, confirming the steady-state conduction assumption.

Water temperature. Two types of precision water-temperature profiles have been obtained during the course of the heat-flow studies. The first is complete from the surface to the bottom with measurement points spaced in such a way as to identify the gross thermal features and the boundaries between water masses. The sample in Figure 2 shows the well-known configuration of warm "Atlantic water" (250 - 1000 m) sandwiched between colder "Arctic water" near the surface and nearly isothermal "bottom water." Systematic trends in such curves will be examined in terms of gross circulation patterns and water depth.

The second type is a near-bottom profile with 10-meter spacing in the bottom 100 meters and 1-meter spacing in the bottom 10 meters. In the sample shown in Figure 3 the bottom is at a depth of 2566 m (shown by lower arrow, Figure 2). The profile in Figure 2 indicates that the gradient is approximately adiabatic below a depth of 2 km. At the site illustrated in Figure 3a and b, the adiabatic gradient (indicated approximately by the dashed line) extends to within 1 meter of the ocean floor, where the temperature rises abruptly by 5 millidegrees. A somewhat similar pattern is illustrated in Figure 4 where the water is shallower and the temperature is decreasing with depth near the bottom as one might anticipate from Figure 2. In this case the gradient for this depth in Figure 2 (dashed line, Figure 3a) extends to within about 20 m of the bottom and once again a temperature increase on the order of 5 millidegrees occurs in the bottom meter. These patterns although widespread

in the Arctic are not universal. Although they have not yet been studied in terms of related observations by the Lamont group and others, they are expected to contain useful information on the vertical transfer of heat and momentum and in the distribution of suspended material in currents in the bottom-most layers of the ocean.

Similar observations from Arlis II in the Denmark Strait have been applied to the analysis of previously undetected bottom-water oscillations important to regional hydrographic patterns (Lachenbruch and Marshall, 1968).

Heat flow. The locations and numbers of heat-flow measurements in the Arctic regions as of the present time are indicated by the blackened areas of Figure 5. The two areas totaling 28 measurements marked with "(S)" indicate Soviet observations from drifting ice stations (Lubimova, 1969; Lubimova et al., 1969). The measurements in the Canadian Archipelago are by Canadians "(C)", and the 14 measurements in Iceland "(I)", were made by Icelandic scientists. The remaining 330 observations were made by the U.S. Geological Survey with support from the Office of Naval Research. Of these, 9 are in the Denmark Strait, and the others are in the Alaskan quadrant.

The dots in Figure 5 represent earthquake epicenters, which delineate the active mid-ocean ridge system from Iceland to the Siberian Arctic shelf. Only two sets of heat-flow measurements have been made on this feature, 8 by the Soviets on the Asian side and 9 by the U.S. Geological Survey near Iceland. Both confirm high heat flow (>2.5 hfu, hfu = heat-flow unit = 10^{-6} cal/cm^{2}sec) within 100 km of the axis. High heat flow is also indicated on land in Iceland. The heat flow was found to fall to normal values (1.4$\pm$ hfu) over a horizontal distance of about 200 km from the ridge (Lachenbruch and Marshall, 1968). The 20 measurements by the Soviets on the Lomonosov Ridge (Lubimova, 1969) indicate a moderately high heat flow there ($\sim$ 2 hfu). Except for local anomalies the heat flow measured in the Alaskan quadrant is in the normal range (1.1 - 1.5 hfu) but the detailed coverage there permits a statistical treatment of small regional differences and in some cases, deterministic models of province boundaries (see, e.g., Lachenbruch and Marshall, 1966, 1969).

Figure 6 summarizes a statistical analysis of 122 U.S. Geological Survey heat-flow values. (It was made prior to the availability of about 200 new values from the large black regions on the Alpha Cordillera, Figure 5.) The multimodal nature of Figure 6(a) is resolved by separating the data into two populations according to depth; one representing the Canada basin and the other the surrounding Alpha-Mendeleyev Cordillera. It is seen that the cordilleran values are considerably more variable and that their mean is lower than the basin values by about 15%. (The greater variability is an expected topographic effect (Lachenbruch, 1968).) This

Try for all data

difference of about 0.2 hfu is quite significant as it exceeds the standard error of these means by an order of magnitude. It is substantially greater than the amount of heat that could be generated beneath the thin oceanic crust that is believed to underlie the deep basins. Hence the mean heat flow through the sea floor at the cordillera is not only less than the mean through the sea floor in the basin, it is also less than the heat flow from the mantle in the basin. As the cordilleran crust is probably thicker, lighter (see, e.g., Vogt and Ostenso, 1970) and more radioactive, than the basin crust, the contrast in mantle heat flows between the cordillera and basin is probably greater than 0.2 hfu, perhaps about 0.3 hfu. Hence the mantles must be significantly different beneath these contrasting tectonic units. Extensive measurements of the radioactive heat production of the Arctic Ocean sediments are being carried out in U.S. Geological Survey laboratories to increase our understanding of this problem.

Vogt and Ostenso (1970) and Hall (1970) have recently summarized a substantial amount of geophysical data which, though incomplete, provides rather convincing evidence that the Alpha Cordillera is an extinct center of sea-floor spreading. They suggest that its activity might have ceased about 40 m.y. ago at which time spreading shifted to the Nansen Cordillera (the region of epicenters in Figure 5). This view is consistent with conclusions by Lachenbruch and Marshall (1966) drawn from preliminary heat-flow data, which indicated a discontinuity in crust-upper mantle properties at the boundary of the Canada Basin and Alpha Cordillera. Subsequent heat-flow data from the cordillera are consistent with the original thermal model and tend to confirm the later views.

These results raise some fundamental questions regarding the nature of sea-floor spreading and the mechanisms of plate tectonics and continental drift. Recent theories (Oxburgh, 1971; Sclater and Francheteau, 1970) attribute the decrease in height of the sea floor and decrease in heat flow away from a ridge to cooling and contraction of aging lithosphere. However, the data from the Arctic indicate that the heat flow is lower in the younger material near the ridge crest, that the mantle is probably cooler beneath the rise than elsewhere, and that its 2 km of relief could hardly be due to thermal expansion. Furthermore if the ridge became inactive 40 m.y. ago, serious constraints are imposed on the depth to which anomalous temperatures could have extended, as cooling of a deep source has a long time constant.

Preliminary inspection of the available Arctic data would seem to suggest that the cordillera is underlain by intrinsically lighter mantle material which is fractionated and depleted in heat sources. If the spreading ceased 40 m.y. ago, it is unlikely that it could have cooled to its present state if the excess thermal energy for spreading extended to depths greater than 100 km or so.

It is expected that analysis of existing data, and that to be obtained in the near future, will help bring some of these fundamental problems of the world oceans into sharper focus. As stated previously the unique opportunity for high density precision measurements from ice islands makes the Arctic the logical place for such studies.

Plans

We consider the results obtained to date to be gratifying, even for this rather substantial logistic effort. We should like to continue the field operation at about the same level and attempt to maintain the heat-flow observations on a 12-month basis in FY 1972 unless the station should stagnate. If T-3 should move southward into the Canada Basin, it will yield much needed data to balance the intensive coverage now available from the cordillera. However, if it should pass north of Greenland, it could traverse several tectonic units including the seismically active spreading center. Geothermal and water-temperature information in this little known region could be of great significance. Hence as long as the station remains in motion along some progressive trajectory, FY 1972 could provide very useful information. If the opportunity should arise for establishing satellite or light-aircraft supported stations, we should like to take advantage of the additional coverage this would provide.

During FY 1972 we shall examine the newly reduced data, identify the most significant scientific findings, and begin work on appropriate research reports.

References

Bullard, E. C., and Day, A., 1961, The flow of heat through the floor of the Atlantic Ocean: Geophys Jour., v. 4, p. 282-292.

Hall, J. K., 1970, Arctic Ocean geophysical studies--The Alpha Cordillera and Mendeleyev Ridge: Ph.D. Thesis, Columbia University.

Lachenbruch, A. H., 1968, Rapid estimation of the topographic disturbance to superficial thermal gradients: Rev. Geophysics, v. 6, no. 3, p. 365-400.

Lachenbruch, A. H., and Marshall, B. V., 1966, Heat flow through the Arctic Ocean floor--The Canada basin-Alpha rise boundary: Jour. Geophys. Research, v. 71, no. 4, p. 1223-1248.

Lachenbruch, A. H., and Marshall, B. V., 1968, Heat flow and water temperature fluctuations in the Denmark Strait: Jour. Geophys. Research, v. 73, no. 18, p. 5829-5842.

Lachenbruch, A. H., and Marshall, B. V., 1969, Heat flow in the Arctic: Arctic, v. 22, no. 3, p. 300-311.

Lubimova, E. A., 1969, Terrestrial heat flow for the USSR and its connection with other geophenomena: Bull. volcanol., v. 33, no. 1, p. 341-367.

Lubimova, E. A., Tomara, G. A., and Aleksandrov, A. L., 1969, Heat flux through the floor of the Arctic Basin in the region of the Lomonosov Ridge: Dok. Akad. Nauk SSR, v. 184, p. 403-405 [translated by E. R. Hope, May 1969, Defence Scientific Information Service, DRB Canada, rept. T 518 R].

Oxburgh, E. R., 1971, Plate tectonics, in Gass, I. G., Smith, P. J., and Wilson, R. C. L., eds., Understanding the Earth, A reader in earth sciences: Sussex, Artemis Press, England, p. 263-285.

Sclater, J. G., and Francheteau, Jean, 1970, The implications of terrestrial heat flow observations on current tectonic and geochemical models of the crust and upper mantle of the earth: Geophys. Jour., v. 20, no. 5, p. 509-542.

Vogt, P. R., and Ostenso, N. A., 1970, Magnetic and gravity profiles across the Alpha Cordillera and their relation to Arctic sea-floor spreading: Jour. Geophys. Research, v. 75, no. 26, p. 4925-4937.

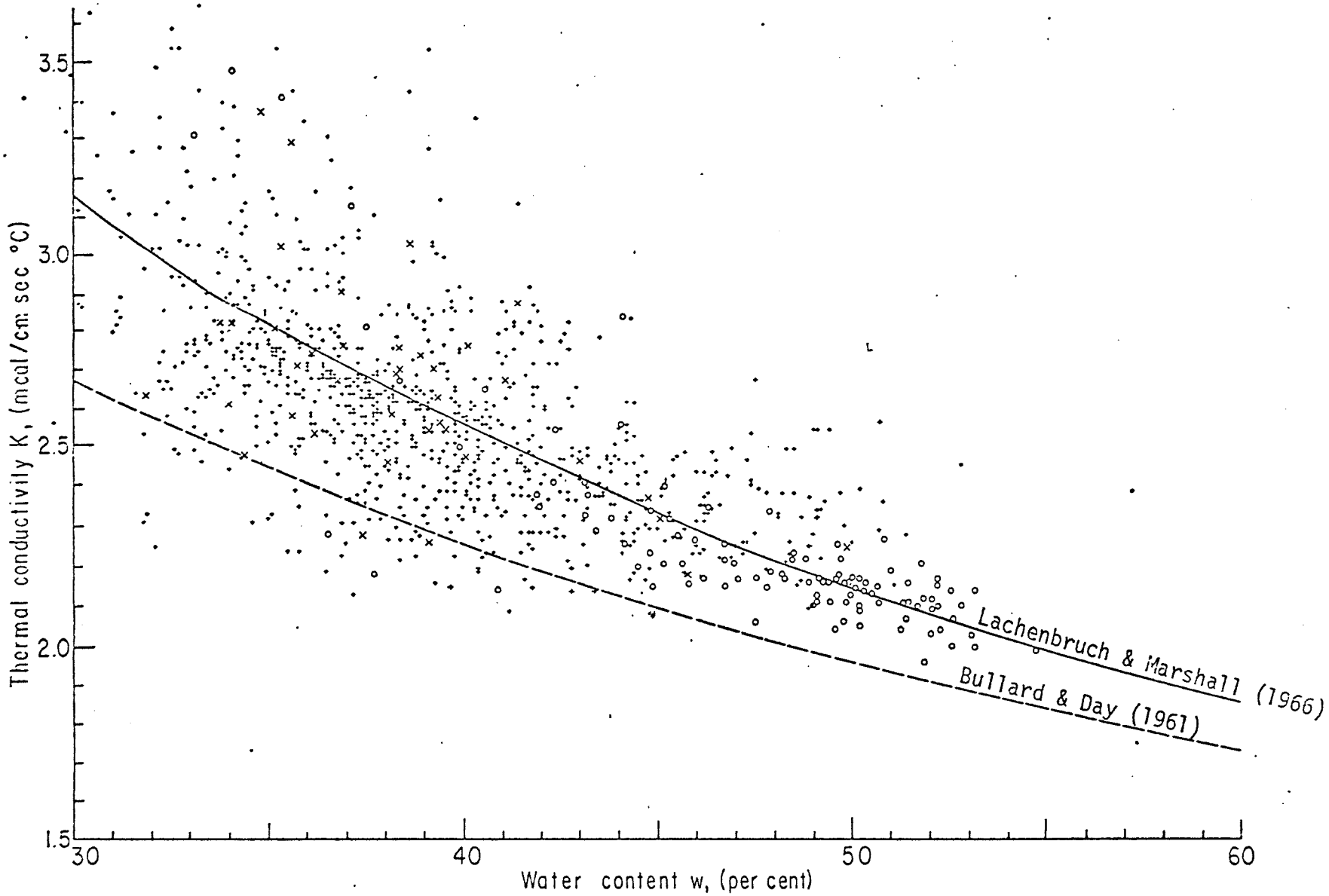

Figure 1. Relation between thermal conductivity and water content for Arctic Ocean sediments. Dashed line is empirical relation for temperate oceans; solid line is least-square fit to preliminary data (circles and crosses). Small pluses represent later observations.

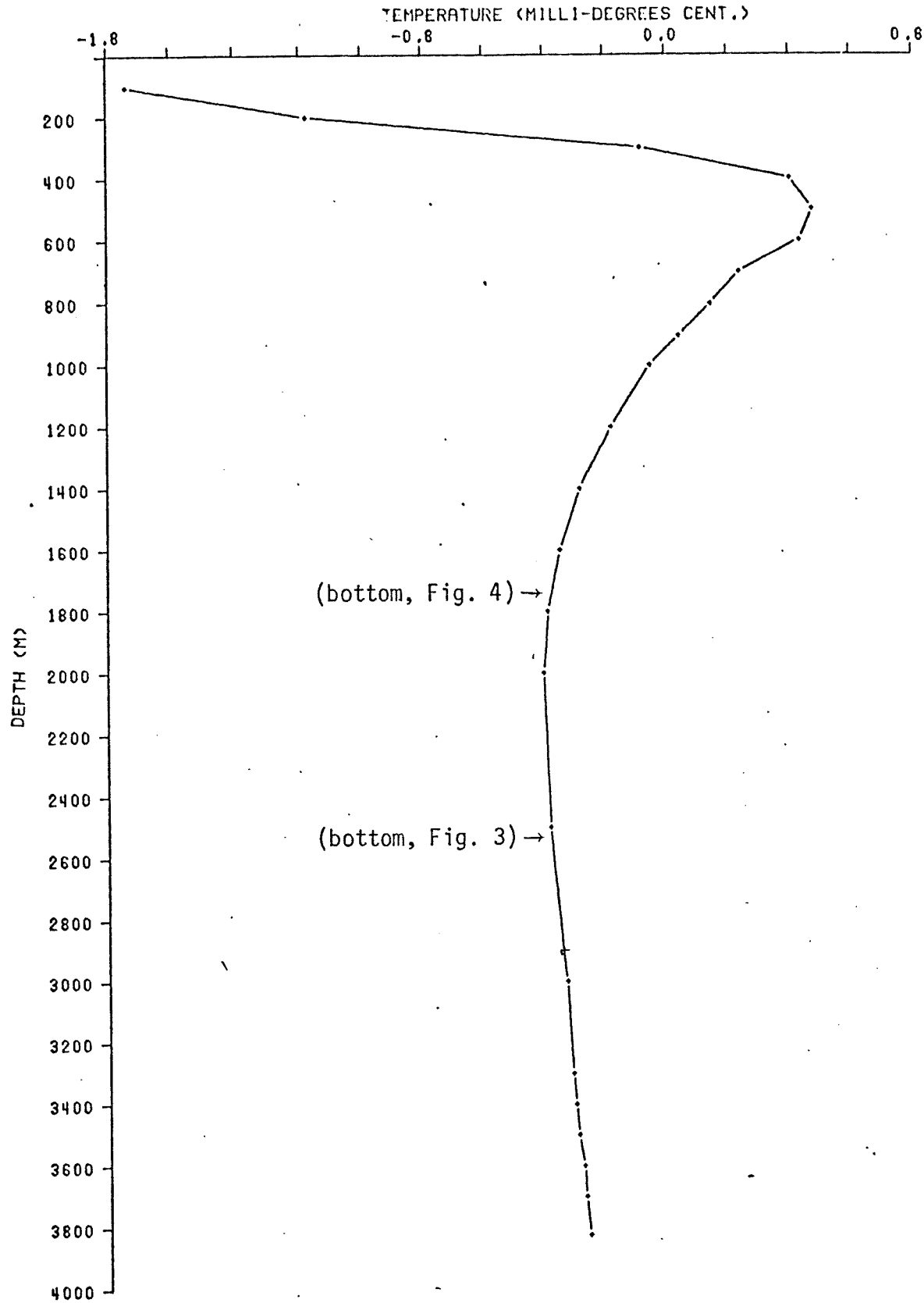

CAST NUMBER FLP-001 DATE 05-08-68

Figure 2. Typical complete water temperature profile for Canada Basin. Arrows indicate depth of bottom for cordilleran bottom water profiles in Figure 3 and Figure 4.

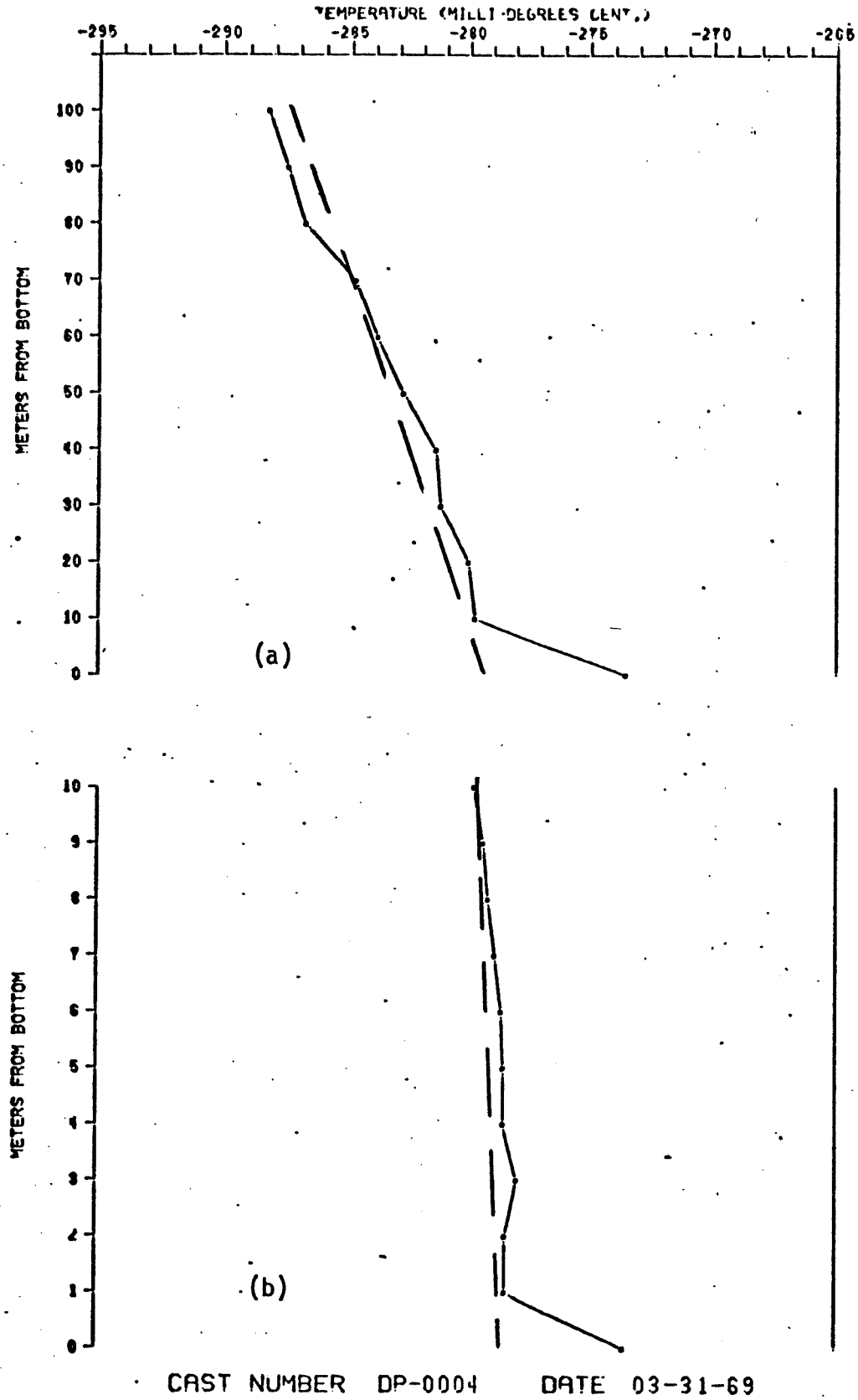

Figure 3. Water temperature profile (a) in bottom 100 meters and (b) in the bottom 10 meters at a cordilleran station. Dashed line is adiabatic gradient, water depth 2566 m.

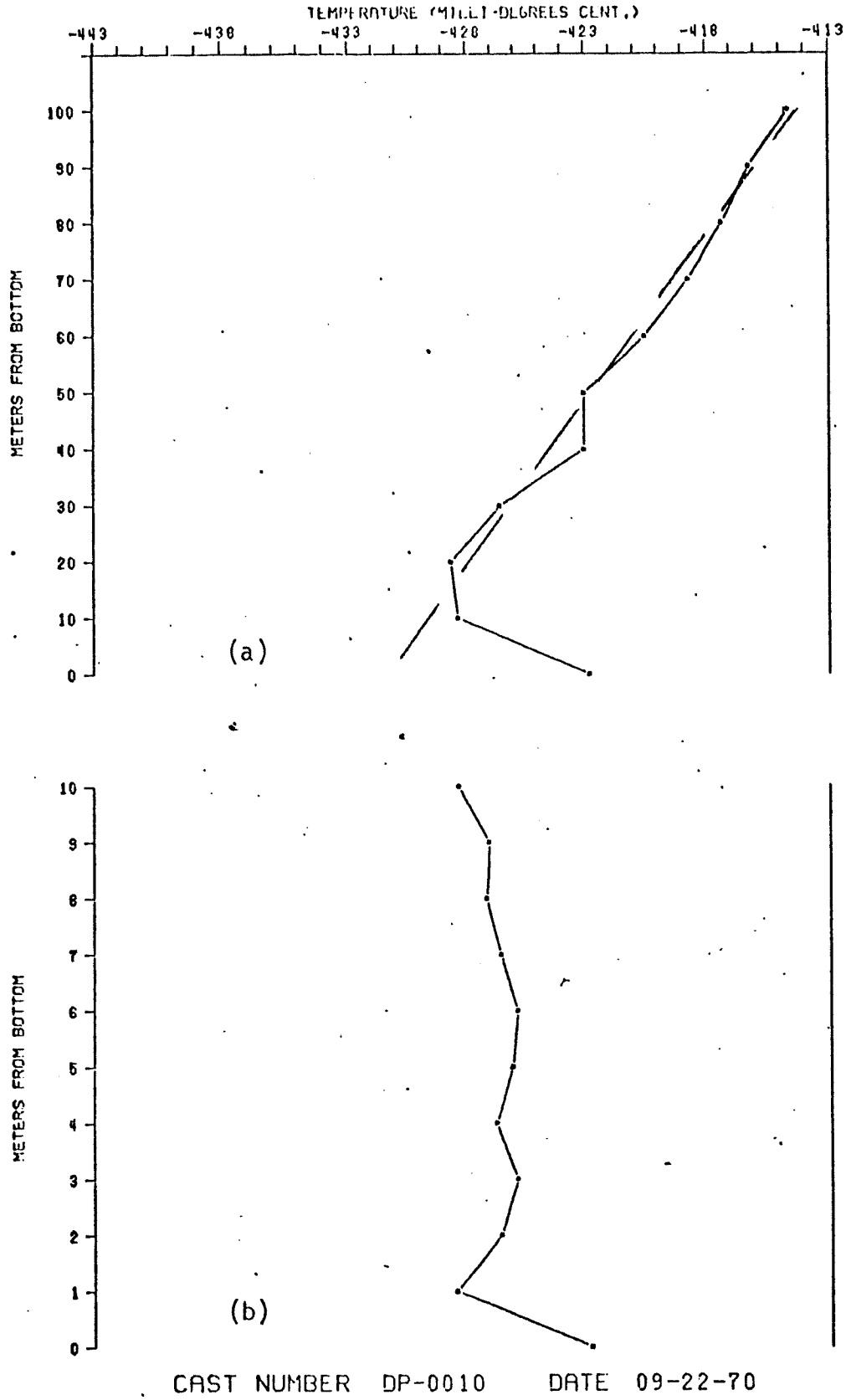

Figure 4. Bottom water temperature profile of type shown in Figure 3. Water depth is 1724 m, dashed line represents gradient at that depth in profile of Figure 2.

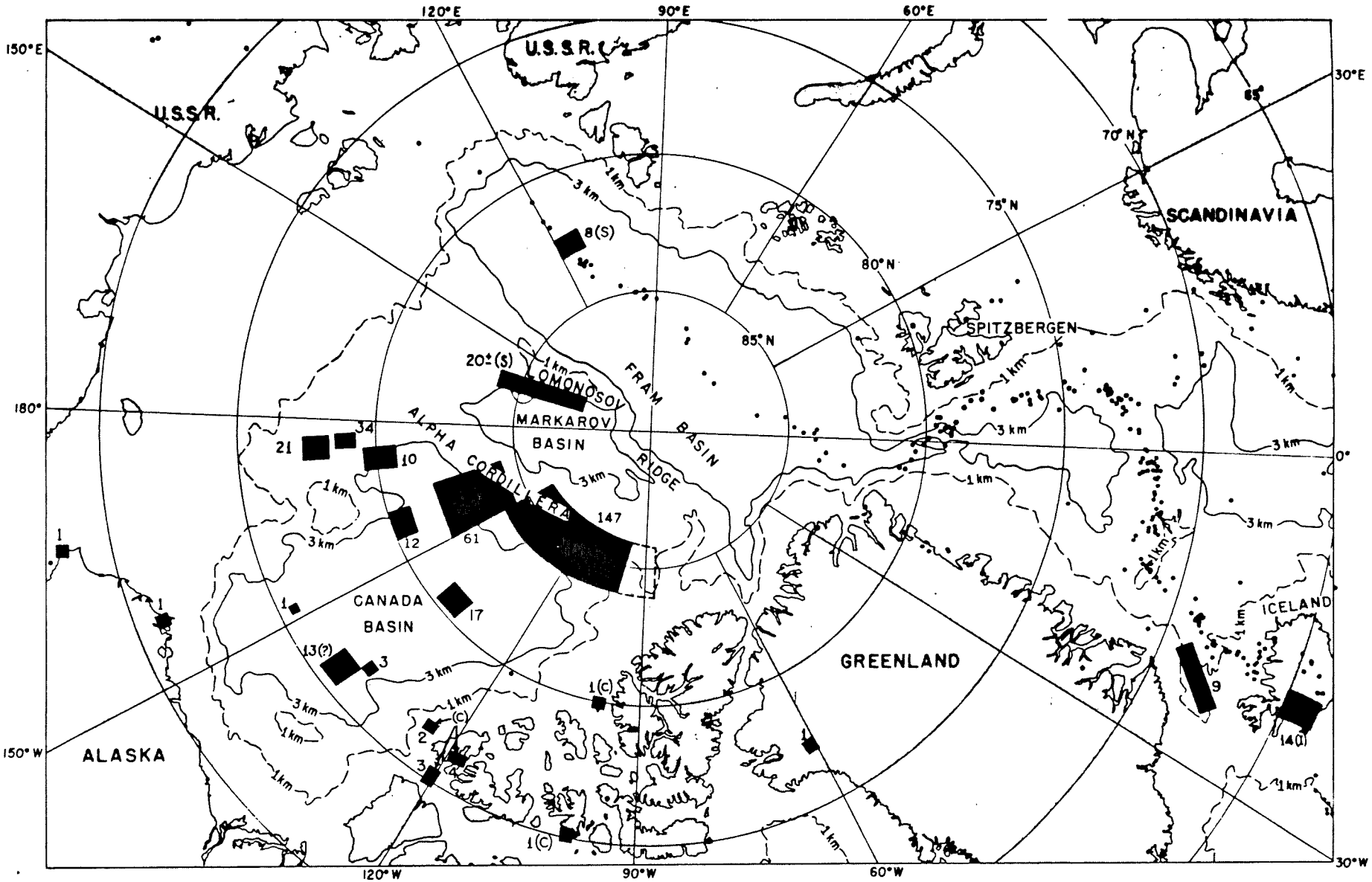

Figure 5. Distribution of heat-flow observation in Arctic regions. Observations by Soviet, Canadian, and Icelandic scientists are denoted respectively by (S), (C), and (I). The others were made by the project. Dots represent seismic epicenters.

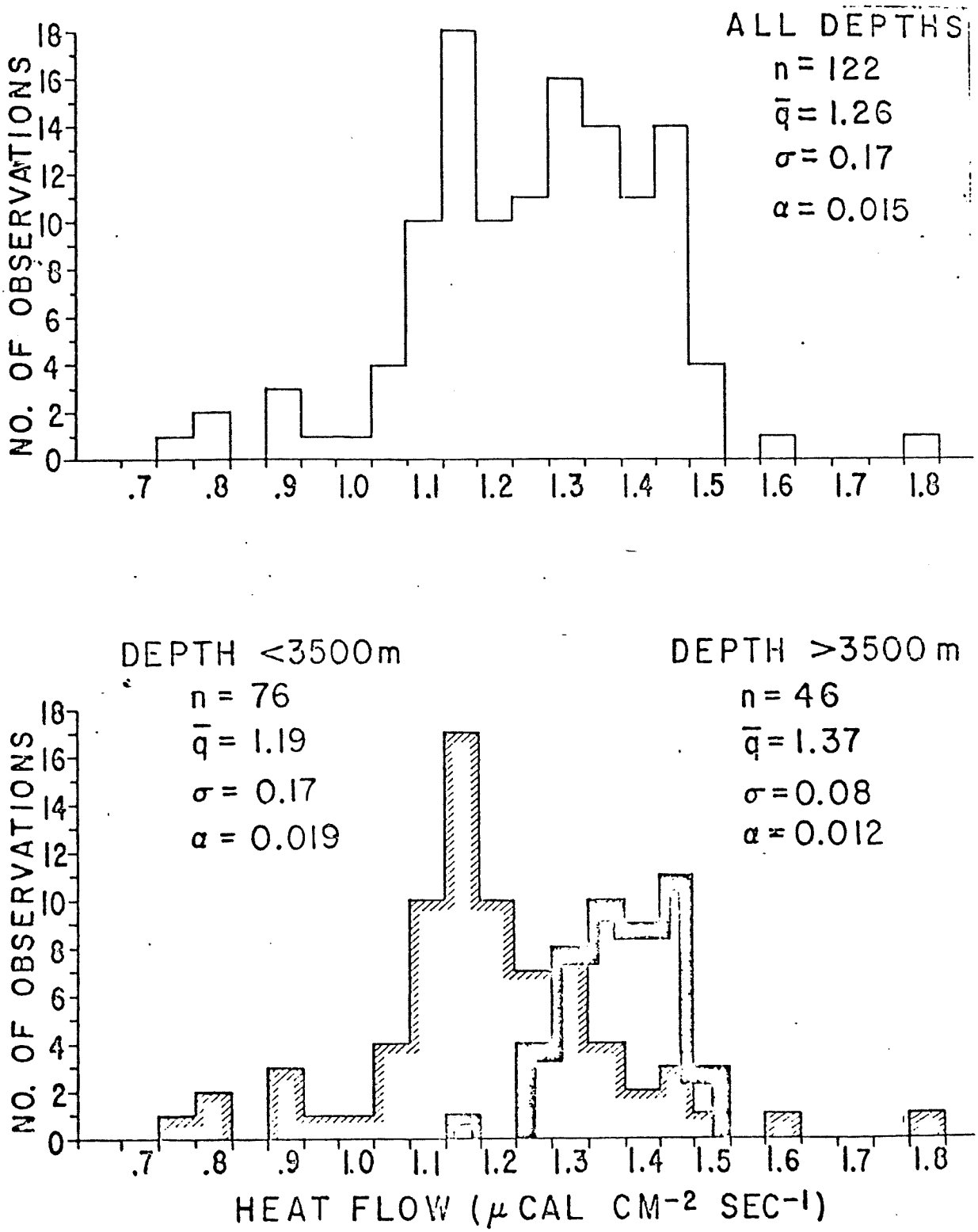

Figure 6. Histogram of the first 122 heat-flow values from the Canada Basin (depth >3500 m) and the Alpha-Mendeleyev Cordillera (depth <3500 m).